ANNUAL REVIEW

INSTITUTE FOR MOLECULAR SCIENCE

1987

ANNUAL REVIEW

INSTITUTE FOR MOLECULAR SCIENCE

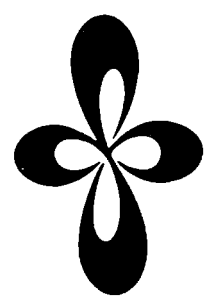

1987

Published by
Okazaki National Research Institutes
Institute for Molecular Science
Myodaiji, Okazaki 444, Japan
Phone 0564-54-1111
Telex 4537-475 KOKKEN J

IMS 1987

First of all, I would like to announce that Prof. S. Nagakura resigned at the end of March after six very fruitful years as Director-General of IMS, and was nominated President of Okazaki National Research Institutes. He had been Director-General since he succeeded Prof. H. Akamatu, the first Director-General of IMS, in April, 1981. During these years, Institute for Molecular Science has expanded its research activities very vigorously and rapidly, and is now recognized as an international centre for molecular science research. Let me take this opportunity to express our sincere gratitude for the efforts and achievements Profs. Akamatu and Nagakura have made during this developmental period.

In 1987, we have accumulated fruitful results in many fields of molecular science. The two main instruments at IMS, the UVSOR facility and the computer centre equipped with a supercomputer, are now in full operation. All of the research activities carried out at IMS in the past year are found in this Review.

During the past year, the movement of scientific staff has been very active. Prof. K. Saito, Director of Coordination Chemistry Laboratories, and I retired from research positions. Prof. H. Iwamura, Director of Department of Applied Molecular Science, moved to Department of Chemistry, University of Tokyo. I am pleased to announce that Dr. K. Isobe was appointed Associate Professor of Applied Molecular Science.

From the viewpoint of promoting international exchange of scientists and joint studies in the field of molecular science, progress has been made in the past year. Two new programmes for international cooperative research were initiated, IMS serving as the key institution on the Japanese side: one is the United States-Japan Cooperative Work in Advanced Materials and the other is the Swedish-Japan Joint Studies on Molecular Science.

Finally, as was mentioned by Prof. S. Nagakura in the previous issue of the IMS Annual Review 1986, I sincerely hope that the coming decade will be even more productive period for IMS on the basis of the high research potentiality cultivated during the past ten years. In order to achieve this goal I will do my utmost to create the optimum research environment at this Institute and continue the excellent progress made during the Akamatu/Nagakura era.

September, 1987

H. Inokuchi

Hiroo INOKUCHI
Director-General

We are saddened to inform you that Professor Hideo Akamatu, the first Director-General, passed away on 8th January 1988, two days after a stroke.

Since his death occurred after this issue was in press, a full tribute to this distinguished scientist will be included in the next issue of Annual Review.

CONTENTS

ORGANIZATION AND STAFF

Organization

The Institute for Molecular Science comprises seventeen research laboratories – each staffed by a professor, and associate professor, two research associates and a few technical associates –, two research laboratories with foreign visiting professors, and six research facilities. The laboratories are grouped into five departments and one facility for coordination chemistry:

Department of Theoretical Studies	Theoretical Studies I
	Theoretical Studies II
	Theoretical Studies III[1)]
Department of Molecular Structure	Molecular Structure I
	Molecular Structure II[1)]
	Molecular Dynamics
Department of Electronic Structure	Excited State Chemistry
	Excited State Dynamics
	Electronic Structure[1)]
	Molecular Energy Conversion[2)]
Department of Molecular Assemblies	Solid State Chemistry
	Photochemistry
	Molecular Assemblies Dynamics
	Molecular Assemblies[1)]
	Synchrotron radiation Research[2)]
Department of Applied Molecular Science	Applied Molecular Science I
	Applied Molecular Science II[1)]
Coordination Chemistry Laboratories	Synthetic Coordination Chemistry
	Complex Catalysis
	Coordination Bond

Research facilities are:	Computer Center
	Low-Temperature Center
	Instrument Center
	Chemical Materials Center
	Equipment Development Center
	Ultraviolet Synchrotron Orbital Radiation (UVSOR) Facility.

1) Professors and associate professors are adjunct professors from universities.

2) Research Laboratories with foreign visiting professors.

Scientific Staff

Hiroo INOKUCHI	**Professor, Director-General**

Department of Theoretical Studies

Theoretical Studies I

Keiji MOROKUMA	Professor
Iwao OHMINE	Associate Professor
Koichi YAMASHITA	Research Associate
Chikatoshi SATOKO	Research Associate (–March '87)[1]
Masaki SASAI	Research Associate
Satoshi YABUSHITA	Technical Associate (September '86–)
Hideki TANAKA	Technical Associate (–June '87)[2]
Mutsumi AOYAGI	Technical Associate (September '87–)
Yuriko AOKI	Graduate Student from Hiroshima Univ.* (October '86–)
Tadahiro OZAWA	Visiting Research Fellow from Kao Corp. (–March '87)[3]

Theoretical Studies II

Hiroki NAKAMURA	Professor
Keiichiro NASU	Associate Professor
Kazuo TAKATSUKA	Research Associate (–March '87)[4]
Masahiro IWAI	Research Associate (July '87–)
Hidemitsu HAYASHI	Research Associate
Akihiko OHSAKI	Technical Associate
Jun-ichi TAKIMOTO	Technical Associate
Masato NAKAMURA	IMS Fellow (April '86–)
Yoshiyuki USAMI	Graduate Student from Keio Univ.* (Arpil '87–)

Theoretical Studies III

Kichisuke NISHIMOTO	Adjunct Professor from Osaka City Univ. (–March '87)
Akira YANASE	Adjunct Professor from Univ. of Osaka Pref. (April '87–)
Koichiro NAKANISHI	Adjunct Associate Professor from Kyoto Univ. (–March '87)
Yuichi FUJIMURA	Adjunct Associate Professor from Tohoku Univ. (May '87–)
Nobuaki KOGA	Research Associate

Department of Molecular Structure

Molecular Structure I

Eizi HIROTA	Professor
Norio MORITA	Associate Professor
Chikashi YAMADA	Research Associate
Yasuki ENDO	Research Associate (–July '87)[5]
Hideto KANAMORI	Technical Associate
Keiichi SATO	Technical Associate (April '87–)
Masatoshi KAJITA	Research Fellow
Takamasa MOMOSE	Graduate Student from Kyoto Univ.* (April '87–June '87)
Masaharu FUJITAKE	Graduate Student from Hiroshima Univ.* (April '87–)

Molecular Structure II

Shuji SAITO	Adjunct Professor from Nagoya Univ. (–March '87)
Akifumi UENO	Adjunct Professor from Toyohashi Univ. of Tech. (April '87–)
Takayoshi KOBAYASHI	Adjunct Associate Professor from Univ. of Tokyo
Kentaro KAWAGUCHI	Research Associate
Takashi OGURA	Research Associate

Molecular Dynamics

Teizo KITAGAWA	Professor
Yasuo UDAGAWA	Associate Professor
Keiji KAMOGAWA	Research Associate
Kazuyuki TOHJI	Research Associate
Takashi FUJII	Technical Associate (–September '87)[6]
Takanori MIZUSHIMA	Technical Associate
Noriyoshi KAKUTA	IMS Fellow (–September '87)[7]
Shoji KAMINAKA	Graduate Student from Osaka Univ.*
Masashi NAKAGAWA	Graduate Student from Univ. of Tokyo*
Mutsumi HARADA	Graduate Student from Toyohashi Univ. of Tech.* (–March '87)
Akira ENDO	Graduate Student from Tokyo Metropolitan Univ.*
Takeshi MIKI	Graduate Student from Toyohashi Univ. of Tech.*
Naoyuki TAKAHASHI	Graduate Student from Toyohashi Univ. of Tech.* (April '87–)

Department of Electronic Structure

Excited State Chemistry

Keitaro YOSHIHARA	Professor
Tadayoshi SAKATA	Associate Professor
Nobuaki NAKASHIMA	Research Associate (–June '87)[8]
Kazuhito HASHIMOTO	Research Associate
Minoru SUMITANI	Technical Associate (–September '87)
Masahiro HIRAMOTO	Technical Associate
Hrvoje PETEK	Visiting Scientist (August '85–)
Nariaki HIROSHIGE	Graduate Student from Saga Univ.* (April '86–March '87)
Keiji IMAGI	Graduate Student from Kyoto Inst. of Tech.* (Spetember '86–March '87)
Yoshihisa FUJIWARA	Graduate Student from Kanazawa Univ.* (April '87–)
Andrew CAMPEN	Graduate Student from Univ. of Southampton (April '87–October '87)
Yoshizumi KAJII	Graduate Student from Tokyo Inst. of Tech.* (April '85–March '87)
Yoshinori YAMADA	Graduate Student from Toyohashi Univ. of Tech.* (April '86–March '87)
Seiji AMAKUSA	Graduate Student from Nagoya Inst. of Tech.* (April '86–March '87)
Takahiko KURODA	Graduate Student from Kyoto Inst. of Tech.* (April '87–)

Excited State Dynamics

Ichiro HANAZAKI	Professor
Nobuyuki NISHI	Associate Professor
Masao TAKAYANAGI	Research Associate (October '86–)
Hisanori SHINOHARA	Research Associate

Teruhiko NISHIYA	Technical Associate
Kazunori YAMAMOTO	Technical Associate
Hiroshi OHOYAMA	IMS Fellow (April '87–)

Electronic Structure

Noboru MATAGA	Adjunct Professor from Osaka Univ. (April '86–)
Hirochika SAKURAGI	Adjunct Associate Professor from Univ. of Tsukuba (April '85–March '87)
Haruo ABE	Visiting Research Fellow (March '85–March '87), Adjunct Associate Professor (April '87–) from Inst of Phys. and Chem. Res.
Ryoichi NAKAGAKI	Research Associate
Hiromi OKAMOTO	Research Associate
Minoru SUMITANI	Research Associate (October '87–)
Yoshio FUKUDA	Technical Assistant (April '86–September '87)[9]

Molecular Energy Conversion

E. TIEMANN	Visiting Professor from Inst. At. Moleculphys., Univ. Hannover (FRG) (June '86–Mar. '87)
J. JESZKA	Visiting Associate Professor from Cent. Mol. Macromol. Stud., Pol. Acad. Sci. (Poland) (May '86–Nov. '86)
G. Black	Visiting Professor from SRI International (April '87–)
H. Toftlund	Visiting Associate Professor from Odense Univ., Denmark (June '87–March '88)

Department of Molecular Assemblies

Solid State Chemistry

Inosuke KOYANO	Associate Professor
Takashi IMAMURA	Research Associate
Shinzo SUZUKI	Technical Associate
Kenichi IMAEDA	Technical Associate
Hitoshi FUJIMOTO	JSPS Post-doctoral Fellow (April '86–)
Hiromichi YAMAMOTO	Visiting Research Fellow (April '86–)
Takashi IMAJO	IMS Fellow (April '87–)

Photochemistry

Katsumi KIMURA	Professor
Kosuke SHOBATAKE	Associate Professor
Kiyohiko TABAYASHI	Research Associate
Katsuhiko OKUYAMA	Research Associate
Atsunari HIRAYA	Technical Associate
Masahiko TAKAHASHI	Technical Associate (Nov. '86–)
Haruo SHIROMARU	IMS Fellow (–March '87)[10]
Nobuo HAYASAKA	Visiting Research Fellow from Toshiba Corp. (May '86–)

Molecular Assemblies Dynamics

Yusei MARUYAMA	Professor
Masatoshi SATO	Associate Professor
Tamotsu INABE	Research Associate
Masashige ONODA	Research Associate
Masafumi SERA	Research Associate (Aug. '87–)
Hajime HOSHI	Technical Associate
Naomi HOSHINO	Technical Associate (–Aug. '87)[11]
Shin-ichi SHAMOTO	Graduate Student from Kyoto Univ.* (–March '87) Technical Associate (April '87–)
Yuji MATSUDA	Graduate Student from Univ. of Tokyo* (–March '87)[12]

Yoichiro KAWAI	Visiting Research Fellow from TOYOTA Motor Co., Ltd. (April '87–)
Shinji KONDOH	Visiting Research Fellow from Asahi Glass Co., Ltd. (June '87–)
Chikako NAKANO	Visiting Research Fellow (Sept. '87–)

Molecular Assemblies

Koji KAYA	Adjunct Professor from Keio Univ. (April '87–)
Ichimin SHIROTANI	Adjunct Associate Professor from Muroran Institute of Technology
Takehiko MORI	Research Associate
Shin-ichi NAGAOKA	Research Associate

Synchrotron Radiation Research

J. Robb GROVER	Visiting Professor from Brookhaven National Laboratory, U.S.A. (June '86–April '87)
P.G. WOLYNES	Visiting Professor from Univ. of Illinois, U.S.A. (June '87–)
J.M. LEE	Visiting Associate Professor from Chonbuk Natl. Univ., Korea (March '86–November '86)
A.L. Verma	Visiting Associate Profssor from North-Eastern Hill Univ., India (Jan. '86–Dec. '87)

Department of Applied Molecular Science

Applied Molecular Science I

Hiizu IWAMURA	Professor (–May '87)[13]
Kiyoshi ISOBE	Associate Professor (January '87–)
Koshiro TORIUMI	Research Associate
Shigeru MURATA	Research Associate (–April '87)[14]
Yoshihito HAYASHI	Graduate Student from Osaka City Univ.* (April '87–)

Applied Molecular Science II

Kazuhiro MARUYAMA	Adjunct Professor from Kyoto Univ. (April '87–)
Hiroharu SUZUKI	Adjunct Associate Professor from Tokyo Inst. of Tech. (July '87–)
Noboru KOGA	Research Associate
Hiroki OSHIO	Research Associate

Coordination Chemistry Laboratories

Kazuo SAITO	Director (–March '87)[16]
Hiizu IWAMURA	Director (April '87–May '87)[13]
Eiji HIROTA	Director (June '87–)

Synthetic Coordination Chemistry

Sigeo KIDA	Professor
Shin-ichi ISHIGURO	Associate Professor
Kazuhiko OZUTSUMI	Research Associate
Masayoshi MIKURIYA	Research Associate (–March '87)[15]
Masahito KODERA	Research Associate (June '87–)
Honoh SUZUKI	Graduate Student from Tokyo Inst. of Tech.* (April '86–)
Eiji ASATO	Graduate Student from Kyushu Univ.* (April '86–)
Makoto HANDA	Graduate Student from Kyushu Univ.* (April '86–)
Kei-ichi SATOH	Graduat Student from Niigata Univ.* (–September '87)
Takamitsu KOUZUMA	Graduate Student from Kanazawa Univ.* (April '86–)

Complex Catalysis

Kazuo SAITO	Professor (–March '87)[16]

Taro SAITO	Adjunct Professor from Osaka Univ. (April '86–)
Shigenobu FUNAHASHI	Adjunct Associate Professor from Nagoya Univ. (April '86–)
Kiyohiko NAKAJIMA	Research Associate (December '86–)

Coordination Bond

Humihiko TAKEI	Adjunct Professor from Tokyo Univ. (April '86–)
Shouzo TERO	Adjunct Associate Professor from Tohoku Univ. (April '86–)

Research Facilities

Computer Center

Keiji MOROKUMA	Director
Hiroshi KASHIWAGI	Associate Professor
Umpei NAGASHIMA	Research Associate
Shigeyoshi YAMAMOTO	Technical Associate
Masahiro SEKIYA	Graduate Student from Hokkaido Univ.* (April '86–)

Instrument Center

Ichiro HANAZAKI	Director
Iwao YAMAZAKI	Associate Professor
Keisaku KIMURA	Research Associate
Naoto TAMAI	Research Associate
Katsuhiro SUMI	IMS Fellow (Sept. '86–Aug. '87)[17]
Takahide MINAMI	Visiting Research Fellow from Kao Corp. (April '86–)
Naoki SATO	Visiting Research Fellow from Kao Corp. (April '86–)

Chemical Materials Center

Keitaro YOSHIHARA	Director
Hidemasa TAKAYA	Associate Professor
Kazushi MASHIMA	Research Associate
Tetsuo OHTA	Technical Associate

Low-Temperature Center

Yusei MARUYAMA	Director
Toshiaki ENOKI	Research Associate (–May '87)[18]

Equipment Development Center

Eizi HIROTA	Director
Tadaoki MITANI	Associate Professor
Yoshihiro TAKAGI	Research Associate
Yoshiki WADA	IMS Fellow (–March '87)[19]

Ultraviolet Synchrotron Orbital Radiation Facility

Katsumi KIMURA	Director
Makoto WATANABE	Associate Professor
Toshio KASUGA	Associate Professor
Hisashi KOBAYAKAWA	Adjunct Associate Professor from KEK (–March '87)
Shun-ichi NAOÉ	Adjunct Associate Professor from Kanazawa Univ. (April '87–)
Hiroto YONEHARA	Research Associate
Kazutoshi FUKUI	Research Associate
Teruo HOSOKAWA	Visiting Research Fellow from NTT (–March '87)

Technical Staff

Akira UCHIDA	Technical Division Head
Keiichi HAYASAKA	Technical Section Chief
Kusuo SAKAI	Technical Section Chief
Satoshi INA	Computer Center (Unit Chief)
Fumio NISHIMOTO	Computer Center
Takaya YAMANAKA	Instrument Center
Shunji BANDOW	Instrument Center
Kiyonori KATO	Low-Temperature Center (Unit Chief)
Shuji NAKANE	Low-Temperature Center
Taeko MAEDA	Chemical Materials Center
Kazuo HAYAKAWA	Equipment Development Center (Unit Subchief)
Hisashi YOSHIDA	Equipment Development Center
Masaaki NAGATA	Equipment Development Center
Toshio HORIGOME	Equipment Development Center (Unit Subchief)
Norio OKADA	Equipment Development Center
Mitsukazu SUZUI	Equipment Development Center
Nobuo MIZUTANI	Equipment Development Center
Shinji KATO	Equipment Development Center
Osamu MATSUDO	UVSOR Facility (Unit Chief)
Toshio KINOSHITA	UVSOR Facility
Masami HASUMOTO	UVSOR Facility
Jun-ichiro YAMAZAKI	UVSOR Facility
Eiken NAKAMURA	UVSOR Facility

* Carries out graduate research at IMS on the Cooperative Education Programs of IMS with graduate schools.

1) Present Address: Nihon Univ., Sakurajosui 3-25-40, Setagaya-ku, Tokyo 156
2) Present Address: Kyoto Univ., Yoshidamotomachi, Sakyo-ku, Kyoto 606
3) Present Address: Nagoya Univ., Fro-cho, Chikusa-ku, Nagoya 464
4) Present Address: Tochigi Res. Lab., Kao Corp., Ichikai 321-34
5) Present Address: Colledge of Arts and Sciences, Univ. of Tokyo, 3-8-1, Komaba, Meguro-ku, Tokyo 153
6) Present Address: Spectra-Physics K.K., 15-8, Nanpeidai, Shibuya-ku, Tokyo 150
7) Present Address: Dept. of Materials Science, Toyohashi Univ. of Tech., 1-1, Hibarigaoka, Tenpaku-cho, Toyohashi 440
8) Present Address: Institute of Laser Engineering, Osaka Univ. Yamada-oka, Suita 565
9) Present Address: Kao Institute for Fundamental Research, 2606, Akabane, Ichikaimachi, Haga, Tochigi 321-34
10) Present Address: Dept. of Chemistry, Tokyo Metropolitan Univ., 2-1-1, Hukazawa, Setagaya, Tokyo 158
11) Present Address: Dept. of Chemistry, Hokkaido Univ., Kita-ku, Sapporo 060
12) Present Address: College of General Education, Univ. of Tokyo, Meguro-ku, Tokyo 153
13) Present Address: Dept. of Chemistry, Faculty of Science, Univ. of Tokyo, Hongo, Bunkyo-ku, Tokyo 113
14) Presnet Address: Dept. of Industrial Chemistry, Faculty of Engineering, Mie Univ., Tsu, Mie 514
15) Present Address: Faculty of Science, Kansai Gakuin Univ.
16) Present Address: Faculty of Science, International Christian Univ.
17) Present Address: Dept. of Biological Chemistry, Univ. of Tsukuba, Sakura-mura, Niiharu-gun, Ibaragi 305
18) Present Address: Dept. of Chemistry, Tokyo Institute of Technology, 2-12-1 Ookayama, Meguro-ku, Tokyo 152
19) Present Address: National Institute for Research in Inorganic Materials, 1-1 Namiki, Sakuramura, Niiharu-gun, Ibaragi 305

Foreign Visiting Staff

Xin Sun	Fudan Univ., China	Jul. 18–Nov. 30, 1986
Ping Wang	Inst. Chem., Acad. Sin., China	Oct. 29, 1986–Oct. 27, 1987
Ivo Plazibat	Univ. Split, Yugoslavia	Nov. 1986–Sep. 1987
Hee S. Yoo	Chungbuk Natl. Univ., Korea	Dec. 23, 1986–Feb. 22, 1987
Sang-Oh Oh	Kyungpook National Univ., Korea	Jan. 6–Mar. 5, 1987
Pill-Soon Song	Univ. of Nebraska, USA	Jan. 5–Mar. 31, 1987
I. H. Munro	Daresbury Lab., SERC, UK	Jan. 22–Apr. 30, 1987
P. G. Mezy	Univ. of Saskatchewan, Canada	Jan.–Feb., 1987
Ye Wen	Inst. Chem., Acad. Sin., China	Feb. 1987–Feb. 1988
Anthony J. Dann	Univ. of Nottingam, UK	May 1987–May 1988
Ronald McKelvey	Univ. of Wisconsin, Lacrosse, USA	May 27–Dec. 21, 1987
S. C. Park	Kangweon Natl. Univ., Korea	Jun.–Aug. 1987
D. Kim	Korea Stand. Res. Inst., Korea	Jul.–Aug. 1987
H. Kim	Seoul Natl. Univ., Korea	Jul.–Sep. 1987
Keitaro Nakatani	E.N.S.ST. Cloud-Fontenay, France	Jul. 27–Sep. 24, 1987
S.M.B. Costa	Inst. Super. Tec., Porutugal	Oct. 1986–Feb. 1987

COUNCIL

Hiroo INOKUCHI **Director-General**

Councillors

Chairman	Kenichi FUKUI	President, Kyoto Institute of Technology
Vice-Chairman	Hiroaki BABA	Professor, The Research Institute of Applied Electricity, Hokkaido University
	Hideo AKAMATU	Professor Emeritus, The University of Tokyo and IMS
	Eiichi FUJITA	President, Osaka University of Pharmaceutical Sciences
	Sachio HAYAKAWA	President, Nagoya University
	Ryuichi HIRANO	Professor Emeritus, The University of Tokyo
	Namio HONDA	President, Toyohashi University of Technology
	Shô ITÔ	Professor, Tohoku University
	Kouzou KUCHITU	Professor, The University of Tokyo
	Michio KURATA	Director-General, Institute for Chemical Research, Kyoto University
	Masatoshi MORITA	Chief Executive Officer, Toyota Central Research & Development Laboratories, INC
	Haruo NISHIHARA	President, Waseda University
	Minoru ODA	Director-General, The Institute of Space and Astoronautical Science
	Yoshihiko SAITO	Professor, Keio University

Kenji TAMARU	Professor, The Science University of Tokyo
Ikuzo TANAKA	President, Tokyo Institute of Technology
Yutaka TOYOZAWA	Professor, Chuo University
Per-Olov LÖWDIN	Professor, University of Florida and Professor Emeritus, Uppsala University (–May '86)
George C. PIMENTEL	Professor, University of California, Barkley (–May '86)
Manfred EIGEN	Head of Department, Max-Planck Institute of Physical Chemistry and Professor, Technical University of Göttingen (August '86–)
Robert Ghormley PARR	Professor, University of Northcarolina (August '86–)

The Council is the advisory board for the Director-General. Two of the councillors are selected among distinguished foreign scientists.

Professor Emeritus

Professor Hideo AKAMATU, ex-Director-General of IMS, was named the first professor emeritus of this institute in September, 1982.

Distinguished Research Consultants

Kenichi FUKUI	President, Kyoto Institute of Technology; Professor Emeritus, Kyoto University
Masao KOTANI	Professor Emeritus, The University of Tokyo
Yonezo MORINO	Professor Emeritus, The University of Tokyo; Director and Supreme Consultant, Sagami Chemical Research Center

Administration Bureau

Kiyoshi INOUE	Director-General, Administration Bureau
Minoru OKAMOTO	Director, General Affairs Department (–March '87)
Yukio OHMURA	Director, General Affairs Department (April '87–)
Hozumi KISHIYAMA	Director, Finance and Facilities Department
Hideo ISHIKAWA	Head, General Affairs Division
Shigeyoshi ONO	Head, Personnel Division (–March '87)
Junsaku NAGATA	Head, Personnel Division (April '87–)
Takeru YAMAKAWA	Head, Research Cooperation and International Affairs Division (–March '87)
Minoru AKIMOTO	Head, Research Cooperation and International Affairs Division (April '87)
Kaichi ONUMA	Head, Budget Division (–March '87)
Takashi TAKIGAWA	Head, Budget Division (April '87)

Yasutaro NAGATA	Head, Accounts Division (–March '87)
Kaoru KATO	Head, Accounts Division (April '87–)
Hirohiko URA	Head, Construction Division (–March '87)
Michitaro MATUI	Head, Construction Division (April '87)
Motokazu FURUYA	Head, Equipment Division

BUILDINGS AND CAMPUS

The IMS campus covering 62,343 m^2 is located on a low hill in the middle of Okazaki City. The inequality in the surface of the hill and growing trees are preserved as much as possible, and low-storied buildings are adopted for conservation of the environment. The buildings of IMS are separated according to their functions as shown in the map. The Research Office Building and all Research Facilities except for the Computer Center are linked organically to the Main Laboratory Building by corridors. Computer Center, Library, and Administration Buildings are situated between IMS and the neighboring National Institute for Basic Biology and National Institute for Physiological Sciences, because the latter two facilities are common to these three institutes.

The lodging facility of IMS called Yamate Lodge, located within 10 min walk, has sleeping accommodations for 19 guests and two families. Since June 1, 1981 a new lodging facility called Mishima Lodge has been opened. Mishima Lodge, located within four minutes' walk east of IMS can accommodate 68 guests and ten families. Scientists who visit IMS as well as the two other institutes can make use of these facilities. Foreign visiting scientists can also live at these lodgings with their families during their stays.

The Institute for molecular Science

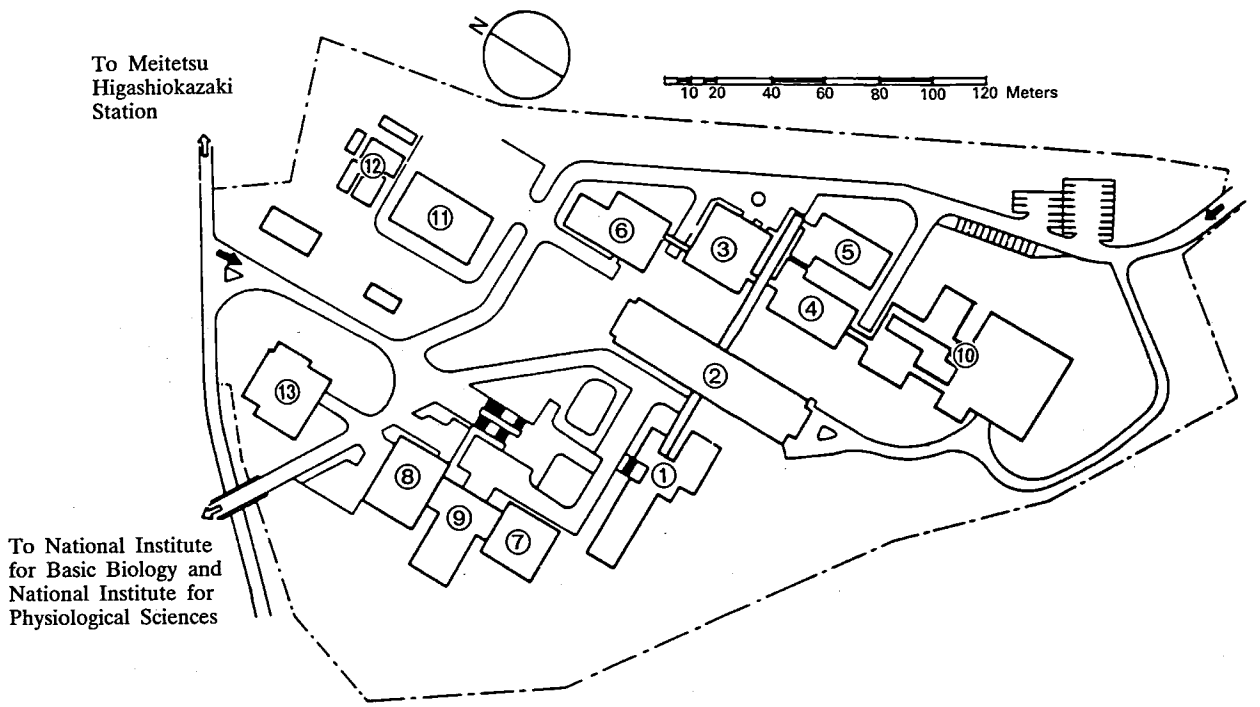

1. Research Office Building
2. Main Laboratory Building
3. Equipment Development Center
4. Instrument Center
5. Chemical Materials Center
6. Low-Temperature Center
7. Computer Center
8. Library
9. Central Administration
10. UVSOR Facility
11. Power Station
12. Waste-Water Disposition Facilities
13. Faculty Club

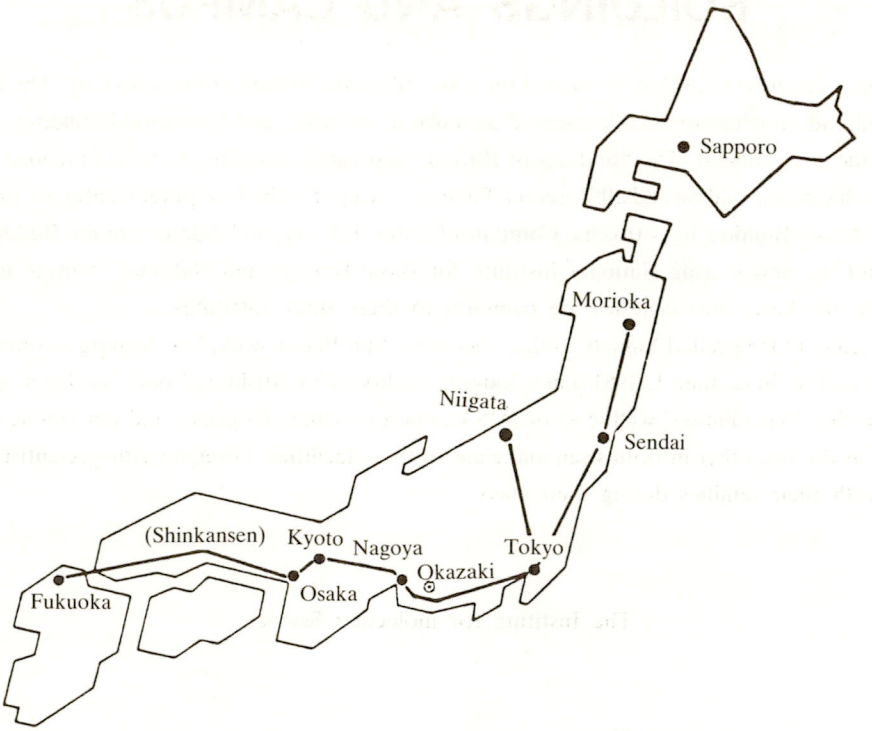

Okazaki (population 280,000) is 260 km southwest of Tokyo, and can be reached by train in about 3 hours from Tokyo via New Tokaido Line (Shinkansen) and Meitetsu Line.
The nearest large city is Nagoya, about 40 km west of Okazaki

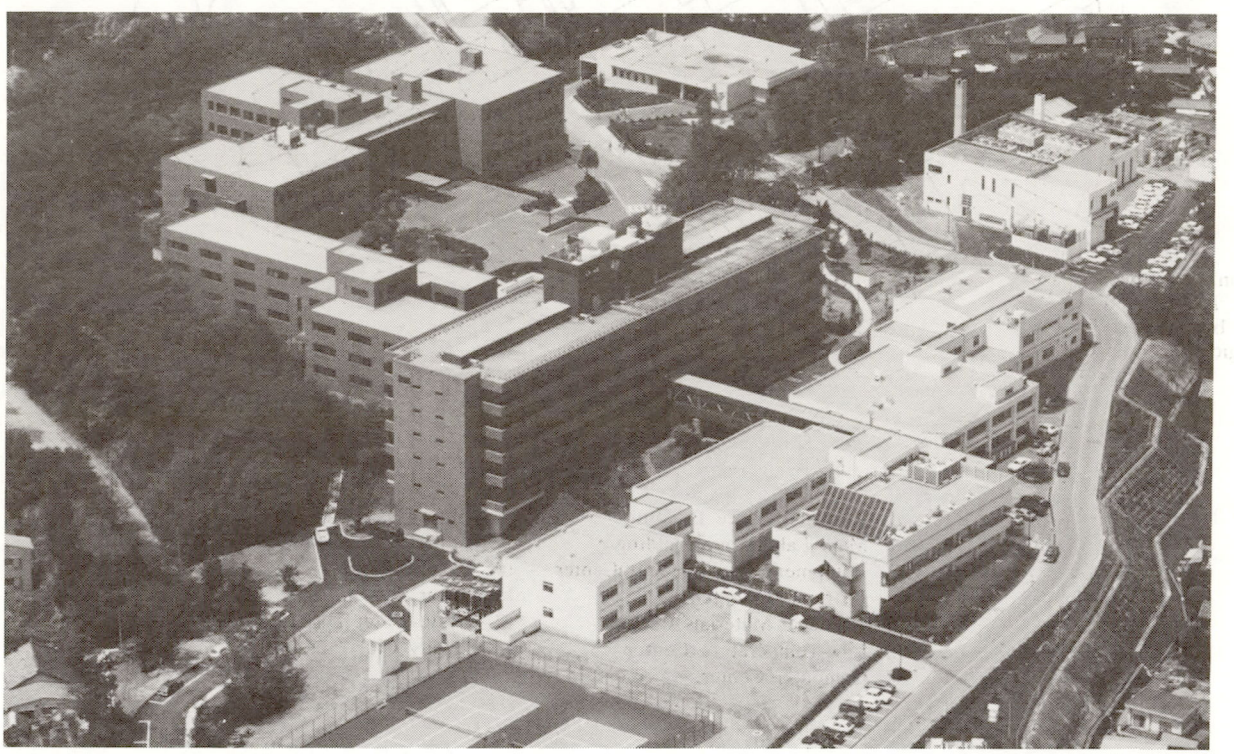

RESEARCH ACTIVITIES I
Department of Theoretical Studies

I–A Potential Energy Surfaces and Dynamics of Chemical Reactions

The study of the potential energy surfaces for chemical reactions has been one of the most important lines of research of the Morokuma group since its start at IMS in the spring of 1977. Dr. Satoshi Yabushita has joined in the project in October, 1986 after postdoctoral work with Profs. M.S. Gordon, C.W. McCurdy and I. Shavitt. We hope to continue to be active in the field, covering a wide range of topics of hot interest that range from the ground to highly excited states, from small triatomic to large organic systems, and from dynamical to static and rather qualitative aspects.

I-A-1 Ab Initio Potential Energy Surfaces and Dynamics of the Na(3S and 3P) + HCl → NaCl + H reactions

Koichi YAMASHITA and Keiji MOROKUMA

The potential energy surfaces of the reactive scattering process between the Na(3S and 3P) atom with the HCl molecule are investigated by ab initio configuration interaction (CI) calculations. The MRSD-CI method is applied using the DZP valence basis set with the Na and Cl effective core potentials as well as the basis sets, [12s7p/8s6p] for Na, [10s7pld/6s6pld] for Cl, and [6s2p/5s2p] for H, by Roos-Siegbahn. A bent-form transition state is found with a late barrier of 10.7 kcal/mol on the ground state. Dependences of reaction probability on vibrational, rotational and translational excitations in the ground state reagents are investigated using classical trajectory calculations on the potential surface fitted to the Murrell-Sorbie type function. The mechanism of the Na atom quenching and the effect of electronic excitation on the dynamics are explained based on the non-adiabatic behavior such as the avoided crossing seam and the coupling between the ground and excited states. The results are discussed in connection with the recent experiments.[1),2)]

References

1) F.E. Bartoszek, B.A. Blackwell, J.C. Polanyi, and J.J. Sloan, *J. Chem. Phys.* **74**, 3400 (1981).
2) M.F. Vernon, H. Schmidt, P.S. Weiss, M.H. Covinsky, and Y.T. Lee, *J. Chem. Phys.* **84**, 5580 (1986).

I-A-2 Theoretical Study on Mode-Selective Chemical Reactions in Cryogenic Matrices

Koichi YAMASHITA and Keiji MOROKUMA

Classical trajectory calculations are performed for the isomerization reaction, HCN ↔ HNC, in the cryogenic Ar matrix. Our theoretical model consists of the twelve first shell and the 42 second shell Ar atoms which surround a central HCN (HNC) molecule. The potential surface of isomerization is described by the Murrell-Sorbie function and the interactions between HCN and Ar and between the Ar atoms are represented by the Lennard-Jones potentials. We discuss the mode-selectivity of the process based on non-RRKM behaviors of lifetime distributions obtained by selective excitations of the CH and NH overtone modes.

I-A-3 Potential Energy Surfaces and Fragment Rotational Excitation of CH_3I and ICN Photodissociation Reaction

Satoshi YABUSHITA and Keiji MOROKUMA

Ab initio CI calculations are performed to investigate the possible mechanism of the fragment rotation in the photodissociation of CH_3I and ICN molecules in the lowest absorption bands. Using the relativistic effective core potential for the I atom, it is found that the lowest excited state of CH_3I is ^3E ($n\rightarrow\sigma^*$), as Mulliken predicted, and that of ICN is $^3\Pi$ ($\pi\rightarrow\sigma^*$), in conflict with McGlynn et al., whose assignment was

$^1\Sigma^-(\pi\rightarrow\pi^*)$. Following the simple spin-orbit CI calculations, we have obtained the excitation energies, which are in reasonable agreement with the experimental peak positions. The potential surface scan of the CH_3I system indicates that the rotational excitation can be induced in the small region of the potential surface, where the $^3Q_0$ and $^1Q_1$ states cross (conical intersection). In the case of ICN, the CN fragment can obtain the large torque to rotate in the wider region, because both the $^3\Pi$ and $^1\Pi$ states are unstable with respect to the bending motion. The recently obserbed large rotational excitation of the CN fragment is therefore qualitatively explained with the potential surface profiles.

I-A-4 The Mechanism of Gas Phase Nucleophilic Substitution Reactions of Carbonyl Containing Molecules

Satoshi YABUSHITA and Keiji MOROKUMA

Nucleophilic substitution reactions of carbonyl groups in solution have long been believed to proceed via "tetrahedral intermediates". It is only recent that the possible role of the tetrahedral adducts as the "transition states" in gas phase is realized. In order to understand the nature of the tetrahedral adducts, we have carried out ab initio calculations for the following three reactions;

(a): Cl^-+CH_3ClCO (1) $\rightarrow$ $Cl^-..CH_3ClCO$ (2) $\rightarrow$ $CH_3Cl_2CO^-$ (3, TS)

(b): $Cl^-+HClCO$ (1) $\rightarrow$ $Cl^-..HClCO$ (2) $\rightarrow$ HCl_2CO^- (3, TS)

(c): F^-+HFCO (1) $\rightarrow$ $F^-..HFCO$ (2) $\rightarrow$ HF_2CO^- (3, IM).

In the above reactions (a) or (b), the adduct (3) was found to be the transition state (TS), however in the reaction (c), it turned out the intermediate (IM). The energetics of the reactant complexes (2) and those of the adducts (3) relative to the reactants (1) are: for a-2..−10.7, a-3..13.3, b-2..−18.0, b-3..8.6, c-2..−29.7, c-3..−32.1 (all in kcal/mol calculated with MP2/6-31G* Ap for (a) and with MP4/6−31+G* for (b) and(c)). C-2 to c-3 are separated by a transition state whose relative energy to c-1 was −18.1 kcal/mol. What is surprising is that the transition states of reactions (a) and (b) have the planar structure, where RCO^+ with a CO triple bond interacts rather weakly with two chlorides.

I-A-5 Theoretical Studies on the Acetylene-Vinylidene Rearrangement with a Metal Atom (Li, Be, B, Mg, and Al)

Shogo SAKAI and Keiji MOROKUMA

[*J. Phys. Chem.* **91**, 3661 (1987)]

Reaction mechanisms of 1,2-hydrogen migration of neutral and anionic acetylene to form corresponding vinylidenes are investigated with the ab initio Hartree-Fock method, the second- and third-order Møller-Plesset perturbation theory, and the localized molecular orbital (LMO) analysis. The LMO analysis shows that in the neutral system the migrating hydrogen bahaves like a hydride (H^-) along the reaction path, while in the anion system it moves as a hydrogen atom. Reaction mechanisms of 1,2-hydrogen migration of neutral acetylene in the presence of a metal atom (Li, Be, B, Na, Mg, and Al) are also studied. The metal-catalyzed acetylene-vinylidene rearrangement can be classified based on the above two mechanisms of the metal-free reaction. In the presence of Li and Na atoms, the reaction mechanism is essentially that of the neutral acetylene, whereas with B, Be(^{3}P), Mg(^{3}P), and Al atoms, the reaction is similar to that of the acetylene anion. This difference has been related to the fact that in the latter atoms an odd electron is in a p orbital, whereas in the former no odd electron exists in a p orbital.

I-A-6 A Theoretical Study of Thermal Reactions of Bicyclo [2.1.0] pent-2-ene

Per N. SKANCKE *(Univ. of Tromsö, Norway and IMS)*, **Koichi YAMASHITA, and Keiji MOROKUMA**

[*J. Am. Chem. Soc.* **109**, 4157 (1987)]

Ab initio molecular orbital calculations, using 3-21G, 6-31G, and 6-31G* basis sets and including electron correlation through CASSCF and Møller-Plesset calculations up to fourth order, have been applied in a study of the thermal walk rearrangement in

bicyclo [2.1.0] pent-2-ene. On the basis of our calculations and estimates, we conclude that this process occurs with inversion at the migrating center and that it probably is a two-step reaction. The activation energy for this symmetry-allowed walk rearrangement is found to be around 10 kcal/mol higher than that for the symmetry-forbidden disrotatory electrocyclic ring opening leading to cyclopentadienen. Estimates have been made of the influence that an electron-withdrawing substituent on the migrating carbon, the $-C\equiv N$ group, has on the activation energies. It is found that the substitution favors the walk reaction energetically relative to the ring opening, in accordance with experimental findings.

I-A-7 Origin of Exo Selectivity in Norbornene, An Ab Initio MO Study

Nobuaki KOGA, Tadahiro OZAWA *(Kao Corp. and IMS)*, **and Keiji MOROKUMA**

[*J. Am. Chem. Soc.*, in press]

The study of the exo selectivity of norbornene has been continued. Models were constructed to evaluate energetic contributions of various proposed factors. Endo deformability, a major portion of the norbornene deformation energy, is singled out as the origin of exo selectivity; norbornene, with the olefinic hydrogens already bent toward endo in the equilibrium geometry, requires less deformation to reach the exo transition state than to the endo transition state. A further analysis has been carried out to elucidate the reason why olefinic hydrogens are bent in norbornene. A similar detailed analysis of the difference in the activation energy between norbornene exo and bicyclo [2.1.1]hex-2-ene indicates that this difference is also dictated by the endo deformability. Bicyclohexene, which has a planar olefinic group, requires more bending energy than the already bent norbornene exo to reach the transition state.

I–B Theoretical Studies of Molecular Structure and Spectroscopy

As in previous years, rearch activities in this field are mostly collaborative work with theoreticians from other universities or with experimentalists. For instance, we have become involved in the theoretical calculation of vibrational circular dichroism with an active experimetal group and hope to have some results in the near future.

I-B-1 On the Binding Energy of Ground State of Be_2

Inge RÖEGGEN *(Univ. of Tromsö, Norway and IMS)*, **Keiji MOROKUMA, and Koichi YAMASHITA**

[*Chem. Phys. Lett.* **140**, 349 (1987)]

The binding energy of the beryllium dimer in the ground state is calculated by an extended geminal model. Compared with a full CI calculation for the valence electrons, adding core-valence intersystem correlation reduces the binding energy of approximately 0.28 kcal/mol, while core-valence intrasystem correlation reduces the binding energy with approximately 0.04 kcal/mol. With a basis set of (8s, 5p, 2d, 1f) contracted GTO's on each atom, the extended geminal model yields a binding energy of 2.10 kcal/mol and an equilibrium bond length of 4.73 a.u.

I-B-2 Theoretical Assignments of the Vibrational Structure of the FHF^- and FDF^- Ions Based on Configuration Interaction and 3D-Vibrational Calculations

Koichi YAMASHITA and Keiji MOROKUMA

Our previous 2-dimensional variational calculations on the vibrational structures of the FHF^- and FDF^- ions using ab initio potential energy surfaces are extended to 3-dimensional ones. The SCF, SDCI and CASSCF-MRSDCI methods with higher excitation corrections (SDQCI and CASSCF-MRSDQCI) are

applied using the DZP basis set augmented with an anion p function on the F atom. The potential energies are calculated as a function of the symmetric stretching, bending, and anti-symmetric stretching normal coordinates to fit to a polynomial of those. It is concluded based on the theoretical calculations that the ν_3 band originally assigned by Kawaguchi and Hirota[1] corresponds to the $\nu_1 + \nu_3$ combination band. The theoretical predictions of frequencies and assignments of lower lying vibrations including the ν_3 mode are in good agreement with those re-assigned by Kawaguchi and Hirota based on their recent observations of new bands.

Reference

1) K. Kawaguchi and E. Hirota, *J. Chem. Phys.*, **84**, 2953 (1986).

I-B-3 Ab Initio Derivative Calculation of Vibrational Circular Dichroism

Keiji MOROKUMA and Hiromu SUGETA *(Osaka Univ.)*

[*Chem. Phys. Lett.* **134**, 23 (1987)]

The recent formalism of Stephens for the calculation of rotational strength in vibrational circular dichroism has been implemented, exploiting the analytical derivative technique for ab initio Hartree-Fock wavefunctions.

I-B-4 Study of Correlation Effects on Stretching Force Constants of the H_3N ... LiF Lithium-Bonded and H_3N ... HF Hydrogen-Bonded Complexes

Zdzistaw LATAJKA *(Univ. of Wrołcaw, Poland)*, **Henryk RATAJCZAK** *(Univ. of Wrłocaw, Poland)*, **Keiji MOROKUMA, and W.J. ORVILLE-THOMAS** *(Univ. of Salford, UK)*

[*J. Mol. Str.* **146**, 263 (1986)]

All quadratic, cubic and quartic force constants associated with high and low vibrational modes of the H_3N ... HF hydrogen-bonded and H_3N ... LiF lithium-bonded complexes have been calculated employing the Møller-Plesset perturbation theory to the second order (MP2) with the 4-31G** basis set.

I-B-5 An Ab Initio MO Study of the Hydrogen Bond Complex between Cyclopropane and Hydrogen Fluoride

Xiao-yuan FU *(Beijing Normal Univ.)*, **Ruo-zhuang LIU** *(Beijing Normal Univ.)*, **and Keiji MOROKUMA**

[*J. Mol. Sci. (Wuhan, China)* **5**, 21 (1987)]

The geometry of the complex between cyclopropane and hydrogen fluoride has been optimized with the ab initio MO energy gradient technique at the HF/3-21G and the HF/4-31G* level. The complex has a C_{2v} symmetry, with the HF molecule perpendicular to one edge of the 3-membered ring and in the same plane with the ring. The calculated hydrogen bond energy is about 70% that of the ethylene-hydrogen fluoride complex. The C_{3v} structure of the complex where HF approaches the molecular plane perpendicularly is only slightly attractive and is not an alternative equilibrium geometry. Cyclopropane behaves like an unsaturated hydrocarbon with its π electrons in the molecular plane.

I–C Structure and Reaction of Transition Metal Complexes

This year we have been able to publish a peper (ref. 1 of I-C-1 below) where the potential energy profile of the full cycle of a homogeneous catalytic system has been calculated theoretically for the first time. While completing a full account of the work, we have extended our study to another catalytic cycle, hydroformylation by a rhodium complex, and have completed a study of very complicated potential surfaces of two important steps: the rearrangement via pseudorotation and the olefin insertion. We also have been able to determine for the first time the transition state of a reaction of a binuclear transition metal complex.

I-C-1 Ab Initio MO Study of the Full Catalytic Cycle of Olefin Hydrogenation by the Wilkinson Catalyst $RhCl(PR_3)_2$

Chantal DANIEL, Nobuaki KOGA, Jin HAN*, Xiao-Yuan FU* *(*Beijing Normal Univ. and IMS)*, **and Keiji MOROKUMA**

In our previous study,[1] we have calculated the potential energy profile of the model catalytic cycle of the olefin hydrogenation by the Wilkinson catalyst with the ab initio MO method, in which PH_3 and ethylen have been used as PR_3 and olefin, respectively. The overall potential energy profile thus obtained is smooth without excessive barriers and without too stable intermediates, and the rate-determining step is olefin insertion combined with the first portion of isomerization. As an extension, we have compared the potential energy profiles of some elementary reactions with those of other transition metal complexes to discuss factors controlling the potential features. For instance, the Pt analogue is not a good catalyst because the β-hydrogen elimination takes place easily and the C_2H_6 reductive elimination has a high barrier. A large cis chloride effect as well as the trans hydride effect plays an important role in determining the potential surface.

Reference

1) N. Koga, C. Daniel, J. Han, X.Y. Fu, and K. Morokuma, *J. Am. Chem. Soc.* **109**, 3455 (1987).

I-C-2 Rearrangement through Berry Pseudorotation and Olefin Insertion of d^8 Five-Coordinate $Rh(H)(C_2H_4)(CO)_2(PH_3)$. An Ab Initio MO Study

Nobuaki KOGA, Su Qian JIN, and Keiji MOROKUMA

[*J. Am. Chem. Soc.*, in press]

The potential energy surface for intramolecular rearrangement and olefin insertion of $Rh(H)(C_2H_4)(CO)_2(PH_3)$, **1**, has been studied by means of ab initio MO method. All the equilibrium structures of **1** are 'trigonal bipyramidal'. The relative stability of such 'trigonal bipyramidal' structures has shown the site preference of axial H and equatorial ethylene. The 'square pyramidal' structures are transition states for intramolecular rearrangement between trigonal bipyramidal equiribrium structures through the Berry pseudorotation, with a very small intrinsic activation barrier. The potential energy surface for olefin coordination to $Rh(H)(CO)_2(PH_3)$ to give **1** has been investigated as well. The transition states for olefin insertion are early and 'square pyramidal' with basal ethylene and basal hydride, in which Rh-H is parallel to the C=C bond. The most important origin of the activation barrier (20-21 kcal/mol at the RHF level) has been ascribed to the skeletal deformation from a 'trigonal bipyramid' to a 'square pyramid'.

I-C-3 CC Coupling between CH_3 and μ-CH_2 in Rh Dinuclear Complex. A Theoretical Study

Nobuaki KOGA and Keiji MOROKUMA

The experimentally studied CC couplig between CH_3 and μ-CH_2 in the Rh dinuclear complex, $\{Cp^*RhCH_3\}_2(\mu\text{-}CH_2)_2$, **1**, has been studied with an ab initio MO method. We have optimized the structure of the model complex, $\{CpRhCH_3\}_2(\mu\text{-}CH_2)_2$, **2**, using energy gradient method with the small basis set (STO-2G) for all the ligands and relativistic effective core potential and double-zeta basis functions for Rh. The structure thus determined is in good agreement with the X-ray structure of **1**. We have also determined the structures of the model reactant, $\{CpRh\}_2(CH_3)(H)(\mu\text{-}CH_2)_2$, the correspondiing product, $\{CpRh\}_2(C_2H_5)(H)(\mu\text{-}CH_2)$, and the transition state connecting them at the same level. The transition state structure of the CC coupling is three-centered and similar to that of the reductive elimination of mononuclear complex, $CpRh(CH_3)_2(PH_3)$, the CC coupling being a reductive elimination. The activation energy of the CC coupling is calculated with the 6-31G* basis set for methyl, methylene and hydride to be 22 kcal/mol with the exothermicity of 8 kcal/mol. The CC coupling of the dinuclear complex is a easier process than the reductive elimination of the mononuclear complex which takes place with a calculated barrier height of 63 kcal/mol and an endothermicity of 15 kcal/mol. The ease of the CC coupling is ascribed to the release of a ring strain during the reaction.

I–D Photochemical Reaction in Gas and Liquid Phases

To understand the chemical reactions in gas and liquid phases, we need to know not only the electronic and dynamic properties of reacting molecules, but also the nature of reactant and solvent molecular interactions such as solvation mechanism. We have made the following three studies for this purpose; (i) potential energy surfaces, nonadiabatic couplings among the excited and ground states of polyenes and the dynamics on these surfaces, (ii) the energy dissipation mechanism of the excited molecules in liquid phases and (iii) the structure and dynamics of the solvent and solute molecules.

I-D-1 Large Local Energy Fluctuations in Water

Hideki TANAKA and Iwao OHMINE

[*J. Chem. Phys.* **87**, 6128 (1987)]

A detailed analysis is made for the dynamical behavior of individual water molecule in liquid water, by using a classical molecular dynamics (MD) calculation. It is found that there exist very large potential energy fluctuations in water; a single water molecule can exhibit a fluctuation of the order of 10~20 kcal/mole. These potential energy fluctuations can be classified into two categories; the fast component (10^{-14}~10^{-13} sec) associated with librational motions of water molecules and the slow component (10^{-12}~10^{-11} sec) associated with water binding structure changes. Both amplitudes can be reached up to 10 kcal/mole. Due to strong coulomb (dipole-dipole) interaction, small mutual geometrical changes, caused by the libration motions, induce large fast potential energy fluctuatoins. Due to large cohesion energy of hydrogen bond and the nature of water binding structure, there exist many water pair interactions which are non attractive or even repulsive; the water molecule potential (binding) energy distribution is inhomogeneous in space. This inhomogeneity alters as the water structure changes. Each water molecule then makes a transition from stable binding to unstable one with surrounding molecules and vice verse, inducing large potential energy changes in the picosecond order. A detailed analysis is made how the hydrogen bonding pattern changes with water molecular motions.

I-D-2 Integral Equation and Monte Carlo Study on Hydrophobic Effects: Size Dependence of Apolar Solutes on Solute-Solute Interactions and Structures of Water

Hideki TANAKA

[*J. Chem. Phys.* **86**, 1512 (1987)]

Hydrophobic effects for various solute sizes was continued to be investigated by the RISM equation and Monte Carlo simulation. The association of solute molecules is enhanced by the hydrogen bonds among water molecules and it's degree depends on the solute size. For a large apolar solute, the structure of water is enhanced, resulting in the exothermic hydration and the negative entropy change in hydration. For a solute comparable with the water size, the hydrogen bonds among water molecules are strengthened but the net hydrogen bonds number does not increase. The analysis of the geometric patterns formed by the hydrogen bond network supports these results. It is shown that the ordered structure of water in the solution of the large solutes gives rise to the large enthalpy of the hydration, and thus they are more soluble in water than the smaller solutes.

I-D-3 Water Local Structure and Dynamics

Hideki TANAKA and Iwao OHMINE

Mechanism of large energy fluctuations in water, found in the previous work, has been analyzed in detail. A long time scale molecular dynamics calculation (~100 psec) was performed to find the probability of occurrence of large fluctuations; they occur once in 9~10 pseconds for each molecule, and they are almost always associated with single large molecular orienta-

tional motions. The latters induce a large reordering of water cluster structure in liquid water.

A model demonstrates the strongly coupled motions with the flustrated interactions are essential for the existence of such fluctuations. There exist, indeed, many flustrated interactions in water, due to the large entropy increases upon the melting from ice to liquid water. Molecular Dynamics calculations for the subsets of a whole system are performed to show that more than few water molecular motions embedded in the other water molecular forces are needed to yield large fluctuations. Further analyses are in progress.

I–E Theoretical Studies of Chemical Reaction Dynamics

Fruitful collaborative works with IMS visiting Professor Michael Baer have been done for quantum mechanical studies of the following reaction systems: He + H_2^+ and $(Ar + H_2)^+$. Approximate hyperspherical coordinate approaches (sudden and adiabatic approximations with respect to rotational motion) are now ready to be applied to practical reaction systems.

I-E-1 Quantum Mechanical Studies of Ion-Molecule Reactions: The He + H_2^+ and the $(Ar + H_2)^+$ Systems

Michael BAER *(Soreq Nuclear Research Center and IMS)* **and Hiroki NAKAMURA**

[*J. Phys. Chem.* **91**, 5503 (1987)]

A quantum mechanical study within the reactive infinite-order sudden approximation for the two prototype ion molecule reactions He + H_2^+ and $(Ar + H_2)^+$ was carried out. He + H_2^+ was studied in the energy range $1.3 \leq E_t \leq 1.8$eV and the two most characteristic features for this system in the above-mentioned energy range, namely the existence of the vibrational propensity rule and the spectator stripping mechanism for exchange, were fully reproduced. The study of $(Ar + H_2)^+$ was carried out for one energy value, $E_t = 0.6$eV. All four possible channels for chemical reactions and charge-transfer processes were treated simultaneously. Integral and differential cross sections were calculated. Qualitative agreement with experiment was found for both. The study of these two ion-molecule reactions revealed the existence of a steric factor which is not associated with the potential but with the kinematics of the exchange process.

I-E-2 A Three Dimensional, Quantum Mechanical Study of Exchange and Charge Transfer Processes in the $(Ar + H_2)^+$ System

Michael BAER *(Soreq. Nuclear Research Center and IMS)* **and Hiroki NAKAMURA**

[*J. Chem. Phys.* **87**, 4651 (1987)]

A three-dimensional quantum mechanical study of the $(Ar + H_2)^+$ system was carried out within the reactive infinite order sudden approximation. All three arrangement channels for exchange and charge transfer were treated simultaneously. Steric factors, opacity functions, angular distributions and integral cross sections were calculated. Whenever possible, these were compared with both experimental and trajectory surface hopping (TSH) results. Whereas the fit with the TSH results was reasonable, the fit obtained with the experiement was less satisfactory. The reason for that can be attributed at least partially to the semiempirical DIM potential employed in the calculation.

I-E-3 Resonance in Collinear Chemical Reaction Caused by Barrier Penetration and Nonadiabatic Coupling

Hiroki NAKAMURA

[*Chem. Phys. Lett.* **141**, 77 (1987)]

A new type of resonance in the collinear Cl + HBr reaction system is analyzed semiclassically and is clarified to be caused by the combined effect of barrier penetration and the Rosen-Zener type nonadiabatic transition. Explicit expressions for the S-

matrix elements are derived in the semiclassical approximation. Semiclassical theory is shown to work quite well for the reaction.

I-E-4 Approximate Quantum Mechanical Treatment of Light Atom Transfer Reactions

Akihiko OHSAKI and Hiroki NAKAMURA

[*Chem. Phys. Lett.* **142**, 37 (1987)]

It is proposed to use the collinear-type hyperspherical coordinates to investigate three dimensional light atom transfer reactions within the framework of the adiabatic approximation with respect to rotational motion originally proposed by Bowman. In the cases of (1) symmetric light atom transfer and (2) near resonant asymmetric light atom transfer reactions, the explicit analytical expressions available for collinear reaction probabilities are suggested to be directly utilized to estimate the three-dimensional reaction cross sections and rate constants. It is also demonstrated that the Rosen-Zener formula is applicable to the collinear asymmetric light atom transfer reactions without introducing any diabatic representation of potentials.

I–F Semiclassical Theoretical Studies of Nonadiabatic Transitions

Nonadiabatic transition is one of the most important mechanism to induce various kinds of physical phenomena, or state-change. Development and application of good analytical semiclassical theories are the aims of our research.

I-F-1 Semiclassical Treatment of Nonadiabatic Transitions: Multilevel Curve Crossing and Nonadiabatic Tunneling Problems

Hiroki NAKAMURA

[*J. Chem. Phys.* **87**, 4031 (1987)]

Nonadiabatic transition in a multilevel curve crossing system and the one accompanying quantum mechanical tunneling are investigated theoretically and numerically for the one-dimensional case. The first problem is analyzed using the semiclassical formulation based on the sophisticated two-state theory for nonadiabatic transition. This formulation is applied to three- and four-level model systems and is found to work surprisingly well even when the avoided crossings (or the transition zones) can not be regarded to be well separated. The significance of the Stokes phase is noticed. As for the second problem, analysis is made not only for the simple tunneling but also for the elastic scattering accompanied by the nonadiabatic tunneling. A combination of the following two formulas is recommended for practical use: (1) the formula essentially based on the one proposed by Coveney et al., and (2) the formula of Ovchinnikova with additional Stokes phase and tunneling corrections.

I-F-2 Semiclassical Theory of Nonadiabatic Transitions

Hiroki NAKAMURA

[*XV-ICPEAC Invited Papers*, in press]

Present status of the semiclassical theory of nonadiabatic transitions is reviewed briefly. Emphasis is put on presenting the most sophisticated two-state formula and the way of unified treatment of various couplings. Also reported are the results of recent research on nonadiabatic tunneling, applicability of the basic two-state theory to multi-level curve crossing problem, and atom-diatom chemical reaction viewed as vibrationally nonadiabatic transition.

I–G Dynamic Processes of Electronically Highly Excited States of Simple Molecules

An ultimate purpose of these studies is to understand the mechanisms of various dynamic processes of higher-(super-) excited states of molecules. Studies are now in progress for the analysis of multi-photon auto-ionization of NO by using the multi-channel quantum defect theory. We have finished the work on ionization of Rydberg atoms in collisions with polar molecules.

I-G-1 Ionization of Rydberg Atoms in Thermal Collisions with Polar Molecules

Toshizo SHIRAI *(Japan Atomic Energy Research Institute)* **and Hiroki NAKAMURA**

[*Phys. Rev. A*, in press]

The title process with simultaneous rotational deexcitation of molecules was investigated theoretically by using the semiquantal approximation. The dipole-Born and dipole-Glauber differential cross sections were employed for the electron-molecule rotational deexcitation process. Numerical applications were made to the following systems: Xe + CO, HCl, HF, and LiF. A comparative study of the two approximations was carried out concerning the dependences of the cross sections on the following various quantities: n (principal quantum number), J (initial rotational quantum number), ΔJ (rotational quantum number change), (dipole moment), and V (relative collision velocity). As the molecular dipole moment becomes larger, there appears a prominent difference in the n-dependence of the cross section. The Glauber approximation brings about a decrease in the cross section and yields a saw-like n-dependence in contrast to a step-like n-dependence in the case of the Born approximation. In the collisions involving lowly excited Rydberg atoms, ionization with simultaneous dipole forbidden transition of a molecule becomes dominant compared to the ionization with simultaneous dipole allowed transition. The cross section was found to be inversely proportional to the relative collision velocity; thus the ionization rate becomes independent of temperature. A comparison was also made with the experiment for the ionization rate at 300K for Xe(27f) + HF and Xe(31f) + HCl.

I–H Unified Theory for CDW, Superconductivity and Superfluidity in Strongly Coupled Electron-Boson Systems

To clarify the nature of the phase transition of many-electron systems in solids, we study the CDW, SDW, superconducting and superfluid states, which are expected to appear through the mediation of quasi-bosonic excitations, such as phonons, plasmons, excitons and magnons.

I-H-1 Superconducting Transition Temperatures of Strongly Coupled Electron-Boson Systems — A Self-Consistent Method for Fluctuation from BCS Limit to Bipolaronic Limit —

Keiichiro NASU [*Phys. Rev. B.*, in press]

Superconducting transition temperatures T_C of a many-electron system coupling strongly with bosonic excitations are studied in the context of polaron theory. The boson clouds that move with electrons are taken into account within the variational method. The effect of fluctuation of the pairing order is also taken into account by the coherent potential approximation. The resultant theory covers the whole region of the three basic parameters characterizing this system: the intersite transfer energy of electron T, the site-diagonal electron-boson coupling energy S, and the energy of boson ω. T_C is found to become maximum in the transition region S~T, which lies between the weak

(BCS) region S≪T and the strong (bipolaronic) region S≫T. The width of this region is narrow in the adiabatic case ω≪T, while wide in the inverse-adiabatic case ω≫T. This region is characterized by the large ratio of the energy gap to k_BT_C. These results are applied to the Cu-O type new ceramics, and the breathing mode of oxygen is shown to be able to give a high-T_C of about 100K. The effects of other quasi-bosons, such as the plasmons and impurity vibrations of high frequencies are also studied, in connection with the room-temperature superconductivity.

I-H-2 Electron-Correlation and Bond-Alternation in One-Dimensional Many-Electron Systems

Chang-qin WU, Xin SUN *(Fudan University and IMS)* **and Keiichiro NASU**

[*Phys. Rev. Letters*, **59**, 831 (1987)]

A variational method is presented to clarify the effect of the inter-electron repulsion on the bond alternation in one-dimensional many-electron systems. This method has a very wide applicability, and can treat any repulsions irrespective of their strengths and force-ranges. The results disclose following new features about the role of the repulsion. The enhancement of the bond-alternation induced by the repulsion increases as the range of the repulsion extends. The bond-alternation is mainly caused by the repulsion itself when the electron-lattice coupling is weak, whereas it is suppressed by the repulsion when the electron-lattice coupling is strong. This second feature is verified in a wide region of the strength and force-range.

I-H-3 Ferromagnetism in a New Type of Organic Polymer Based on Benzene Rings Bridged by Carbons

A. MISHIMA *(Kanazawa Institute of Technology)* **and K. NASU**

[*Synthetic Metals*, **22**, 23 (1987)]

A new organic polymer with a three-dimensional network of carbons is proposed as a prototype of organic ferromagnet. It is composed of benzene rings bridged by carbon atoms. The ground and the excited states of π electrons of this polymer are studied within the Hubbard model combined with the mean-field theory, and it turns out that this polymer becomes a ferromagnet (ferrimagnet). The one-electron energy band and the spin density at each carbon atom as well as the magnon spectrum are calculated, in connection with the exotic ferromagnetism absent in the traditional one in transition metals.

I-I Theory for Resonant Raman, Hot Luminescence and Ordinary Luminescence with Nonradiative Processes

To study the dynamics of lattice relaxation of optical excitations in solids and molecules, we derive a systematic theory that can describe all components of the resonant secondary radiation, the resonant Raman scattering, the hot luminescence and the ordinary luminescence. We are especially interested to clarify the dynamics of self-localization of exciton in molecular solids.

I-1-1 Tunneling and Relaxation from Free State to Self-Localized State of Exciton — Nonadiabatic Multi-Step Theory —

Keiichiro NASU [*J. Luminescence*, in press]

A new theory for the rate of tunneling from the free(F) state to the self-localized (S) state of an exciton is worked out, so as to clarify the nonadiabatic effect of exciton-phonon coupling on this rate. The tunneling is assumed to occur through a multi-step process wherein the exciton passes successively a series of intermediately localized states between F and S states. In contrast to the adiabatic theory due to Lashba, the rate is found to be determined mainly by the nonadiabatic overlap between the F state and the top state of the potential barrier. The rate of the rapid relaxation after the tunneling is also determined in connection with the hot

luminescence from around the exit of the tunnel. These results are compared with recent experiments on pyrene in good agreement.

I-I-2 Hot Luminescence in F Center under One- and Two- Photon Excitations

S. MURAMATSU *(Utsunomiya Univ.)*, K. NASU and M. AIHARA *(Yamaguchi Univ.)*

[*J. Luminescence*, in press]

The spectra of hot luminescence from F center in KCl excited by one and two photons are theoretically investigated on the basis of a vibronic model. The depolarization spectra as well as the total emission intensity are calculated, and compared with experiments in good agreement. It is also shown that the non-Markov effect plays very important roles in the vibrational relaxation of this system, especially in the intensity of the hot-luminescence.

I–J Non-linear Excitations in Conducting Polymers and Other One-Dimensional Materials

In one-dimensional materials such as conducting polymers both electron-lattice and electron-electron interactions are important, and as a consequence, excited states in these materials are highly non-linear in character (solitons, breathers, etc.). We especially stress the importance of the electron-electron interaction, which is frequently overlooked. Our aim is to understand not only static but also dynamical properties of these non-linear excitations, including their creation, mutual conversion and destruction. To this end, we are trying to develop new theoretical methods, for treating those excitations.

I-J-1 Generation of Neutral Soliton Pair from the ^1A_g State in Conducting Polymers.

Masaki SASAI

In conjugated π-electron systems such as polyacetylene the electron-electron interaction is important and the lowest singlet excited state is not an electron-hole pair but a dipole-forbidden exciton state with neutral character (the ^1A_g state). Recently it is conjectured that in polyacetylene a neutral soliton pair may be created from this state via lattice relaxation. Our aim is to check this conjecture theoretically.

To study such an excited state with strong correlation we use the method of boson representation and transform the electronic degree of freedom into a quantum phase variable $\theta(x)$ ($\nabla\theta(x)$ has the meaning of spin density at x). By applying semiclassical approximation to this bose field $\theta(x)$ we can simulate the lattice relaxation process in the ^1A_g state. In this approximation the internal structure of ^1A_g state is represented by the so called "breather" (non-linear oscillation of $\theta(x)$ as shown in Figure 1(b)). At t=0 the center of mass of the excitation is in an extended state. If we follow the time evolution of this state (Figure 1), the center of mass gradually localizes and the lattice relaxes (a)-(c).

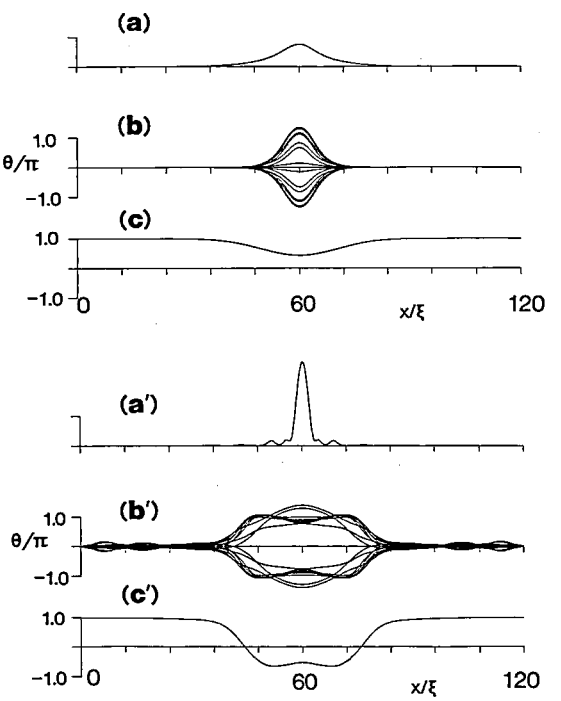

Figure 1. (a), (a') Probability distribution of the center of mass of the excitation, (b), (b') internal structure of the excitation and (c), (c') the amplitude of bond alternation as functions of x/ξ, where ξ is the coherence length (=2.6 lattice constant). (a)-(c) are at t=8.8 fsec and (a')-(c') at t=48.4 fsec.

The internal structure also changes gradually, and the neutral soliton pair is formed (a')-(c'). Thus our method provides a clear physical picture of a complex time dependent process in a strongly correlated system. This work was carried out in cooperation with Dr. Jun-ichi Takimoto.

I-J-2 Zwitterionic and Diradical Breathers in trans-Polyacetylene

Masaki SASAI and Hideo FUKUTOME *(Kyoto Univ.)*

[*Prog. Theor. Phys.*, in press]

Photoinduced absorption data of $(CH)_x$ suggest that some of the photogenerated solitons are confined to bound states.[1] A possible explanation is that solitons may be bound to form dynamical states called breathers, which are localized nonlinear oscillations of electrons and lattice. We study effects of the π electron Coulomb interaction on breathers utilizing the Pariser-Parr-Pople model. Charged solitons with opposite charges and neutral solitons with antiparallel spins, respectively, have attractive interactions and make breathers of two kinds, zwitterionic and diradical ones. We numerically simulate adiabatic lattice motion to demonstrate the breather oscillations. The zwitterionic and diradical breathers have different energies, spatial extents and oscillation periods but have similar oscillation patterns. They may explain the ionic and neutral excitations oberved in the photoinduced absorption spectra of trans-$(CH)_x$. The zwitterionic breather may also explain the self-pinning of photogenerated charged solitons.

Reference

1) J. Orenstein in "Handbook of Conducting Polymers" ed. by T.A. Skotheim (Marcel Dekker, New York, 1986).

I–K Electronic Structure of the Solids and Surfaces

The local density functional (LDF) method has supplied useful informations for the electronic structures of the many kinds of the solids and their surfaces. The electronic structures of the superconducting oxides with Cu ions and the heavy fermion materials with Ce are studied by the LDF methods mainly in this year.

I-K-1 The Mechanism of the Large Residual Resistivity in $CePd_3$

Akira YANASE and Akira HASEGAWA *(Niigata Univ.)*

[*Jpn. J. Appl. Phys.* **26** (1987) Suppl. 26-3 483]

To investigate an origin of the large residual resistivity in $CePd_3$, we calculate the energy band structure by a full-potential LAPW method and a local density approximation to the density functional theory. We suggest that small Fermi surfaces in the 4f bands may play an essential role in the electrical conduction. The observed sharp rise of the resistivity by the replacement of Pd with Ag or Cu may be due to the Anderson localization in the 4f bands.

I-K-2 Electronic Structure of Superconducting Oxide Effect in Non-Metalic Elements

Akira YANASE, Takahiro YAMASAKI *(Osaka Univ.)*, **Michihiko ONOZAI** *(Univ. of Osaka Pref.)*, **Kiyoyuki TERAKURA** *(Univ. of Tokyo)*, **and Key Taeck PARK** *(Univ. of Tokyo)*

[*Proc Yamada Conf. XVIII*, in press]

The self-consistent LAPW band calculations for $YCuO_3$, $YCuO_3H$ and $YCuO_2OH$ have been done using the local density approximation. When O atoms replaced by OH radicals, the hydrogen atoms act as a donors and the valence bands are filled with the electron introduced by the hydrogen addition.

I–L Theoretical Studies on Molecular Multiphoton Processes

I-L-1 Theory of Coherent Polarization Anisotropy in Time-resolved Two-photon Ionization of Isolated Molecules: Effects of Coriolis Couplings

Shinichiro SATO *(Tohoku Univ.)*, **Yasushi NOMURA** *(Tohoku Univ.)*, **and Yuichi FUJIMURA** *(Tohoku Univ., and IMS)*

[*J. Chem. Phys.* in press]

Effects of vibration-rotation couplings on the coherent polarization anisotropy in a time-resolved two-photon ionization of isolated molecules are theoretically studied. It is shown that oscillatory behaviors in the degree of polarization, which is characteristic of the coherent polarization anisotropy, should be observed as a result of the creation of the rovibronic coherence induced by the vibration-rotation coupling.

I-L-2 Mechanism of Time-Resolved Multiphoton Ionization of Molecules

Yasushi NOMURA *(Tohoku Univ.)*, **Yuichi FUJIMURA** *(Tohoku Univ. and IMS)*, **and Hirohiko KONO** *(Yamagata Univ.)*

An expression for the probability of time-resolved three-photon ionization via coherently excited resonant states of a molecular system is derived in the perturbative density matrix formalism with the aid of the Liouville space Feynman diagram. The three-photon ionization process consists of the simultaneous and sequential processes. The role of the direct and redistributed processes is discussed. The redistributed process is induced by the intramolecular processes in the resonant state. The theoretical treatment is applied to the (1 + 2) three-photon ionization of pyrazine observed by Knee et al.[1] It is demonstrated that the fast decay component (~110 ps) of the pyrazine spectra originates from the intramolecular dephasing of the

vibronic coherence created by the pumping laser.

Reference

1) J.L. Knee, F.E. Doany, and A.H. Zewail, *J. Chem. Phys.* **82**, 1042 (1985).

I-L-3 Theory of Time-Resolved Coherent Anti-Stokes Raman Scattering from a Molecular System

Michitoshi HAYASHI *(Tohoku Univ.)*, **Yasushi NOMURA** *(Tohoku Univ.)*, **and Yuichi FUJIMURA** *(Tohoku Univ., and IMS)*

Picosecond or femtosecond time-resolved coherent anti-Stokes Raman scattering (CARS) spectroscopy is a new powerful tool for directly measuring the transient behaviors of the coherently excited molecules strongly interacting with the heat bath. The purpose of this project is to theoretically study the dephasing effects on the ultla fast time-resolved CARS spectra of the molecular system. For this purpose we derive an expression for the intensity of the time-resolved CARS by using the density matrix method. We show that effects of the coherent transfer induced by the molecule-perturber interaction are reflected on the time-resolved CARS spectra in addition to the T_2 processes.

RESEARCH ACTIVITIES II
Department of Molecular Structure

II–A High Resolution Spectroscopy of Transient Molecules and Ions

During the course of chemical reactions many transient molecules and ions appear as intermediates. Because of their high reactivities, i.e. their short lifetimes, these transient species have remained to be explored and some of them have even escaped detection. Many of these molecules have open-shell electronic structure, which characterizes them as free radicals. Unpaired electrons in a molecule cause splittings in high resolution spectra of such species through fine and hyperfine interactions, and, when properly analyzed, these splittings provide us with information on the electronic properties of the molecule which is not obtainable for molecules without unpaired electrons. High resolution spectroscopy not only provides molecular constants of transient molecules at very high precision, but also allows us to unambiguously identify chemical species occuring in reaction systems and to unravel the details of reaction mechanisms, in particular, when it is combined with some time-resolved detection methods. The present project will also be of some significance in related fields such as astrophysics and environmental sciences, and even in semiconductor fabrication.

II-A-1 Diode Laser Spectroscopy of the ν_3 and ν_2 Bands of FHF^- in 1300 cm^{-1} Region

Kentarou KAWAGUCHI and Eizi HIROTA

The ν_3, ν_2 and $\nu_1+\nu_3 - \nu_1$ bands of a linear molecular anion FHF^- have been detected by diode laser spectroscopy in 1300 cm^{-1} region. The previously reported 1848 cm^{-1} band [K. Kawaguchi and E. Hirota, *J. Chem. Phys.*, **84**, 2953 (1986)] was re-assigned to the $\nu_1+\nu_3$ combination band. Analysis of the observed spectra gave the fundamental frequencies; ν_1 = 583.0539 (13), ν_2 = 1286.0284 (22), and ν_3 = 1331.1502 (7) cm^{-1} with three standard deviations in parentheses. From the obtained rotational constants the equilibrium F-F internuclear distance was calculated to be 2.27771 (7) Å.

II-A-2 The Vibrational Assignment for the $A^2\Pi$-$X^2\Sigma^+$ Band System of the SiN Radical: The 0-0 Bands of ^{29}SiN and ^{30}SiN

Chikashi YAMADA, Eizi HIROTA, Satoshi YAMAMOTO *(Nagoya Univ.)*, **and Shuji SAITO** *(Nagoya Univ. and IMS)*

The vibrational assignment for the A-X system of the SiN radical was reexamined by observing the spectra in the 5 μm region of ^{29}SiN and ^{30}SiN in natural abundance. The original assignment of Mulliken for the A state was found to be correct, rather than the one currently accepted, i.e. the 5 μm spectrum was assigned to the 0-0 band of the A-X system. The term value of the A state was thus modified to T_e (A) = 2032.4 (1) cm^{-1} and the equilibrium internuclear distance in the A state was recalculated to be 1.641 879 (20) Å, with the uncertainty in parentheses which was primarily due to that in Planck's constant. The vibrational and isotopic variations observed for the Λ-type doubling and the spin-orbit interaction contants of the A state and for the spin-rotation interaction constants in the X state were explained by treating the electronic matrix elements of the spin-orbit interaction and of the orbital angular momentum between the A/X, B/A, and D/X states as paramenters.

II-A-3 The Diode Laser Spectrum of the NO_3 Radical in 2500 cm^{-1} Region

Takashi ISHIWATA *(Tokyo Inst. Tech.)*, **Kentarou KAWAGUCHI, Ikuzo TANAKA** *(Tokyo Inst. Tech.)*, **and Eizi HIROTA**

In view of the complexities of the energy level

structure of the NO_3 radical,[1] the measurement has been extended to 2500 cm^{-1} region, where a combination band, i.e. the 1490 cm^{-1} band [1] plus the ν_1 mode, was expected to appear. We have observed two bands; one exhibited the structure very similar to that of the 1490 cm^{-1} band and was thus assigned to the combination band, in accordance with the expectation. Its band origin was determined to be 2518.7094 cm^{-1}. The second one at 2580 cm^{-1} region showed much narrower spin splittings than the first one, and is thus very likely to be a purely vibrational band.

Reference

1) T. Ishiwata, I. Tanaka, K. Kawaguchi, and E. Hirota, *J. Chem. Phys.*, **82**, 2196 (1985).

II-A-4 The Submillimeter-Wave Spectrum of the Deuterated Vinoxy Radical, CD_2CDO

Yasuki ENDO and Eizi HIROTA

[*J. Mol. Spectrosc.*, in press]

The a-type R-branch transitions of N=17-16 up to 22-21 of the fully-deuterated vinoxy radical, CD_2CDO, were observed in the 320 to 370 GHz region. They showed splittings caused by spin-rotation interaction, indicating the vinoxy radical to be an open-shell molecule. Analysis of the observed spectrum yielded ground-state molecular constants including the rotational constants, which were then combined with those of CH_2CHO previously reported to determine the structural parameters of the skeleton: r(C-C) = 1.408Å, r(C-O) = 1.261Å, and θ(C-C-O) = 122.4°.

II-A-5 Laser Magnetic Resonance of NH_2 in $\tilde{A}^2A_1$ and Highly Excited Vibrational States of $\tilde{X}^2B_1$

Kentarou KAWAGUCHI, Tetsuo SUZUKI, Shuji SAITO, and Eizi HIROTA

[*J. Opt. Soc. Am.*, **B4**, 1203 (1987)]

The CO_2/N_2O laser magnetic resonance spectra of NH_2 of the $\tilde{A}^2A_1$ (0,12,0)-(0,11,0) band and also of transitions between the $\tilde{A}^2A_1$ (0,11,0) state and highly excited vibrational states ("u") of $\tilde{X}^2B_1$ were observed at sub-Doppler resolution, by using an infrared-optical double resonance technique. The observed lines were analyzed to determine the Zeeman parameters and hyperfine coupling constants of the states involved and also to make rotational assignments for the "u" levels. The observed hyperfine structure gave support for identifying the "u" level to be associated with the $\tilde{X}$ state.

II-A-6 Infrared Diode Laser and Microwave Spectra and Molecular Structure of an Unstable Molecule, FBO

Yoshiyuki KAWASHIMA *(Ikutoku Tech. Univ.)*, **Kentarou KAWAGUCHI, Yasuki ENDO, and Eizi HIROTA**

[*J. Chem. Phys.*, **87**, 2006 (1987)]

The FBO molecule was generated by a dc discharge in a mixture of BF_3, O_2, and He and its vibration-rotation and rotation spectra were observed by using infrared diode laser spectroscopy and microwave spectroscopy, respectively. The ν_1 B-O stretching mode of $F^{11}BO$ and $F^{10}BO$ and the $\nu_1+\nu_2-\nu_2$ hot band of $F^{11}BO$ were observed in the region, 2050 to 2140 cm^{-1}. Subsequently, the pure rotational spectrum was observed for the following isotopic species: $F^{11}BO$, $F^{10}BO$, $F^{11}B^{18}O$, and $F^{10}B^{18}O$. The rotational, centrifugal distortion, and ℓ-type doubling constants were determined from the observed spectra, and the partial r_s structure of FBO was calculated from r_s coordinates and the first moment equation to be r(F-B) = 1.2833 (7) Å and r(B-O) = 1.2072 (7) Å.

II-A-7 Dye Laser Excitation Spectroscopy of Two New Bands of the DSO Radical in 6100 Å Region

Nobukimi OHASHI *(Kanazawa Univ.)*, **Shuji SAITO, Tetsuo SUZUKI, and Eizi HIROTA**

Two new bands of the DSO radical are studied by Doppler-limited dye laser excitation spectroscopy. The observed lines in both of the bands are assigned and analyzed to determine molecular constants for each of the excited states. The band origins of the two bands

are 16 281.5550 (2.5σ = 0.0014) cm^{-1} and 16 536.1666 (2.5σ = 0.0015) cm^{-1}. A force field analysis in the $\tilde{A}^2A'$ state is made by using available fundamental frequencies and inertia defects. This leads to a revision of the vibronic assignment for the band studied previously (N. Ohashi et al., *J. Mol. Spectrosc.*, **84**, 204-224 (1980)); this band observed at 16 413.8740 (20) cm^{-1} is reassigned to $\tilde{A}^2A'$ (012) ← $X^2\tilde{A}''$(000), whereas two new bands detected at 16 281.5550 (14) and 16 536.1666 (15) cm^{-1} are interpreted as $\tilde{A}^2A'(021) \leftarrow \tilde{X}^2A''(000)$ and $\tilde{A}^2A'(003) \leftarrow \tilde{X}^2A''(000)$, respectively. An additional support for the present assignment is obtained by calculating Franck-Condon factor.

II-A-8 The Microwave Spectrum of the PH_2 Radical

Masatoshi KAJITA, Yasuki ENDO, and Eizi HIROTA

[*J. Mol. Spectrosc.*, **124**, 66 (1987)]

Five more rotational transitions of the PH_2 radical in the ground state were observed in the sub mm-wave region. Sixty one fine and hyperfine components were measured for the five transitions.

An analysis of the observed spectra, combined with the microwave spectra reported in the previous paper, far-infrared and mid-infrared laser magnetic resonance spectra, and laser-induced fluorescence spectra obtained by other workers, improved the accuracy of most of the molecular constants given in the previous paper.

II-A-9 Diode Laser Spectroscopy of the ν_3 (CN Stretch) Band of $HCNH^+$

Masatoshi KAJITA, Kentarou KAWAGUCHI, and Eizi HIROTA

[*J. Mol. Spectrosc.*, in press]

The ν_3 band of the $HCNH^+$ ion has remained to be detected, while the other four fundamental bands or states have been investigated by infrared laser spectroscopy. In the present study the ν_3 band was detected by infrared diode laser spectroscopy combined with either magnetic field modulation or discharge current modulation. The $HCNH^+$ ion was generated by a hollow-cathode discharge either in a mixture of C_2H_3CN (10 mTorr) and H_2 (0.6 Torr) or in a mixture of HCN (100 mTorr) and H_2 (1 Torr), cooled to dry ice temperature. Five P branch and five R branch transitions were observed, yielding the band origin ν_0 = 2155.6975 (17) cm^{-1}, the rotational constant B_3 = 36 865.5 (10) MHz, and the centrifugal distortion constant D_3 = 0.0538 (50) MHz, with one standard deviation in parentheses. By combining the present B_3 constant with the rotational constatnts in other fundamental states already reported, the equilibrium rotational constant B_e was calculated to be 37 273.8 MHz.

II-A-10 Infrared Diode Laser Spectroscopic Study of the Active Nitrogen. The Electronic Transition between the Lowest Singlet Metastable States $a^1\Pi_g$-$a'^1\Sigma_u^-$, 0-0 Band

Chikashi YAMADA and Eizi HIROTA

[*J. Chem. Phys.*, in press]

The $a^1\Pi_g$-$a'^1\Sigma_u^-$, 0-0 band of the molecular nitrogen was observed in an electric discharge plasma of nitrogen using infrared diode laser spectroscopy at Doppler-limited resolution. Precise values were obtained for the rotational constants and the energy separation between the two electronic states. The effect of Λ-type doubling in the $a^1\Pi_g$ state was observed as small shifts of Q-branch and P/R branch transitions to higher and lower frequencies, respectively, than those expected if Λ-doubling were absent.

II-A-11 Microwave Spectroscopy of HCO^+ and DCO^+ in Excited Vibrational States

Eizi HIROTA and Yasuki ENDO

[*J. Mol. Spectrosc.*, in press]

The J=3-2, 4-3, and 5-4 transitions of DCO^+ and the J=3-2 and 4-3 transitions of HCO^+, both in the ν_2, $2\nu_2$, ν_1, and ν_3 states, were observed to derive the rotational, centrifugal distortion, and ℓ-type doubling constants. The Fermi resonance between the ν_1, and $4\nu_2^0$ states of DCO^+ was analyzed using the observed

molecular constants of the ν_1, ν_2, and $2\nu_2$ states. The effect of the discharge electric field was noticed on the ν_2 and $2\nu_2$ spectra.

II-A-12 Infrared Diode Laser and Microwave Spectroscopy of Molecular Ions

Eizi HIROTA

[*Phil. Trans. R. Soc.*, in press]

Some of the recent results on FHF^-, HBF^+, H_2Cl^+, H_3S^+, HCO^+, and DCO^+ are reviewed. The last two molecules are studied to detect the effect of the discharge electric field on ℓ-type doublets in the $\nu_2 = 1$ and $\nu_2 = 2$ states. The Fermi interaction between ν_1 and $4\nu_2^0$ in DCO^+ is also discussed. These experimental results are followed by introduction of a simple procedure which, based upon the Hellmann-Feynman theorem, allows us to estimate the electron distributions in ions in comparison with those in related neutrals. Three isoelectronic series (1) NH^-, OH, and FH^+, (2) HBF^+, HBO, HCO^+, HCN, HNN^+, HNC, and HOC^+, and (3) NH_2^-, OH_2, and FH_2^+ are discussed by this method.

II-A-13 The Millimeter- and Submillimeter-Wave Spectrum of the DCO Radical

Yasuki ENDO and Eizi HIROTA

[*J. Mol. Spectrosc.*, in press]

The pure rotational spectrum of the DCO radical was observed in the millimeter- and submillimeter-wave regions for both a-type and b-type transitions. Spin splittings were clearly resolved, whereas deuterium hyperfine splittings were partially resolved. Analysis of the observed spectrum yielded precise ground-state molecular constants of DCO: A = 441 714.02 (16), B = 38 417.03 (27), C = 35 116.48 (27), ε_{aa} = 7130.59 (40), ε_{bb} = 5.5 (17), ε_{cc} = −174.2 (16), $|\varepsilon_{ab} + \varepsilon_{ba}|/2$ = 74.7 (18), a_F = 58.413 (74), T_{aa} = 2.191 (93), T_{bb} = 0.16 (12), and χ_{aa} = 0.22 (21) in MHz with 2.5 standard deviations in parentheses.

II-A-14 Submillimeter-Wave Spectroscopy of $a^1\Delta$ SO in Excited Vibrational States Produced by 193 nm Photolysis of Cl_2SO

Yasuki ENDO, Hideto KANAMORI, and Eizi HIROTA

[*Chem. Phys. Lett.*, in press]

The pure rotational spectrum of the $a^1\Delta$ SO radical in the vibrational states of v up to 5 has been observed in the submillimeter-wave region of 300 to 400 GHz. The SO radical was produced by the excimer laser photolysis of Cl_2SO at 193 nm, and its absorption signal was detected by a transient digitizer followed by a desktop computer for signal processing. The present method was discussed as a means of studying short-lived molecules.

II-A-15 Detection of HBNH by Infrared Diode Laser Spectroscopy

Yoshiyuki KAWASHIMA *(Ikutoku Tech. Univ.)*, **Kentarou KAWAGUCHI, and Eizi HIROTA**

[*J. Chem. Phys.*, in press]

The infrared spectrum of a transient species HBNH was observed in the gas phase using a diode laser spectrometer. The HBNH molecule is formed in an ac discharge plasma of a diborane/ammonia or diborane/nitric oxide mixture. The ν_3 band origin and the rotational constants of $H^{11}BNH$ were determined to be ν_0 = 1786.193 08 (72), B_0 = 1.099 335 (81), and B_3 = 1.093 481 (72) cm^{-1}, with three standard deviations in parentheses. The ν_3 band of $H^{10}BNH$ was also observed and analyzed.

II-A-16 Diode Laser Spectroscopy for Monitoring the Yield of Metastable Cl from Photodissociation of Simple Molecules

Eberhard TIEMANN *(Univ. Hannover and IMS)*, **Hideto KANAMORI, and Eizi HIROTA**

Time resolved spectroscopy of the atomic fine structure transition of Cl, $^2P_{1/2}$-$^2P_{3/2}$ at 882.35 cm^{-1} is applied to derive relative yields of the metastable level $^2P_{1/2}$ of Cl(Cl*) from the photodissociation by excimer

laser radiation of KrF or ArF. Molecules such as HCl, CH_3Cl, CH_2Cl_2, phenyl chloride, and PCl_3 are studied, getting for the first time the possibility of systematic comparison of yields for Cl* and also of earlier results on heavier halogens obtained by other authors using different methods. Most yields determined in the present work are close to a value as calculated from the statistical weights of the two fine structure levels of Cl. This finding is related in a simple diabatic picture to the small spin-orbit interaction in Cl compared to that in iodine. Additionally some rate constants for the collisional quenching of the metastable Cl by the parent molecule are derived.

II-A-17 Infrared Diode Laser Kinetic Spectroscopy of SO in the $a^1\Delta$ State Generated by the Photolysis of Cl_2SO and SO_2 at 193 nm

Hideto KANAMORI, Eberhard TIEMANN *(Univ. Hannover and IMS)*, **and Eizi HIROTA**

Sulfur monoxide molecules generated by photolyzing Cl_2SO at 193 nm were shown to be distributed in the $a^1\Delta$ state as well as in the $X^3\Sigma^-$ state; the vibration-rotation spectrum of $a^1\Delta$ SO was observed for v up to 6-5 by infrared diode laser kinetic spectroscopy. Vibrational and rotational molecular parameters were precisely determined and were employed to calculate an RKR potential energy curve. The branching ratio of the two channels leading to $a^1\Delta$ and $X^3\Sigma^-$ SO was estimated to be 1:4 for the 193 nm photolysis of Cl_2SO, in contrast with the ratio less than 0.01 for the SO_2 photolysis.

II-A-18 Infrared Diode Laser Kinetic Spectroscopy of the CCH Radical Hot Bands

Hideto KANAMORI and Eizi HIROTA

We have previously shown [1] that the photolysis of pure acetylene at 193 nm yields hot CCH radicals and the ν_3 band of CCH can be observed only after CCH is vibrationally relaxed by an appropriate buffer gas such as H_2, D_2, and CH_4. This observation suggests that a number of absorption lines observed in 1700 to 1900 cm^{-1} region are assigned to hot band transitions of CCH. In fact, we have succeeded in observing two Π-Π bands. One of them was assigned to the $\nu_2 + \nu_3 - \nu_2$ band, because the lower- and upper-state constants agreed with those previously determined. [2,3] The other Π-Π band was assigned to either $7\nu_2$-ν_2 or $5\nu_2$-ν_2. Recently we found that many of the remaining absorption lines with intermediate lifetimes corresponded to transitions from the ν_3 state to two Π states at 3600 and 3693 cm^{-1} which Curl et al.[4] detected by color-center laser spectroscopy. Table I summarizes molecular parameters derived from the observed spectra.

References

1) H. Kanamori, K. Seki, and E. Hirota, *J. Chem. Phys.*, **87**, 73 (1987).
2) IMS Ann. Rev. 1986 II-A-21.
3) IMS Ann. Rev. 1987 II-A-19.
4) R. F. Curl, P. G. Carrick, and A. J. Merer, *J. Chem. Phys.*, **82**, 3479 (1985).

Table I. Molecular Constants of the CCH Radical in Excited Vibronic States (cm^{-1})[a]

Constant	$\Pi(01^10)$[b]	$\Pi(01^11)$	$\Pi(07^10)$ or (05^10)	Π(3600 cm^{-1})	Π(3693 cm^{-1})
B	1.451 288 9 (9)	1.434 313 (6)	1.450 764 (7)	1.405 30 (2)	1.411 660 (9)
$D \times 10^6$	3.80 (3)	7.27 (7)	−3.68 (4)	17.5 (2)	−5.63 (5)
$\gamma \times 10^3$	−1.545 (7)	−1.66 (3)	−0.45 (3)	−13.2 (1)	16.79 (5)
A	−0.346 5 (4)	−1.0175 (4)	−0.654 (1)	−7.242 (2)	−5.4033 (8)
$p \times 10^3$	0.15 (2)	0.18 (5)	0.05 (13)	−2.75 (5)	−2.3 (2)
$p_D \times 10^6$	[0.0][c]	0.9 (3)	0.2 (9)	16 (4)	−2.9 (9)
$q \times 10^2$	1.1359 (2)	1.6907 (9)	2.6140 (9)	−0.813 (3)	−0.946 (2)
$q_D \times 10^7$	0.5 (3)	−30 (2)	2.8 (6)	35 (3)	−14.1 (8)
T_{vib}	371.3228 (6)	2090.8402 (5)	2166.2327 (9)	3600.3636 (6)	3692.6088 (3)

a. Values in parentheses denote one standard deviation and apply to the last digits of the constants.
b. IMS Ann. Rev. 1987 II-A-19.
c. Fixed.

II-A-19 Microwave Spectroscopy of the CCH and CCD Radicals in Excited Bending States

Yasuki ENDO and Eizi HIROTA

The CCH radical in the $\tilde{X}^2\Sigma^+$ ground electronic state shows some anomalies in its spectra, which are probably caused by a low-lying electronic state $\tilde{A}^2\Pi$. For example, a Π-Π type hot band was observed and was assigned to $7\nu_2$-ν_2 or $5\nu_2$-ν_2, but this sort of a band is unlikely to be observed in most cases. In order to clarify the anomalous behaviors of the molecule, the microwave spectra of CCH and CCD in excited bending states were observed using a 1.2 m long discharge cell cooled to −100°C. A mixture of C_2H_2 or C_2D_2 (3 mTorr) and He (60~70 mTorr) was discharged with the current of about 200 mA to generate the radical. The N=2-1, 3-2, and 4-3 transitions were observed for CCH in the $\nu_2 = 1$ state, whereas the N = 3-2, 4-3, and 5-4 transitions were detected for CCD in the $\nu_2 = 1$, $\ell = 1$ and $\nu_2 = 2$, $\ell = 0$ states. The observed transitions were analyzed by a least-squares method using a Hamiltonian which included the spin-orbit interaction term. Table I summarizes molecular parameters thus determined. It is interesting to note that the changes of the rotational constants with ν_2 are quite anomalous: B_1-B_0 = −165.970 MHz for CCH and B_1-B_0 = +9.508, B_2−B_1 = +102.554 MHz for CCD. The spin-rotation interaction constant $|\gamma|$ and the hyperfine coupling constants b and c decrease considerably from the ground state to the ν_2 = 1 state.

Table I. Molecular Constants of CCH and CCD in Excited Bending States (in MHz)[a]

Constant	CCH $\nu_2 = 1$, $\ell = 1$	CCD $\nu_2 = 1$, $\ell = 1$	CCD $\nu_2 = 2$, $\ell = 0$
B	43 508.544 (67)	36 077.539 (182)	36 180.093 (52)
D	0.114 0 (24)	0.074 16 (43)	−0.048 72 (130)
q	340.531 (120)	298.961 (32)	
q_D	−0.0016 (22)	−0.002 21 (39)	
A	−10 386.4 (30)	−6 365.7 (22)	
γ	−46.31 (49)	−45.596 (195)	−38.09 (73)
γ_D			−0.013 1 (135)
p	4.34 (52)	6.697 (165)	
o_F	40.5 (90)		
c	8.1 (23)		

a. Valeues in parentheses denote 2.5 standard deviations and apply to the last digits of the constants.

II-A-20 Infrared Diode Laser Spectroscopy of the PS Radical

Kentarou KAWAGUCHI, Eizi HIROTA, Masatoshi OHISHI *(Nobeyama Radio Obs.)*, **Hiroko SUZUKI** *(Nobeyama Radio Obs.)*, **Shuro Takano** *(Univ. Tokyo)*, **Satoshi YAMAMOTO** *(Nagoya Univ.)*, **and Shuji SAITO** *(Nagoya Univ.)*

Attention has been paid to P-containing molecules in space, especially in stellar atmosphere, but so far only PN has been detected in space. Tsuji[1] predicted the PS radical to be abundant in stellar atmosphere where oxygen dominates carbon in abundance. In the present study the radical was detected by infrared diode laser spectroscopy. Before searching for PS lines, the PO spectrum was observed with a good S/N ratio by using $POCl_3$ of 30 mTorr diluted with 900 mTorr of He as a precursor. So the PS radical was produced from 50 mTorr of $PSCl_3$ in 1 to 1.5 Torr of He. At an initial stage Zeeman modulation was employed to observe lines in the $^2\Pi_{3/2}$ state. It was later replaced by discharge current modulation of 500 Hz to observe lines in $^2\Pi_{1/2}$ and high-J lines in $^2\Pi_{3/2}$. Some 19 lines were observed, which yielded the ground-state rotational constant of B = 0.296 709 (44) cm^{-1} with one standard deviation in parentheses. This result facilitated the microwave study to be carried out at Nagoya University.

Reference

1) T. Tsuji, *Astron. Astrophys.*, **23**, 411 (1973).

II-A-21 Microwave Spectroscopy of the $^{13}CH_3O$ Radical

Takamasa MOMOSE *(Kyoto Univ. and IMS)*, **Yasuki ENDO, Eizi HIROTA, and Tadamasa SHIDA** *(Kyoto Univ.)*

The pure rotational spectrum of the isotopically substituted methoxy radical $^{13}CH_3O$ was observed in the submillimeter-wave region. The $^{12}CH_3O$ radical was also studied in the submillimeter-wave region and the molecular parameters of the previous work were reexamined. It was found necessary to add a few terms for the centrifugal distortion. The hyperfine coupling constants of the carbon nucleus were determined for the first time. With reference to the rotational constant of CD_3O, the r_s structure of the methoxy radical was determined.

II-A-22 Time-Resolved Microwave Spectroscopic Study of the Oxidation Reaction of Acetylene

Yasuki ENDO and Eizi HIROTA

The following two channels have been proposed as possible initial steps for the oxidation reaction of acetylene:

$$\begin{aligned} HCCH + O &\rightarrow HCCO + H \quad (a) \\ &\rightarrow CH_2 + CO \quad (b) \end{aligned}$$

In order to determine the branching ratio, microwave kinetic spectroscopy[1] was applied to this system; oxygen atoms were generated by Hg-sensitized decomposition of N_2O and the microwave spectra of HCCO[2] and CO were monitored. Because the signals were weak, the source klystron was tone-burst modulated at 50 kHz. The time resolution was about 0.3 ms. The Hg-lamps were lighted for 4 ms. As shown in Figure 1, the HCCO signal appeared immediately after the Hg-lamps were switched on and were steadily increased while the lamps were lighted, whereas the CO signal showed a much slower rise. These qualitative observations indicate that channel (a) is a dominant route at the initial stage and CO is mainly produced by subsequent reactions. In fact, analysis of the time profiles of the signals assuming appropriate secondary reactions led to the rate constant for (a) to be 8.0×10^{-13} cm^3 molecule^{-1}s^{-1} and (b) to be slower than 3×10^{-13} cm^3 molecule^{-1}s^{-1}.

Reference

1) Y. Endo, H. Kanamori, and E. Hirota, *Laser Chem.*, **7**, 61 (1987).
2) Y. Endo and E. Hirota, *J. Chem. Phys.*, **86**, 4319 (1987).

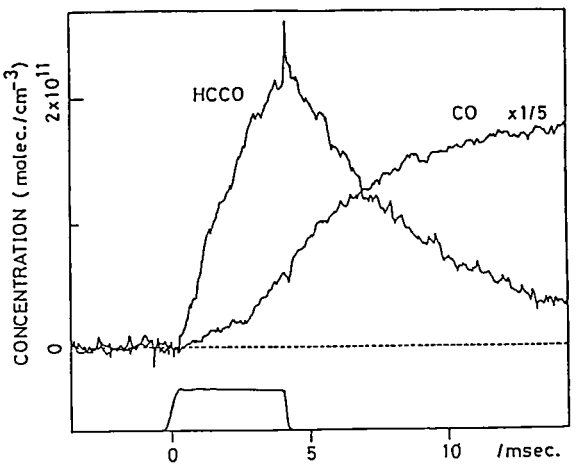

Figure 1. Time variations of the HCCO and CO concentrations.

II-A-23 Deuterium Isotope Effect on the Branching Ratio in $O(^3P)$ + Ethylene Reaction

Seiichiro KODA *(Univ. Tokyo)*, **Yasuki ENDO, Eizi HIROTA, and Soji TSUCHIYA** *(Univ. Tokyo)*

The branching ratio of the two channels of $O(^3P)$ + ethylene reaction, one yielding vinoxy+ atomic hydrogen (a) and the other, methyl + formyl (b), was determined for C_2H_4 and C_2D_4 by means of a microwave kinetic spectroscopic method. The ratio of (b)/(a) was found to be 6 ± 1.5 in the C_2D_4 reaction compared with 1.2 ± 0.2 in the C_2H_4 reaction. This fact could be interpreted by a reaction mechanism in which the unimolecular dissociation on the triplet surface [(a) channel] competes with the intersystem crossing to a singlet surface followed by 1,2-hydrogen migration and C-C cleavage [(b) channel].

II-A-24 Infrared Diode Laser Kinetic Spectroscopy of the CCD Radical ν_3 Band

Hideto NANAMORI and Eizi HIROTA

In order to obtain detailed information on an interesting free radical CCH, infrared kinetic spectroscopy has been applied to its deuterated species. Deuterated acetylene of about 0.8 Torr was diluted with hydrogen to the total pressure of 2.5 Torr, and was photolyzed at 193 nm. About one hundred of transient absorption lines with the lifetime shorter than 10 μs were observed in the region of 1690-1790 cm^{-1}. As in the case of CCH,[1] the spin splitting was of some help to assign the ν_3 band. Nineteen P and R branch transitions were thus observed, of which twelve were resolved into two spin-rotation components. A least-squares analysis yielded molecular constants as listed in Table I. The band origin agrees well with the matrix value,[2] 1746.3 cm^{-1}. As in the case of CCH, the spin-rotation interaction constant is changed by as much as 36 % upon ν_3 excitation.

References

1) H. Kanamori and E. Hirota, *J. Chem. Phys.*, **87**, 73 (1987).
2) M. E. Jacox and W. B. Olson, *J. Chem. Phys.*, **86**, 3134 (1987).

Table I. Molecular Constants of CCD in $\tilde{X}^2\Sigma^+$ $v_3 = 1$ $(cm^{-1})^a$

B	1.190 932 7 (29)
$D \times 10^6$	2.546 9 (65)
$\gamma \times 10^3$	−2.441 (15)
T_{vib}	1743.178 47 (23)

a. Values in parentheses denote one standard deviation and apply to the last digits of the constants. Ground-state parameters were fixed to the microwave result of M. Bogey, C. Demuynck, and J. L. Destombes, *Astron. Astrophys.*, **144**, L15 (1985).

II-B Development of New Instruments and New Experimental Methods for High Resolution Spectroscopy

The scope of a research is limited by the techniques and the capabilities of instruments available to a researcher. This is particularly true for spectroscopic investigations of simple molecules, free radicals, and ions, which are main research themes this Department is interested in. The high precision with which we determine molecular paramaters often unravels new features of molecular structure which have previously escaped experimental observation. The diversity of molecular systems which we can detect and analyze is often limited by the sensitivity of the spectrometer employed. It is thus imperative for us to steadily improve our research facilities and to develop equipments of radically new conceptual design. The rewards of these efforts will include not only the detailed knowledge of the molecules under investigation, but also contributions to related fields. Various technical problems need to be solved to attain these goals. In this respect the collaboration of the Equipment Development Center is indispensable. New instruments developed in this program promise to open new research area in the field of molecular science.

II-B-1 Direct Observation of Inversion in the $v = 5$ State of NH_3 by Millimeter Wave-Optical Double Resonance

Yukari MATSUO *(Univ. Tokyo)*, **Yasuki ENDO, Eizi HIROTA, and Tadao SHIMIZU** *(Univ. Tokyo)*

[*J. Chem. Phys.*, in press]

A powerful method for detailed studies of the static and dynamic properties of molecules in highly excited vibrational states is presented. NH_3 molecule is excited to the $v = 5$ state in the N-H stretching mode by a pulsed dye laser and a subsequent transient change in the millimeter wave absorption due to the inversion transition in the excited state is observed before the distribution returns to thermal equilibrium. The determined inversion transition frequencies are more accurate by 3 digits than those reported in the previous work.

II–C High Resolution Spectroscopy of Molecules of Fundamental Importance

The need for high quality spectroscopic data has recently been increasing, especially for molecules of fundamental importance. Perhaps such spectroscopic data have been accumulated in the past because of interest in precise molecular structure determination. However, research activities in other related fields such as reaction kinetics, environmental sciences, plasma chemistry and physics, astronomy, and semiconductor technology have recently been advanced such that precise spectroscopic data are indispensable as a means of monitoring molecules. Spectroscopic data which are available at present are not necessarily good enough and must often be replaced by new data that meet necessary requirements. Such spectroscopic data on chemically stable molecules of fundamental importance will be presented in this section.

II-C-1 The Microwave Spectrum of Cyclopropane-1,1-d_2. Molecular Structure of Cyclopropane

Yasuki ENDO, Man Chai CHANG *(Sun Cheon Natl. Univ. and IMS)*, **and Eizi HIROTA**

[*J. Mol. Spectrosc.*, in press]

The microwave spectrum of cyclopropane-1,1-d_2 has been observed in the frequency region from 320 to 400 GHz using a source-frequency modulation microwave spectrometer. Sixty four observed a-type R branch transitions were analyzed by the least-squares method to determine the rotational and centrifugal distortion constants to be A = 18 835.662 (18), B = 16 370.2703 (70), C = 11 409.2285 (67), Δ_J = 0.011 246 (12), Δ_{JK} = 0.005 087 (35), Δ_K = 0.007 06 (12), δ_J = 0.003 028 0 (79), and δ_K = 0.005 561 (27), in MHz with three standard errors in parentheses. The observed rotational constants of the 1,1-d_2 species and the B_0 and C_0 constants of C_3H_6 and the B_0 constant of C_3D_6 available in the literatures were corrected for harmonic terms to derive an average structure: r_z(C-H) = 1.0797 (34) Å, r_z(C-C) = 1.5157 (23) Å, θ_z(HCH) = 115.47 (38)°, and r_z(C-H)-r_z(C-D) = 0.000 29 (16) Å with standard deviation of the fit in parentheses. Using the vibration-rotation constants reported, the equilibrium structure was also estimated, where only two "diagonal" third-order anharmonic terms were taken into account.

II-C-2 Molecular Parameters of ν_2 Band of $^{15}N^{16}O_2$

Naoki TANAKA *(Univ. Tokyo)*, **Yoshiaki HAMADA** *(Univ. Tokyo)*, **Chikashi YAMADA, and Eizi HIROTA**

The high resolution infrared diode laser spectrum of $^{15}N^{16}O_2$ was observed in the region from 780 to 670 cm^{-1}, and was analyzed by combining the existing microwave spectrum. A set of molecular constants was derived which reproduces the vibration-rotation energies of the ν_2 state within the error of 0.0005 cm^{-1} in the range of K up to 5 and N up to 40.

II-C-3 The Microwave Spectra of Deuterated Cyclobutanes

Eizi HIROTA, Yasuki ENDO, and James S. CHICKOS *(Univ. Missouri-St. Louis)*

A number of infrared and Raman spectroscopic studies have been carried out on cyclobutane and cyclobutane-d_8 to explore the puckering motion in the molecule. Recently Egawa et al.[1] reported an electron diffraction study combined with Fourier-transform infrared spectroscopy of the normal species. The present study aimed at supplying further detailed information on the molecular structure of cyclobutane through observation of the microwave spectra of deuterated species.

Two 1,2-d_2 species, trans and cis, were investigated. As shown in Figure 1, the trans form exists in either an axial-axial (ax-ax) or an equatorial-equatorial (eq-eq) configuration, converted each other by puckering, whereas the cis form consists of two equivalent configurations, equatorial-axial (eq-ax) and axial-equatorial (ax-eq). The trans form thus behaves as a

mixture of two distinctive species, both being of C_2 symmetry, while the cis form may exhibit the effect of degeneracy on its rotational spectrum. Assignment has been made for the trans ax-ax and eq-eq forms and also for the cis form, yielding the rotational constants shown in Table I.

Reference

1) T. Egawa, T. Fukuyama, S. Yamamoto, F. Takabayashi, H. Kambara, T. Ueda, and K. Kuchitsu, *J. Chem. Phys.*, **86**, 6018 (1987).

Table I. Rotational Constants of Cyclobutane -1,2-d_2, trans and cis (in MHz)

	trans		cis
	eq-eq	ax-ax	
A	9794.388	9738.229	9938.754
B	9758.328	9693.440	9577.005
C	5782.655	6048.548	5913.201

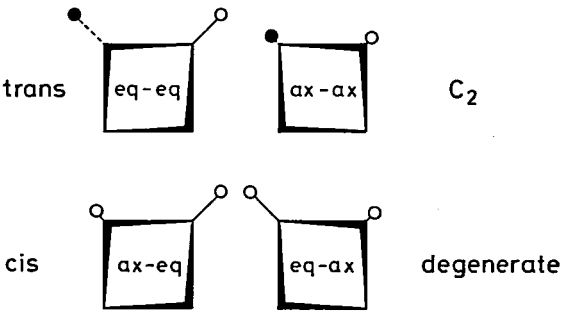

Figure 1. Cyclobutane-1,2-d_2, trans and cis.

II–D Laser Spectroscopy of Highly Excited Atoms and Molecules in Vacuum Ultraviolet Region

Narrow bandwidth and high brightness are the most significant properties of lasers and have been playing important roles in various spectral regions. Recent technical progress has extended these properties to the vacuum ultraviolet (VUV) region. One of the methods for the application of lasers to the VUV region is the generation of coherent VUV light by nonlinear multiwave mixing in gaseous media. The use of this technique allows us to observe highly excited states of atoms and molecules with higher resolution than other methods can provide. This method is useful mainly in the observation of excited states that can be reached by one-photon absorption from ground states. On the other hand, multiphoton or multi-step excitation spectroscopy is an alternative method. This method is essentially indispensable to the observation of highly excited states whose wavefunctions have very small overlaps with those of ground states. The aim of this project is to investigate the structure of highly excited states of atoms and molecules lying in VUV region with high resolution and to study the photochemical dynamics of these states by using each of the above methods or by combining them.

II-D-1 Construction of Coherent VUV Light Source with Narrow Bandwidth, High Intensity and Wide Tunability

Norio MORITA and Keiichi SATO

Various generation methods of coherent VUV have been investigated so far; for example, the third-order harmonic generation, four-wave mixing, stimulated anti-Stokes Raman scattering and so on. Among them, we use two-photon-resonant four-wave difference mixing, because it is expected to have not only high efficiency and high spatial quality but also broader tunability than other methods. The latter property is due to the less restriction of the phase-matching condition. We use 4p-5p two-photon transition of Kr atom to generate as short wavelength as possible. The UV input light (216 nm) resonant with this transition can be generated with high efficiency by using a recently devised nonlinear crystal, β-BaB_2O_4. The fundamental light for this UV light is produced by four-stage amplification of a single-mode cw dye laser in order to obtain as narrow bandwidth as possible. While we usually use a pulsed dye laser as the other

input light for the mixing, we prepare another cw dye laser with an amplifier chain. This scheme is expected to generate 120-200 nm VUV light with high intensity and uniform tunability. We also prepare another generation scheme of sum-frequency-mixing with Mg atom in order to generate farther short wavelength or to obtain more intense light at a particular wavelength. As a preliminary result, we have generated coherent VUV light at around 140 nm with high efficiency by using the above scheme with Kr atom. Farther improvement and precise measurement are in progress.

II-D-2 Laser Spectroscopy of High Lying Doubly Excited States of Ca Atom

Norio MORITA and Keiichi SATO

It has been predicted by many theories that high lying doubly excited states of atoms, which are called planetary atoms, have various interesting features. In particular, when two electrons are in the states with nearly equal principal quantum numbers, a strong correlation exists between them and causes a specific level structure, which is called a super multiplet. This is interpreted as a ro-vibronic structure of two correlated electrons and an ionic core, which behave as if the system were a linear floppy XYX triatomic molecule. In spite of this interesting prediction, there have been only a few experimental works. We have carried out the observation of such high lying doubly excited states of Ca atom by double two-photon excitation, which is equivalent to the method used by Cooke et al. for Ba atom. One-electron excited state 4s11s or 4s12s was firstly produced by two-photon absorption of a blue dye laser, and then two-photon transition spectra from this state was observed by using another UV laser light. These spectra were observed by the detection of CaIII ions. The scanned region of the UV laser was 235-208 nm, corresponding to around 140,000 cm^{-1} above the ground states. Although the results were preliminary yet, we observed several sharp lines (width < 1 cm^{-1}) and a few broad structures, all of which were confirmed to be two-photon absorption lines from 4s11s or 4s12s state. The analysis of these lines and an experiment with higher sensitivity are in progress.

II-E Raman Spectroscopy and Its Application

Raman scattering reveals the vibrational spectrum of a molecule which is sensitive to a molecular structure and bond strength. We apply this technique to study the following three projects; 1) elucidation of the structure-function relationship of biological molecules, 2) structure of short-lived molecules, 3) solution structure. The first project utilizes resonance enhancement of Raman intensity, which enables us to observe selectively the vibrational spectra of chromophores of large molecules with a small amount of a dilute solution. Various kinds of heme proteins, flavoproteins, retinoid proteins, and metalloproteins and their model compounds are investigated. Currently, we focus our attention to reveal two main problems; the mechanism of the proton- and electron transfers by proteins and of biological activation of oxygen. So far we have used visible lasers to see the spectra of chromophores, but we are extending the excitation wavelength to UV region (~200 nm) to enhance selectively the Raman bands of aromatic amino acid residues of proteins. The second project aims to determine resonance Raman spectra of transient states, i.e. reaction intermediates and excited molecules by using the pump-probe technique. In order to observe Raman spectra of fluorescent molecules, we developed an improved method for fluorescence rejection. The third project intends to evaluate a relative size of solute-solvent and solvent-solvent interactions for a binary mixtures of liquids and to elucidate a concentration-dependent assembled structure of molecules. For this purpose a system to measure Raman difference spectra was constructed.

II-E-1 Improved Fluorescence Rejection in Measurements of Raman Spectra of Fluorescent Compounds

Keiji KAMOGAWA, Takashi FUJII, and Teizo KITAGAWA

[*Appl. Spectrosc.*, in press]

Practical ways for fluorescence rejection were developed by using the technique of Raman difference spectroscopy and a gated diode-array detector. The basic idea is to observe a Raman-plus-fluorescence spectrum (S_T) and a pure fluorescence spectrum (S_F) separately with a high S/N ratio and to obtain a Raman spectrum (S_R) as their difference. With a CW Ar^+ laser, S_T and S_F were excited at different wavelengths but recorded in the same wavelength region. This was easy and quite successful for compounds with the Raman to fluorescence intensity ratio (I_R/I_F) of greater than 0.01 such as methyl orange and methylene blue. With a mode-locked and Q-switched Nd:YAG laser, S_T and S_F were obtained from different timings of the detector gate (6 ns), i.e., -6 to 0 ns for S_T and 3 to 9 ns for S_F. The temporal discrimination between Raman and fluorescence photons combined with the Raman difference technique significantly improved the 532-nm excited Raman spectrum of the tetraphenylporphyrin solution. This method is applicable to compounds with the I_R/I_F of smaller than 0.01. The time-correlated single photon counting method with a time-to-amplitude converter was improved to work with a high repetition rate and applied to a Rhodamine 6G solution, which was also examined by the gated Raman difference technique. Advantages and problems associated with each technique and appropriate methods for a given sample will be discussed.

II-E-2 Observation of the $Fe^{IV} = O$ Stretching Raman Band for a Ferryl Porphyrin π Cation Radical

Shinji HASHIMOTO, Yoshitaka TATSUNO and Teizo KITAGAWA

[*J. Am. Chem. Soc.*, in press]

The $Fe^{IV} = 0$ stretching ($\nu_{Fe=O}$) Raman band was identified at 828 cm^{-1} for an oxo-iron (IV) porphyrin π cation radical for the first time. The observed ^{18}O and ^{54}Fe isotopic frequency shifts were quite close to those expected for an isolated Fe = O stretching vibration. This indicates that the vibrational coupling of the $\nu_{Fe=O}$ mode with other porphyrin vibrations is insignificant. The $\nu_{Fe=O}$ frequency was lower by 15 cm^{-1} than that of the five coordinate oxo-iron (IV) neutral complex, suggesting that the oxidation of the porphyrin ring to the cation radical slightly reduces the double bond character of the axial $Fe^{IV} = O$ bond. Since the radical complex was photolabile, the Raman experiment was successful only when the sample was spun at $-80°C$ and the measurement was completed within a few minutes with a diode array detector.

II-E-3 Transient Resonance Raman Spectra of Bacteriorhodopsin and Its pH Dependence: Observation for Precursors of Two M Forms.

M. NAKAGAWA, T. OGURA, A. MAEDA, and T. KITAGAWA

Transient resonance Raman spectra were observed for μs to ms intermediates of bacteriorhodopsin by using the pump-probe double-beam flow technique and their pH dependence was investigated. Although the L_{550} intermediate is currently considered to give split C = C stretching bands at ~1540 and ~1552 cm^{-1}, they were found to arise from different molecular species. The rise time of the 1540 cm^{-1} band was pH dependent but that of the 1552 cm^{-1} was not so; it was faster at alkaline pH. The decay time of the 1540 cm^{-1} band was also pH dependent and 75 and 300 μs at pH 7.0 and 10.5, respectively at 4°C, while that of the 1552 cm^{-1} band depended little on pH and was much slower. These decay times of the 1540 cm^{-1} band were in reasonable agreement with the reported rise times of two M intermediates [Hanamoto J. H., Dupuis, P., El-Sayed, M. A., *Proc. Natl. Acad. Sci. U.S.A.* **81**, 7083 (1984)]. Consequently, only the 1540 cm^{-1} band was assigned to the L species. This suggests the presence of another intermediate with the 1552 cm^{-1} band in this time scale of the photocycle of bR. The single beam power-difference spectrum and spectral changes due to variation in residence time of bR in the laser beam were also measured with both the flow technique and the spinning cell for a common preparation, and differences in observations due to differences in techniques are discussed.

II-E-4 Functional Activity of Haemoglobins Adsorbed on Colloidal Silver: A SERRS Study

J. DE GROOT, R. E. HESTER, S. KAMINAKA, and T. KITAGAWA

[*J. Phys. Chem.*, in press]

Surface enhanced resonance Raman spectra from submicromolar concentrations of human and carp haemoglobins adsorbed on colloidal silver are reported. The adsorbed haemoglobins show reversible dioxygen and carbon monoxide binding and undergo a reversible R- to T-state transition. The Fe-N_{His} stretching vibration is unperturbed by adsorption at the silver surface, indicating that the intact haem environment is preserved and the tetrameric structure is retained, even at submicromolar concentrations. Molecular graphics representations of haemoglobins indicate that the propionate groups attached to the porphyrin macrocycle provide suitable binding groups for adsorption of the haemoglobin at the positively charged silver surface.

II-E-5 An Interpretation for the UV and Visible Spectral Changes of Bacteriorhodopsin in Alkaline pH

Akio MAEDA, Masashi NAKAGAWA, and Teizo KITAGAWA

The pH dependent changes in the visible and UV absorption spectra were observed for the dark- and light-adapted bacteriorhodopsin (bR) in the purple membrane and their lysine-acetylated forms and interpreted based on the pH difference spectra of amino acid derivatives. For weak alkalization of native bR we observed a small red shift of the visible band, which gave apparent increase of absorbance around 620 nm, and appearance of a structured feature around 290 nm, which could be mimicked by the pH difference spectrum of tryptophane but not of tyrosine. The red shift was observable only for bR with the all-trans chromophore. For the acetylated bR the visible absorption band was shifted to blue upon alkalization. Resonance Raman spectra of the blue shifted acetylated bR demonstrated that its chromophore has the protonated Schiff base. Therefore, the blue shift was thought to have arisen from the appearance of a negative charge near the Schiff base. The visible and UV spectral change of native bR upon weak alkalization consisted of the reversible and irreversible parts. The irreversible parts resembled the spectral changes observed for the acetylated bR, for which the changes in the visible and UV regions were parellel, and was attributed to deprotonation of a carboxylic side chain of Glu or Asp. The reversible parts of the UV spectral change (~290 nm) was deduced to be caused by deprotonation of an amino group located nearby the tryptophane residue.

II-E-6 An Optical Device to Measure Absorption Spectra in a Raman Exciting Laser Beam.

Takashi OGURA AND Teizo KITAGAWA

Resonance Raman spectroscopy provides detailed structural information on the chromophore of biological pigments. However, irradiation of laser light on those molecules at the wavelength within the absorption band often causes undesirable photoreaction by which unexpected species are generated. Particularly for studies of reaction intermediates, it is essentially important to identify the species that gives a Raman spectrum. For this purpose we constructed an optical device to measure the absorption spectrum of molecules in the laser beam by using an optical fiber. This device has successfully been applied to photolabile reaction intermediates, compound I of horseradish peroxidase and carbonmonoxy hemoglobin.

II-E-7 Resonance Raman Studies of Hydrogenase-catalyzed Reduction of Cytochrome c_3 by Hydrogen

A. L. VERMA, K. KIMURA, A. NAKAMURA *(Ajinomoto Corp.)*, **T. YAGI** *(Shizuoka Univ.)*, **H. INOKUCHI and T. KITAGAWA**

We report the first resonance Raman studies of hydrogenase-catalyzed reduction of a tetraheme protein cytochrome c_3 with hydrogen. We have observed splittings of Raman lines in the intermediate redox states obtained under controlled pressure of hydrogen suggesting that the four hemes in the protein are non-equivalent and interact with each other. Observation of well-defined Raman peaks due to individual hemes in the partially reduced states at the characteristic positions for the reduced or the oxidized form indicates that the electron exhange rates either intramolecular within the four hemes or intermolecular between different cytochrome c_3 molecules is much

slower than the time scale of the RR scattering process while the recent NMR studies indicate the intramolecular exchange rates is faster than the NMR time scale. We have attempted to estimate the relative importance of the dispersion, induction, orientational and repulsive interactions for understanding the "vibrational exciton" type splitting of the Raman bands in the intermediate states of reduction of cytochrome c_3. The dipole-dipole coupling mechanism can be ruled out while the dispersion interactions may contribute predominantly for the splittings of the Raman bands.

II-E-8 Resonance Raman Characterization of Tetra-, Penta-, and Hexa-Coordinated Cobalt(II)-Porphyrin Complexes

Y. OZAKI *(Jikei Univ.)*, **K, IRIYAMA** *(Jikei Univ.)*, **K. AOYAMA** *(Fukushima College of Tech.)*, **H. OGOSHI** *(Tech. Univ. of Nagaoka)* **and T. KITAGAWA**

Resonance Raman (RR) spectra were observed for tetra-, penta- and hexa-coordinated octaethylporphyrinato-cobalt(II) [Co(OEP)] complexes. RR bands due to the methine-bridge or C_bC_b stretching modes showed small to medium (1-8 cm^{-1}) and large (8-22 cm^{-1}) downward shifts, respectively, upon the conversion from the tetra- to penta- and hexa-coordinated complexes. This suggests that the coordination of axial ligand(s) causes the core-size expansion and the extent of the core expansion is larger for the penta-coordination than for the hexa-coordination. It seems that the size of the core expansion depends not only on the coordination number but also on a species of axial ligands; for instance, the core size is larger for $Co(OEP)(Py)_2$ (Py: pyridine) than $Co(OEP)(Im)_2$ (Im: imidazole) within the six-coordinate complexes. The RR frequency of the totally symmetric C_aN stretching mode was independent of the coordination number or the core-size, but it changed with the species of axial ligands. The RR spectra in the low frequency region of the Co(OEP) complexes were also very sensitive to the coordination number and a species of axial ligands.

II-E-9 Resonance Raman Characterization of N-Methyl-Octaethylporphyrinato-Cobalt(II)

Y. OZAKI *(Jikei Univ.)*, **K. IRIYAMA** *(Jikei Univ.)*, **K. AOYAGI** *(Fukushima College of Tech.)*, **H. OGOSHI** *(Tech. Univ. of Nagaoka)*, **and T. KITAGAWA**

Resonance Raman (RR) spectra were observed for $Co(N\text{-}CH_3OEP)AcO$ ($N\text{-}CH_3OEP$: N-methyl-octaethylporphyrin, AcO: acetate), $Co[(N\text{-}CH_3OEP)\text{-}d_4]AcO$, $Co[(N\text{-}CH_3OEP)\text{-}^{15}N_4]AcO$, and $Co(N\text{-}CD_3OEP)AcO$. The ν_{10}, ν_2, ν_{19}, and ν_3 modes of $Co(N\text{-}CH_3OEP)AcO$ were observed at 1616, 1585, 1570, and 1482 cm^{-1}, respectively which exhibited an isotopic frequency shift by 14, 2, 11, and 8 cm^{-1}, respectively, upon the meso-deuteration. The tendency of the meso-deuteration shifts of $Co(N\text{-}CH_3OEP)AcO$ was similar to that of Co(OEP), although their magnitudes were somewhat different between the two kinds of complexes. The frequencies of RR bands in the 1650-1450 cm^{-1} region of $Co(N\text{-}CH_3OEP)AcO$ were much lower than those of Co(OEP)(2-MeIm) (2-MeIm: 2-methylimidazole), indicating that the core-size of the former is much larger than that of the latter. The ν_4 band of $Co(N\text{-}CH_3OEP)$ appeared as a doublet, suggesting the splitting between the C_aN stretching modes of pyrrole rings with and without the bound methyl group. A Raman line of $Co(N\text{-}CH_3OEP)AcO$ at 179 cm^{-1} exhibited a large (23 cm^{-1}) and a small (5 cm^{-1}) upward shift upon the N-methyl-deuteration and ^{15}N substitution, respectively. Accordingly, this band is associated with the motion of N-methyl group. Interestingly, the RR frequency of this band was sensitive to solvent and the exchange of the fifth ligand. Probably the relative location of N-methyl group is altered upon the change of solvent of fifth ligand.

II–F Structure of Noncrystalline Solids by EXAFS

It is very important to know the structure of supported catalyst in order to understand the roles of catalysts in catalytic reactions. EXAFS is best suited for the purpose because the local structure around the selected elements can be determined irrespective of the phase. Very tiny metal or metal oxide clusters in the supported catalyst, which TEM and XRD fail to observe, can be studied. Especially, the structure under the reaction conditions can be probed by the use of an in situ cell, since EXAFS measurement can be done with the presence of reacting gas.

In the past years, our efforts was mainly concentrated on the determination of the structures of several supported mono- and bimetallic catalysts. Structural changes at the several stages of the preparation procedure and under the presence of reacting gases have also been investigated. Studies above these lines have been continued. Local structures around the metals in solutions and glassy materials have been studied as joint studies program.

This year a new double-crystal spectrometer for EXAFS study was constructed (II-F-1) and proved to be especially useful in high energy region (>15 keV). A possibility of x-ray Raman spectroscopy as a new method for structure determination has been continuously pursed in laboratory (see Special Research Project) as well as with synchrotron radiation, and some positive results have been obtained (II-F-4).

The followings are the abstracts of the manuscripts submitted to several journals in the past year.

II-F-1 A Double Crystal Spectrometer for Laboratory EXAFS Spectroscopy

Kazuyuki TOHJI, Yasuo UDAGAWA, Tsutomu KAWASAKI*, and Kimitoshi MIENO* *(*Rigaku Co.)*

[submitted to *Rev. Sci. Instrum.*]

A double crystal x-ray spectrometer designed for in-laboratory EXAFS (extended x-ray absorption fine structure) study is constructed. By the use of two curved crystals with different structure factor such as Ge(220) and Ge(111), reflections other than the desired order are virtually eliminated and monochromatic as well as intense x-ray flux can be obtained by applying higher voltage to the x-ray generator. As a result, data of very high quality can be collected in a short period by measuring the incident and the transmitted beam intensity simultaneously. It can cover a wide spectral range (7–26 keV) and is especially useful in the high energy region, where the laboratory EXAFS system previously reported has some difficulties.

II-F-2 Characterization of Silica Supported Bimetallic Iron-Nickel Catalysts by EXAFS

Takanori MIZUSHIMA, Kazuyuki TOHJI, and Yasuo UDAGAWA, Mutsumi HARADA*, and Akifumi UENO* *(*Toyohashi Univ. of Technology and IMS)*

[submitted to *J. Catal.*]

Fe-Ni/SiO_2 bimetallic catalysts with various composition were prepared by two kinds of preparation procedures; alkoxide and impregnation method. The size distribution of the metal clusters and the local structure around each kind of metal atom in the clusters are studied by TEM, XRD, and EXAFS. Fe as well as Ni atoms are concluded to be in small clusters with fcc structure; that is, alloy is formed. The metal particles are, however, not uniform in composition and consists of Ni rich kernel covered with outer laysers which contain more Fe. This tendency is more pronounced in the catalyst prepared by the alkoxide method. The reason of the evolution of such inhomogeneous clusters is examined by EXAFS through the local structure change during the preparation procedure.

II-F-3 Molybdenum Oxide Structure on Silica-Supported Catalysts Studied by Raman Spectroscopy and EXAFS

Noriyoshi KAKUTA, Kazuyuki TOHJI, and Yasuo UDAGAWA

[*J. Phys. Chem.*, in press]

Raman as well as EXAFS (extended x-ray absorption fine structure) spectroscopy have been used to

investigate the formation of molybdenum oxide on silica supported catalysts. The existence and the structure of interaction species at low loadings is elucidated by both the spectroscopies. The Raman data of the catalyst at higher loadings confirmed the previously reported observations, that is, the presence of MoO_3 phase after the calcination at 773 K, while EXAFS spectra clearly demonstrate that the major molybdenum species is different from MoO_3 crystallite. The reason of the apparent contradiction is discussed.

II-F-4 A Novel Approach for the Structure Analysis by X-Ray Raman Scattering

Kazuyuki TOHJI and Yasuo UDAGAWA

[*Phys. Rev.*, **B** in press]

An EXAFS like oscillation was observed in the x-ray Raman spectra of graphite by exciting 8265eV x-rays from synchrotron radiation. From an analysis employing the formula used for EXAFS, the carbon-carbon interatomic distances are obtained which are in good agreement with the ones in graphite. Thus, x-ray Raman scattering is a very promising method for the determination of the local structure around light elements.

II-F-5 Pronounced Effect of Particle Size on Selectivity Observed for Carbon Monoxide Hydrogenation over Ruthenium-Aluminum Catalyst

Z. Z. LIN*, T. OKUHARA*, M. MISONO*, Y. UDAGAWA, and K. TOHJI *(*Univ. of Tokyo)*

[*J. Chem. Soc., Chem. Commun,*, **1986**, 1673]

The sizes of Ru crystallites on alumuna support were characterized by EXAFS spectroscopy and TEM picture in relation to selectivity. The size of Ru crystallites affected markedly the selectivity for CO hydrogenation in contrast to previous reports; small particles (10 A) produced significant proportions of higher hydrocarbons and large single crystallites (110 A) gave mainly methane.

II-F-6 Characterization of Iron Oxide in Fe_2O_3/SiO_2 Catalyst

T. IDA*, A. UENO*, K. TOHJI, Y. UDAGAWA, K. IWAI, and H. SANO**** *(*Toyohashi Univ. of Technology and IMS, **Tokyo Metropolitan Univ.)*

[*J. Catal.*, **106**, 428 (1987)]

Silica supported iron oxide catalyst was prepared by hydrolysis of a mixed solution of ethyl silicate and iron (III) nitrate dissolved in ethylene glycol. A gel obtained by the hydrolysis was dried and calcined at various temperatures. The iron oxide particles thus prepared were maghemite (γ-Fe_2O_3) deduced by EXAFS measurements and the sample color. The maghemite particles were classified into two groups; one is small but detectable by TEM and the other is too small to be detected by TEM. The former was well controlled in an even size level, which depended on the calcination temperature, and exhibited ferrimagnetic properties. The latter showed super-paramagnetic properties and was estimated smaller than 10 A in the particle size by magnetic and Mösbauer measurement at low temperature.

For comparison, the catalyst was also prepared by a conventional impregnation method using silica powder and an aqueous solution of iron (III) nitrate. Iron oxide thus prepared was hematite (α-Fe_2O_3) and the particle sizes were broadly distributed.

II-F-7 An EXAFS Study of Local Structure by GeO_2-P_2O_5 Glasses

Y. SIMIZUGAWA*, C. D. YIN*, M. OKUNO*, H. MORIKAWA*, F. MARUMO*, Y. UDAGAWA, N. MOCHIDA, and T. SEKIYA**** *(*Tokyo Inst. Technology, **Yokohama National Univ.)*

[*Yogyo Kyokaishi*, **95**, 418 (1987)]

The Ge EXAFS (extended x-ray absorption fine structure) above its K absorption edge was measured for GeO_2-P_2O_5 glasses containing up to 49 mol% $PO_{5/2}$. The Ge-O distance was determined to be 1.72-1.76 A by the curve fitting method. It was shown that a part of Ge atoms changes their cooordination number form 4 to 6 on introducing P_2O_5 into GeO_2 glass. The fraction of six-coordinated Ge atoms (N_6) was estimated from

the Ge-O distances obtained by EXAFS analysis and the result agreed with the value of N_6 estimated from molar volume using partial molar volumes. N_6 approximately followed a formula $N_6 = x/2(1-x)$, where x is the molar fraction of $PO_{5/2}$.

RESEARCH ACTIVITIES III
Department of Electronic Structure

III–A UV and VUV Photochemistries of Olefins, Alkylbenzenes, Phenol, and Anisole

Irradiation of molecules with UV or VUV light often induces photodissociation. Besides direct and pre-photodissociation, we have been investigating another type of photodissociation, which consecutively involves excitation of electronically excited state, efficient internal conversion to the ground state, and dissociation. The ground electronic state thus produced has a very high vibrational energy, in other words the corresponding vibrational temperature is thousands Kelvin. Since the internal energy of this state is determined by photon energy and unique, we are able to directly obtain the specific rate constants of unimolecular dissociation. We show that the dissociation rate constants of olefines can be predicted on the basis of RRKM theory. However, we have found that predissociation is predominant in case of phenoxy radical formation.

III-A-1 Direct Measurements of Formation Rate Constants of Allylic Radical from Hot Olefins Formed by Internal Conversion. I.

Nobuaki NAKASHIMA, Noriaki IKEDA, Nobuo SHIMO *(Cen. Res. Lab. Idemitsu Kosan)*, **and Keitaro YOSHIHARA**

[*J. Chem. Phys.*, in press]

The photofragmentation of 2,3,3-trimethyl-1-butene (TMB), 2,3-dimethyl-2-pentene (DMP), and tetramethylethylene (TME) has been studied in the gas phase by ArF (193 nm) laser flash photolysis. For the first time, the formation rate constants to the common product of trimethylallyl (TMA) radical have been measured directly under collision free conditions. The C-C bond (the C-H bond for TME) at the position β to the double bond dissociates and TMA radical is formed. The formation rate constants of the TMA radical are found to be $5.6 \times 10^7 s^{-1}$ for TMB, $2.7 \times 10^7 s^{-1}$ for DMP, and $1.7 \times 10^7 s^{-1}$ for TME. These rate constant values can be explained in terms of the RRKM theory by assuming that the absorbed photon energy is redistributed in all the vibrataional modes. Formation of the TMA radical is reduced by adding a foreign gas, however, a small amount of the radical was still detected under a high pressure. TMA and methyl radicals were formed by a one-photon process as shown in Figure 1. The unquenched processes are interpreted in terms of predissociation.

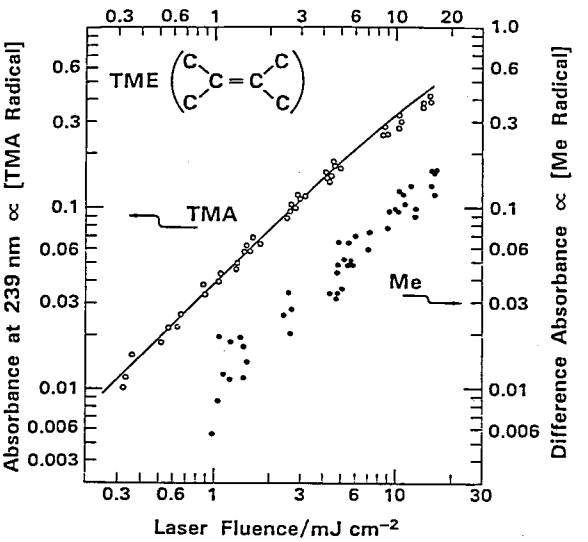

Figure 1. Laser fluence vs. absorption intensities of the trimethylallyl (TMA) and methyl (Me) radicals formed from tetramethylethylene (TME). Absorbances of TMA radical were measured at 239 nm at 50 ns are plotted vs. laser fluences in the presence of 800 Torr of nitrogen. The solid curve was calculated by assuming a one-photon process without any inner filter effect. The difference absorbances for methyl radical was obtained by subtracting the background from the absorbance at the peak of methyl radical (216.4 nm). The absorbances were measured at a delay time of 80 ns in the presence of 400 Torr of propane. TMA pressures were 1.0–4.26 Torr. All The absorbances for the two systems were normalized to those observed at 4.26 Torr of TME.

III-A-2 ArF Laser Flash Photolysis of Phenol and Anisole

Yoshizumi KAJII *(Tokyo Inst. of Tech.)*, **Kinichi OBI** *(Tokyo Inst. of Tech.)*, **Nobuaki NAKASHIMA, and Keitaro YOSHIHARA**

[*J. Chem. Phys.*, in press]

Absorption spectra of phenoxy radical in the gas phase are observed in the range of 210~300 nm in the ArF excimer laser (193 nm) flash photolysis of phenol and anisole. An intense absorption band is obtained around 230 nm and a broad band around 270~300 nm. In the photolysis of anisole, simultaneous formation of methyl and phenoxy radicals makes it possible to determine the molar extinction coefficient of phenoxy radical which is determined to be 7800 $M^{-1}cm^{-1}$ at 230 nm. The phenoxy radicals are formed in the time range of shorter than 1 ns as shown in Figure 1. They are produced from phenol, anisole, pentafluorophenol, and pentafluoroanisole on irradiation with the ArF laser light. The photodissociation is not explained in terms of the hot molecule mechanism but of predissociation.

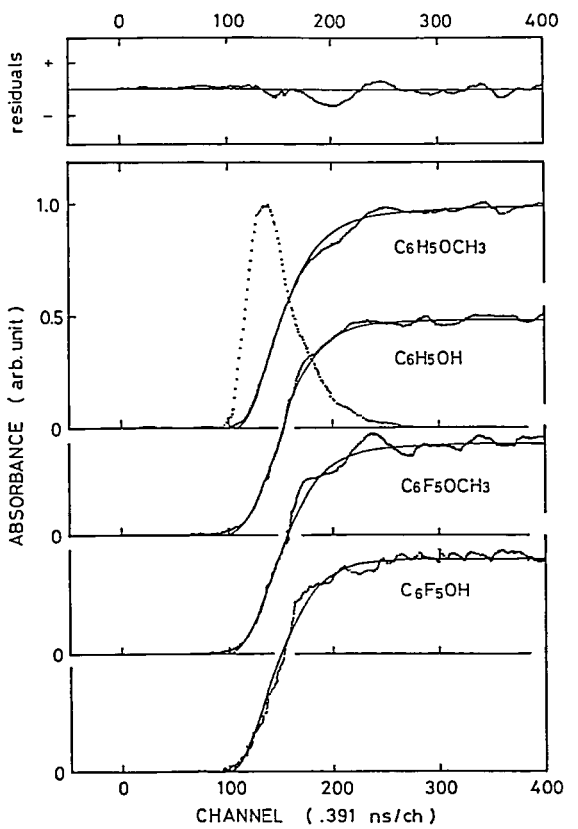

Figure 1. Rise curves of hot phenoxy radicals formed in the photolysis of anisole, phenol, pentafluoroanisole, and pentafluorophenol measured under collision free conditions. The dotted line with a pulse shape is a typical irradiation laser pulse. Solid lines are integrated curve of the laser pulse.

III-A-3 Hot Molecule Mechanism in the Photochemistries of Benzene, Alkylbenzenes, and Olefins

Nobuaki NAKASHIMA and Keitaro YOSHIHARA

[*Phys. Org. Chem.* 1986, Elsevier Science, in press]

The primary intermediate of photochemical reactions of gaseous benzene has been found to be a hot molecule (S_0**: a highly excited vibrational state in the ground electronic state) by nanosecond laser (ArF 193 nm) photolysis. Time-resolved spectra are measured in relation to isomerization to fulvene. A comment is given on the mechanism of collisional relaxation of S_0**. A typical decay curve is shown in Figure 1. The decay curve is analysed in terms of an energy dependent model. The differences between reactions activated by thermal energy and those via the hot molecule mechanism are discussed. The latter mechanism is operative in the photodissociation of olefins and alkylbenzenes. For the first time, the specific dissociation rate constants from S_0** were measured in more than 50 molecules.

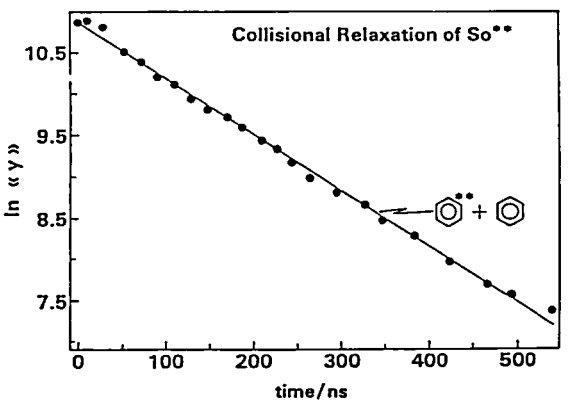

Figure 1. Collisional relaxation of hot benzene produced by an ArF laser excitation. Absorption intensity has been converted to internal energy of benzene (≪y≫) expressed in units of cm^{-1}. The decay is well expressed as a single exponential one. The pressure of benzene is 8 Torr.

III-A-4 Oscillator Strengths of The Ultraviolet Bands of Hot and Relaxed Methallyl, Allyl, and Methyl Radicals

Nobuaki NAKASHIMA and Keitaro YOSHIHARA

[*Laser Chem.*, **7** 177 (1987)]

Absorption spectra of methallyl, allyl, and methyl radicals were measured in the ArF laser flash photolysis of halogenated methanes and olefins, and 2-methyl-1-butene. Broad absorption spectra were detected immediately after excitation, indicating that the radicals carried high internal energy (called "hot" radicals here). The spectra were sharpened with time due to collisions with foreign gases and finally reached equilibrium (spectra in relaxed states), as shown in Figure 1. The oscillator strengths (f) of methallyl and allyl radicals were found to remain about the same for hot and relaxed states. The values (f) in the relaxed states were determined with errors of ±10% to be 0.14 for the methallyl radical, 0.26 for the allyl redical, and 1.57×10^{-2} (including the partition function) for the methyl radical. The molar extinction coefficients of the allylic radicals were 1.4~1.8 times as great as ones previously reported. Rate constants of collisional relaxation by nitrogen were discussed for seven hot radicals and molecules. Larger species gave greater rate constants. The hot methyl radical relaxed with a rate constant of 1.0×10^{7} s^{-1} in the presence of 760 Torr of nitrogen, while for the trimethylallyl radical it was 20 times as great as that of the methyl radical.

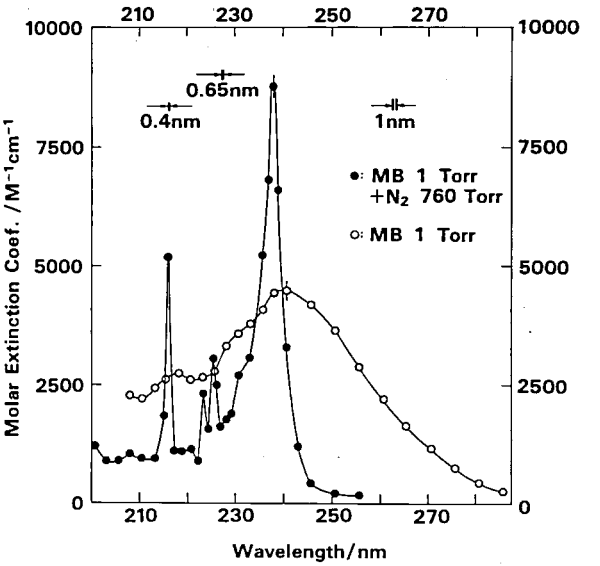

Figure 1. Absorption spectra of hot (○) and relaxed (●) methallyl radical. (○) Obtained at 10 ns after excitation of 1 Torr of 2-methyl-butene (MB); (●) at 60 ns delay time for 1 Torr of MB in the presence of 760 Torr nitrogen. Molar extinction coefficients are evaluated by assuming that the formation yield of the radical is unity. The spectral resolution is 0.4~1 nm as indicated. Error bar corresponds to a single σ.

III-B Photochemical cis-trans Isomerization of Isolated Olefinic Molecules

The photochemical cis-trans isometrization of an olefinic carbon bond is a fundamental chemical transformation that is important in chemical and biological sciences. Although much work has been done in this field, especially on model systems such as stilbenes, the isomerization dynamics and the photochemical intermediates are poorly understood. The S_1 state of cis-stilbene, in gas and solution, has been found to decay on sub-picosecond time scale presumably due to barrierless isomerization. Emission from cis-stilbene has only been observed in low temperature glasses where the viscosity of the host material prevents isomerization. The fluorescence excitation of supersonically cooled cis-stilbene has been measured in order to determine whether there exists a local minimum in the S_1 state of cis-stilbene. The fluorescence excitation spectrum of supersonically cooled diphenylsuberene, which has electronic structure that is similar to cis-stilbene but cannot isomerize, is measured in order to study the electronic structure of cis-stilbene like molecules.

III-B-1 Fluorescence Excitation Spectroscopy of Supersonically Cooled cis-Stilbene

Hrvoje PETEK, Yoshihisa FUJIWARA *(Kanazawa Univ.)*, **Dongho KIM** *(Korea Standards Res. Inst.)*, **and Keitaro YOSHIHARA**

The fluorescence excitation spectrum of supersonically cooled cis-stilbene is investigated from 354 nm to 308 nm; it is structureless even after extreme vibrational and rotational cooling, confirming the absence of a local minimum in the S_1 state of cis-stilbene. The fluorescence spectrum rapidly increases in intensity

from 351 nm, where the emission is below detection sensitivity, and does not reach a maximum in the observed region. Likewise the emission spectrum maximum is significantly red-shifted (maximum at 420 nm) from the excitation wavelength. These observations are consistent with a large change in the equilibrium geometries between the ground and excited states. The fluorescence quantum yield increases with higher seeding gas pressure, and it is at least an order of magnitude higher for Ar and Ne than for equal pressure of He. Although the influence of the seeding gas on cis-stilbene quantum yield is not yet understood, it is likely that the quantum yield depends on either cluster formation or rotational cooling.

III-B-2 Fluorescence Excitation Spectroscopy of Diphenylsuberene

Hrvoje PETEK, Yoshihisa FUJIWARA *(Kanazawa Univ.)*, **Dongho KIM** *(Korea Standards Res. Inst.)*, **and Keitaro YOSHIHARA**

The fluorescence excitation spectrum of 2:3, 6:7-Dibenzocyclo-hepta-2:4:6-triene (diphenylsuberene-DPS), a fluorescent isomorph of cis-stilbene, has been measured in order to further the understanding of electronic structure and photochemical cis-trans isomerization in stilbenes. Unlike cis-stilbene, DPS is strongly fluorescent because the two stilbene phenyl groups are tied together by a CH_2 group thereby preventing cis-trans isomerization. Therefore sharp vibrational structure can be observed in the fluorescence excitation spectrum (Figure 1).

The spectrum is dominated by two progressions of a 29 cm^{-1} vibrational modes that have different origins, and whose intensities monotonically increase for at least 25 quanta above the origin. Since the molecule is expected to undergo a large change in geometry between the ground and excited states due to retarded cis-trans isomerization, the progressions are due to a cycloheptatriene skeletal mode that is closely associated with the isomerization coordinate. The two close lying electronic states observed for DPS should also exist in cis-stilbene, however only one excited state has been considered in previous work on cis-stilbene isomerization.

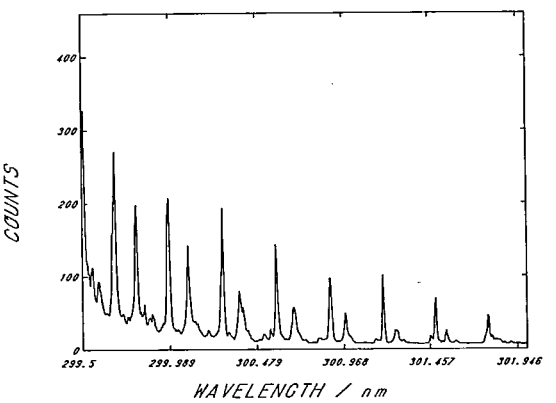

Figure 1. A portion of the fluorescence excitation spectrum of diphenylsuberene. The sample is seeded in 2.7 kgf/cm^2 of He and expanded through a 0.2 mm pulsed nozzle orifice.

III-C Dynamical Behavior of Excited Dye Molecules Adsorbed on Organic Single Crystals: A Novel System for Study of Electron Transfer

The system of dye molecules adsorbed on a single crystal allows unique opportunities for separate measurements of energy and electron transfer. A few years ago we studied two-dimensional energy transfer among adsorbed dye molecules on naphthalene and phenanthrene single crystals. Uninfluenced by energy transfer at a coverage of about 0.01, electron transfer has been studied with anthracene, pyrene, and other single crystals for which the free energy of electron transfer reaction, ΔG_0, is negative. In this chapter, we firstly describe electron transfer from anthracene, pyrene, and perylene single crystals to adsorbed molecules of Rhodamine B in the temperature range of 300-77 K. Experimental results were analysed with quantum mechanical electron transfer theory. We found a very small reorientational energy in this solvent-free, dry system and strong coupling of electron transfer to low frequency lattice modes and weaker coupling to the intramolecular vibrational modes. This model system is a potentially valuable for

biological systems. Secondly we describe the system with inorganic semiconductor single crystals of α-SiC, β-SiC and GaP. Electron transfer seems to occur with different rates at different adsorption sites.

III-C-1 Electron Transfer of Isolated Molecules of Rhodamine B Adsorbed on Organic Single Crystals. A Solvent-Free Model System

Klaus KEMNITZ, Nobuaki NAKASHIMA, and Keitaro YOSHIHARA

Electron transfer from anthracene, pyrene, and perylene single crystals to adsorbed molecules of Rhodamine B in the low coverage regime has been studied in the temperature range of 300-77K. A very small reorientation energy of 0.18 eV was obtained for this solvent-free, dry system with an electron exchange matrix element of 0.0023 eV. The electron transfer is analysed to be coupled to low frequency lattice or intermolecular modes (10~100 cm^{-1}) in addition to the 1400 cm^{-1} breathing mode of the aromatic skeleton of donor and acceptor. A pronounced decrease of the rate of electron transfer was found in the wet systems with an increased value of the reorientation energy, 0.4 eV at decreased electron exchange matrix element of 5.7×10^{-4} eV. The rate constant of electron transfer was determined to be $1.3 \times 10^{11} s^{-1}$ for the dry anthracence system. The measurement of the temperature dependence at three values of the energy gap allowed the confinement of potential fitting parameters. The small reorientation energy together with the coupling to low frequency modes at fixed distance and orientation renders above system into a potentially valuable model for biological systems.

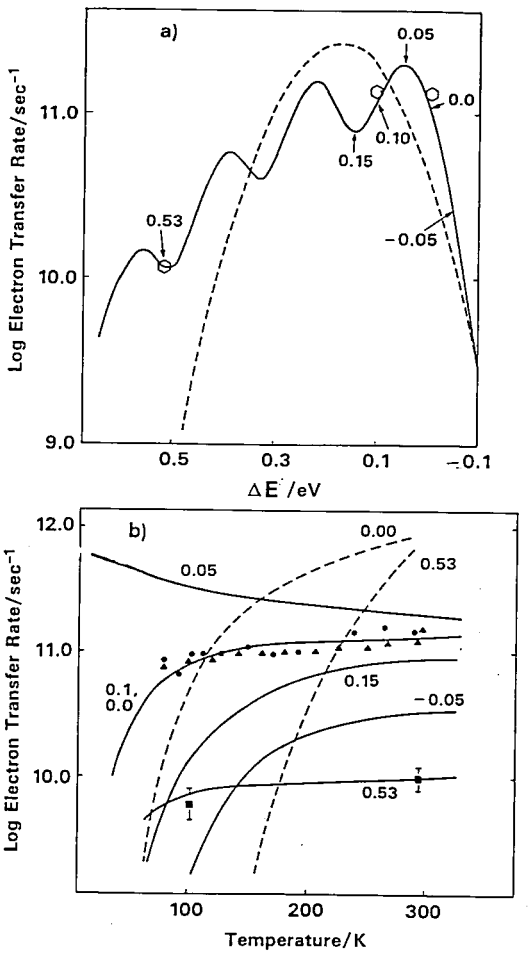

Figure 1. (a) Energy gap dependence of electron transfer; A calculated plot (solid line) of the energy-gap dependence of the electron transfer rate constant using the following equation, which is Sarai's three-mode-variant[1] of Jortner's original equation:[2]

$$W = (2\pi/\hbar^2\omega_s)|V|^2 \exp\left[-\frac{1}{2}\sum_i^N \Delta_i^2(2\bar{v}_i+1)\right] \prod_i^{N-N'} \sum_{n_i=-\infty}^{\infty} [(\bar{v}_i+1)/\bar{v}_i]^{n_i/2} I_{n_i}(\Delta_i^2(\bar{v}_i(\bar{v}_i+1))^{1/2}) \times [(\bar{v}_s+1)/\bar{v}_s]^{p'(n_1\ldots n_N)/2} I_{p'(n_1\ldots n_N)}(2S_s(\bar{v}_s(\bar{v}_s+1))^{1/2}),$$

$$p'(n_1\ldots n_N) = \left[\Delta E - \sum_i^{N-N'}{}' n_i\hbar\omega_i\right]/\hbar\omega_s,\ S_s = \frac{1}{2}\sum_s^{N'}\Delta_s^2,$$

with thermal populations $\bar{V}_i = (\exp(\hbar\omega_1/kT) - 1)^{-1}$, the modi ified Bessel functions $I(n_i)$ and I_p and the reduced displacement $\Delta_i^2 = (m_i\omega_i/\hbar)(\Delta R_i)^2$, with m_i the reduced mass and ΔR_i the displacement. Analyses are made with $\hbar\omega_s = 20\ cm^{-1}$, $\hbar\omega_1 = \hbar\omega_2 = 1400\ cm^{-1}$, $S_s = 20$, $S_1 = S_2 = 0.375$, V = 0.0023 eV, k(ac) = k(py) = $1.25 \pm 0.25 \times 10^{11} s^{-1}$, k(pe), = $1.04 \pm 0.15 \times 10^{10} s^{-1}$, ΔE: 0.532 (perylene), 0.10 (pyrene), 0.00 (anthracene) eV. The dashed lines show energy-gap and temperature dependence according to the classical Marcus theory with reorganization energy, $\lambda = 0.18$ eV. (b) Temperature dependence; the dashed lines according to classical theory are arbitrarily shifted along vertical axis, (•) anthracene, (▲) pyrene, and (■) perylene are data points from fluorescence lifetime measurements.

References

1) A. Sarai, *Chem. Phys. Lett.*, **63**, 360 (1979).
2) J. Ulstrup and J. Jortner, *J. Chem. Phys.*, **63**, 4358 (1975).

III-C-2 Fluorescence Decay of Isolated Molecules of Rhodamine B Adsorbed on Semiconductor Single Crystals

Klaus KEMNITZ, Nobuaki NAKASHIMA, Keitaro YOSHIHARA, and Hiroyuki MATSUTNAMI(*Kyoto Univ.*)

Fast nonexponential fluorescence decays of Rhodamine B monomers adsorbed on single crystals of α-SiC, β-SiC, and GaP have been observed. The decays are fitted with three exponentials and are interpreted in terms of different absorption sites with differing electron transfer capability. A thermal equilibrium if postulated to exist among the ground state populations of these sites. The electron transfer rate is only weakly dependent on temperature but is considerably slowed down by addition of water and by aging of the semiconductor surface.

III-D Dynamic Behavior of Excited States

Optical excitation of molecules to electronic excited sates causes a variety of dynamical behavior, depending upon the nature of electronic structures and environments, such as energy transfer, proton transfer, chemical reaction, radiationless transition, ionization, and others. Most of these processes fall into the nanosecond, picosecond and femtosecond timescale. Firstly, we describe a study of intramolecular vibrational redistribution of benzene in the channel three region with picosecond two-color two-photon ionization method. Secondly, picosecond transient absorption spectral and kinetic study of microcrystals by diffuse reflectance lasser photolysis is described. Thirdly, photochemical and photophysical properties of phenylethynyldisilanes is studied by means of picosecond spectroscopy. Fourthly, we describe resonance Raman spectroscopy of supersonically cooled acetylene. Finally, construction of femtosecond tunable dye laser system is briefly described.

III-D-1 Direct Measurement of the Intramolecular Vibrational Redistribution Rate of Benzene in the Channel Three Region

Minoru SUMITANI and Keitaro YOSHIHARA

The rate of the intramolecular vibrational redistribution (IVR) process of benzene in the channel three region is measured by the picosecond two-color two-photon ionization method. Figures 1(a) and 1(b), respectively, show the intensity of time-dependent ion current observed upon excitation of the 7^1 and $6^1 1^3$ bands in a supersonically cooled beam. Both 7^1 and $6^1 1^3$ band are excited just above the channel three threshold. Excitation to the 7^1 band gives the decay rate constant coincident with the fluorescence lifetime.[1] The dispersed fluorescence gives no evidence of the IVR process,[2] seemingly IVR does not take place at the 7^1 band excitation. On the other hand, upon excitation to the $6^1 1^3$, which is located only 210 cm^{-1} higher than the 7^1 band, a very short decay component is observed. (i) This short decay has not been observed in the total fluorescence decay measurement, (ii) the main component of fluorescence spectrum is constructed with the very broad one which should be caused by the fluorescence after IVR

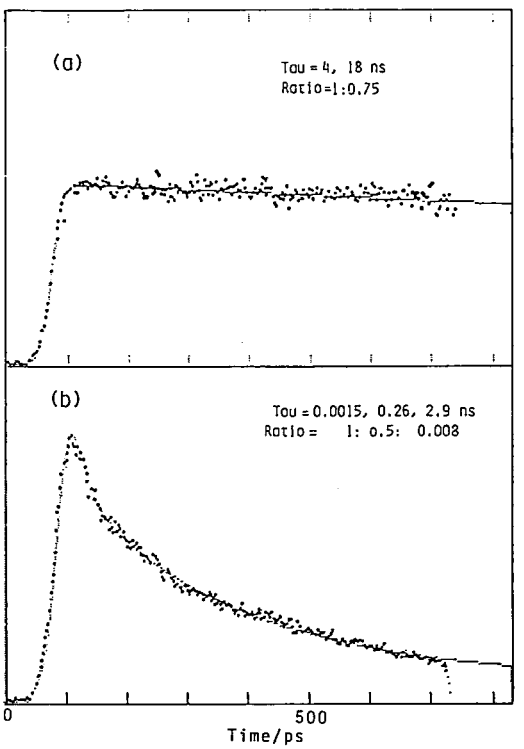

Figure 1. Intensity profiles of time-dependent ion current. (a) Excitation of the 7^1 band with 242.2 nm light and ionization with 266 nm light. (b) Excitation of the $6^1 1^3$ band with 241.7 nm light and ionzation with 266 nm light. •; experimental points, –; simulated curve using the value in the each figure.

process, (iii) the $S_1 \leftarrow S_0$ absorption band width is broadened and the band width gives the same order of phase decay rate as the observed short decay time. These three pieces of evidence indicate that this short decay component is caused by the IVR process. Therefore, it is very clear that the channel three process is the different process with the IVR process.

Reference

1) M. Sumitani, D.V. O'Connor, Y. Takagi, N. Nakashima, K. Kamogawa, Y. Udagawa, and K. Yoshihara, *Chem. Phys.*, **93**, 359 (1985)
2) M. Ito, private communication.

III-D-2 Picosencond Transient Absorption Spectral and Kinetic Study on Benzophenone Microcrystals by Diffuse Reflectance Laser Photolysis Method

Noriaki IKEDA *(Kyoto Inst. of Tech.)*, **Keiji IMAGI** *(Kyoto Inst. of Tech.)*, **Hiroshi MASUHARA** *(Kyoto Inst. of Tech.)*, **Nobuaki NAKASHIMA, and Keitaro YOSHIHARA**

[*Chem. Phys. Lett.* in press]

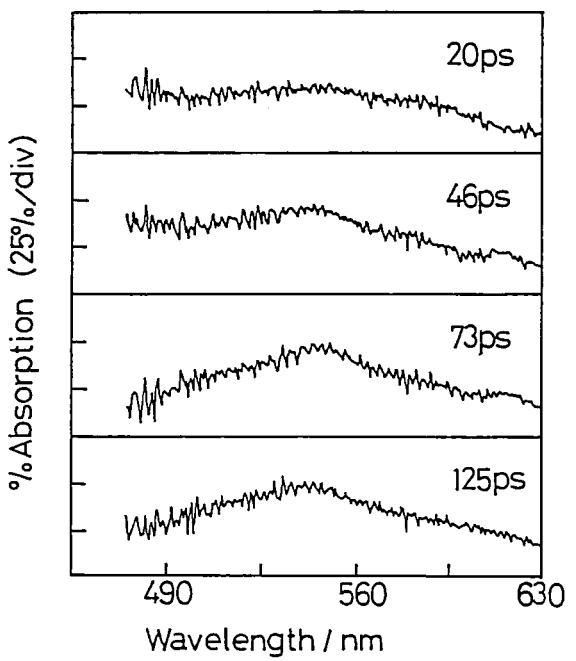

Figure 1. Transient absorption spectra of benzophenone microcrystals which were corrected with respect to the phosphorescence contribution. The delay times are indicated in the Figure.

Absorption spectrum and formation dynamics of the triplet benzophenone in microcrystal were measured for the first time, as shown in Figure 1, by analyzing diffuse reflected spectra of the picosecond continuum. The absorption spectral shape is similar to that of 2-propanol solution, and no appreciable difference was observed on their rise curves.

III-D-3 Excited-State Behavior of Phenylethynyldisilanes: An Intramolecular Charge-Transfer Emission

Haruo SHIZUKA *(Gunma Univ.)*, **Katsuhiko OKAZAKI** *(Gunma Univ.)*, **Hideaki TANAKA** *(Gunma Univ.)*, **Masayuki TANAKA** *(Gunma Univ.)*, **Mitsuo ISHIKAWA** *(Kyoto Univ.)*, **Minoru SUMITANI, and Keitaro YOSHIHARA**

[*J. Phys. Chem.*, **91**, 2057 (1987)]

Photochemical and photophysical properties of phenylethynyldisilanes in MP (methylcyclohexane/isopentane, 3:1 v/v) have been studied by means of picosecond and nanosecond spectroscopy along with steady-state experiments. Intramolecular charge transfer in the excited singlet state of phenylethynyldisilanes occurs very rapidly (<10ps) at both 77 and 294 K. This finding shows that internal rotation (or twisting) or solvation is not necessary for the intramolecular CT formation of phenyl-ethynyldisilanes. The mechanism on the intramolecular CT from the $^1(\pi,\pi^*)$ state to the $^1(2p\pi, 3d)$ CT state of the compounds is quite different from that of the usual TICT (twisted intramolecular charge transfer). Two decay components (fast and slow) of the ^{1}CT state are observed, which are ascribed to the intersystem crossing rates from ^{1}CT to $^3(\pi,\pi^*)$, depending upon the molecular conformations of the ^{1}CT state of phenylethynyldisilanes. The photochemical reaction to produce silacyclopropenes takes place effectively via the ^{1}CT state at room temperature, but not in MP glass at 77 K.

III-D-4 Resonance Raman Spectroscopy of Supersonically Cooled Acetylene

Hrvoje PETEK, Yoshihisa FUJIWARA *(Kanazawa Univ.)*, **and Keitaro YOSHIHARA**

The structure A (236.9~210.0 nm) and B (200~155 nm) states of acetylene are investigated by measuring the resonance Raman spectra in a neat supersonic expansions using 266 and 212.8 nm excitation sources. The spectra of A and B excited states of acetylene have been assigned to trans-bent structures. At about the same energy, two cis-bent excited states are predicted by theory but have not been experimentally observed.[1] The Raman spectra measured at 266 and 212.8 nm are shown in Figure 1. At 266 nm only the totally symmetric ν_2 (C≡C stretch) and ν_1 (C–H stretch) fundamentals are observed. At 212.8 nm, in addition to the ν_1 and ν_2 fundamentals, $\nu_2 + 2\nu_4$ (C≡C stretch and transbend) and $\nu_2 + 2\nu_5$ (C≡C stretch and cis-bend) combination bands are observed. The Raman activity at 212.8 nm of cis and trans bend vibrations can be explained by resonance enhancement from nearby electronic states that are cis and trans bent. The fact that the cis-bend combination band has the highest intensity in the 212.8 nm spectrum strongly suggests the presence of a previously unidentified cis-bent electronic state. It is probable that at least part, if not all of the B state oscillator strength is due to a cis-bent excited state.

Reference

1) H. Lischka and A. Karpfen, *Chem. Phys.*, **102**, 77 (1986).

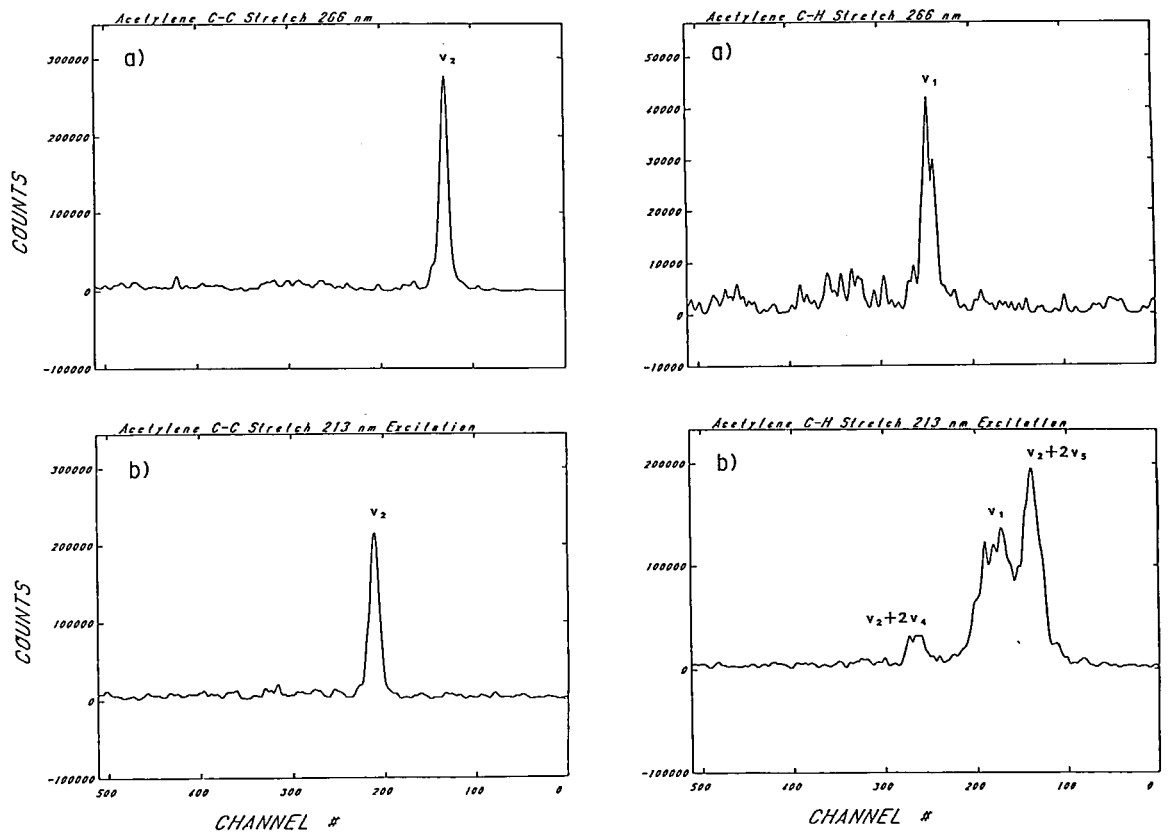

Figure 1. Acetylene Raman spectra produced by a) 266 nm, and b) 212.8 nm excitation. The sample is expanded from 300 Torr stagnation pressure through 0.6 mm nozzle.

III-D-5 Construction of Femtosecond Tunable Dye Laser System

Hiromi OKAMOTO, Yoshihiro TAKAGI, and Keitaro YOSHIHARA

Construction of high power high repetition rate femtosecond tunable dye laser system with excitation by a CW mode-locked YAG laser and amplification with a copper-vapor laser is described in section *Special Research Projects*.

III-E Solar Energy Conversion by Using Photocatalytic Effects of Semiconductors and Dyes — Decomposition of Water and Application to Organic Synthesis —

Essential roles are played by semiconductors and dyes in the photocatalytic effects to which a particular attention has been paid in connection to the direct conversion of solar energy to chemical energy. One of the most important application is the water splitting reaction. Photocatalytic reactions of water with various organic compounds are also interesting not only from the view point of hydrogen production but also from that of the application to organic synthesis. In order to elucidate the mechanism of these photocatalytic reactions, we need detailed knowledges on the electronic structures of adsorbed molecules, the fundamental processes of photoinduced electron transfer at the semiconductor-liquid interface and catalysis on the surface. Work on the following topics is in progress with the purpose of clarifying the photocatalytic effects of semiconductors and dyes from the view point of solar energy conversion.

III-E-1. Ultramicrostructured Electrode System Prepared from the Multilayered Thin Film and Its New Electrochemical Properties

Masahiro HIRAMOTO, Kazuhito HASHIMOTO, and Tadayoshi SAKATA

The ultramicrostructured electrode systems with the scale of nm orders have been prepared and the vertical sections of the multilayered thin films have been applied to electrochemistry. The vertical section was obtained by cutting the multilayer perpendicularly using the photolithography technique. Figure 1A shows the example of the surface structure of this ultramicrostructured electrode system made of metal and insulator layers.

For this type of electrode, supporting electrolyte is not necessary for the electrochemical reaction due to the very short distance between electrodes. Particularly, it was confirmed that this type of electrode can work in the gas phase. Figure 1B shows the current(j)-potential(U) curves for the ultramicrostructured electrode system which consists of two Ni electrodes separated by 130 nm from each other. Under vacuum condition, only hysteresis was observed. However, when H_2O vapor was introduced, stable current was observed. This phenomenon was quite reversible. Current density which was increased by H_2O vapor introduction was very large. Moreover, the applied voltage that the current starts to flow is almost the same to that in liquid water containing a supporting electrolyte. Above results clearly indicate that the ultramicrostructured electrode system can work even in the gas phase. Furthermore, it is confirmed that this electrode responds under CO_2, N_2 atmosphere at low-temperature.

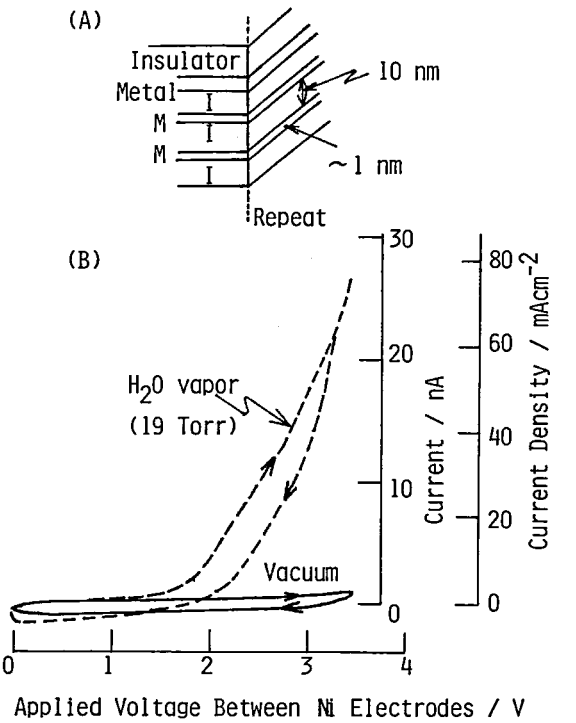

Figure 1. (A) Ultramicrostructured electrode system. (B) The current(j)-potential(U) curves for the ultramicrostructured electrode system in the gas phase.

III-E-2 Electrochemical Transistor Effect of pn-Junction Semiconductor

Tadayoshi SAKATA, Masahiro HIRAMOTO, and Kazuhito HASHIMOTO

In order to clarify the semiconductor electrode processes, especially the reaction of minority carriers on the semiconductor surface, the electrochemical properties of several kinds of semiconductor electrodes with a pn-junction have been investigated.

For a pn-Si electrode, in which the surface is composed of a thin p-layer (thickness:10~20 micron), it was proved that the electrons are injected from the inside n-layer into the surface p-layer without recombination. Figure 1 shows one of the results which demonstrates the electron injection together with an electric circuit of the electrochemical cell used for the experiment. The cell has a similar structure with that of a bipolar transistor and the circuit corresponds to the base-earthed one. For this circuit, I_C vs V was measured with keeping the magnitude of I_E constant. The result is shown in the same Figure. As shown in this Figure, I_E is almost equal to I_C, indicating that the majority carriers (electrons) are injected to the surface p-Si layer with almost 100% efficiency. Due to the injection, hydrogen was evolved vigorously from the p-Si surface. By making use of this effect, electricity can be amplified. This result indicates that a pn-semiconductor electrode can function as an electrochemical transistor. It was also observed that irradiation of this pn-Si electrode enhances dramatically the injection current.

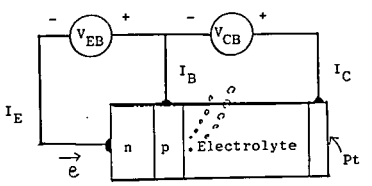

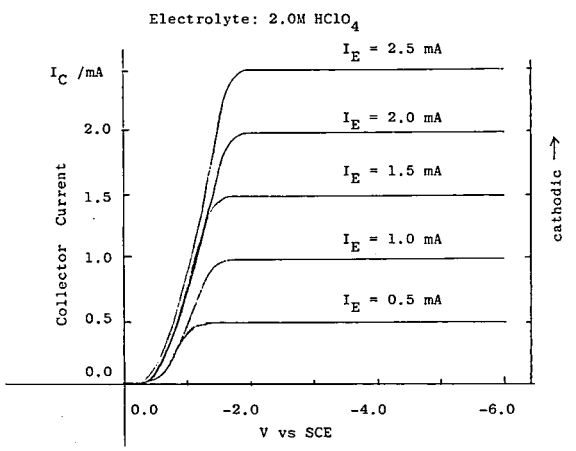

Figure 1. The electric circuit for a pn-Si electrode in an electrolyte solution (2.0M $HClO_4$) and the I_C vs V under the condition of constant I_E.

III-E-3 Amorphous Films Prepared from $Fe(CO)_5$ and SiH_4 by Plasma CVD

Sigetada OHKUBO *(Tokai Univ.)*, **Tadayoshi SAKATA, Nariaki HIROSHIGE** *(Saga Univ.)*, **Masahiro HIRAMOTO, Kazuhito HASHIMOTO, Tohru HIRAYAMA** *(Tokai Univ.)*, **and Hiroshi OGAWA** *(Saga Univ.)*

Various nonstoichiometric materials have been prepared from gaseous compounds by plasma CVD. We have prepared amorphous thin films from $Fe(CO)_5$ and SiH_4 by using this method. Uniform films were formed on various substrates. Their growth rates were 150~500 A/min. The color of the films depends on the flow ratio. Figure 1 shows the dependence of the optical band gap of those films on the flow ratio of $Fe(CO)_5$ and SiH_4. The films are conductive. In the same Figure, the resistivity of the films are shown against the flow ratio. Interestingly, the resistivity of the films remains small even when the flow ratio, $SiH_4/Fe(CO)_5$, is increased up to 10^2. These films contains a small quantity of Fe and O. They showed p-type semiconductivity. For p-type amorphous Si, boron is commonly used as a dopant. The resistivity of boron depod a-Si is about 10^3 ohm cm for the flow ratio of B_2H_4/SiH_4 = 10^{-2}. On the other hand, the resistivity of the present film is about 10^2 ohm cm for $Fe(CO)_5/SiH_4$ as shown in Figure 1. This result indicates that the present film has a excellent electrical property.

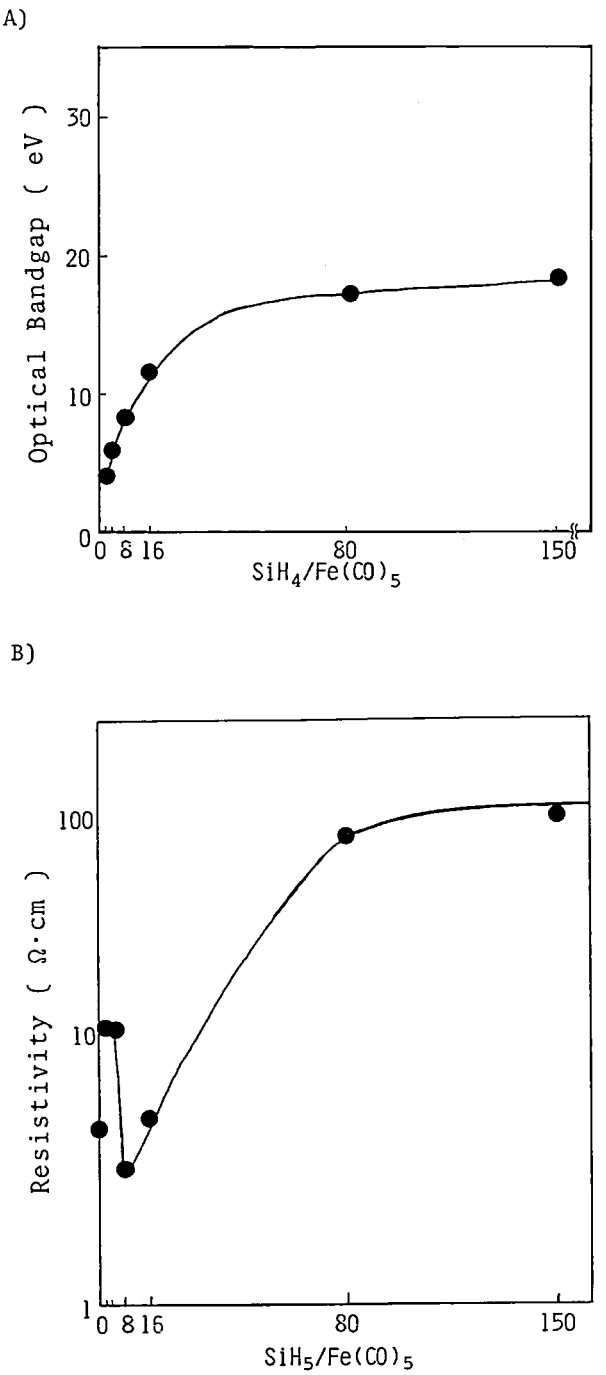

Figure 1. The dependence of optical band gap (A) and resistivity (B) on the flow ratio of $SiH_4/Fe(CO)_5$.

III-E-4 pH Effect on Electrochemical and Photoelectrochemical Reaction Products of Lactic Acid

Hisashi HARADA *(Meisei Univ.)*, **Tadayoshi SAKATA, and Toyotoshi UEDA** *(Meisei Univ.)*

Semiconductor dependence of the photocatalytic reactions of lactic acid have been reported[1]; for Pt/TiO_2, the main products were H_2, CO_2 and CH_3CHO, whereas for Pt/CdS they were H_2 and $CH_3COCOOH$. The similar reaction selectivity was also observed in the photoanodic reactions. In order to elucidate the mechanism of this selectivity, pH effect was investigated on the photoanodic (TiO_2) and dark-potentiostatic (Pt and glassy carbon) reactions.

Figure 1 shows the pH dependence on photoanodic reaction products using TiO_2 electrode. When the pH value of the solution was above 12, the major product was the pyruvic acid instead of acetaldehyde. The ratio of products was changed suddenly in the narrow pH range (11 to 13). On the other hand, in the electrochemical reactions with a Pt electrode, pH dependence was a little bit different from that for TiO_2, although pyruvic acid became the major product at a high pH region. The amount of pyruvic acid increased gradually with increasing pH, while the that of acetaldehyde decreased through a wide pHrange (6 to 12). Inter-

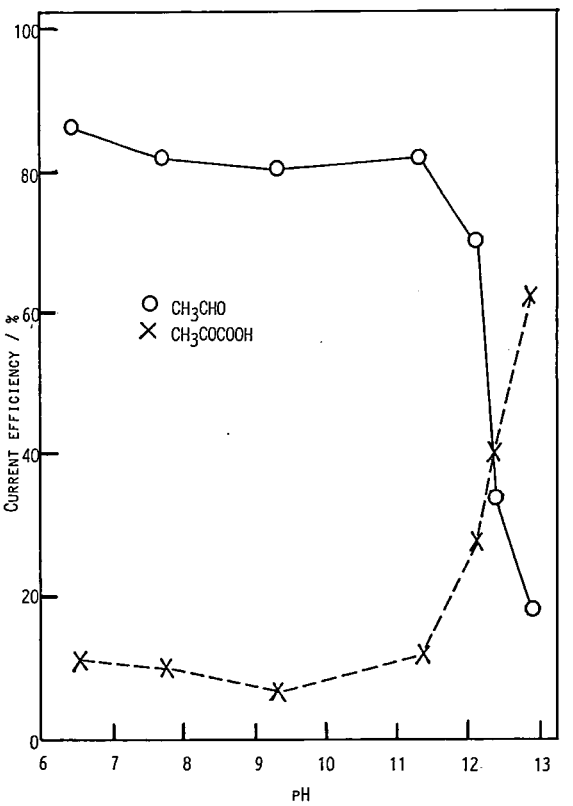

Figure 1. pH dependence on photoanodic reaction products of sodium lactate on TiO_2 electrode. Amount of electricity: 9.65C, supporting electrolyte: K_2SO_4(0.1M), applied potential: 1.3V vs. SCE, irradiation source: 1-kW Xe lamp (500 W operation).

estingly, on a glassy carbon electrode acetaldehyde remained to be the main product even at a high pH region. Thus each electrode showed different characteristic pH dependence. Different electrochemical properties was observed on the i-V curves for the oxidation of sodium lactate with a Pt and glassy carbon electrodes.

These results indicate that the adsorption and electrocatalytic properties of reactants on a semiconductor or metal surface are important to control the reactions.

Reference

1) H. Harada, T. Sakata and T. Ueda, *J. Am. Chem. Soc.*, **107**, 1773 (1985).

III-E-5 Luminescence Decays of Ru(II) Complexes Adsorbed on Metal Oxide Powder in Vacuo: Energy Gap Dependence of Electron Transfer Rate

Kazuhito HASHIMOTO, Masahiro HIRAMOTO, and Tadayoshi SAKATA

Luminescence decays of $Ru(bpy)_3^{2+}$ and $Ru(bpz)_3^{2+}$ adsorbed on powdered SiO_2, $SrTiO_3$, TiO_2(anatase), TiO_2(rutile), ZnO and SnO_2 were measured in vacuo. The decay curves depended on the substrates, and were fitted with the sum of four exponentials. Electron transfer rates from the excited state of the Ru(II) complexes to semiconductor were calculated from the decay rates and were plotted versus energy difference of the redox potential for excited state of the complexes and band edge of the conduction band of semiconductors. Each complex on the different adsorption site has a different electron transfer rate, but the energy gap dependence is almost parallel for these four components, suggesting that it is not the FC factor but electron matrix element that is changed for the different adsorption species. Moreover, the electron transfer rate of each component is smoothy related with the energy level of the conduction band edge of semiconductor as shown in Figure 1. The rate increases slightly with a larger energy difference, and even in the region that the energy difference is more than 1 eV the rate still increases. This may be the first observation of the energy dependence of the electron transfer rate from adsorbed molecule to inorganic semiconductor.

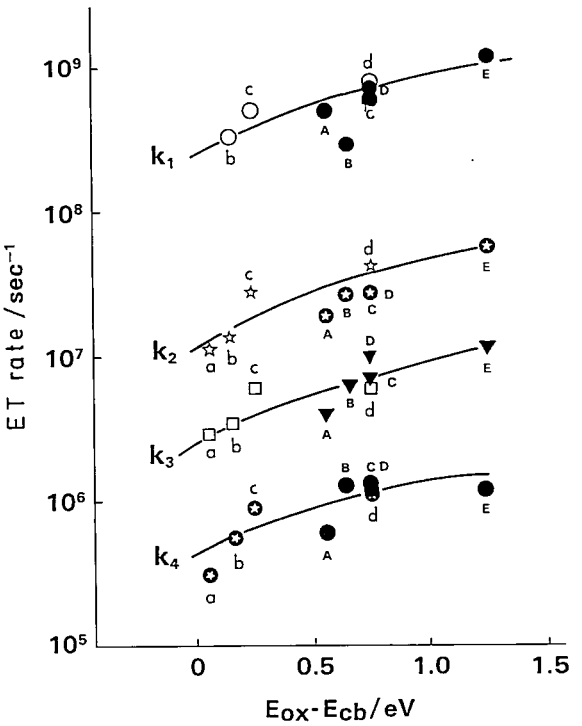

Figure 1. Dependence of electron transfer rates from photoexcited Ru(II) complexes to semiconductors on the energy difference.

III-E-6 Photoinduced Electron Transfer and Photoluminescence Quenching of ZnS Particles Deposited on Porous Vycor Glass

Masahiro HIRAMOTO, Kazuhito HASHIMOTO, Tadayoshi SAKATA, and Shozo YANAGIDA *(Osaka Univ.)*

Photoinduced electron transfer processes between ZnS particles deposited on porous Vycor glass (ZnS/PVG) and various redox species were investigated by measuring the luminescence quenching. An intense photoluminescence was observed at 520 nm for ZnS/PVG after a heat treatment (Figure 1(a)). The time-resolved spectrum of the luminescence shifted to longer wavelengths with time, indicating that the luminescence was due to a transition between a donor-acceptor pair. Although most electron donors hardly quench the luminescence, many electron acceptors such as oxygen, methyl viologen, benzoquinone, etc. effectively quench it. The quenching effect of oxygen is shown in Figure 1. Luminescence decay measurements revealed that the

quenching was static for any type acceptor. These results can be explained on the basis of a donor-acceptor pair model. In this model, an isolated coactivator, such as Cl, works as a donor and a Zn vacancy with a nearest-neighbor coactivator, works as an acceptor; the luminescence is due to a transition between a donor-acceptor pair. The quenching mechanism is discussed in relation to an electron transfer between electrons in the conduction band of ZnS and electron acceptors on the surface.

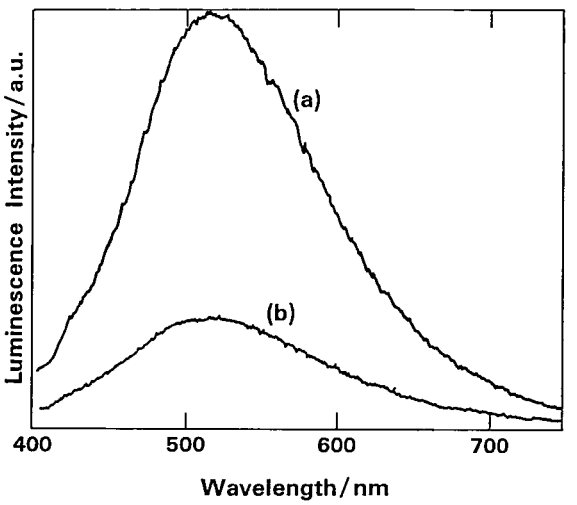

Figure 1. Photoluminescence spectra of ZnS/PVG after a heat treatment in a He atmosphere at 500°C for 30 min. (a) Under vacuum (1×10^{-5} Torr). (b) Under an O_2 atmosphere (0.66 atm). Excitation wavelength is 350 nm.

III-E-7 Photoluminescence Dynamics of CdS Particles Deposited on Porous Vycor Glass — Temperature Dependence of Interfacial Electron-Transfer Rate

Masahiro HIRAMOTO, Kazuhito HASHIMOTO, and Tadayoshi SAKATA

[*Chem. Phys. Lett.*, **133**, 440 (1987)]

Photoinduced electron transfer between semiconductor and redox species in an electrolyte is one of the elementary processes in electrochemical cells, photocatalysis. Recently, we reported that the red emission of CdS particles deposited on porous Vycor glass (CdS/PVG) was effectively quenched by electron acceptors adsorbed on the CdS surface, such as benzoquinone, methyl viologen, Fe^{3+}, and the quenching ratio was related with the electron-transfer rate between CdS and the acceptor. Here, we report the

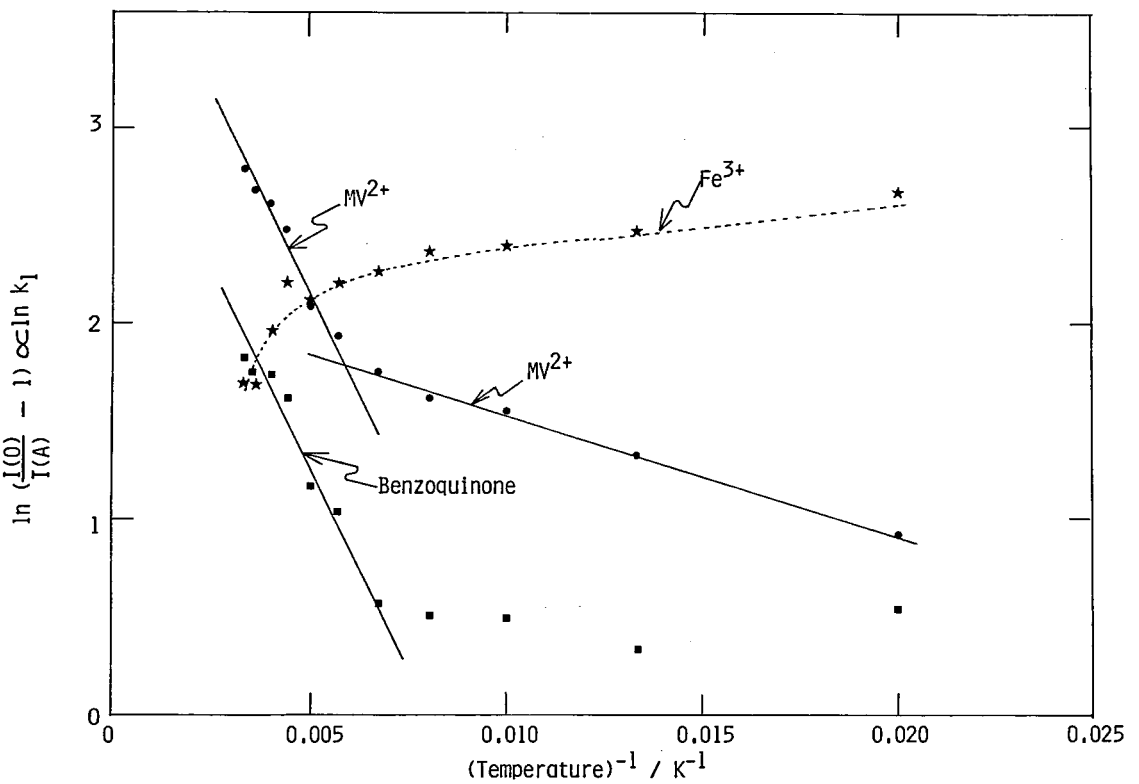

Figure 1. Temperature dependence of the quenching ratio ($\ln[I(O)/I(A)-1]$) for methyl viologen, benzoquinone, and Fe^{3+}. I(A) and I(0) denote the photoluminescence intensity at 800 nm with and without electron acceptors, respectively. Quenching ratio is proportional to the interfacial electron-transfer rate (k_1).

temperature dependence of this interfacial electron-transfer rate.

The intensity of the red emission of CdS/PVG located around 800 nm (I(0)) increased about 11 times by lowering the temperature below 100 K. The intensity of the red emission which was quenched by electron acceptors (I(A)) also increased by cooling and their temperature dependence much depend on the kind of acceptors. Recently, we presented the SA (self-activated) center model in which the emission center is a Cd vacancy associated with a halogen atom. In this model, the quenching ratio $(I(0)/I(A))-1$ is proportional to the electron-transfer rate (k_1) between electrons in the conduction band of CdS and adsorbed electron acceptors. Thus, we can plot the temperature dependence of k_1 (Figure 1). In the case of benzoquinone and methyl viologen, k_1 decreased and finally became constant by lowering the temperature. However, in the case of Fe^{3+}, k_1 increased by lowering the temperature.

III-E-8 Luminescence Decays and Spectra of $Ru(bpy)_3^{2+}$ Adsorbed on TiO_2 in Vacuo and in the Presence of Water Vapor

Kazuhito HASHIMOTO, Masahiro HIRAMOTO, Takashi KAJIWARA *(Toho Univ.)*, **and Tadayoshi SAKATA**

The luminescence of $Ru(bpy)_3^{2+}$ was quenched strongly on TiO_2 and its decay rate was increased remarkably due to electron transfer from the excited $Ru(bpy)_3^{2+}$ to TiO_2. The decay curve was nonexponenetial and could be analyzed with a sum of four exponentials. Each decay component was ascribed to the luminescence from an adsorption species on a different site. The time resolved spectra of the faster decay components were shifted to shorter wavelength by about 500 cm^{-1} compared to those of the slower ones. On introducing water vapor into the system, the decay rate of the fastest component became slower, indicating that the electron transfer from the photoex-

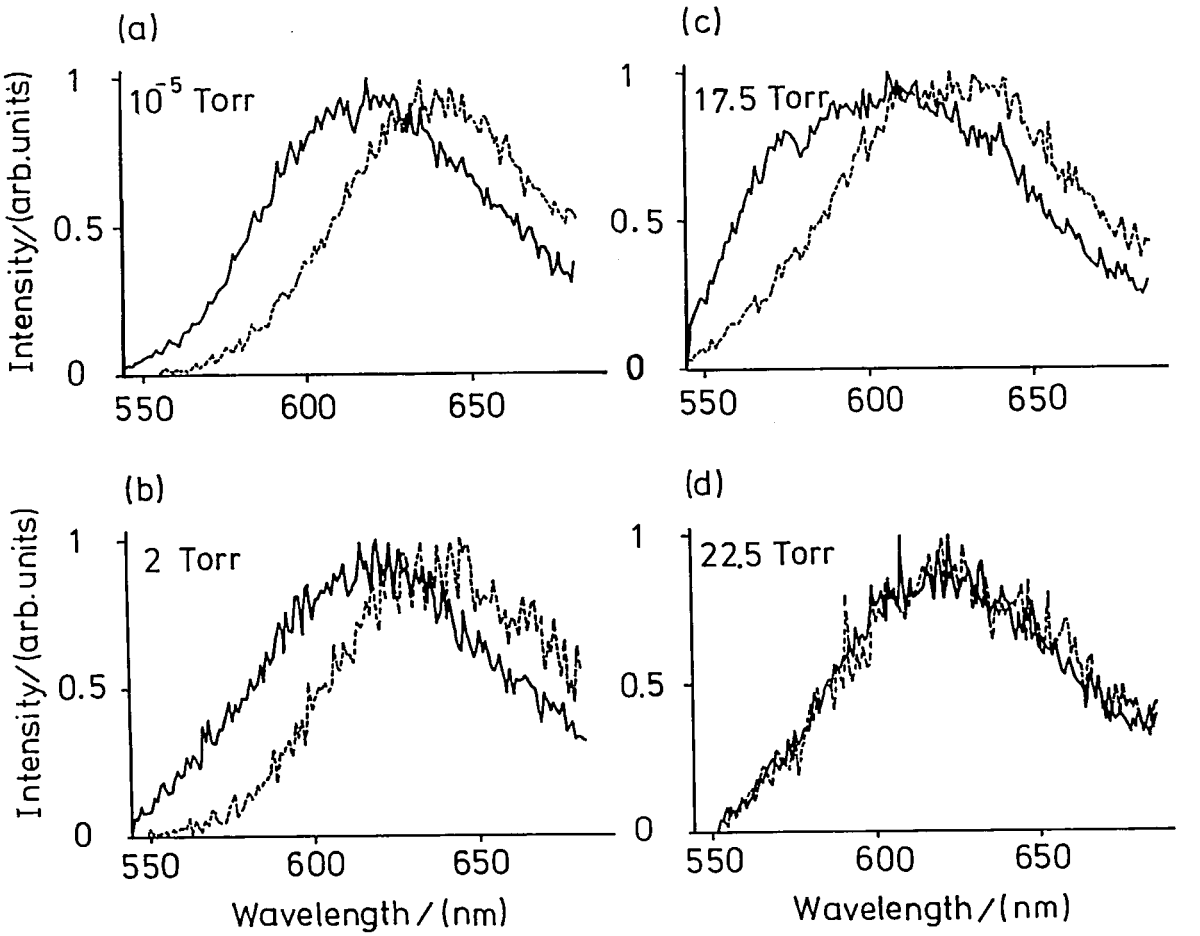

Figure 1. Time resolved spectra of luminescence from $Ru(bpy)_3^{2+}$ adsorbed on TiO_2 in the presence of water vapor. Gated at the time range of 0 to 20 ns (solid lines) and 500 to 1000 ns (dotted lines) after excitation.

cited $Ru(bpy)_3^{2+}$ adsorbed on the most favorable site for the electron transfer to TiO_2 substrate was decreased by the solvation effect of water. When the vapor pressure exceeded the saturated value, the blue shift of the faster decay components disappeared and the time resolved spectra of the faster decay component became almost the same as those of the slower ones (Figure 1). These results show that the interaction of the Ru complex and TiO_2 surface is decreased by the physisorbed water molecule on the surface.

III-F Dynamical Processes in Electronically and/or Vibrationally Excited Molecules

III-F-1 Formation and Identification of Carbon Molecules in Low-Temperature Rare-Gas Matrices.

Teruhiko NISHIYA, Masaaki BABA *(Kobe Univ.)*, **and Ichiro HANAZAKI**

Spectroscopic properties of carbon molecules (C_n) in the gas phase have not yet been studied for $n \geqq 4$, because of the difficulty in obtaining such clusters with reasonable concentration in the vapor phase.

Matrix isolation is an alternative method for the spectroscopic study of such a system. It offers specific isolated condition by controlling initial sample concentration and/or by annealing the matrices. We evaporated C_n by resistance-heating of two graphite rods at the contact point.

In Figure 1, bands around 410 nm are assigned to the $^1\Pi_u \leftarrow {}^1\Sigma_g^+$ transition of C_3. By exciting the 247 nm band, we obtained two emission bands around 327 and 650 nm. These are thought to be the emission from the relaxed excited states of a cluster larger than C_3, since the absorption intensity increased with the initial sample concentration. Other absorption features around 311 and 492 nm may be due to larger clusters than that of the 247 nm band. We are now trying another evaporation method and investigating the effect of annealing to identify these absorption bands.

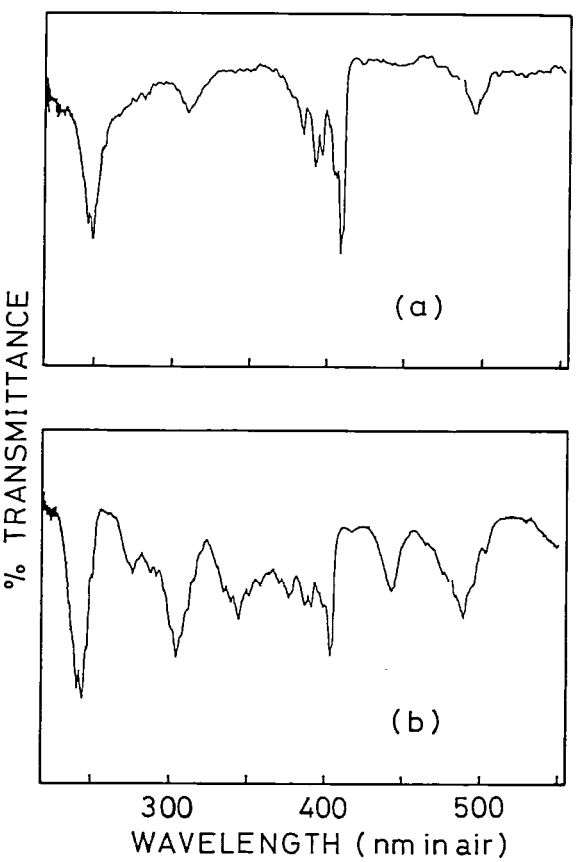

Figure 1. Absorption spectra of C_n in Ar matrices at 20 K with low (a) and high (b) initial concentrations.

III-F-2 REMPI Studies of Metastable Species

Graham BLACK *(SRI International and IMS)*, **Teruhiko NISHIYA, and Ichiro HANAZAKI**

[*Chem. Phys. Lett.*, in press]

The REMPI (resonance-enhanced multiphoton ionization) technique has been applied to the study of metastable species originating in a microwave discharge in N_2. In the absence of the discharge, ionization signals arise from (2 + 2) ionization of N_2 ($v'' = 0$) *via* various vibrational levels of the $a^1\Pi_g$ state. Such spectra have been previously reported[1,2] for N_2.

When the discharge is activated, and the flow time to the laser interaction region is <10 ms, many new spectral features are observed (Figure 1). The strongest of these arises from very highly vibrationally excited

nitrogen (v'' = 23–26) which are photoionized *via* the $a^1\Pi_g$ state in a (1 + 1) process. These findings have been further confirmed by a study of the power dependences of the various photoionization processes.

References

1) N. van Veen, P. Brewer, P. Das and R. Bersohn, *J. Chem. Phys.*, **77**, 4326 (1982).
2) S.T. Pratt, P.M. Dehmer and J.L. Dehmer, *J. Chem. Phys.*, **81**, 3444 (1984).

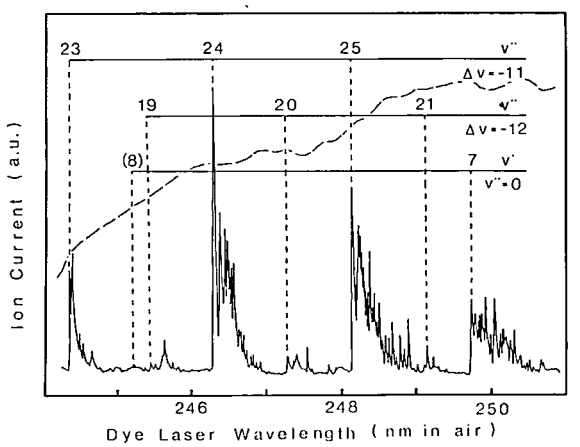

Figure 1. Low resolution REMPI spectrum of nitrogen subjected to a microwave discharge.

III-F-3 Multiphoton Ionization Study of Aliphatic Carbonyl Molecules

Masaaki BABA *(Kobe Univ.)*, **Teruhiko NISHIYA and Ichiro HANAZAKI**

The multiphoton ionization spectra of aliphatic carbonyl compounds have been observed in a supersonic nozzle beam. In the previous study we have shown the laser induced fluorescence excitation spectra (LIF) near the 0–0 band of the $S_1(n, \pi^*)$ state. We found that the sharp vibronic bands could not be observed at higher energy region. It is considered that the predissociation takes place during relatively long radiative lifetimes of the S_1 states.

We observed the multiphoton ionization (MPI) spectra of acetaldehyde and cyclobutanone in an Ar supersonic pulse nozzle beam. Figure 1 shows the LIF and MPI spectra. The spectral features are very similar, although the relative intensities of several bands are different. Again we could not observe sharp vibronic features above the predissociation limit. It indicates that the rate of depopulation of the $S_1(n, \pi^*)$ state by predissociation is even faster than the ionization process. This result seems to be consistent with the previous results of the MPI mass spectroscopy at 248 nm[1].

Reference

1) M. Baba *et al.*, *Chem. Phys.*, **83**, (1984) 221.

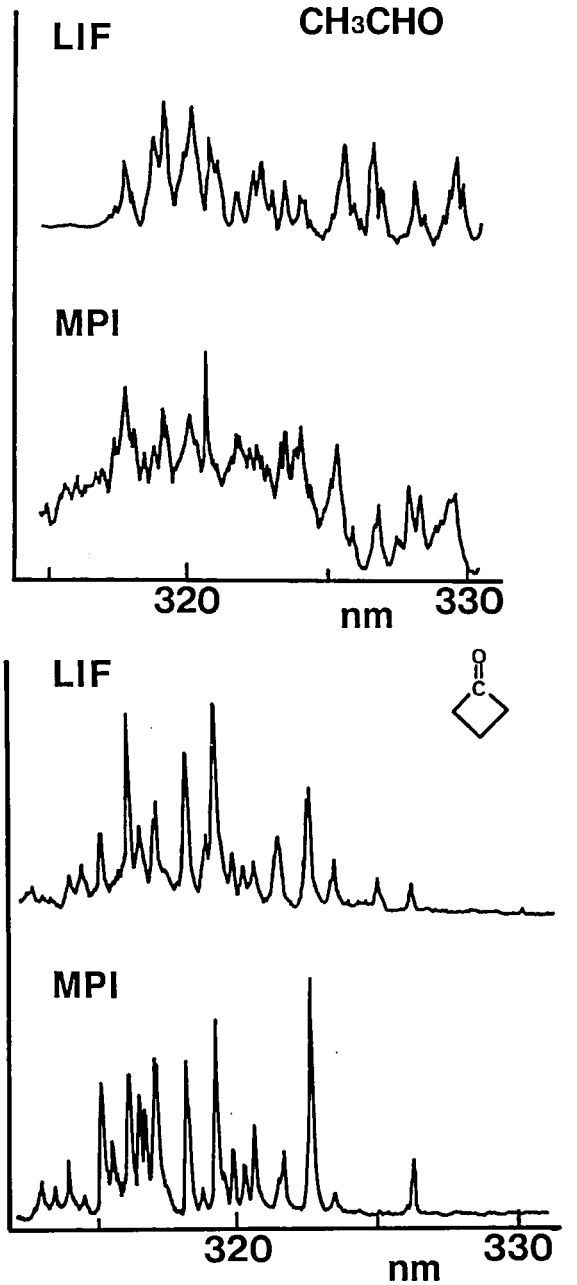

Figure 1. LIF and MPI spectra of S_1 (n, π^*) acetaldehyde and cyclobutanone.

III-F-4 Laser Fluence Dependence of Infrared Photodissociation of Benzene Dimers

Masao TAKAYANAGI, Hiroshi OHOYAMA and Ichiro HANAZAKI

We reported previously the dissociation spectra of benzene dimer in a supersonic molecular beam (IMS Annual Review 1983, 1984). We have suggested the observed power broadening would contain the information on the IVR and photodissociation processes. However there remains possibility that the broadening is only apparent, being caused by the existence of the larger clusters and/or by an inappropriate correction for the velocity distribution of the parent beam.

Therefore we have recently reexamined the broadening very carefully by choosing the source condition which minimizes the contributions from larger clusters and by applying careful correction for the velocity distribution and laser profile. The result is illustrated in Figure 1, where the solid curve represents the results simulated assuming a constant cross section for dissociation. The good agreement with the experimental values suggests that the broadening previously reported is only apparent, mainly due to an inappropriate treatment in the velocity distribution correction. We are now investigating hetero dimers to see the effect of the excitation energy to the dissociation probability of van der Waals molecules.

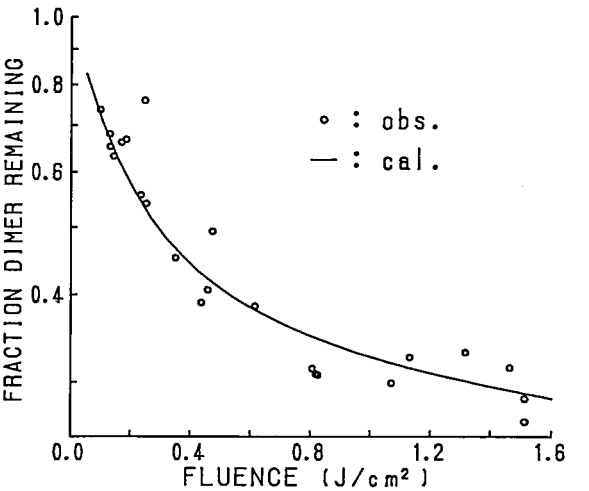

Figure 1. Observed and calculated laser fluence dependence of infrared photodissociation of benzene dimers.

III-G Mass Spectrometrical Study of Molecular Association in Aqueous Solution Systems

The "Flickering Cluster" model, proposed by Frank and Wen and by Nemethy and Scheraga, has been shown to describe various properties of liquids very well. Hydrogen bond formation of water molecules in aqueous solutions is thought to form clusters with "ice-like" structure which are stabilized by the presence of hydrophobic groups. Understanding of the chemistry of aqueous solutions in terms of "fragments" is highly necessary for analyzing the real situation since measurement of overall average properties of a solution does not provide realistic information on the local structure.

Simple adiabatic expansion of a drop of liquid in vacuum causes instantaneous fragmentation by dissociating molecules which are weakly bound to hydrogen-bonded clusters through van der Waals forces. Evaporation of weakly bound or "freely rotating" molecules cools the clusters by the transfer of internal energy to kinetic energy. In the expansion process, the relative distance between free molecules and clusters gets longer very quickly. The cluster beams are detected mass spectrometrically after the electron impact ionization. Although electron impact dissociates relatively weak intermolecular bond(s) of parent clusters to some extent, the detected ions are still "fragments" of the liquids.

Here we report the characteristics of molecular association in aqueous systems studied by this technique.

III-G-1 Highly Stable Kempter-Mecke Sequence of Ethanol Olygomers $(C_2H_5OH)_n$ in Aqueous Solution

Nobuyuki NISHI, Kunimasa KOGA *(Suntory Res. Inst.)*, **Chikako OHSHIMA** *(Suntory Res. Inst.)*, **Kazunori YAMAMOTO, and Kenzo NAGAMI** *(Suntory Res. Inst.)*

Cluster composition in ethanol-water mixed solutions has been investigated by the mass spectrometrical analysis of the cluster beams produced by adiabatic expansion of the solutions in vacuum. According to the ab-initio studies, hydrogen-bonding energy of ethanol-ethanol dimer is about the same as those of ethanol-water complex and water-water dimer (5.4~5.8 kcal/mol). Nevertheless, the aqueous solutions with ethanol mole fractions higher than 0.03 were found to be composed of ethanol polymer chains $(C_2H_5OH)_n$ which destroy "ice-like" water clusters contrary to the well-known former explanation. Figure 1 shows the cluster spectra of three different solutions at an liquid temperature of 80°C. The spectra are composed of the main sequence of the protonated $(C_2H_5OH)_n$ species (Kempter-Mecke sequence). The bottom spectrum of the solution with 10% ethanol volume-content reveals the water sequences attached to the alcohol polymers. At lower temperatures, however, the coordinated water signals became weaker and the dehydrated polymer sequence grew as if the ethanol concentration was apparently increased. The spectrum of the 10% ethanol system at 40°C was similar to that of the 20% system at 80°C (Figure 1-B). Liquid ethanol (99.6%) showed very weak polymer signals, while the addition of 10% of water in neat ethanol grew the polymer species drastically. Formation of ethanol polymer chains requires surrounding water molecules.

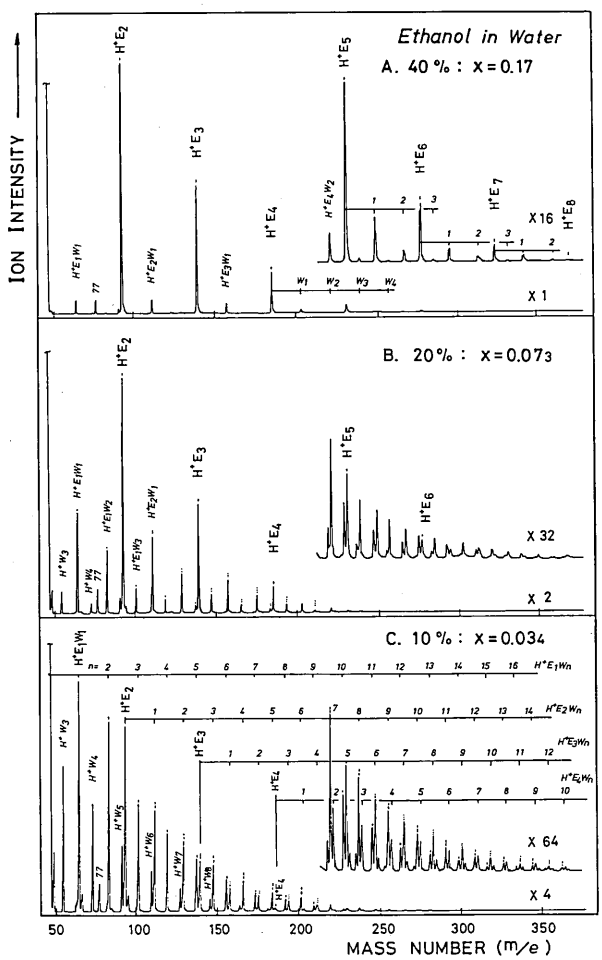

Figure 1. Mass spectra of the cluster beams generated from ethanol-water solution at 80°C. Ethanol concentration is A: 40 vol.%, B: 20 vol.%, and C: 10 vol.%. The water sequences which follows the ethanol monomer, dimer, trimer, and tetramer ion signals become weaker in lower temperature spectra where the non-hydrated ethanol-polymer signals are dominant.

III-G-2 Enthalpy Changes of Cluster Formation Processes in Aqueous Solution

Nobuyuki NISHI and Kazunori YAMAMOTO

An aqueous solution of ethanol with an alcohol mole fraction of 0.01 showed complicated cluster spectra due to the appearance of hydrated higher-order oligomers at lower temperatures. At higher temperatures, monomer-hydrates and pure water signals became stronger. The change of the cluster compositon is originated in the change of the equilibrium of the cluster evolution-destruction processes in a liquid, such as;

$$(H_2O)_n + A \underset{}{\overset{K_1^n}{\rightleftarrows}} A(H_2O)_{n-1} + H_2O, \quad (1)$$

and,

$$A(H_2O)_n + A \overset{K_2^n}{\rightleftarrows} A_2(H_2O)_{n-1} + H_2O. \quad (2)$$

The equilibrium constant, K_i^n, is related to the enthalpy and entropy changes (ΔH_i^n and ΔS_i^n) of the above processes.

$$\ln K_i^n = -(\Delta H_i^n/R)(1/T) + \Delta S_i^n/R. \quad (3)$$

This equation is rewritten in terms of the observed intensity ratio:

$$\ln \frac{[H^+A_i(H_2O)_{n-s-1}]}{[H^+A_{i-1}(H_2O)_{n-s}]} = -(\Delta H_i^n/R)(1/T) + \Delta S_i^n/R + \ln x_1/x_2. \quad (4)$$

Thus, the logarithmic plot of the intensity ratios against T^{-1} gives the enthalpy and the entropy changes of an exchange process. Figure 1 summarizes the obtained enthalpy changes for the above exchange processes and water-molecule attachment-detachment processes. Important is that the stabilization energies for the addition of one ethanol molecule to pure water clusters are

nearly the same as those for the ethanol-addition to monomer-hydrates and dimer-hydrates (~4.5 ± 0.9 kcal/mol). The observed trend of ethanol-ethanol association is attributed to the hydrophobic hydration of an ethyl group in aqueous environment.

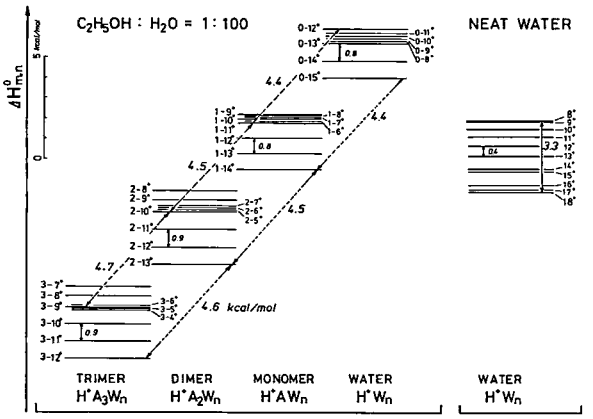

Figure 1. Enthalpy changes for molecular exchange processes (eqs. (1) and (2), shown by dotted arrows) and for water attachment processes in an ethanol-water (1:100) solution. Errors for the respective values are ±0.3 kcal/mol. For a comparison, enthalpy changes of water attachment processes in pure water are shown with the values reliable.

III-G-3 Stability of Hydrated Binary Clusters in Solution

Nobuyuki NISHI and Kazunori YAMAMOTO

Isolation of molecular clusters from solution by the adiabatic expansion method made it possible to determine the stability of hydrated clusters formed in liquid environment. If the intermolecular interaction in a solution is equivalent for all molecular pairs, a stochastic distribution of solute and solvent molecules in the detected clusters is expected. In this model, the population ratio of the $A_{r+1}W_{n-1}$ cluster to the A_rW_n cluster is expressed as; $[A_{r+1}W_{n-1}]/[A_rW_n] = (n/(r+1))(x_A/x_W)$, (1), where x_A and x_W are the mole fractions of solute and solvent, respectively. Namely, the population ratio is proportional to the number of solvent molecules (n) in the cluster A_rW_n and to the molar ratio of solute to solvent. Based on the model, the stability constant of hydrated clusters ($\varkappa_{r+1}$) was defined:

$\varkappa_{r+1}=([H^+A_{r+1}W_{n'-1}]/[H^+A_rW_{n'}])((r+1)/(n'-n_0))(x_W/x_A)$,

where n' is the number of water molecules in the observed ion and $-n_0$ is the number of lost water molecules on ionization. The plots of the ion intensity ratios against n' showed linear slopes which originate at n_0. The slope gives the value of $\varkappa_{r+1}$ that indicates the degree of deviation from the stochastic model. Larger values mean higher stability of the hydrated clusters. The obtained values are listed in Table 1. Among 13 solute species, alcohols and carboxylic acids showed higher stabilities, but even among the alcohols the stability varies largely indicating that the role of the

Table 1. Stability of monomer hydrate-clusters and dimer hydrate-clusters in aqueous solutions represented as observed abundances of the respective hydrate-clusters relative to stochastic abundance expected. The solutions are at 65°C under a pressure of 3.0 bar. Definitions of $\varkappa_1$, $\varkappa_2$, and n_0 are given in the text.

Solute species	$\varkappa_1$ Stability of monomer hydrates	$\varkappa_2$ Stability of dimer hydrates	Cluster size valid for $\varkappa_1$	n_0
CH_3OH	4.0	4.0	$4 \leq n \leq 19$	−3
C_2H_5OH	5.3	8.4	$4 \leq n \leq 13$	−1
iso-C_3H_7OH	5.2	8.0	$2 \leq n \leq 14$	−1
$HOCH_2CH_2OH$	1.6	2.7	$2 \leq n \leq 8$	−1
HCOOH	7.5	8.4	$14 \leq n \leq 18$	−2
CH_3COOH	5.9	8.0	$4 \leq n \leq 10$	−2
CH_3NH_2	1.3	0.9	$5 \leq n \leq 14$	−1
$C_2H_5NH_2$*	1.4	1.0	$5 \leq n \leq 14$	−1
H_2NCHO*	1.8	1.9	$5 \leq n \leq 14$	−2
CH_3NHCHO	1.3	1.6	$5 \leq n \leq 11$	−2
$CH_3NHCOCH_3$	0.5	–	$5 \leq n \leq 15$	−2
CH_3CN	0.003	–	$6 \leq n \leq 20$	−1
CH_3COCH_3	0.19	–	$9 \leq n \leq 19$	−1
Stochastic Model	1.0	1.0		−1

* in D_2O solution.

hydrophobic group is of great importance to the stabilization.

III-G-4 Molecular Association in Aqueous Solution of Formic and Propionic Acids

Kazunori YAMAMOTO and Nobuyuki NISHI

Molecular association in aqueous solution of carboxylic acids has been studied by means of the mass spectrometry of the cluster beams generated through the adiabatic expansion of liquid jets of binary solutions. Cluster composition was measured at various liquid temperatures and the enthalpy changes of the following reactions were obtained from the van't Hoff plots of ion intensity ratios. A: water-solute exchange reaction; $(RCOOH)_m(H_2O)_n + RCOOH \rightleftharpoons (RCOOH)_{m+1}(H_2O)_{n-1} + H_2O$, B: water attachment reaction; $(RCOOH)_m(H_2O)_n + H_2O \rightleftharpoons (RCOOH)_m(H_2O)_{n+1}$. The results of the analyses are summarized in Figure 1. In an aqueous solution of HCOOH with $[HCOOH]/[H_2O] = 0.005$, all water attachment reactions are exothermic ($\Delta H \sim -0.3$ kcal/mol), which is almost the same as those in neat water. On the contrary, all the water-solute exchange reactions are endothermic ($\Delta H \sim 1.0$ kcal/mol). This indicates that the carboxylic group changes the hydrogen bonding networks of water molecules. In an aqueous solutions of C_2H_5COOH with $[C_2H_5COOH]/[H_2O] = 0.005$, the situation changes drastically. In this system, the water attachment reactions are endothermic ($\Delta H \sim 0.3$ kcal/mol) and the water-solute exchange reactions are exothermic ($\Delta H \sim 2.3$ kcal/mol). Propionic acid has an ethyl group, so the observed trend of the stabilization for the addition of one propionic acid to pure water clusters, $(H_2O)_n$, and to monomer-hydrate clusters, $C_2H_5COOH(H_2O)_n$, are attributed to the hydrophobic hydration of an ethyl group in aqueous environment.

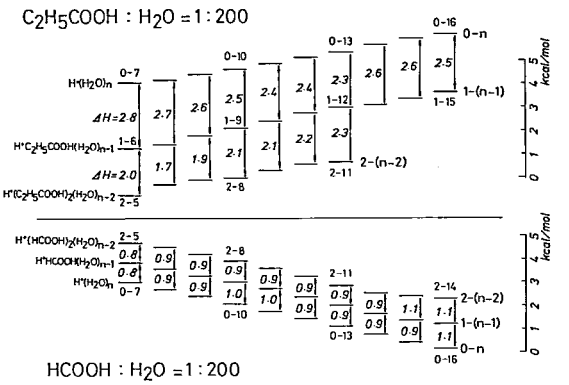

Figure 1. Enthalpy changes for water-solute exchange processes and for water attachment processes in a propionic acid-water (1:200) solution (top) and a formic acid-water (1:200) solution (bottom). It is expected that the clusters with two excess water molecules are the parent species of these cluster ions, [m-n = $H^+(RCOOH)_m(H_2O)_n$].

III-H Study of Molecular Clusters through Wavelength Selected One-photon and/or Multi-photon Ionization Method

Advent of wavelength-tunable high power UV lasers has opened the door of the new field. We have started the study of the electronic structure and excited state chemistry of molecular clusters by using high-resolution UV lasers as well as conventional VUV light sources.

III-H-1 Resonance-Enhanced 2PI Detection of Ammonia Clusters via a Linear Reflectron TOF Mass Spectrometer

Hisanori SHINOHARA and Nobuyuki NISHI

Ammonia clusters, produced via adiabatic expansion, are resonantly two-photon ionized by using a tunable pulsed UV dye laser (208~215 nm) and are subjected to time-of-flight (TOF) mass analysis equipped with a linear ion reflector. The linear reflectron has an ion reflector to compensate for the initial spread of ion velocities in the acceleration region and thus provides high mass resolution even with the present short drift-free length (53.6 cm). The technique produces a whole cluster mass spectrum with a single laser shot and yet exhibits a high mass resolution which

is essential to the study of the ion-molecule reactions of the ammonia clusters.

Figure 1 shows a vibronic TOF mass spectrum of the ammonia clusters and monomer over the wavelength region studied. The ion signal variation of the monomer upon exciting wavelength exactly reproduce a known vibronic transition of ammonia, $\tilde{A}^1A_2''(v=2)$, which has the absorption maximum at 208.9 nm. The clusters behave differently. The fact that all of the observed clusters (from dimer to heptamer) show a similar intensity dependence on laser wavelength seems to suggest that properties of the electronic excited states of the various clusters are primarily governed by those of the dimer unit, at least in the wavelength region investigated.

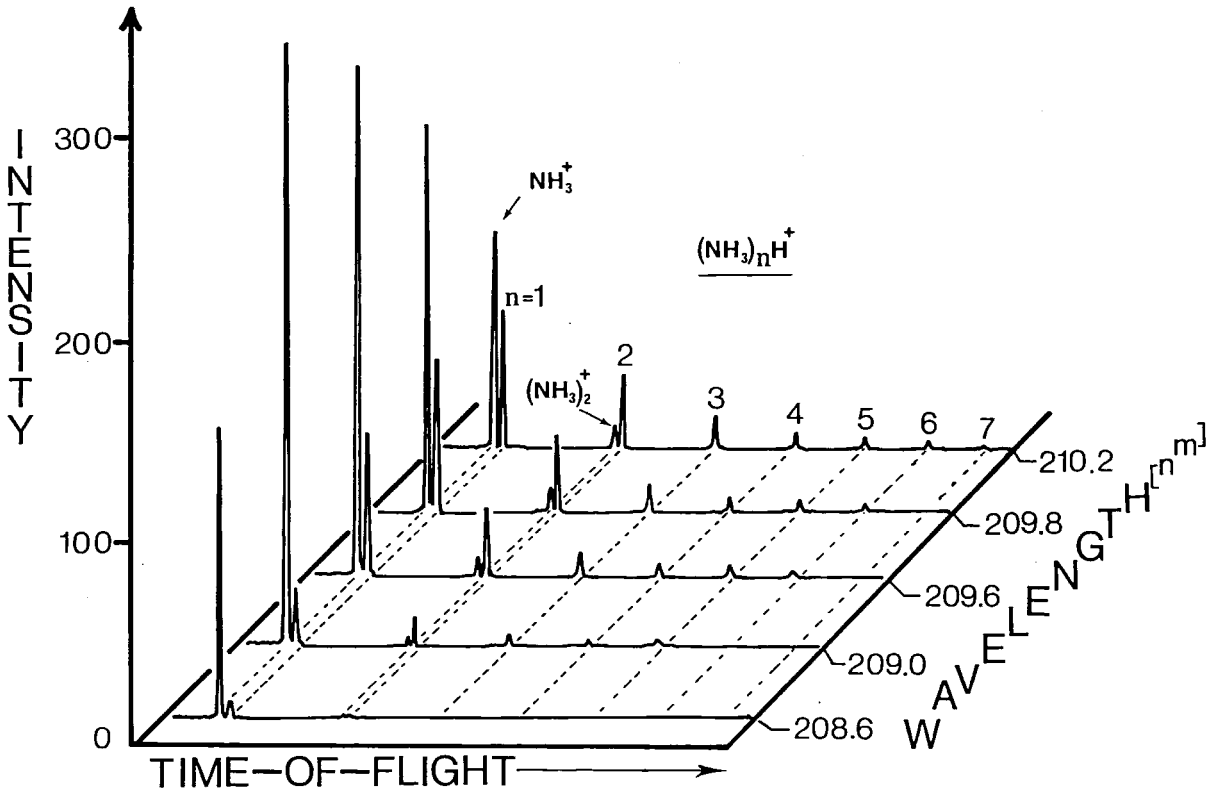

Figure 1. Two-dimentional resonance-enhanced 2PI vibronic mass spectrum of ammonia clusters in the wavelength region 208.6~210.2 nm. Nozzle conditions: neat NH_3 expansion at a backing pressure of 1.2 atm and 31°C nozzle temperature.

III-H-2 Higher Electronic Excited States of Benzene Clusters

Hisanori SHINOHARA and Nobuyuki NISHI

Benzene and benzene clusters are resonantly two-photon ionized in a linear TOF reflectron mass spectrometer by incorporating a tunable pulsed UV dye laser. Figure 1 displays time-of-flight (TOF) mass spectra obtained by using two different exciting laser wavelengths. In the excitation of the $S_1(^1B_{2u})$ state, the spectrum exhibits the conventional various types of the fragment ions (C_1~C_5) in addition to the parent benzene ion (cf. Figure 1-(a)). Benzene dimer ion, $(C_6H_6)_2^+$, appears only very weakly in the spectrum as compared with the monomer and the fragment ions, and the larger cluster ions are not seen at this spectral sensitivity.

By exciting the onset of the higher electronic excited state (S_2), however, the spectrum gives an entirely different feature (Figure 1-(b)). The intensity of the fragment ions is greatly reduced to such an extent that the various fragment ions other than the C_4^+ series are almost missing. What is more important in the spectrum is that the cluster ions, $(C_6H_6)_n^+$, up to the heptamer can be observed and the signal intensity of the dimer ion is particularly enhanced. By scanning the

laser wavelength, it has been found that a similar spectral feature was obtained at the wavelength regions down to 215 nm where the molecular fragment ions are totally absent. The higher electronic excited states of the various benzene clusters (corresponding to the $^1B_{1u}$ state of the monomer) are shifted to the red by at least several nanometers.

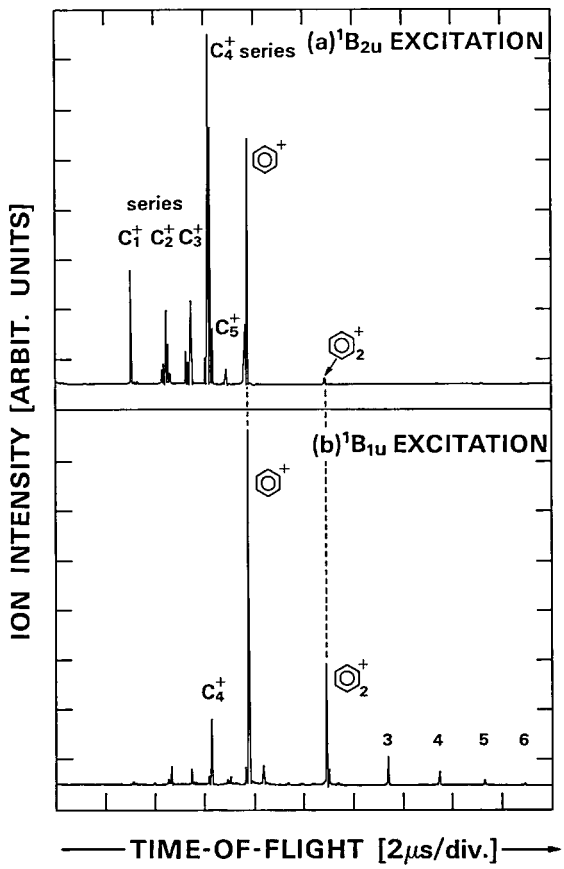

Figure 1. Resonance-enhanced 2PI time-of-flight mass spectrum of benzene and benzene clusters at two different laser excitations under otherwise similar experimental conditions: (a) S_1(243.11 nm), (b) S_2(211.0 nm). Experimental conditions: 63 μJ/pulse laser intensity, Ar-seeded 900 Torr stagnation pressure, and 40°C nozzle temperature. Each TOF spectrum was obtained by 500 laser shots.

III-H-3 Extensive MPI Fragmentation of Benzene Clusters

Hisanori SHINOHARA and Nobuyuki NISHI

Extensive multiphoton-ionization (MPI) fragmentation of benzene clusters have been observed, for the first time, in a linear reflectron time-of-flight (TOF) mass spectrometer under intense laser irradiation. Additional several photons (1~3) imparted to the benzene cluster ions, $(C_6H_6)_n^+$, have induced extensive fragmentation, where two types of series of fragment ions are important as a result of intracluster ion-molecule reactions.

Figure 1-(a) exhibits the observed MPI-TOF mass spectrum of benzene clusters and their fragments which was obtained under strong laser field (0.54 mJ/pulse). The most distinct feature of the spectrum is the appearance of the various fragment ions in addition to the main peaks corresponding to $(C_6H_6)_{1\sim3}^+$. The observed cluster fragments can be classified into three categories: $[(C_6H_6)_nCH_m]^+$, $[(C_6H_6)_nC_3H_m]^+$, and $[(C_6H_6)_nC_4H_m]^+$. A second class of fragment ions in the mass spectrum is dehydrated cluster ions, $[(C_6H_6)_n$-$mH]^+$. These intracluster ion-molecule reactions are intrinsic to the MPI/fragmentation of the clusters since

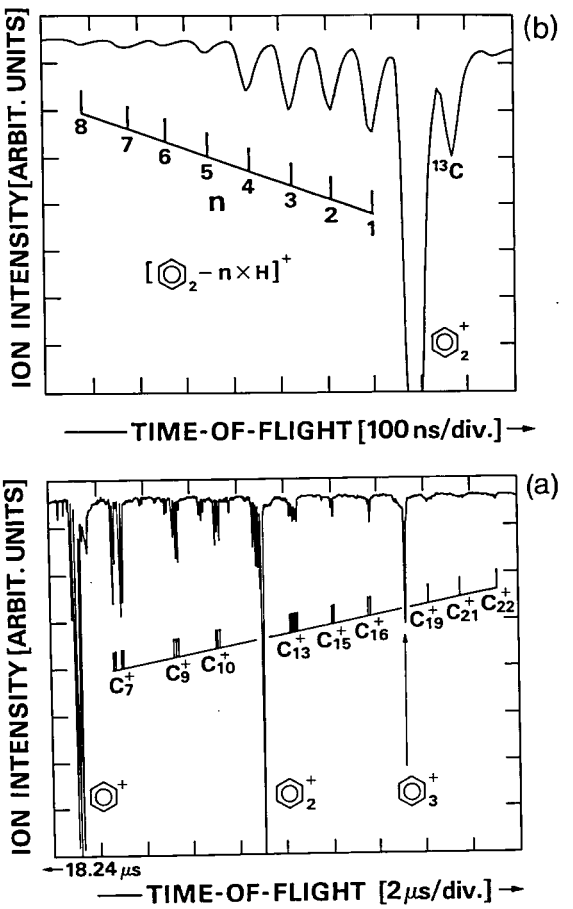

Figure 1. Multiphoton ionization/fragmentation time-of-flight mass spectrum of benzene clusters at 213 nm: (b) the same TOF spectrum in the dimer region, but the time axis is expanded 20-fold.

the above types of fragmentation are totally absent in electron-impact ionization of the benzene clusters. Photons imparted to the ionized clusters must primarily induce the cleavage of the C-C and C-H bonds of benzene in the clusters.

III-H-4 Experimental Evidence of the Magic Number Stability of the Hydrated Ammonia Cluster Ions $(H_2O)(NH_3)_{0\sim4}NH_4^+$

Hisanori SHINOHARA, Nobuyuki NISHI, and Nobuaki WASHIDA *(Nat. Inst. for Environmental Studies and IMS)*

Especially stable hydrated cluster ions $(H_2O)(NH_3)_{0\sim4}NH_4^+$ have been observed in a mass spectrometer via VUV one-photon and electron-impact ionization of the corresponding neutral binary clusters $(H_2O)_m(NH_3)_n$ produced in a supersonic jet. Figure 1 summarizes the results of the normalized cluster ion intensities, $(NH_3)_nNH_4^+$ and $(H_2O)[(NH_3)_nNH_4^+]$, vs. clustering number n, which is obtained by both electron and the VUV one-photon ionization at 11.83 eV. A distinct feature is readily discerned from the plots: there exist the intensity breaks between n=4 and 5 in otherwise monotonic decrease of the cluster distributions. This is suggestive of the fact that at n=4 the inner solvation shell is completed forming a stable $(NH_3)_4NH_4^+$ ion and in the further clustering stage above n=4 the outer shell, such as $(NH_3)[(NH_3)NH_4^+]$ and $(H_2O)[(NH_3)NH_4^+]$, is beginning to form.

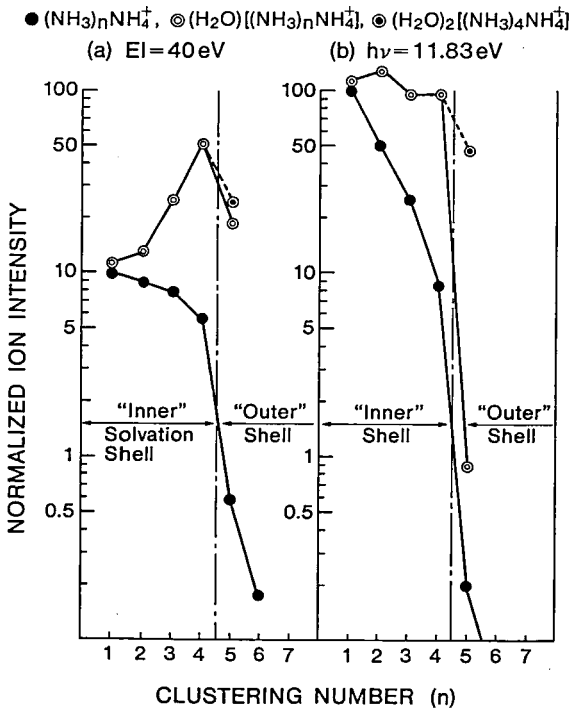

Figure 1. Semilogarithmic plots of the normalized cluster intensities vs. clustering number n: (a) electron-impact ionization (40 eV) and (b) the VUV photoionization (11.83 eV). In each case two plots are shown for pure ammonia clusters $(NH_3)_nNH_4^+$ (●) and mixed clusters containing one (H_2O) $[(NH_3)_nNH_4^+]$ (◎) and two $(H_2O)_2[(NH_3)_4NH_4^+]$ (◉) water molecules. The inner solvation shell is completed at n=4.

Figure 1-(b) indicates that the mixed cluster ions $(H_2O)(NH_3)_nNH_4^+$ are especially stable up to n=4 and also the $(H_2O)_2(NH_3)_4NH_4^+$ ion is relatively stable. However, the stability of the $(H_2O)(NH_3)_nNH_4^+$ cluster suddenly drops at n=5. The results can be interpreted to mean that in the outer shell water is taken up preferentially by the inner shell to construct the $(H_2O)[(NH_3)_4NH_4^+]$ ion rather than (NH_3) $[(NH_3)_4NH_4^+]$, which leads to a larger stabilization energy.

III-H-5 Fragmentation of Hydrogen-bonded Molecular Clusters on Photoionization

Nobuyuki NISHI, Hisanori SHINOHARA, Kazunori YAMAMOTO, Umpei NAGASHIMA, and Nobuaki WASHIDA *(Nat. Inst. for Environmental Studies and IMS)*

[*Faraday Discuss. Chem. Soc.* **81**, 359 (1986)]

Photofragmentation mechanisms on the near threshold ionization of $(H_2O)_m(Ar)_n$, $(CH_3NH_2)_{1,2}$ $(H_2O)_n$, and (N-methylformamide)$_{1,2}(H_2O)_n$ clusters have been investigated based on the molecular-beam VUV-photoionization mass spectroscopy with Ar(11.83, 11.62 eV) and Kr(10.64 and 10.03 eV) resonance lamps. In the Ar lamp ionization of $(H_2O)_m(Ar)_n$ clusters, $(H_2O)_k^+$ $(2\leq n\leq 10)$ ions were observed as well as $(Ar)_{1,2}(H_2O)_n^+$ $(2\leq n\leq 5)$ clsuters. This suggests that excess energy dissipation among H_2O-Ar and/or Ar-Ar vibrational modes, finally leads to dissociation of the bond(s), preventing the activation of the proton transfer reaction in an H_2O^+-H_2O hydrogen bonding unit. In the Kr lamp ionization of methylamine hydrated clusters and N-methylformamide hydrated clusters, proton transfer reactions are found to be negligible. Even at 11.83 eV,

$CH_3NH_2^+(H_2O)_n$ and $HNCH_3CHO^+(H_2O)_n$ ions were dominant fragments. The origin of protonated ions was attributed to the ionization of the CH_3NH_2-CH_3NH_2 or the $HNCH_3CHO$-$HNCH_3CHO$ dimer unit in the hydrated clusters based on the solute concentration dependence of the ion signals. When an H_2O molecule was ionized directly, the hydrogen atom of an adjacent molecule was abstracted by H_2O^+ forming an H_3O^+ ion. Increase of excess energy did not change the degree of fragmentation as much but changed the fragmentation pathways to the production of protonated ions. Selective ionization of a solute molecule enabled us to specify the bond dissociated primarily. The fragmentation mechanisms were elucidated by identifying the character of the ionized solute molecule in the hydrogen bond; electron donor (base) or hydrogen donor (acid).

III-I Dynamical Study of Surface Photochemistry with an UV Laser

III-I-1 Photocatalytic Disproportionation Reaction of Butadiene Thin Films at the Interface of Submonolayer $Co_2(CO)_8$

Nobuyuki NISHI

[*Rev. Laser Engineering*, **15**, 686 (1987)]

UV laser induced surface photoreaction has been studied by measuring time-of-flight spectra of photodesorbed molecular species mass-spectrometrically.

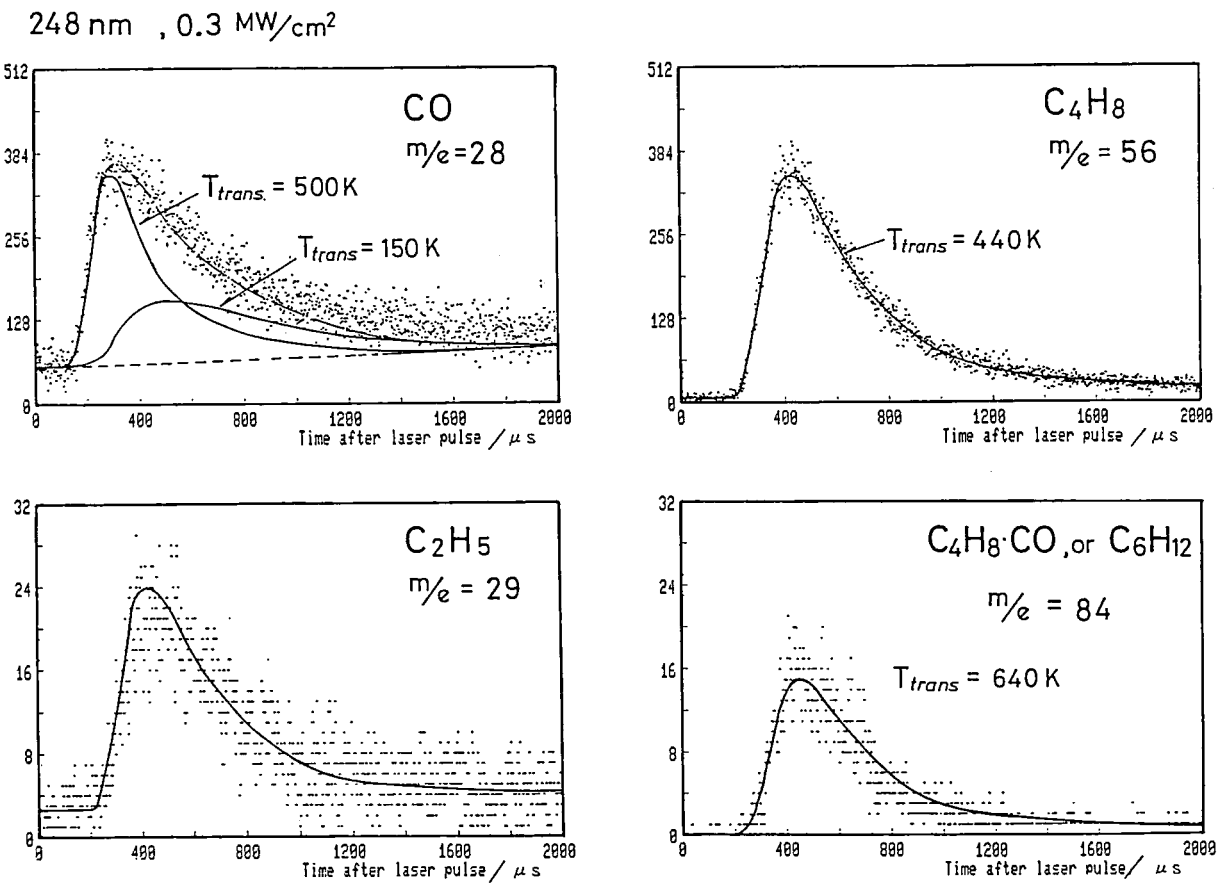

Figure 1. Time-of-flight spectra of photo-catalytic reaction products photodesorbed by the irradiation of 248 nm laser on a butadiene solid with sub-monolayer coverage of $Co_2(CO)_8$ which absorbs 248 nm light dissociating a CO fragment in the interface of the two layers. The signal at mass 29 was attributed to a secondary fragment of C_2H_5 generated from C_4H_8 in the electron impact ionizer.

Butadiene(C_4H_6: mass number=54) was deposited on a quartz surface at 100 K forming a film with a thickness of ~100 μm, on which submonolayer $Co_2(CO)_8$ was deposited. Butadiene solid is transparent at 248 nm, while the extinction coefficient of the cobalt carbonyl at that wavelength is larger than 3×10^4 $dm^3mol^{-1}cm^{-1}$. Upon the irradiation of 248 nm laser pulses at weak power levels less than 0.5 MW/cm^2, four signals were observed at mass numbers 28, 29, 56 and 84. Figure 1 shows the time-of-flight spectra of the four signals. The upper two are strong and the lower two are very weak. The signal at mass 28 was analyzed as a composite of the two Maxwell-Boltzmann components at translational temperature of 500 K and 150 K. This signal is due to dissociated CO molecules, since the primary photoreaction of cobalt carbonyl is;

$$Co_2(CO)_8 + h\nu \rightarrow Co_2(CO)_7 + CO. \quad (1)$$

The high temperature component has an average energy of 1.5 kcal/mol, which is very low compared with usual kinetic energy of recoiling fragments. This indicates that the fragments are ejected after collisional deactivation processes losing a large part of the initial energy. The strongest signal comes from butene (C_4H_8) which contains 2 hydrogen atoms more than butadiene. Reaction (1) was found to induce a bimolecular condensation reaction of butadiene.

III-J Photodissociation Dynamics Studied by Photofragment Time-of-flight Spectroscopy

III-J-1 Photofragment Energy Distribution of p-Dichlorobenzene Molecular Beam Excited by Linearly Polarized Light at 193 nm

Teijiro ICHIMURA *(Tokyo Inst. of Tech.)*, **Yuji MORI** *(Tokyo Inst. of Tech.)*, **Hisanori SHINOHARA, and Nobuyuki NISHI**

[*J. Spectrosc. Soc. Jpn.*, **35**, 299 (1986)]

Time-of-flight spectra of Cl photofragments were measured for a molecular beam of p-ClC_6H_4Cl irradiated by a 193 nm excimer laser beam polarized parallel or perpendicular to the detection axis. The total translational energy distribution, $P(E_T)$, of fragments has three peaks at around 3, 13, and 28 kcal/mol as shown in Figure 1. The broad distribution with the peak E_T value of ~3 kcal/mol in Figure 1 can be expressed by a Maxwell-Boltzmann function and the two higher energy distributions may be explained by Gaussian-type functions. Only the highest energy component showed an anisotropic angular distribution similar to those of the fast predissociation processes in chloroethylenes. This indicates that the excitation of p-dichlorobenzene is followed by a fast predissociation via a repulsive (n, σ^*) state. The major channels in the photolysis are the slow dissociation processes which showed isotropic angular distribution. The broad distribution with a peak at 13 kcal/mol is not reproduced

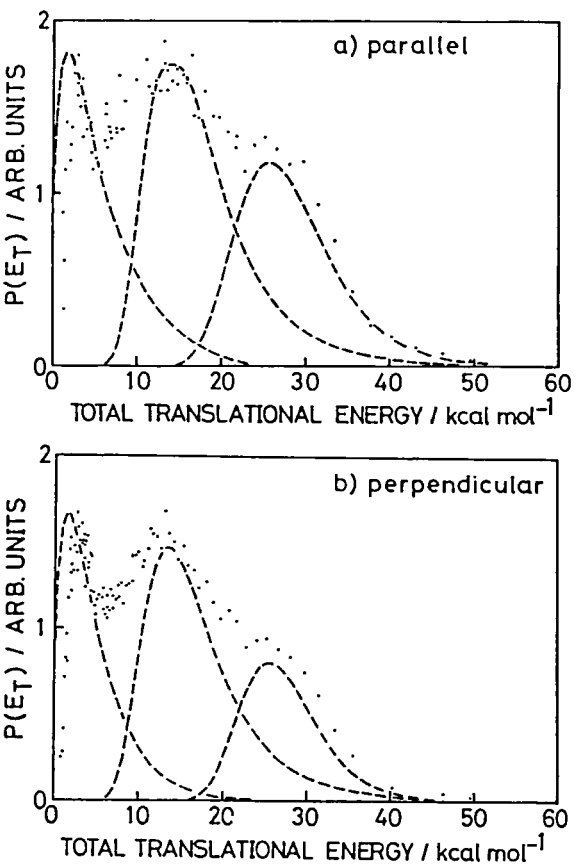

Figure 1. Total center-of-mass translational energy distribution $P(E_T)$ obtained from the time-of-flight spectrum of Cl fragments formed by the polarized light excitation of p-dichlorobenzene at 193 nm. The observed distributions were simulated by the superposition of a Maxwell-Boltzmann and two Gaussian functions.

by a Maxwell-Boltzmann function. The non-statistical distribution suggests that the process should be faster than the complete thermalization seen in the process of the lowest energy component. This second component was attributed to the dissociation from the highly vibrationally excited triplet state, and the last one was that from the vibrationally excited S_0 state.

III-J-2 Photodissociation of Tetramethyltin at 193 nm

Masahiro KAWASAKI *(Mi'e Univ.)*, **Hiroyasu SATO** *(Mi'e Univ.)*, **Hisanori SHINOHARA, and Nobuyuki NISHI**

[*Laser Chem.* **7**, 109 (1987)]

Tetramethyltin absorbs UV photons continuously from a long wavelength limit at 225 nm. By analogy with an analysis of the UV spectra of a series of alkyl metal compounds, the first electronic transition of tetramethyltin weakens the Sn-C bond. In this case two body and three body dissociation processes are expected as seen in the photolysis of dimethylcadmium.[1] For the 193 nm excimer laser irradiation, the only fragments detectable (at a detection axis orthogonal to the molecular beam) were those of mass 15. The time-of-flight distribution of CH_3 radicals is shown in Figure 1. In order to measure the bond dissociation energy D_0(C-Sn), a neat solid of $Sn(CH_3)_4$ on the quartz plate was photodissociated to give signals of methyl radicals as shown in the insert of Figure 1. Since the substrate has an infinite mass, the fastest photofragment can carry all the excess energy as translational energy, i.e. $D_0 = h\nu - E_T^{max}$. The bond dissociation energy is found to be 61 kcal/mol from the threshold of the time-of-flight signal. The obtained value is in good agreement with 60 ± 2 kcal/mol reported by Lampe and Niehaus.[2] The analysis of the translational energy distribution showed that the relative contribution of the three body dissociation to the two body process is 0.6.

References

1) C. Jonah, P. Chandler and R. Bersohn, *Chem. Phys. Lett.*, **83**, 304 (1971).
2) F.W. Lampe and A. Niehaus, *J. Chem. Phys.*, **49**, 2949 (1968).

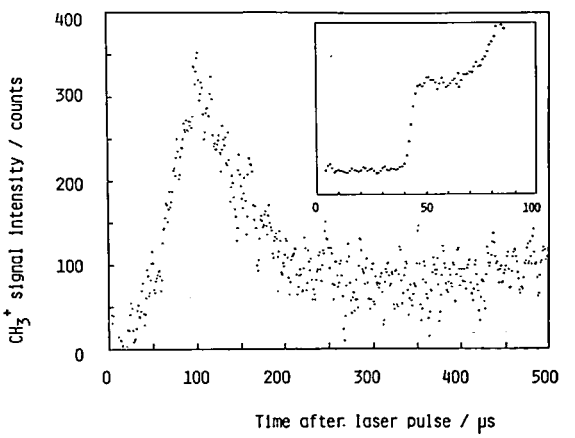

Figure 1. Time-of-flight spectra of CH_3 photofragments observed in the photolysis of a molecular beam of $Sn(CH_3)_4$ at 193 nm. The insert shows the threshold region of the time-of-flight spectrum of CH_3 photofragments generated in the photolysis of solid neat $Sn(CH_3)_4$ at 193 nm. For both cases, the drift time in the quadrupole mass filter is 17 μs for CH_3^+ ions.

III-K External Magnetic Field Effects upon Chemical Reactions

Magnetic field effects upon chemical reactions provide us with useful methods for studying reaction mechanism and technique for controlling reaction rates, product yields, and concentration of a certain isotope. In the recent decade, the magnetic field effects upon photochemical reactions in the solution phase have been extensively studied by several methods, *e.g.* magnetic-field-modulated fluorescence measurement, kinetic analysis of reaction intermediates by laser photolysis including two-step laser excitation, and chemical analysis of photoproducts obtained by steady-state irradiation. In particular, photochemistry of aromatic carbonyls in micellar media and of bifunctional chain molecules in homogeneous solutions have been investigated in some detail. In addition, we have also examined the magnetic field effects on afterglow activated by a microwave discharge and the mechanism of magnetic quenching of CS_2 fluorescence in the gaseous state.

III-K-1 Formation of Triplet Biradicals by Norrish Type I Cleavage of 2,2-Diphenylcycloalkanones and Magnetic Field Effects upon Their Dynamical Behavior

Hirochika SAKURAGI *(Univ. of Tsukuba and IMS)*, **Itsuko SUZUKI** *(Univ. of Tsukuba)*, **Ryoichi NAKAGAKI, Hiroaki MISAWA** *(Univ. of Tsukuba)*, **Katsumi TOKUMARU** *(Univ. of Tsukuba)*, **and Saburo NAGAKURA**

Cyclic ketones containing two phenyl groups at 2 position with respect to the carbonyl group undergo intramolecular photochemistry classified as Norrish type I reaction, which involves methylene-linked biradicals in the triplet manifold. Photoproducts derived from the triplet biradicals depend on the ring size. Namely, small ring ketones yield unsaturated aldehydes, while cyclophane derivatives are obtained from large cycloalkanones. Figure 1 summarizes the photochemical behavior of cyclic ketones. It is noteworthy that the lifetime of the triplet biradicals lengthens on application of an external magnetic field. This finding shows that the hyperfine coupling mechanism is more important than the Zeeman mechanism. On the other hand, no magnetic field effects are observed on the endproduct yields. This can be explained in terms of two intersystem crossing (ISC) pathways: magnetic-field-dependent ISC due to the radical pair mechanism and magnetic-field-independent ISC due to the spin-orbit coupling.

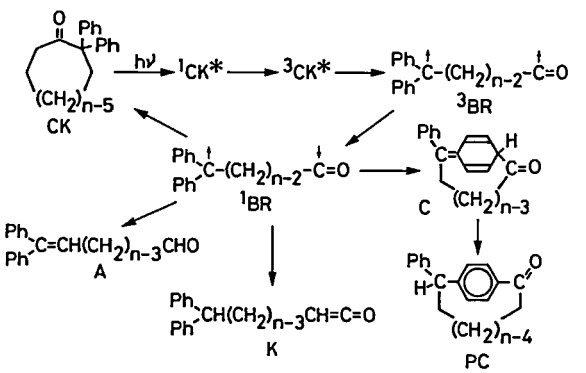

Figure 1. Photochemical reaction pathways of n-membered cyclic ketones (CK-n).

III-K-2 Photochemistry of Bichromophoric Species in the Presence of γ-Cyclodextrin and External Magnetic Field Effect upon the Branching Ratio between the Escape and Cage Products

Ryoichi NAKAGAKI, Kiyoshi MUTAI *(Univ. of Tokyo)*, **Mitsuo HIRAMATSU** *(Hamamatsu Photonics K.K.)*, **and Saburo NAGAKURA**

Photodecomposition of N-[12-(4-nitro-1-naphthoxy)dodecyl]aniline (NNDA) in $(CH_3)_2$-NCHO: H_2O mixed solvent (80:20 volume ratio) was studied in the presence and absence of γ-cyclodextrin (γ-CD). NNDA undergoes an intramolecular photoredox reaction yielding **Product 1** through a cage process and **Product 2** via an escape process (Figure 1). The branching ratio between the cage and escape products R_b=**[Product 2]**/**[Product 1]** drastically changes on application of an external magnetic field (0.64 T), namely, $R_b<1$ when H=0 T and $R_b>1$ when H=0.64 T in the presence of γ-CD. In other words, **Product 1** is dominant in the absence of the external magnetic field, whereas **Product 2** predominates in the presence of the magnetic field. Addition of γ-CD increases the yield of the escape product, since the inclusion of the donor or the acceptor moiety depresses the intramolecular cage process leading to **Product 1**. No magnetic field effects were observed for disappearance of NNDA or formation of aniline.

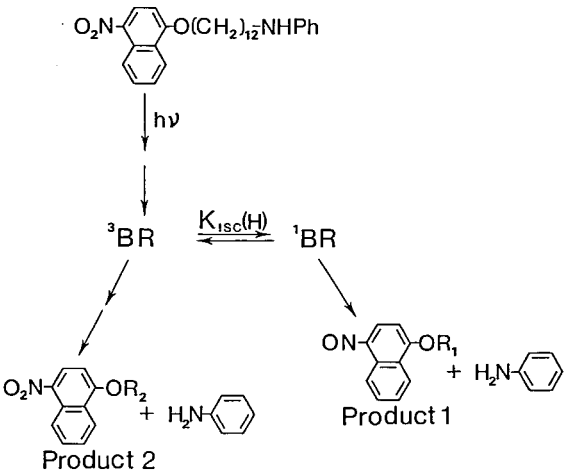

Figure 1. Photochemical decomposition of NNDA yielding **Product 1**, **Product 2**, and aniline.

III-K-3 Magnetic Field Effects and Long-range Oxygen Transfer in Intramolecular Photooxidation of N-Alkyldiphenylamine and 10-Alkylphenothiazine by Nitro-aromatic Moieties

Ryoichi NAKAGAKI, Kiyoshi MUTAI *(Univ. of Tokyo)*, **Mitsuo HIRAMATSU** *(Hamamatsu Photonics K.K.)*, **and Saburo NAGAKURA**

Bifunctional chain molecules containing an electron donor (N-alkylated diphenylamine or phenothiazine) and an acceptor (4-nitro-1-naphthoxyl group) undergo an intramolecular photoredox reaction involving nitro to nitroso reduction and an oxidative N-dealkylation. This photoreaction can be characterized as intramolecular oxidation by a nitro group at an anomalously remote site:

4-O_2N-$C_{10}H_6$-1-O$(CH_2)_{12}$-(Donor) → 4-ON-$C_{10}H_6$-1-O$(CH_2)_{11}$CHO + H-(Donor), where (Donor) = -N=$(C_6H_5)_2$ or -N=$(C_6H_4)_2$=S (see Figure 1).

The formation yield for nitroso-aromatic species decreases by about 10% in the presence of an external magnetic field (0.64 T). The observed magnetic field effects can be explained in terms of the radical pair mechanism.

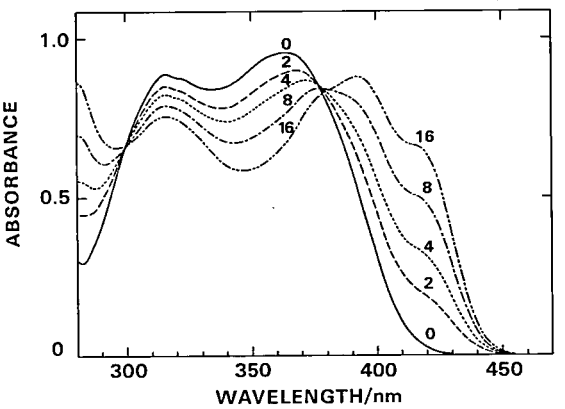

Figure 1. Development of the photoredox reaction of 10-[12-(4-nitro-1-naphthoxy)dodecyl]phenothiazine in benzene as revealed by UV-absorption spectroscopy. The absorption band around 393 nm is attributable to a 4-nitroso-1-naphthoxyl chromophore. The number refers to the irradiation time in min.

III-K-4 Magnetic Field Effects on the Exciplex Fluorescence of Phenanthrene and N,N-Dimethylaniline

Yoshifumi TANIMOTO *(Kanazawa Univ.)*, **Kiyoshi HASEGAWA** *(Kanazawa Univ.)*, **Michiya ITOH** *(Kanazawa Univ.)*, **Kaoru IWAI** *(Nara Women's Univ.)*, **Fukuo TAKEMURA** *(Nara Women's Univ.)*, **Ryoichi NAKAGAKI, and Saburo NAGAKURA**

The external magnetic field effects on the intermolecular exciplex fluorescence of phenanthrene (Phen) and N,N-dimethylaniline (DMA) have been studied by magnetic-field-modulated (MFM) fluorescence spectroscopy. Figure 1 shows the magnetic field dependence of the exciplex fluorescence intensity monitored at 500 nm. The field strength $B_{1/2}$, at which the MFM fluorescence intensity reaches half the saturation value obtained at higher fields (>60 mT), increases with increasing DMA concentration: 5 mT ([DMA] = 0.005 M), 8 mT ([DMA] = 0.01 M), 8 mT ([DMA] = 0.03 M), 10 mT ([DMA] = 0.06 M), and 10 mT ([DMA] = 0.1 M).

The magnetic field effects on the exciplex fluorescence is attributable to those on the radical ion pair, which is in dynamical equilibrium with the exciplex and undergoes the intersystem crossing induced by hyperfine coupling.[1)]

Reference

1) Y. Tanimoto, M. Okada, M. Itoh, K. Iwai, K. Sugioka, F. Takemura, R. Nakagaki, and S. Nagakura, *Chem. Phys. Lett.*, **136**, 42 (1987).

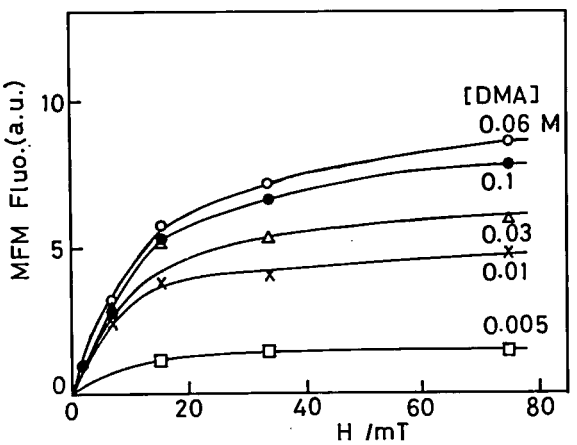

Figure 1. Magnetic field effect on the fluorescence intensity of the Phen-DMA exciplex in methanol measured by MFM fluorescence spectroscopy.

III-K-5 Magnetic Field Effects on the Hydrogen Abstraction Reaction of Fluorenylidene in SDS Micellar Solution

Yoshifumi TANIMOTO *(Kanazawa Univ.)*, **Chikako JINDA** *(Kanazawa Univ.)*, **Yoshihisa FUJIWARA** *(Kanazawa Univ.)*, **Michiya ITOH** *(Kanazawa Univ.)*, **Hideo TOMIOKA** *(Mi'e Univ.)*, **Ryoichi NAKAGAKI, and Saburo NAGAKURA**

The magnetic field effects on the photochemical primary process of a carbene, fluorenylidene (FL) have been studied by laser photolysis. Upon laser pulse excitation (308 nm and 15 ns FWHM) of 9-diazafluorene (DAF) in sodium dodecyl sulfate (SDS) micellar solution, transient absorption appears in the region of 450~500 nm, which is attributable to 9-fluorenyl radical (FLH˙). This observation indicates that fluorenylidene formed by N_2 elimination of the excited DAF abstracts a hydrogen atom from SDS ion (HD). In order to elucidate the spin multiplicity of FL, the transient decay of the 500 nm band was examined in the absence and presence of a magnetic field (Figure 1).

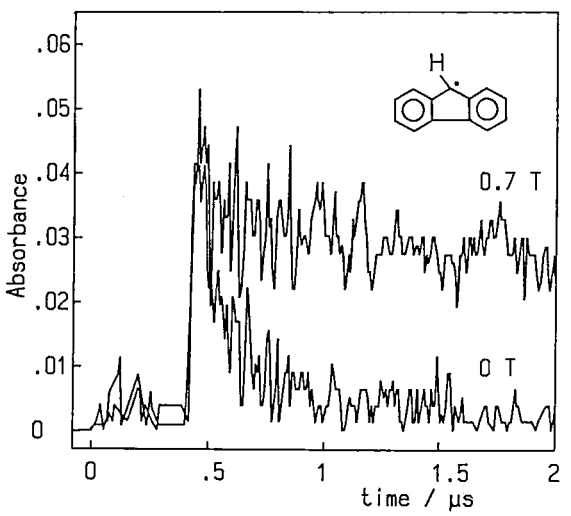

Figure 1. Magnetic field effect on the decay of the 9-fluorenyl radical. Tansient absorption was monitored at 500 nm.

The magnetic field effect shows unequivocally involvement of the FL triplet state. The reaction scheme can be summarized as follows:

DAF $\xrightarrow{h\nu}$ ^{1}FL → ^{3}FL (carbene formation and intersystem crossing)

$^3\overline{\text{FLH}^{\cdot\cdot}\text{D}}$ → $^1\overline{\text{FLH}^{\cdot\cdot}\text{D}}$ (hydrogen abstraction)

$^3\overline{\text{FLH}^{\cdot\cdot}\text{D}}$ → $^1\overline{\text{FLH}^{\cdot\cdot}\text{D}}$ (intersystem crossing)

$^3\overline{\text{FLH}^{\cdot\cdot}\text{D}}$ → FLH˙ + ˙D (escape process)

$^1\overline{\text{FLH}^{\cdot\cdot}\text{D}}$ → FLH-D (product formation).

III-K-6 External Magnetic Field Effects on the Fluorescence of CS_2 Excited to the $^1B_2$ State with Nanosecond and Picosecond Lasers

Takashi IMAMURA, Naoto TAMAI, Yoshio FUKUDA, Iwao YAMAZAKI, Saburo NAGAKURA, Haruo ABE *(Inst. of Phys. and Chem. Res. and IMS)*, **and Hisaharu HAYASHI** *(Inst. of Phys. and Chem. Res.)*

[*Chem. Phys. Lett.*, **135**, 208 (1987)]

External magnetic field effects on the banded emission from V^1B_2 state of gaseous CS_2 have been studied. The observed results are summarized as follows: (1) the integrated intensities of the excitation spectra are reduced by a magnetic field for all vibronic

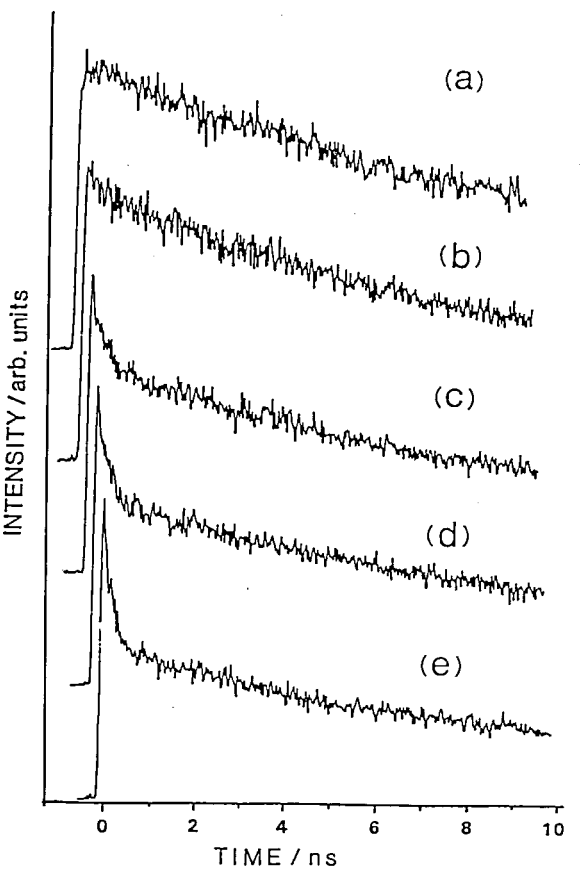

Figure 1. Fluorescence decay curves of CS_2 obtained by picosecond laser pulse excitation: (a) at 0 kG, (b) at 4.0 kG, (c) at 8.3 kG, (d) at 11.1 kG, and (e) at 15.1 kG. On excitation at 30526 cm^{-1}, the CS_2 fluorescence was monitored at 346 nm.

bands (6V, 9V, 10V, and 15V) measured even under a supersonic jet condition, (2) the magnetic quenching pattern shows no systematic dependence on the rotational quantum number and varies from line to line within one vibronic band, (3) the emission lifetime measurement shows the presence of the fast decay component in the subnanosecond time scale and the magnetic field quenching of the slow decay component, and (4) application of the external magnetic field causes shortening of the lifetime of the fast decay component and remarkable change in the ratio of the pre-exponential factors of the fast and slow decay components as shown in Figure 1. These findings suggest that the energy relaxation process of CS_2 is classified as the so-called intermediate case and that the magnetic quenching of the CS_2 fluorescence can be explained in terms of the enhancement of some intramolecular nonradiative relaxation processes induced by the magnetic field.

III-K-7 Magnetic Field Effects upon Atomic and Molecular Collisions

Yoshio FUKUDA

[*Chem. Phys.*, **118**, 199 (1987)]

Full quantal theory of heavy-particle collisions in the presence of static magnetic field, B, has been formulated. A new mechanism of magnetic field effect was found which depends on velocity of molecular center of mass and plays an important role at high-speed collisions. A power series expansion of cross section as a function of B was obtained, which can be applicable to collisions at weak field. It was also found that differential cross section can become zero due to magnetic field when a rovibronic energy level of a molecule is in resonance with another energy level. Figure 1 shows an example of these resonance effects, where two energy levels, 1A and 2A, of a product is nearly degenerate. A perturbation causes a mixing of these two levels. The mixing coefficient, ϱ, depends also upon energies, E_1 and E_2, of the two levels, which are functions of external magnetic field, B, due to Zeemann interaction. Thus, transition rates, W_a^{1A} and W_a^{2A}, into these two levels depend on magnetic field.

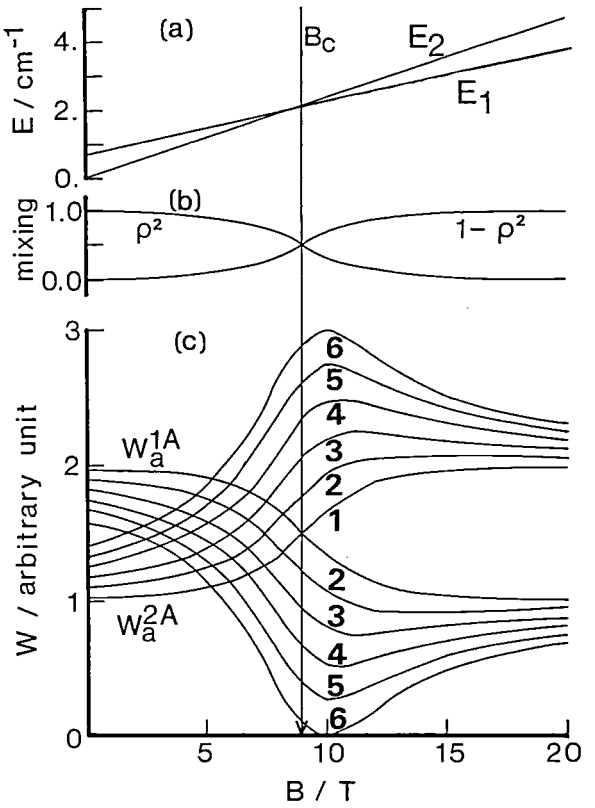

Figure 1. Dependences of energy levels(a), mixing coefficients(b) and transition rates W(c) upon strength of magnetic field B, calculated for ideal $^2S_{1/2}$ and $^2P_{1/2}$ states of an atom. Used parameters. U=0.1 cm^{-1}, δE(0)=0.7 cm^{-1} and w_1/w_2=2. In trace(c), transition rates were calculated with u=0.0(1), 0.2(2), 0.4(3), 0.6(4), 0.8(5) and 1.0(6).

RESEARCH ACTIVITIES IV
Department of Molecular Assemblies

IV–A Photoelectron Spectroscopy of Organic Solids in Vacuum Ultraviolet Region

UPS study of organic solids and polymers has been carried out. UVSOR-UPS apparatus was used to observe intramolecular band mapping of hexatriacontane.

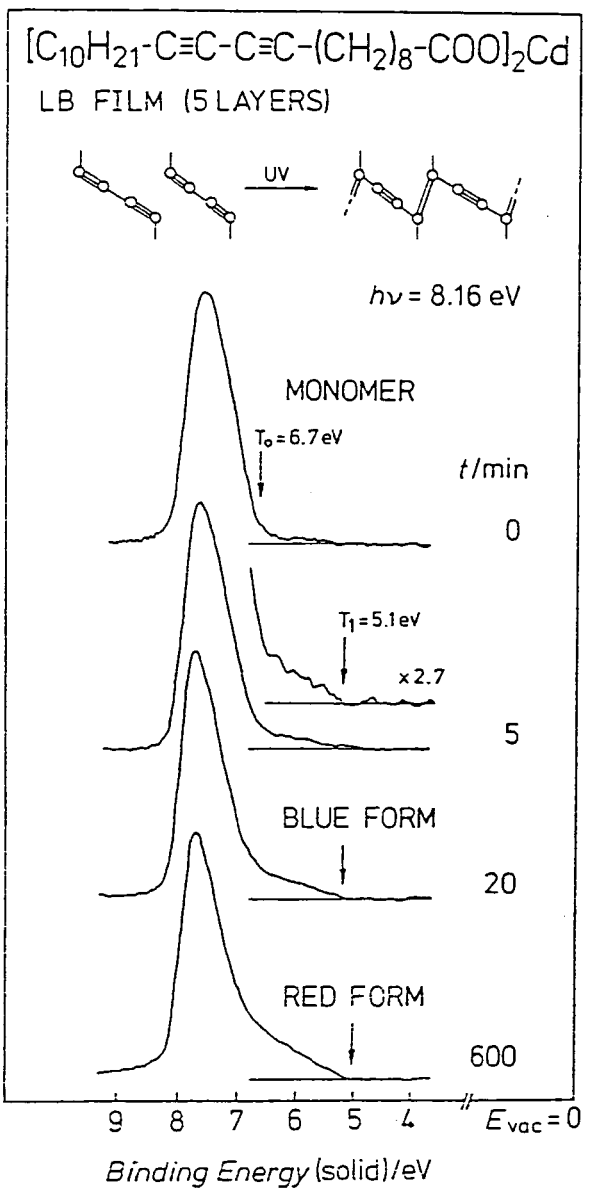

Figure 1. Change of the photoelectron spectra of the multilayer films at hv = 8.16 eV on polymerization. The time of UV irradiation is shown for each spectrum. Threshold energies are indicated by arrows.

IV-A-1 UV photoelectron Spectroscopic Study of the Photopolymerization of Long-Chain Diacetylene Monocarboxylic Acid in the Langmuir-Blodgett Films

Hiroo NAKAHARA*, Kiyoshige FUKUDA*, Kazuhiko SEKI, Satoshi ASADA, and Hiroo INOKUCHI**
*(*Saitama Univ., **Toyota Motor Co. and IMS)*

Photopolymerization of diacetylene multilayer monocarboxylic acid (tricosa-10,12-diynboic acid) in the Langmuir-Blodgett films was studied by UV photoelectron spectroscopy. Upon polymerization, the ionization threshold energy decreased by 1.6 eV from 6.7 eV (monomer) to 5.1 eV (polymer), as shown in Fig. 1. No change of the threshold was found between the blue and red forms of the polymer. This suggests that the polymer chain is in the acetylenic form in both forms. The mechanism of spectral sensitization by dyes is also discussed.

IV-A-2 Characterization of Vacuum-deposited Perfluorocarboxylic Acid Monomolecular Film by Penning Ionization Electron Spectroscopy

Munehisa MITSUYA*, Hiroyuki OZAKI, Yoshiya HARADA**, Kazuhiko SEKI, and Hiroo INOKUCHI**
*(*Hitachi Ltd., ** Univ. Tokyo)*

The molecular arrangement of perfluorocarboxylic acid monomolecular film, vacuum-deposited on a dehydrated SiO_2 substrate, is studied through cyclic thermal treatment using Penning ionization electron spectroscopy. The film was ascertained to cover the substrate surface up to 60°C (curves a-d in Fig. 1). Reversible spectral change due to the thermal fluctua-

tion of fluorocarbon tails is observed in the temperature range of 80-100°C (e-g), while irreversible disordering of the molecules occurs above 150°C (h-j). The film prepared on an undehydrated substrate easily desorbs in ultrahigh vacuum even at room temperature. The results indicate that the chemical bond between the molecules and the substrate appears to dominate the stability of the film.

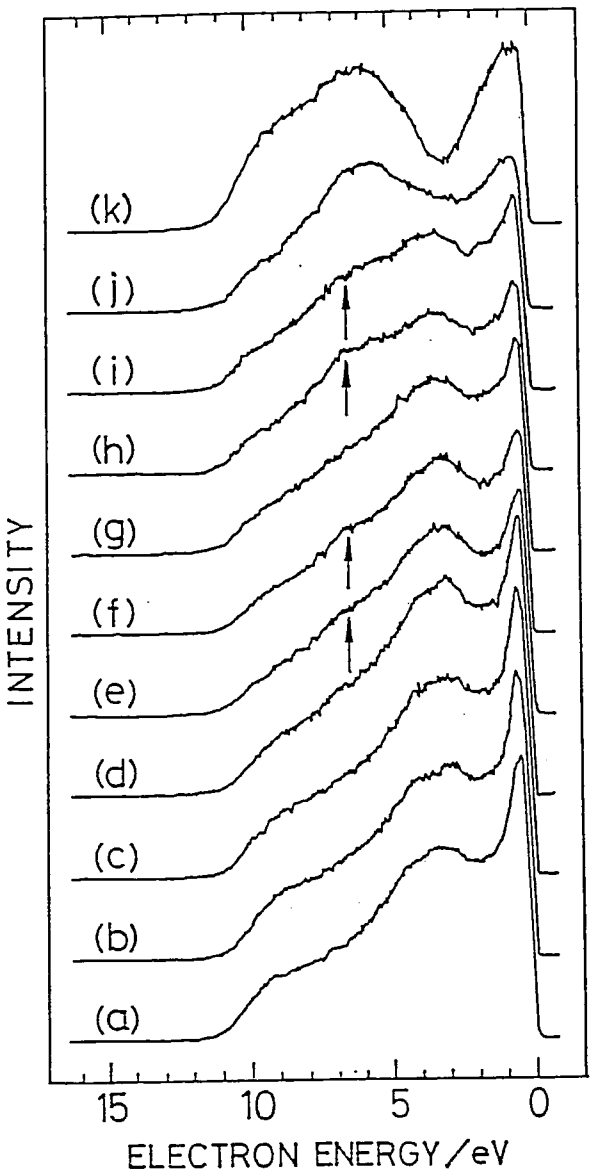

Figure 1. Penning ionization electron spectra of the perfluorocarboxylic acid film (a-j) and the substrate (k). Sample temperatures are, (a) 0°C, (b) room temperature, (c) 40°C, (d) 60°C, (e) 80°C, (f) 100°C, (g) room temperature after cooling case (f), (h) 150°C, (i) room temperature after cooling case (h), and (j) 200°C. Arrows indicate substrate emission.

IV-A-3 Skeleton-Pendant Interaction in Organopolysilane

Kyozaburo TAKEDA*, Masaie FUJINO*, Kazuhiko SEKI, and Hiroo INOKUCHI *(*NTT)*

[*Phys. Rev.* **B**, in press]

Skeleton-pendant interaction due to σ-π mixing in organopolysilane $(SiXY)_n$, where X and Y are methyl (Me) and phenyl (ϕ) groups, has been theoretically investigated. The results were discussed on the basis of UPS experiments. The σ-π interaction at the VB edge causes not only the delocalized σ-states along the Si skeleton, but also the localized π-states in the individual pendants. On the other hand, the σ-π interaction at the CB edge is inhibited owing to the orbital symmetry. This paper also presents the results of theoretical investigations on the influence of side-group substitution and of ϕ-group-pendant rotation on the electron distribution along the Si skeleton.

IV-A-4 Molecular Fasteners: Extraordinarily Strong Interactions in Tetrakis(alkylthio)tetrathiafulvalenes (TTC_n-TTFs)

Kazuhiko SEKI, Tong Bor TANG *(Hong Kong Baptist College and IMS)*, **Takehiko MORI, Peiji WU** *(Academia Sincica and IMS)*, **Gunji SAITO** *(Univ. Tokyo)*, **Kenichi IMAEDA, Zurong SHI** *(Academia Sinica and IMS)*, **Toshiaki ENOKI, Yoshiki HIGUCHI** *(Himeji Inst. Tech.)*, **Noritake YASUOKA** *(Himeji Inst. Tech.)*, **and Hiroo INOKUCHI**

[*Studies Org. Chem.*, **31**, 575 (1987)]

The synthesis, crystal structures, and properties of the title compounds, with carbon number n = 1-18 in each alkyl chain, are described. Long-chain members showed high electrical conductivities up to 10^{-5} Scm^{-1}. Crystal structure analyses of these long-chain compounds revealed extraordinarily short S-S distances (357 pm). The strong intermolecular interaction resulting in such short distances is expected to be due to the attractive (fastening) force among alkyl chains, hence we call these compounds molecular fasteners. Measurements of ionization energies and charge carrier mobilities also indicated the effect of the strong intermolecular interactions which contribute to the high conductivities.

IV-A-5 Ionization Potentials of Carbon Tetraiodide and Tetraiodoethylene in the Solid State

Naoki SATO *(Univ. Tokyo)* **and Hiroo INOKUCHI**

[*Chem. Phys.*, **113**, 445 (1987)]

Ultraviolet photoelectron spectra measured for vapor-desposited thin films of carbon tetraiodide and tetraiodoethylene allowed to determine the threshold ionization potentials in the solid state to be 5.5_0 and 5.0_4 eV, respectively. The spectral features do not necessarily correspend to each other between the gaseous and solid states; the energy differences between the adiabatic ionization potentials in the gas phase and the threshold ionization potentials are obtained to be 3.5_0 and 3.5_3 eV for the respective compounds above. These values are much larger than the polarization energies of any other organic solids reported so far. The large energy differences are explained by a strong intermolecular interaction working in those solids, extra to the van der Waals force; this is supported by the results of their crystal structure analyses.

IV-A-6 Simple Gun for Vapor Deposition of Organic Thin Films

Naoki SATO *(Univ. Tokyo)*, **Kazuhiko SEKI** *(Hiroshima Univ.)*, **and Hiroo INOKUCHI**

[*Rev. Sci. Instrum.*, **58**, 1112 (1987)]

A simple evaporation gun for preparing organic thin films was fabricated using commercially available parts of an electron gun for a TV Braun tube. The device, of which schematic is shown in Figure 1, permits sample heating to be easily controlled because of the small heat capacity.

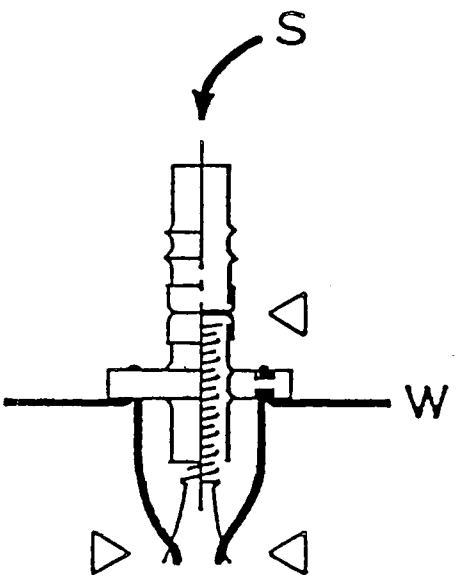

Figure 1. Fabricated gun: s, sample materials to be charged into the upper tube; w, nickel-chromium wires. Triangles indicate the positions where spot-welded.

IV-A-7 Reevaluation of Electronic Polarization Energies in Organic Molecular Crystals

Naoki SATO *(Univ. Tokyo)*, **Hiroo INOKUCHI, and Edger A. SILINSH** *(Acad. Sci. Latvian SSR)*

[*Chem. Phys.*, **115**, 269 (1987)]

Effective electronic polarization energies for positive P^{+}_{eff} and negative P^{-}_{eff} charge carriers in polyacene crystals have been reevaluated. By comparing the P^{+}_{eff} and P^{-}_{eff} values obtained from the analyses of reported energy parameters with calculated data, it is shown that the widely accpted assumption that $P^{+}_{eff} = P^{-}_{eff}$ in polyacene crystals is not valid. By applying recently reported data on optical E_G^{Opt} and adiabatic E_G^{Ad} energy gap values, the contribution of molecular (vibronic) polarization in the total effective polarization energy W^{+}_{eff} and W^{-}_{eff} has been estimated, and modified energy diagrams for polyacene crystals have been presented. Further, due to practically constant values of observed and calculated P^{+}_{eff} and P^{-}_{eff} in polyacenes, the gap energies between positive and negative charge carrier conduction levels have been estimated for several related aromatic hydrocarbons.

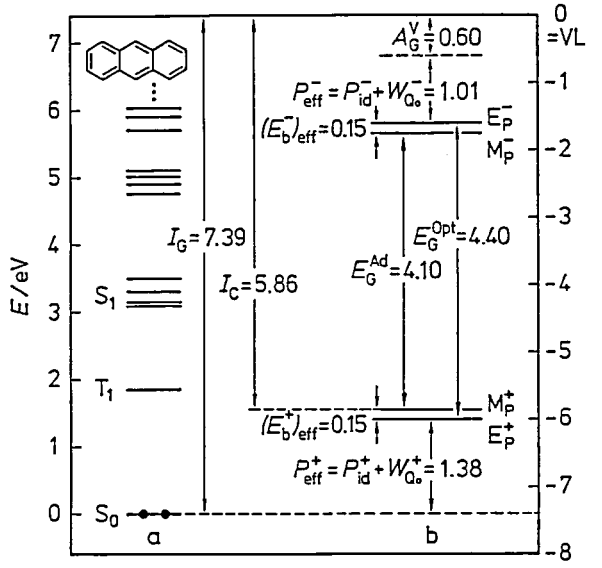

Figure 1. A modified energy level diagram for an anthracene crystal; (a) neutral and (b) ionized state levels; I_G and I_C – ionization potentials in the gaseous and solid states; A_G^V – vertical electron affinity in the gas phase; P_+^{eff} and P_-^{eff} – effective electronic polarization energies for positive and negative charge carriers; E_G^{Opt} and E_G^{Ad} – optical and adiabatic energy gaps; E_p^+, E_p^- – electronic polaron states; M_p^+, M_p^- – conductivity states for molecular polarons. (For other notations see the article cited above).

IV-A-8 Change of the Electronic Structures of Tetrakis(alkylthio)tetrathiafulvalenes (TTC_n-TTFs) during the Solid-Melt Transition

Hiromichi YAMAMOTO, Kazuhiko SEKI *(Hiroshima Univ.)*, **Hiroo INOKUCHI, and Gunzi SAITO** *(Univ. Tokyo)*

[*J. Chem. Soc. Faraday Trans.* **2**, in press]

The ultraviolet photoelectron spectra of tetrakis(alkylthio)tetrathiafulvalenes (TTC_n-TTFs) in the solid and molten states have been measured for n = 2 and 10, where n is the number of carbon atoms in each chain. The ionization threshold and spectral features of TTC_{10}-TTF are different in the solid and molten states, while no change is observed for TTC_2-TTF. This result proves that the low-ionization threshold of TTC_{10}-TTF in the solid state is caused by the much closer packing of TTF moieties than that of TTC_2-TTF. The absorption spectra of these compounds have been also measured in the solid, molten, and solution states. Comparison of the observed spectra reveals that the electronic structure of TTC_2-TTF in the solid state is dominated by that of an isolated molecule, while that of TTC_{10}-TTF in the solid state is strongly affected by the intermolecular interactions. The relationship between these findings on the electronic structures and the reported electric conductivities is also discussed.

IV-A-9 Intramolecular Band Mapping of *n*-$CH_3(CH_2)_{34}CH_3$ over the Whole Brillouin Zone by Angle-resolved Photoemission

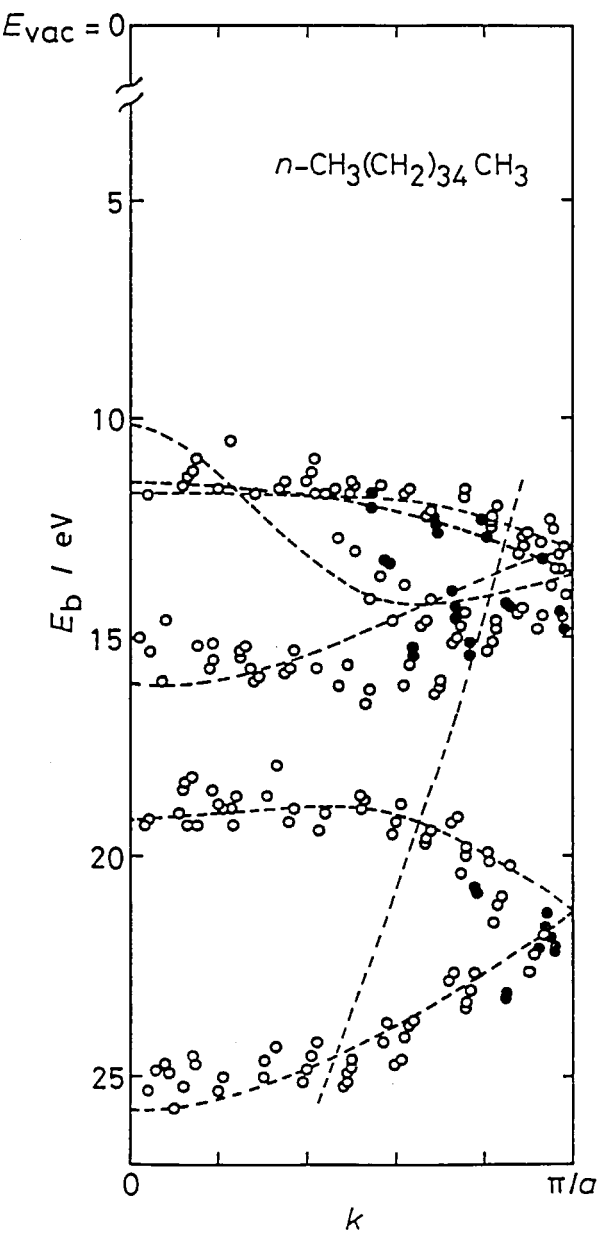

Figure 1. Energy-band dispersion of *n*-$CH_3(CH_2)_{34}CH_3$. The part at the right side of the vertical broken line could not be accessed in the previeous work.[1] The calculated band structure for idealized polyethylene by Karpfen[2] is also shown by broken line.

Hitoshi FUJIMOTO, Takehiko MORI, Hiroo INOKUCHI, Nobuo UENO *(Chiba Univ.)*, **Kazuyuki SUGITA** *(Chiba Univ.)*, **and Kazuhiko SEKI** *(Hiroshima Univ.)*

[*Chem. Phys. Lett.*, **141**, 485 (1987)]

The angle-resolved photoemission spectra were measured for an oriented film of a model compound of polyethylene (hexatriacontane n-$CH_3(CH_2)_{34}CH_3$) using synchrotron radiation at the UVSOR Facility, IMS. The photon energy ($h\nu$)-dependence of normal emission spectra was confirmed to be due to the intramolecular energy-band dispersion, and the dispersion over the whole Brillouin zone was determind.

The band structure obtained from photoelectron spectra is shown as the points in Figure 1. It should be noted that the data after passing the edge of the Brillouin zone ($h\nu \geqq 61$ eV and 65 eV for the upper and lower bands, respectively), which are marked with filled circles, fit well with these at lower photon energies (open circles). Thus, the observed $h\nu$-dependence can be explained as due to the intramolecular dispersion.

References

1) K. Seki, N. Ueno, U. O. Karlsson, R. Engelhardt, and E. E. Koch, *Chem. Phys.*, **105**, 247 (1986).
2) A. Karpfen, *J. Chem. Phys.*, **75**, 238 (1981).

IV–B Electrical Conduction of Organic Solids

The first series of works on organic semiconductors were single component systems. Since 1954, multi-component systems have been developed strongly. However, multi-component systems have some disadvantageous properties such as air and thermal instability. Therefore, semiconducting single component organic compounds are likely to more suitable for use as molecular device. As a single component organic semiconductors, a series of uncapped alkyl-substituted tetrathiafluvalenes has been studied.

IV-B-1 A High-mobility Organic Semiconductor: Tetrakis(methyltelluro)-tetratiafulvalene ($TTeC_1$-TTF)

Hiroo INOKUCHI, Kenichi IMAEDA, Toshiaki ENOKI, Takehiko MORI, Yusei MARUYAMA, Gunzi SAITO *(Univ. Tokyo)*, **Naoko OKADA** *(Univ. Tokyo)*, **Kazuhiko SEKI** *(Hiroshima Univ.)*, **Yoshiki HIGUCHI* and Noritake YASUOKA** *(*Himeji Inst. Tech.)*

[*Nature* **329**, 39 (1987)]

We have found a new class of highly conductive single-component organic semiconductors: tetrakis (methyltelluro) tetrathiafulvalene. Its resistivity is 8.1 $\times$ 10^4 Ωcm, having zigzag chalcogen chains formed from quasi-covalent bonds. This semiconductor has a high room-temperature charge mobility, 20-30 cm^2/V.sec., which is about one order of magnitude greater than the mobilities of other organic solids.

IV-B-2 Electrical Conductivities of Tetrakis (alkylthio)tetrathiafulvalene (TTC_n-TTF) and Tetrakis(alkyltelluro)tetrathiafulvalene($TTeC_n$-TTF).

Kenichi IMAEDA, Toshiaki ENOKI, Zurong SHI,* Peiji WU,* Naoko OKADA,$^+$ Hideki YAMOCHI,$^+$ Gunzi SAITO$^+$ and Hiroo INOKUCHI *(*Institute of Chemistry, Academia Sinica) ($^+$Univ. Tokyo).*

[*Bull. Chem. Soc. Jpn.* **60**, 3163 (1987)]

Electrical conductivities have been measured for TTC_n-TTF and $TTeC_n$-TTF. In the case of TTC_n-TTF, the compounds with short alkyl chains (n=1-3) show the high resistivities above 10^{10} Ωcm, while the resistivities of the compounds with long alkyl chains are attributed to the considerable reduction in intermolecular distance between adjacent TTF skeletons caused by intermolecular interactions through alkyl chain groups taking into account the results of their crystal structures, thermal properties and densities. As for $TTeC_n$-TTF compounds, the carbon number dependence of

resistivity is almost similar to that of TTC_n-TTF in the range of large n ($n \geqq 8$). Exceptionally, $TTeC_1$-TTF exhibits noticeably low resistivity of 8.1×10^4 Ωcm. X-ray diffraction study confirms that the high conductivity of $TTeC_1$-TTF is caused by the formation of zigzag Te chains due to the presence of strong intermolecular Te···Te atomic contacts.

IV–C Characterization of Cytochrome c_3 and Hydrogenase

We succeeded to make single crystal of hydrogenase.

IV-C-1 Single Crystals of Hydrogenase from *Desulforibrio vulgaris* Miyazaki F.

Yoshiki HIGUCHI,* Noritake YASUOKA,* Masao KAKUDO,* Yukiteru KATSUBE *(Osaka Univ.)*, **Takehiko YAGI** *(Shizuoka Univ.)*, **and Hiroo INOKUCHI** *(*Himeji Inst. Tech.)*

[*J. Biol. Chem.* **262**, 2823 (1987)]

The hydrogenase solubilized from the particulate fraction from *Desulfovibrio vulgaris* Miyazaki F. has been crystallized. The apparently homogenous hydrogenase has been separated into three components of similar molecular weights by high performance liquid chromatography of DEAE-Toyopearl. Preliminary x-ray experiments reveal that crystals grown form one component are in space group of $P2_12_12_1$ with a = 102.1(1), b = 126.8(3), and c = 66.9(1) Å. The unit cell volume of 8.66×10^5 Å^3 suggests that it contains one molecule /asymmetric unit (Vm = 2.43). The crystals grown from another component are in the same space group with a = 99.6(1), b = 126.8(3), c = 66.9(1) Å and the unit cell volume is 8.45×10^5 Å^3 (Vm = 2.37). The crystals diffract more than 2.5 Å and are suitable for complete crystal analysis. Up to 4 Å resolution native data have been collected on a diffractometer.

IV–D Physics and Chemistry of Graphite Intercalation Compounds

Graphite-alkali metal intercalation compounds absorb hydrogen chemisorptively, leading to the occlusion of hydrogen in intercalate layers. The introduction of hydrogen gives effects on the electronic and lattice properties of the compounds due to the strong electron affinity of hydrogen and the occupation of the sites by hydrogen species in the intercalate layer. We investigate the properties of the alkali metal-hydrogen-graphite ternary intercalation compounds by means of ESR and proton-NMR to clarify the electronic and lattice structures of the compounds.

Fluorine-graphite intercalation compounds show anomalous properties which are associated with the motion of fluorine atoms in intercalate space. We investigate the electronic properties of the fluorine-graphite intercalation comopounds. (See also VII-J)

IV-D-1 ESR Study of the Hydrogen-Potassium Graphite Ternary Intercalation Compounds

Toshiaki ENOKI, Hiroo INOKUCHI and Mizuka SANO *(Kumamoto Univ.)*

The electronic properties of the stage-1 and -2 hydrogen potassium graphite ternary intercalation compounds (KH-GIC's) $C_{4n}KH_X$(n = 1,2, X~0.8) were investigated by means of ESR measurements. The observed temperature dependence of diffusion time is found to be associated not only with the conduction electron spins but also with the localized spins. The behaviors of the paramagnetic susceptibilities and the g-values give additional evidence for the presence of localized spins which interact with the conduction electron spins. The KH-GIC's possess the ionic lattice of the donor intercalant with sandwich layers K^+-H^--K^+, which is affected by the conduction electrons on the graphite layers. The compositon $C_{4n}KH_{0.8}$ suggests hydrogen deficiency in the K^+-H^--K^+ ionic interca-

lant, which gives defects in the intercalant. The presence of the localized spins is attributed to trapped electrons at the defects in the intercalants. The spin relaxation at high temperatures is explained with the Elliott mechanism. The exchange intercations between graphite π and alkali metal s electrons and the large spin-orbit interaction of alkali metal atoms play important roles in the relaxation process.

IV-D-2 Structural and Electronic Properties of Hydrogen in Potassium-Hydrogen-Graphite Ternary Intercalation Compound, $C_8KH_{0.55}$: A Nuclear Magnetic Resonance Study

Seiichi MIYAZIMA *(Nihon Univ.)*, **Takehiko CHIBA** *(Nihon Univ.)*, **Toshiaki ENOKI, Hiroo INOKUCHI and Mizuka SANO** *(Kumamoto Univ.)*

Proton NMR study was carried out on a second stage potassium-hydrogen-graphite intercalation compound, C_8KH_x (x = 0.55), in a powder form within the temperature range, 1.5–77 K. An inhomogeneously broadened NMR signal (ca. 40 kHz in full width) was observed, but the intrinsic linewidth of the spin isochromat, ca 3.6 kHz, was determined from the spin echo envelope. The shape of the echo envelope was explained by assuming regular two-dimensional structure of dissociated hydride ions. The inhomogeneous broadening is possibly ascribed to localized electron spins of the order of 100 ppm. The spin-lattice relaxation mechanisms were divided into two contributions, the metallic process and the process due to localized electron spins as shown in Fig. 1. The analysis of the metallic relaxation component revealed the existence of small local density of states at Fermi level at hydrogen sites, $N(E_F)_H$ = 0.014 states/eV per spin per hydrogen atom. The hydrogen atomic plane was revealed to be weakly metallic. A possible electronic structure is discussed.

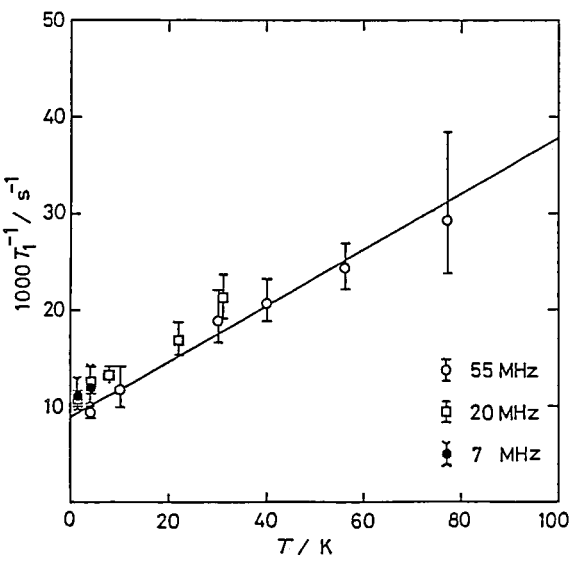

Figure 1. Temperature and frequency dependences of spin-lattice relaxation rates. The experimental data, ●, □, and ○ stand for 7, 20, and 55 MHz respectively. The solid line represents the best-fit linear function for the 55 MHz data.

IV-D-3 Fluorine-Graphite HOPG Intercalation Compounds

Hidekazu TOUHARA *(Kyoto Univ.)*, **Yoshihito GOTO** *(Kyoto Univ.)*, **Nobuatsu WATANABE** *(Kyoto Univ.)*, **Kenichi IMAEDA, Toshiaki ENOKI, Hiroo INOKUCHI and Yasuo MIZUTANI** *(Kyoto Univ.)*

[*Synth. Metals*, in press.]

Fluorine-graphite intercalation compounds C_xF ($15 > x \geq 5.6$) have been obtained by exposing HOPG to fluorine with available highest purity, at 50°C for periods exceeding 30 days. The identity period and the intercalant thickness of pure stage-2 comound $C_{6.4}F$ are, respectively, 9.46 and 2.76 Å. In-plane electrical conductivities of C_xF are ca. 8–10 times that of the pristine HOPG. The c-axis resistivity of the stage-2 compound vs. temperature shows a maximum at 194 K; metallic-like behavior at lower temperatures and semiconductor-like behavior at higher ones, as shown in Fig.1. The compound also shows an anomalous

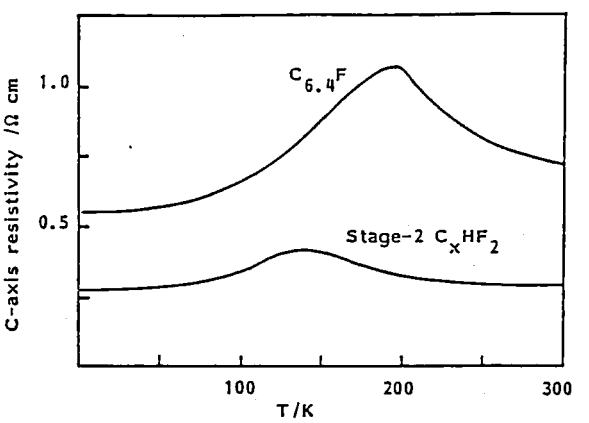

Figure 1. C-axis resistivity vs. temperature for $C_{6.4}F$ and stage-2 C_xHF_2.

c-axis thermal expansion at 130 K and a drastic motional narrowing in the linewidth of ^{19}F-NMR at 150K, suggesting a kind of in-plane phase transition of intercalated fluorine.

IV–E Organic Metals

In an attempt to develop a new organic superconductor and to explore the related phenomena, several new organic charge-transfer complexes are prepared, and their structural and physical properties are investigated.

IV-E-1 BEDT-TTF Complexes Including Divalent Gold, Au(II)

Takehiko MORI and Hiroo INOKUCHI

[*Chem. Lett.*, **1986**, 2069]
[*Solid State Commun.*, **62**, 525 (1987)]

The organic donor BEDT-TTF forms 2:1 and 1:1 salts with $AuCl_2^-$. The 2:1 salt is the β'-type which is isostructural with the ICl_2^- and $IBrCl^-$ salts, and has one-dimensional electronic structure. In the 1:1 salt, half of $AuCl_2$, which are incorporated in the sheet of BEDT-TTF (Figure 1), are likely to be formally neutral and to include anomalous divalent gold, Au(II). On the other hand, electrochemical crystallization of BEDT-TTF in the presence of $AuCl_4^-$ yields (BEDT-TTF)-$AuCl_2AuCl_4$, where $AuCl_2$ is again incorporated in the BEDT-TTF sheet and includes Au(II).

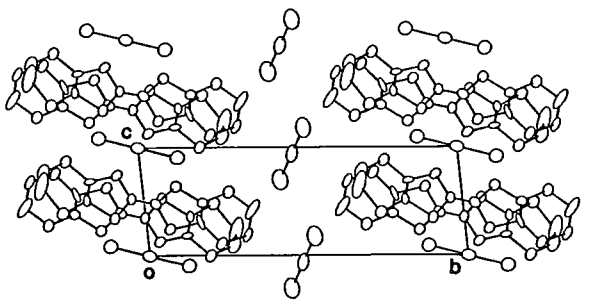

Figure 1. Crystal structure of (BEDT-TTF)$AuCl_2$. The gold atoms of $AuCl_2$ on (0,0,0) and (1/2,1/2,0) are formally Au(II) and Au(I), respectively.

IV-E-2 A Novel Organic Superconductor, $(BEDT\text{-}TTF)_3Cl_2(H_2O)_2$

Takehiko MORI and Hiroo INOKUCHI

[*Chem. Lett.*, **1987**, 1657]
[*Solid State Commun.*, **64**, (1987)]

An organic superconductor $(BEDT\text{-}TTF)_3Cl_2(H_2O)_2$ has been prepared by using $[(C_2H_5)_4N]_2CoCl_4$ as an electrolyte. This complex shows as high conductivity as 500 S cm^{-1} at room temperature, while undergoes a metal-semiconductor transition around 100 K. This transition is gradually suppressed by pressure, and under the pressure of 16 kbar a superconducting state appears at 2 K (Figure 1). The pressure dependence of the resistivity and the anisotropy of the superconducting critical field are investigated.

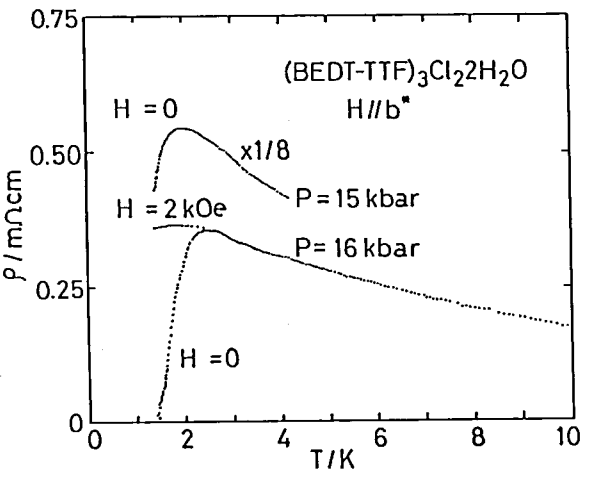

Figure 1. Superconductivity of $(BEDT\text{-}TTF)_3Cl_2(H_2O)_2$. At 15 kbar, the resistivity starts to drop at 2 K. At 16 kbar, the onset, the mid point, and the end point temperatures are 2.5 K, 2 K, and 1.4 K. The breakdown of the superconducting state by the external magnetic field is shown. The field was applied perpendicularly to the BEDT-TTF conducting sheet.

IV-E-3 New Series of Organic Metals, DCNQI Family

Hayao KOBAYASHI*, Reizo KATO*, Akiko KOBAYASHI *(Univ. Tokyo)*, **Takehiko MORI, Kenichi IMAEDA, and Hiroo INOKUCHI** *(*Toho Univ.)*

[*Chem. Lett.*, **1987**, 1579]
[*Solid State Commun.*, **64**, 45 (1987)]
[*J. Phys. Soc. Jpn.*, **56**, 3429 (1987)]

The structural and physical properties of new radical anion salts of DMDCNQI and MClDCNQI have been investigated. Though $(DMDCNQI)_2Cu$ retains a metallic state down to 1.5 K at ambient pressure, a metal-semiconductor transition appears above 4.5 kbar, and the transition temperature increases with an increase in pressure. The salt $(MClDCNQI)_2Cu$, just like the Ag and alkali-metal salts of DMDCNQI and MClDCNQI, undergoes a metal-semiconductor transition even at ambient pressure. In the copper salts, the Cu atom is coordinated in the tetrahedral fashion by the N atoms of four cyano groups. The observation of $2k_F$ reflections and the XPS investigation indicate the formal oxidation state of the copper is $Cu^{1.3+}$ (Figure 1). This may be the first evidence of the molecular metal having the mixed-valent transition metal atoms interacting with the conduction band of organic molecules.

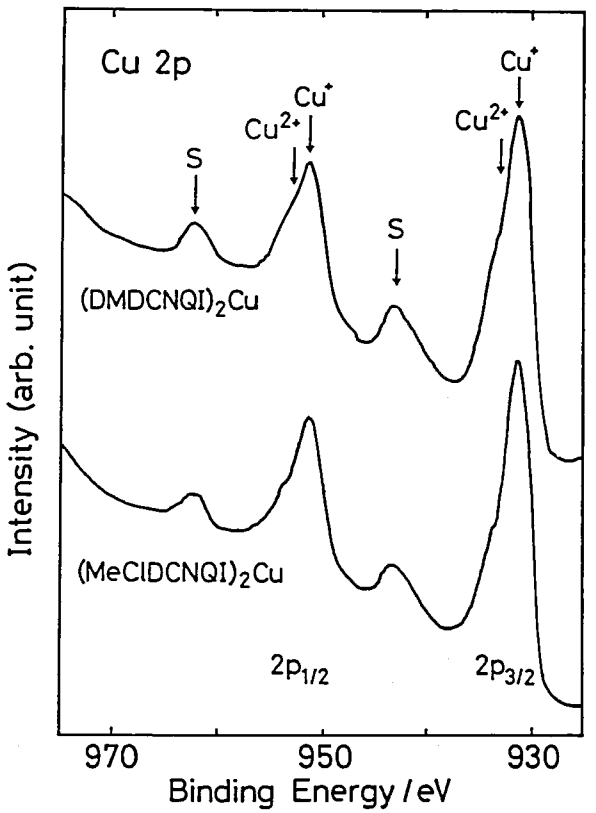

Figure 1. X-ray photoelectron spectra of the Cu 2p levels of $(DMDCNQI)_2Cu$ and $(MClDCNQI)_2Cu$. Both the $2p_{3/2}$ and the $2p_{1/2}$ peaks are respectively, composed of two lines, which can be attributed to Cu^+ and Cu^{2+}. The ratio of Cu^+ and Cu^{2+} is 2:1. The appearance of the shake-up satellites gives another evidence of the existence of Cu^{2+}.

IV-E-4 Structural and Electrical Properties of $(BEDT\text{-}TTF)_3CuBr_3$

Takehiko MORI, Fumiko SAKAI*, Gunzi Saito*, and Hiroo INOKUCHI *(*Univ. Tokyo)*

[*Chem. Lett.*, **1987**, 927]

An organic conductor $(BEDT\text{-}TTF)_3CuBr_3$ has been prepared and its structural and electrical properties have been investigated. The donors form a two-dimensional network (Figure 1), where a charge

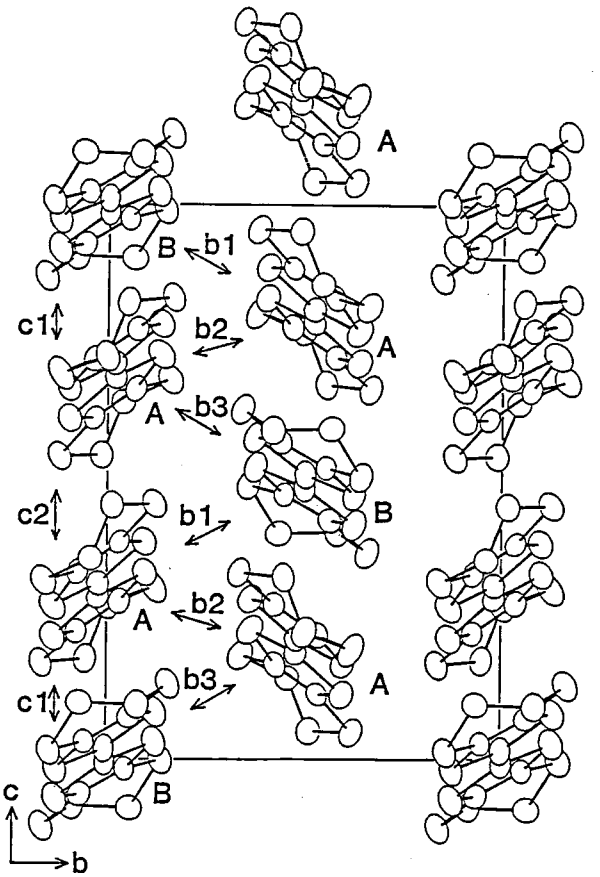

Figure 1. Two-dimensional network of the donors in $(BEDT\text{-}TTF)_3CuBr_3$

separation takes place as $(D^{3/4+}D^{3/4+}D^{0})_2$-$CuBr_2^{-}CuBr_4^{2-}$. The resistivity at room temperature is 0.6 Ωcm and semiconductive.

IV-E-5 Thermal Expansion and Stepwise Superconducting Transition of β-(BEDT-TTF)$_2$(I$_3$)$_{1-x}$-(AuI$_2$)$_x$

Hayao KOBAYASHI*, Reizo KATO*, Akiko KOBAYASHI *(Tokyo Univ.)*, **Takehiko MORI, and Hiroo INOKUCHI** *(*Toho Univ.)*

[*Solid State Commun.*, **60**, 473 (1986)]

The temperature dependence of the lattice parameters and electrical resistivities of β-(BEDT-TTF)$_2$(I$_3$)$_{1-x}$(AuI$_2$)$_x$ are examined. A stepwise resistivity drop similar to that of so-called "high-T_c" and "low-T_c" transitions of the $x = 0$ salt is observed in the $x = 0.9$ salt, where the periodical lattice modulation wave characteristic of the $x = 0$ salt is not observed down to 98 K. On the other hand, no superconducting behavior is observed down to 1.5 K in the $x = 0.1$ salt, whose X-ray investigation gives strong satellite reflections.

IV-E-6 Magnetic Susceptibility of Low-dimensional Organic Conductors with Bis(ethylenedithio)tetrathiafulvalene:(BEDT-TTF)$_3$(ClO$_4$)$_2$ and (BEDT-TTF)$_2$ClO$_4$(C$_2$H$_3$Cl$_3$)$_{0.5}$

Mototada KOBAYASHI, Toshiaki ENOKI, Kenichi IMAEDA, Hiroo INOKUCHI and Gunzi SAITO *(ISSP, Univ. of Tokyo)*

[*Phys. Rev.* **B36**, 1457 (1987)]

The magnetic susceptibilities, χ, have been measured for two-dimensional metallic bis(ethylenedithio) tetrathiafulvalene(BEDT-TTF)-perchlorate salts under slow or rapid cooling conditions. (BEDT-TTF)$_3$(ClO$_4$)$_2$ shows a semimetal-insulator transition due to Peierls instability at 175 K which is independent of the cooling rate. (BEDT-TTF)$_2$ClO$_4$(C$_2$H$_3$Cl$_3$)$_{0.5}$ shows a semimetal-semimetal transition associated with nesting of a part of the Fermi surface at 25 K under slow cooling. Under rapid cooling this transition disappears. this transition disappears.

The dependence of the transition observed for χ on the cooling rate is confirmed by resistivity measurements. The properties and the origin of anomalies observed for χ with the two salts are discussed in connection with the motion of ethylene groups and $C_2H_3Cl_3$ molecules.

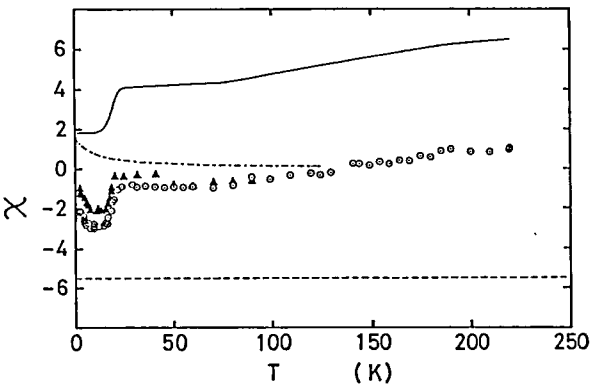

Figure 1. Temperature dependence of χ for the (2:1:0.5) phase with H//b* under the slow cooling condition (10^{-7} cgs emu/g in unit). The symbols ▲ and ⊙ are the results for the first run and the second run, respectively. The dashed, the dash-dotted and the solid lines show the values of χ_c, χ_I and χ_s, respectively, which contribute to χ represented by the symbol ⊙.

IV-E-7 Novel Peri-Condensed Weitz-Type Donors: Synthesis, Physical Properties, and Crystal Structures of 3,10-Dithiaperylene (DTPR), 1,6-Dithiapyrene (DTPY), and Some of Their CT Complexes

Kazuhiro NAKASUJI*, Hirohisa KUBOTA*, Tomoyuki KOTANI*, Ichiro MURATA* *(*Osaka Univ.)*, **Gunzi SAITO** *(Univ. of Tokyo)*, **Toshiaki ENOKI, Kenichi IMAEDA, Hiroo INOKUCHI, Masako HONDA**, Chuji KATAYAMA**, and Jiro TANAKA**** *(**Nagoya Univ.)*

[*J. Am. Chem. Soc.*, **108**, 3460 (1986)]

3,10-Dithiaperylene (DTPR), 1,6-dithiapyrene (DTPY), and their diphenyl derivatives, Ph$_2$DTPR and Ph$_2$DTPY, were prepared as examples of molecular design for condensed type donors with two sulfur atoms. The electrochemistry indicates that these heterocycles are actually two-stage redox systems with low oxidation potentials. We obtained relatively high conductive CT complexes utilizing these donors and

TCNQ-type acceptors. In addition, especially noteworthy is the high conductivity of $Ph_2DTPY\text{-}DDQ_{0.75}$ (σ = 0.5 Scm^{-1}) despite the fact that the complex consists of neither TTF-type donor nor TCNQ-type acceptor. These heterocycles gave stable iodine complexes. The conductivities of these iodine complexes of compressed powder samples are the same order of magnitude with that of the iodine complex of perylene.

IV-E-8 Methylthio and Ethanedithio Substituted 1,6-Dithiapyrene and Their Charge-Transfer Complexes: New Organic Molecular Metals

Kazuhiro NAKASUJI*, Mitsuru SASAKI*, Tomoyuki KOTANI*, Ichiro MURATA*, *(*Osaka Univ.)*, **Toshiaki ENOKI, Kenichi IMAEDA, Hiroo INOKUCHI, Atsushi KAWAMOTO**, and Jiro TANAKA**** *(**Nagoya Univ)*

[*J. Am. Chem. Soc.*, in press]

The synthesis and physical properties of 2,7-bis(methylthio)-1,6-dithiapyrene (MTDTPY) and 2,3:7,8-bis(ethanedithio)-1,6-dithiapyrene (ETDTPY), and their charge-transfer complexes were reported. These two new donors showed reversible two-stage redox behavior with potentials comparable to that of TTF. MTDTPY produced two crystalline phases of 1:1 TCNQ complexes, α-form (monoclinic, $P2_1/c$) and β-form (triclinic, $P\bar{1}$), which consist of mixed stacks and uniform segregated stacks of donors and acceptors, respectively. The single crystal conductivity of the β-form was metallic (σ_{rt} = 110 Scm^{-1}, T_{MI} = 110 K), while that of the α-form was semiconductive (σ_{rt} = 3.4 × 10^{-6} Scm^{-1}). MTDTPY-chloranil crystallized in uniform segregated stacks of donors and acceptors (triclinic, $P\bar{1}$). The single crystal conductivity was metallic (σ_{rt} = 140 Scm^{-1}, T_{MI} = 240 K). MTDTPY-bromanil also showed metallic conductivity (σ_{rt} = 230 Scm^{-1}, T_{MI} = 125 K).

IV-E-9 Electronic Properties of 3,3',5,5'-Tetramethylbenzidine Complexes with TCNQ Derivatives

Kenichi IMAEDA, Toshiaki ENOKI, Gunzi SAITO *(Univ. of Tokyo)*, **and Hiroo INOKUCHI**

[*Mol. Cryst. Liq. Cryst.*, **141**, 131 (1986)]

The charge-transfer complexes of 3,3',5,5'-tetramethylbenzidine (33'55'TMB) with five TCNQ derivatives (F_4TCNQ, FTCNQ, TCNQ, Me_2TCNQ, and $(MeO)_2TCNQ$) were investigated by electrical conductivities, electronic spectra, and vibrational spectra. The physical properties of these complexes are summarized in Table 1. 33'55'TMB-FTCNQ and 33'55'TMB-TCNQ showed the relatively high conductivites. Two charge-transfer bands were observed in the electronic spectra of these complexes. From the correlation between the observed first charge-transfer band and the eastimated one, it was found that FTCNQ and TCNQ complexes were in the intermediate state between ionic and non-ionic states. Including a qualitative estimation of a degree of charge-transfer from IR spectra, the relatively high conductivities of FTCNQ and TCNQ complexes among the benzidine complexes were confirmed to be caused by partial charge-transfer.

Table I. Electrical resistivities and absorption bands of 33'55'TMB complexes.

X in 33'55'TMB-X	Resistivity at room temperature (Ωcm)	Activation energy (eV)	Absorption bands: solid (KBr) (10^3cm^{-1}) 1st	solid (KBr) (10^3cm^{-1}) 2nd	soln (CH_2Cl_2) (10^3cm^{-1}) 1st	soln (CH_2Cl_2) (10^3cm^{-1}) 2nd
F_4TCNQ	2.3 × 10^5	0.45	7.9	15.5	9.8	15.7
FTCNQ	4.6 × 10^2	0.22	7.4	17.5	9.9	17.1
TCNQ	3.6 × 10^3	0.28 0.20	7.2	18.4	10.2	18.0
Me_2TCNQ	8.8 × 10^6	0.40	6.9	18.4	10.3	18.6
$(MeO)_2TCNQ$	1.1 × 10^7	0.46	7.8	19.0	10.9	18.4

IV-E-10 Magnetic Property of an Organic Conductor, (TTM-TTF)$(I_3)_{0.823}$

Kenichi IMAEDA, Toshiaki ENOKI, Takehiko MORI, Peiji WU *(IMS and Inst. Chem., Academia Sinica, China)*, **Mototada KOBAYASHI, Gunzi SAITO** *(Univ. of Tokyo)*, **and Hiroo INOKUCHI**

[*Synth. Met.*, **19**, 721 (1987)]

The magnetic property of an organic conductor, (TTM-TTF)$(I_3)_{0.823}$, with an incommensurate structure has been investigated by means of ESR measurement.

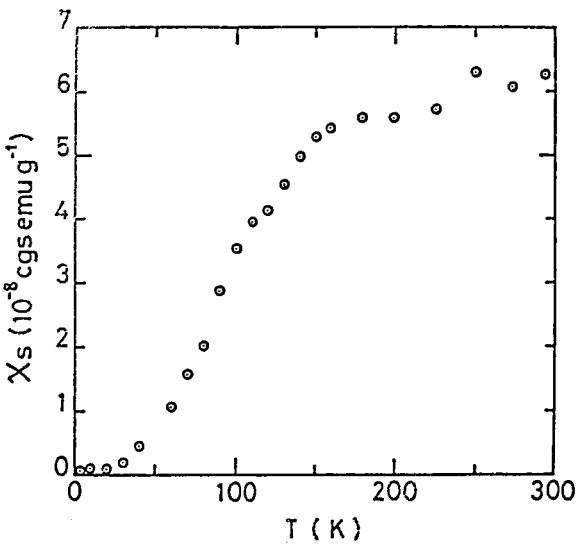

Figure 1. Temperature dependence of the spin susceptibility (χ_s) for the sharp signal.

ESR spectra with a superimposed sharp signal on a broad signal were observed between liquid helium and room temperatures. The sharp signal is assigned to be due to conduction electron spins on TTM-TTF molecules, while the broad one due to localized spins on iodine molecules. The spin susceptibility associated with the sharp signal shows a metal-insulator transition at 100 K, as shown in Figure 1. The temperatures 160 and 100 K with the anomalies of the spin susceptibility for the sharp signal are close to those of the g-value for the broad signal. In addition to these facts, the strong temperature dependence of the g-value for the broad signal suggests that this transition is accompanied by a change in the electronic state of the iodine anion through the mixing of the electronic states of TTM-TTF donor and iodine acceptor.

IV-E-11 Electronic Structure of (BEDT-TTF)$CuCl_2$ Complex

Masashi TANAKA*, Atsushi KAWAMOTO*, Jiro TANAKA*, Mitsuru SANO* *(*Nagoya Univ.)*, **Toshiaki ENOKI and Hiroo INOKUCHI**

[*Bull. Chem. Soc. Jpn.* **60**, 2531 (1987)]

The X-ray photoelectron spectra and the ESR spectra of the (BEDT-TTF)$CuCl_2$ complex were taken. The analysis of the X-ray photoelectron spectra shows that the Cu atoms in (BEDT-TTF)$CuCl_2$ are in a mixed valence state consisting of mono and bivalent cations and the concentration ratio of Cu(I) and Cu(II) is determined to be 2:1. The ESR signals show the presence of the BEDT-TTF cation radical and Cu(II)Cl_2. The temperature dependence of the magnetic susceptibility of these components were obtained from the ESR spectra.

IV–F Studies of Ion-Molecule Reactions by a Threshold Electron-Secondary Ion Coincidence (TESICO) Technique

The knowledge of the microscopic reaction cross sections for evolution of a system in a single reactant quantum state (translational, rotational, vibrational, and electronic) to a single product quantum state is essential for a complete understanding of a chemical reaction. Ion-Molecule reactions are particularly suited for studying such microscopic cross sections since ions can readily be prepared in various internal states in the initial ionization processes, such as photoionization, and the emitted photoelectrons provide information on the distribution among these states.

In this project, we study state-selected ion-molecule reactions by the use of a photoionization technique which utilizes the threshold photoelectron-secondary ion coincidence. The technique allows direct determination of $\sigma(i, v)$, i.e., the reaction cross section as a function of the internal and collisional energies of reactants. The selection of electronic, vibrational, rotational, and fine-structure states are possible by this technique.

IV-F-1 Dynamics of the Reaction $CH_4^+ + CH_4 \rightarrow CH_5^+ + CH_3$. Separation of Two Microscopic Reaction Mechanisms by TOF Coincidence

Shinzo SUZUKI and Inosuke KOYANO

Ion-molecule reactions of the type $MH^+ + MH \rightarrow MH_2^+ + M$ generally have two apparent microscopic reaction mechanisms, viz., proton transfer from ion to neutral and hydrogen atom transfer from neutral to ion. In the present paper, we distinguish these two direct mechanisms in the reaction $CH_4^+ + CH_4 \rightarrow CH_5^+ + CH_3$ using the TESICO technique.[1)]

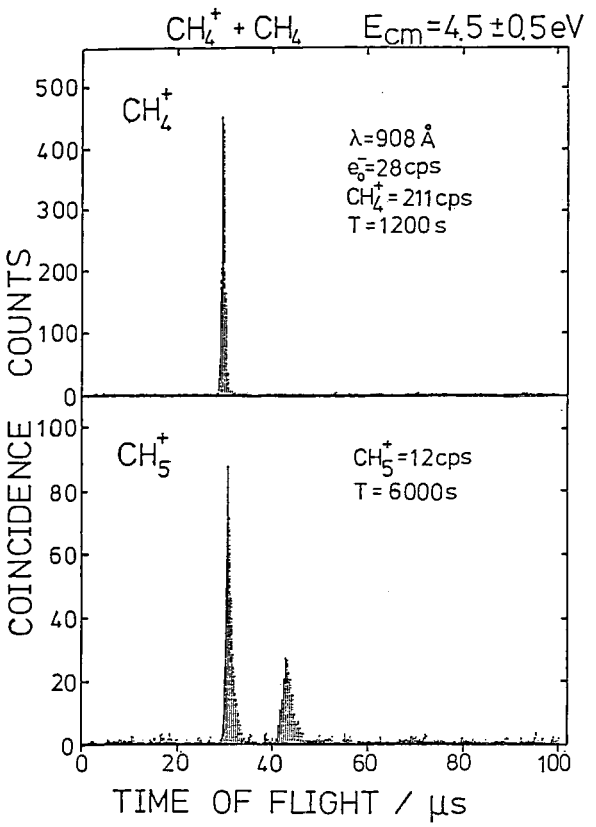

Figure 1. TOF coincidence spectra of the primary and secondary ions of the reaction $CH_4^+ + CH_4 \rightarrow CH_5^+ + CH_3$.

Figure 1 shows an example of the TOF coincidence spectra of the primary (CH_4^+) and secondary (CH_5^+) ions of the reaction. It is clearly seen that the TOF spectrum of the mass-selected ion consists of two peaks, the faster one of which almost coincides with that of the primary ion. This is consistent with the interpretation that the faster one corresponds to the H atom transfer mechanism, which produces the product ion with mass and initial velocity that are almost identical with those of the primary ions at the position of reaction. The slower one then most probably corresponds to the H^+ transfer mechanism.

Reference

1) I. Koyano and K. Tanaka, *J. Chem. Phys.*, **72**, 4858 (1980).

IV-F-2 Dynamics of the Reaction $D_2^+ + D_2 \rightarrow D_3^+ + D$. Separation of Two Microscopic Reaction Mechanisms by TOF Coincidence

Shinzo SUZUKI and Inosuke KOYANO

We have so far investigated internal and collisional energy dependence of the two microscopic reaction mechanisms, viz., H^+ transfer from ion to neutral and H atom transfer from neutral to ion, in the reaction of

the type $MH^+ + MH \rightarrow MH_2^+ + M$. Here we report a preliminary result in the simplest system $D_2^+ + D_2 \rightarrow D_3^+ + D$.

Figure 1 shows a TOF coincidence spectra of the primary (D_2^+) and secondary (D_3^+) ions. As in the previous cases (see **IV-F-1** above and **IV-F-3** of *IMS Ann. Rev.* 1986), it is clearly seen that the TOF spectrum of the mass selected product ion consists of two peaks, the faster one corresponding to the D-atom transfer mechanism and the slower one to the D^+ transfer mechanism. The relative cross sections for the two mechanisms determined from such coincidence spectra show that the importance of the D^+ transfer and D-atom abstraction mechanisms is almost the same at 5.0 eV of c.m. collision energy.

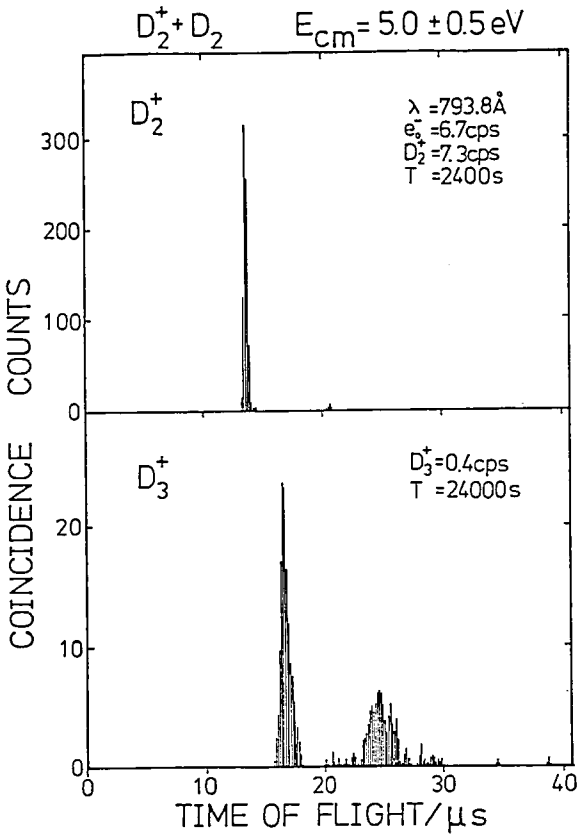

Figure 1. TOF coincidence spectra of the primary and secondary ions of the reaction $D_2^+ + D_2 \rightarrow D_3^+ + D$.

IV-F-3 Vibrational State Dependence of the $H^+(D^+)$ Transfer and the D(H) Abstraction Cross Sections in the $ND_3^+(v) + NH_3$ and $NH_3^+ + ND_3$ Reactions

Shinji TOMODA *(Osaka Univ.)*, **Shinzo SUZUKI, and Inosuke KOYANO**

The effects of the vibrational excitation of the ν_2 mode of ND_3^+ and NH_3^+ on the three reaction channels with NH_3 and ND_3, respectively, are investigated up to $v(\nu_2) = 12$ in the center-of-mass kinetic energy range from 0.9 to 4.5 eV by use of the TESICO technique. The ratio (γ) of the hydrogen (or deuterium) atom abstraction cross section over the competing deuteron (or proton) transfer cross section systematically has a maximum at a vibrational level slightly higher than that giving maximum Franck-Condon factor for the neutralization of each $ND_3^+(v)$ (or $NH_3^+(v)$), as shown in Fig. 1. A new theoretical model based on a non-adiabatic transition theory as well as the proton transfer potential energy surface of the ammonia dimer cation is presented to explain the experimental results. The hydrogen (or deuterium) atom abstraction reaction is interpreted as an electron jump followed by proton (or deuteron) stripping process which proceeds via "electron (charge) transferred" potential surface by near resonant electron transfer process at larger intermolecular separation.

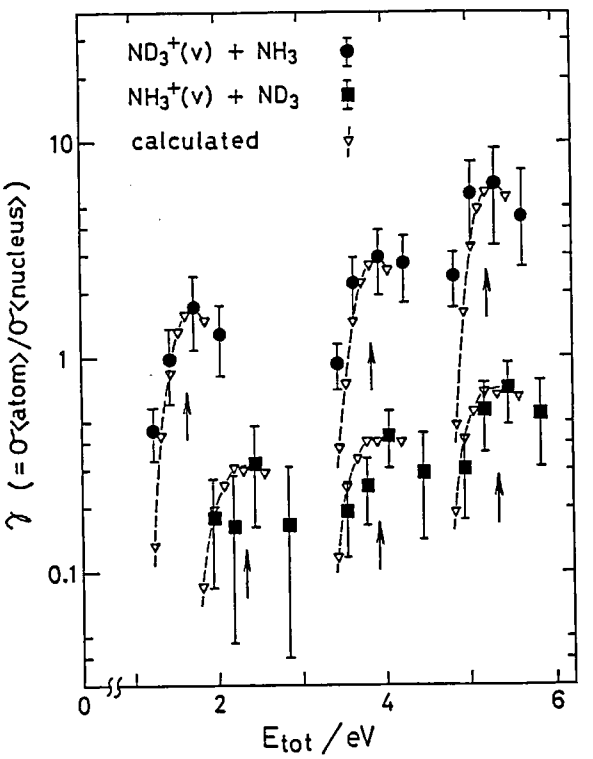

Figure 1. The ratio γ of the "atom transfer" cross section to the competing "nucleus transfer " cross section plotted against the total reaction energy (E_{tot}).

IV-F-4 Internal Energy Selected Reactions in the $C_3H_4^+ + C_3H_4$ Systems

Teruhiko OGATA *(Shizuoka Univ.)*, **Shinzo SUZUKI, and Inosuke KOYANO**

Three channels of the title reaction have been studied for all combinations of reactant ions and neutrals from allene, propyne, and cyclopropene using the TESICO technique. Particular emphasis has been placed on the formation of the $C_3H_3^+$ ions, whose structure, heat of formation, and reactivity have been a controversial issue for a long time. Figure 1 shows the TOF coincidence spectra for the parent and product ions of the cyclopropene$^+$ + allene reaction obtained with the incident photon wavelength of 124.95 nm (0.35 eV internal energy) at 5.0 eV of collision energy. It is clearly seen that the product $C_3H_3^+$ ion shows peculiar TOF profile distinct from those of parent and other product ions. The situation was the same for all $C_3H_3^+$ ions produced by bimolecular reactions, while those

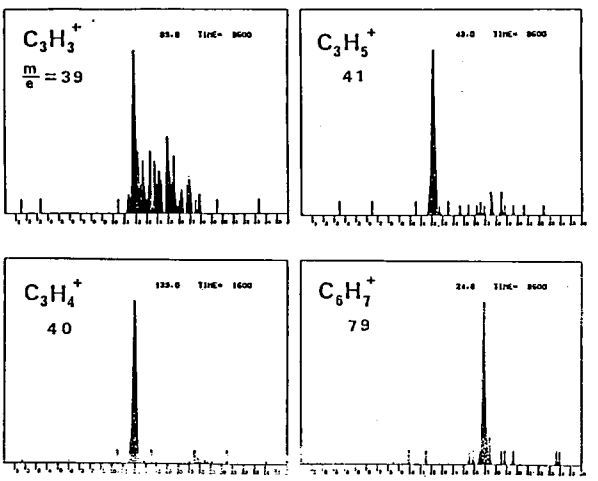

Figure 1. TOF coincidence spectra for the parent and product ions of the $C_3H_4^+$ (cyclopropene) + C_3H_4 (allene) reaction.

produced by unimolecular decomposition of parent ions (at photon energies above dissociation threshold) always had a TOF profile of comparable width as that of the parent ions. These facts would indicate that the $C_3H_3^+$ product is formed via a long lived intermediate complex, in which considerable internal excitation of products takes place.

IV-F-5 State Selected Charge Transfer and Rearrangement Reactions in Four-Atom Ion-Molecule Systems

Inosuke KOYANO, Kenichiro TANAKA *(Natl. Lab. for High Energy Physics)*, **Tatsuhisa KATO** *(Kyoto Univ.)*, **and Shinzo SUZUKI**

[*Faraday Discuss. Chem. Soc.* **84**, in press]

An extensive study of charge transfer and chemical (rearrangement) reactions in four-atom ion-molecule systems $(AB + CD)^+$, where each of AB and CD stands for a diatomic molecule, has been performed by selecting vibrational and vibronic states of reactant ions using the 'TESICO' coincidence technique. Systems studied include $(H_2 + N_2)^+$, $(HD + N_2)^+$, $(D_2 + N_2)^+$, $(O_2 + H_2)^+$, $(NO + H_2)^+$ and $(N_2 + O_2)^+$, and the reactions starting from both $AB^+ + CD$ and $AB + CD^+$ have been studied in each system. Some systems show exactly the same vibrational state dependence for the charge transfer and chemical reactions, while some others show quite different dependence between the two channels. It has also been found that the two reactions $AB^+ + CD$ and $AB + CD^+$ leading to the same product ABC^+ show sometimes similar and sometimes dissimilar internal energy dependences. The experimental internal-state dependence is compared with that calculated from a model appropriate to a long-range electron-jump mechanism. Based on this comparison, some features of the potential-energy surfaces for each system are discussed.

IV–G Probing Transition State in Ion-Molecular Reactions

The experimental knowledge of chemical reactions has long been obtained from detailed observations of the states of reagents and products. Much effort has been made to accomplish state-selection to as detailed an extent as possible. Recently, direct probing of the transition state of a chemical reaction has begun to pave the way for a deeper understanding of the reaction path and is forming a new field in reaction dynamics.

In this project, we attempt to probe transition states of ion-molecule reactions by use of a variety of experimental techniques, including a beam-chamber and/or a supersonic free jet combined with a tunable dye lasers. Detection of stimulated transitions in colliding systems induced by the non-resonant laser irradiation might provide new information on the structure and potential energy surfaces and is expected to open new area in the reaction dynamics. Weakly bound species such as ion-molecule complex prepared in a supersonic expansion is another target for the study of transition state. We attempt to detect the ion-molecule complexes by means of the laser induced fluorescence technique. Such a detection would give an important piece of information on the dynamics of half-collisions in systems where full-collision reactions can also be studied.

IV-G-1 Construction of a Tandem Mass Spectrometer for Probing Transition State in Ion-Molecule Reactions

Takashi IMAMURA, Toshio HORIGOME, Shinzo SUZUKI, Takashi IMAJO, and Inosuke KOYANO

An apparatus for the title purpose is under construction. The system consists of a 60° sector magnetic analyzer which serves as a source of mass-selected primary ion beams, collision chamber, and a quadrupole mass filter as a detector. As an ion source, duoplasmatron is used. This allows us to get high ion-current density up to the space-charge-limit by the accelarator. The mass-selected ion beam is decelerated to tens of eV and injected into the collision chamber held in an octahedral aluminium housing. Transition states in ion-molecule reactions are probed by monitoring fluorescence and/or variation in the ion intensity induced by non-resonant laser irradiation.

IV-G-2 An Investigation of Ion-Molecule Complexes using Laser Induced Fluorescence

Takashi IMAJO, Shinzo SUZUKI, Takashi IMAMURA, and Inosuke KOYANO

It is widely known that the formation of an intermediate complex plays an important role in ion-molecule reactions. However, no direct observation of an ion-molecule complex has been reported. A major difficulty in detecting intermediate complex arises from the short lifetime of it. In the present project, we aim at a direct detection of such complexes. Using free jet expansion, the ion-molecule complex is expected to be frozen and detected by laser induced fluorescence. Vibrational and rotational analyses of a fluorescence excitation spectrum would give information on the structure of the complex, which in turn would yield an important piece of information on the bimolecular ion-molecule reaction mechanism.

IV–H Studies of Unimolecular Decomposition of Simple and Complex Molecular Ions

The TEPSICO and the TEPSICO-II apparatus which we have developed for the study of state selected ion-molecule reactions (see **IV-F** above and **IV-F-4** of *IMS Ann. Rev.* 1984) are also applicable to the study of unimolecular decomposition of molecular ions. In this technique, ions can be prepared with defined amounts of internal energy and their subsequent decomposition investigated. In the present project, we study unimolecular decomposition of both simple and complex molecular ions mainly following valence and inner valence photoionization. Both laboratory and synchrotron light sources are used. Processes following core photoionization

constitute another project (see **IV-I** below).

IV-H-1 Dissociation Mechanism of State Selected NO_2^+ Ions

Kazuhiko SHIBUYA *(Tokyo Inst. of Tech.)*, **Shinzo SUZUKI, Takashi IMAMURA, and Inosuke KOYANO**

In order to elucidate dissociation mechanisms of NO_2^+ from various electronic states, we have measured the threshold electron spectrum (TES) of NO_2, the photoionization efficiency (PIE) curves for its parent and fragment ions, and the threshold electron-ion TOF coincidence spectra in the range 40–80 nm using TEPSICO-II. Figure 1 shows the TOF coincidence spectra for the parent and two fragment ions obtained with excitation at 65.4 nm, corresponding to the onset of the $^3B_2$ $v_1 = 0$ state of NO_2^+. The O^+/NO^+ branching ratio was obtained to be 0.66. The vibrational dependence of the ratio was not observed within the $^3B_2$ state to an appreciable extent.

From similar measurements at 57.9 nm (formation of $^1B_2$ and/or $^3A_1$), the ratio of O^+/NO^+ was found to be 0.16, which is four times as small as the ratio derived for $^3B_2$. Possibly, the fragmentation pattern of excited NO_2^+ could be quite different depending on whether the relevant surface is singlet or triplet.

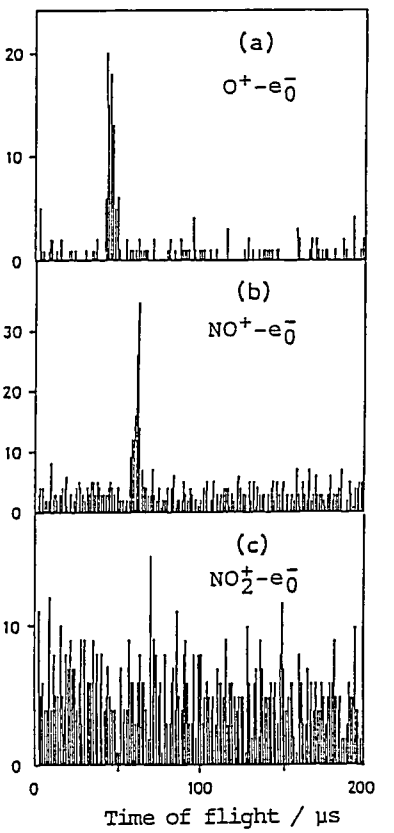

Figure 1. TOF coincidence spectra for the parent and fragment ions of NO_2 at 65.4 nm of incident photons.

IV–I Investigation of Ionic Fragmentation Following Core Level Ionization in the Vapor Phase Using Synchrotron Radiation

Shallow valence level ionization and subsequent fragmentation of molecules have been studied extensively using various kinds of light source in recent years. However, the investigation of processes following core level excitation have not been so extensive, because, for the purpose of such investigation, the conventional light sources are insufficient both in photon energy and intensity. Synchrotron radiation is expected to provide a powerful means to obtain information about the core level excitation. In contrast to the case of the valence electrons delocalized over the molecule, the core electrons in a molecule are localized near the atom to which they belonged originally. As a result, the photoionization from the core level is expected to produce dissociation pathways quite different from those following photoionization from the valence level.

IV-I-1 Production of Pb^+ Ion Following 5d Core Photoionization of Tetramethyl Lead as Revealed by a Coincidence Experiment

Shin-ichi NAGAOKA, Shinzo SUZUKI, and Inosuke KOYANO

[*Phys. Rev. Lett*, **58**, 1524 (1987)]

Ionic fragmentation following Pb 5d core level ionization in tetramethyllead ($PbMe_4$) has been studied with synchrotron radiation. In the wavelength range between 45 and 75 nm, photoionization of the Pb 5d core levels is observed in the threshold electron spectrum of $PbMe_4$. The efficiency for the production of Pb^+ ions increases dramatically in this region, while those of other fragment ions decrease. It is shown that the Pb^+ ion is predominantly produced following 5d photoionization by use of the threshold electron-photoion coincidence technique.

IV-I-2 Investigation of Fragmentation Processes following Core Photoionization of Organometallic Molecules in the Vapor Phase

Shin-ichi NAGAOKA, Shinzo SUZUKI and Inosuke KOYANO

[*Nucl. Instr. Meth.*, in press.]

Ionic fragmentation processes following (n-1)d core level photoionization of organometallic molecules have been studied in the vapor phase using synchrotron radiation. Results on tetramethyllead, tetramethyltin and tetramethylgermanium are reported. The threshold electron spectra and the photoionization efficiency curves of these molecules are presented and discussed. It is concluded that the $(n-1)d^9$ core-hole state of $M(CH_3)_4$ (M = Pb, Sn or Ge) is split into five sublevels owing to both the spin-orbit coupling and the electrostatic perturbations by the methyl groups, and that the M^+ ions are predominantly produced following (n-1)d photoionization.

IV–J Application of Excited-State Photoelectron Spectroscopy to Photophysics and Photochemistry

Laser photoelectron spectroscopy for excited states of gaseous molecules has been developed by means of a multiphoton ionization technique by K. Kimura and his coworkers in this Institute since 1980 [*IMS Annual Review* (1980-87); *Advance in Chemical Physics*, **60**, 161 (1985)]. Since any excited states can in principle be ionized by an appropriate pulse laser, the laser photoelectron spectroscopic technique is especially powerful for studying non-radiative excited states. In this project, we are continuing to use this technique for studying photophysical and photochemical processes in molecular science.

IV-J-1 Molecular Dynamic Photoelectron Spectroscopy Using Resonant Multiphoton Ionization for Photophysics and Photochemistry

Katsumi KIMURA

[*Internat. Rev. Phys. Chem.*, **6**, 195 (1987)]

This is a review article on gas-phase laser excited-state photoelectron spectroscopy. Photoelectron spectra of resonant multiphoton ionization of gaseous molecules are regarded as photoelectron spectra of the resonant intermediate excited states. Therefore, such a technique using a tunable pulse UV/visible laser makes it possible to observe excited-state photoelectron spectra for various molecules and molecular complexes in the gas phase. Molecular nonradiative electronic states for which direct observation is difficult by fluorescence spectroscopy can in principle be studied by this technique. It is also possible to study not only static aspects but also dynamic aspects of molecular excited states from a photoelectron spectroscopic point of view. In this sense, such a spectroscopy is dynamic photoelectron spectroscopy. This is in striking contrast to the VUV photoelectron spectroscopy which is mostly concerned with static aspect of ground-state molecules, and prosperous especially in studies of the dynamic aspect of molecular excited states from photophysical and photochemical points of view. This article is concerned mainly with dynamic photoelectron spectroscopy and its applications to molecular processes such as photodissociation, autoionization, and intramolecular relaxation.

IV-J-2 Photoelectron Spectroscopic Evidence for the Competition of Ionization and Internal Conversion at the S_2 Excited State of Trimethylamine

Hiroyasu SATO *(Mie Univ.)*, **Masahiro KAWASAKI** *(Mie Univ.)*, **Kenzo TOYA** *(Mie Univ.)*, **Kenji SATO, and Katsumi KIMURA**

[*J. Phys. Chem.* **91**, 751 (1987)]

Laser excited-state photoelectron spectroscopy by resonant multiphoton ionization is very useful for characterization of various electronically excited states of molecules in the gas phase. When photoionisation occurs at an excited state in competition with some intramolecular relaxation such as internal conversion or intramolecular vibrational redistribution, photoelectrons can be ejected from relaxed states as well as from the optically prepared excited state. Previously this technique has been applied to benzene, naphthalene, and triethylamine, indicating photoelectron evidence of fast intramolecular vibrational relaxation in the vibrationally excited states. In the present study, we have carried out photoelectron energy measurements for trimethylamine at the laser wavelengths of 192.1, 208.8, 228.7 and 252.7 nm. It has been found that the photoelectron spectra observed at 192.1 and 208.8 nm can be attributed to two ionization processes competing with each other: One from the optically prepared S_2 state and the other from the vibrationally excited S_1 state ($S_1^{\pm}$) produced from the internal conversion $S_2^* \rightsquigarrow S_1^{\pm}$.

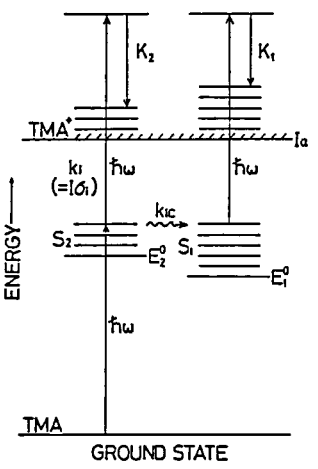

Figure 1. Schematic energy diagram of trimethylamine (TMA) showing two kinds of ionization processes a and b, which take place before and after the internal conversion $S_2^* \rightsquigarrow S_1^{\pm}$.

IV-J-3 Selection Rule and Efficiency for Autoionization of Diazabicyclooctane as Studied by Two-Color Double-Resonance Spectroscopy

Masaki FUJII *(Tohoku Univ.)*, **Kenji SATO, and Katsumi KIMURA**

[*J. Phys. Chem.*, in press]

Photoelectron spectra due to autoionization for two series of high Rydberg states have been observed for diazabicyclooctane (DABCO) in a supersonic jet. The selection rule of the autoionization has been found to be $\Delta v = -1$ for each vibrational mode involved in the Rydberg states, consistent with Berry's theory available for the vibrational autoionization of a polyatomic molecule. The relative autoionization efficiencies for the high Rydberg series have also been determined from two-color MPI and fluorescence dip spectra. The irregular variation in the relative autoionization efficiency with the principal quantum number has been found for the two Rydberg series, suggesting the irregular variation in their non-radiative rates.

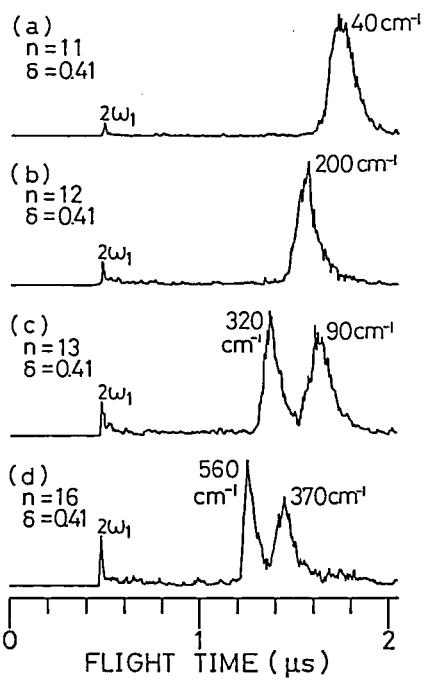

Figure 1. Photoelectron spectra of jet-cooled DABCO obtained through the $\delta = 0.41$ Rydberg states a) n = 11, b) n = 12, c) n = 13, and d) n = 16. The Rydberg vibrational level is $3^1 20^1$, dominantly produced by two-color double-resonant excitation via the S_1 $3^1 20^1$ level. Peaks at 0.5 μs are due to the (1 + 1) ω_1 ionization via the S_1 state. The observed photoelectron energies are indicated on the individual bands.

IV-J-4 Picosecond Laser Photoelectron Spectra of Excited-State Benzene

Katsumi KIMURA and Kenji SATO

Photoionization of a molecular excited state is more or less in competition with its dynamic processes such as electronic and vibrational relaxation processes. So far, nanosecond UV/visible lasers have been used in most excited-state photoelectron studies.[1] Previously, in this laboratory we have obtained photoelectron spectra due to the optically prepared levels and their relaxed vibrational levels after IVR.[2]

In the present work, we have been able to obtain photoelectron spectra due to the (1 + 1) resonant ionization of benzene at three different wavelengths of 208.8, 228.7, and 252.7 nm, using picosecond UV laser radiations (17 ps) which we produced by the second harmonic generation (532 nm) of a modelocked picosecond Quantel Nd-YAG laser (35 ps, 10 mJ, 10 Hz) through a hydrogen Raman shifter (10 atm). Photoelectron spectra were measured with a TOF electron analyzer. From our picosecond work, we have found three kinds of photoelectron bands of benzene: (1) two-photon resonant ionization given by ($2h\nu$-I_a); (2) two-photon resonant ionization from the optically prepared vibronic level; and (3) two-photon two-step ionization through IVR levels.

Reference

1) K. Kimura, *Adv. Chem. Phys.* **60**, 161 (1985); *Internat. Rev. Phys. Chem.*, **6**, 195 (1987).
2) Y. Achiba, A. Hiraya and K. Kimura, *J. Chem. Phys.*, **80**, 36047 (1984).

IV-J-5 Construction of Heat Pipe Ovens for Generation of Tunable VUV Laser

Ivo PLAZIBAT *(Univ. of Split, Yugoslavia)*, **Katsuhiko OKUYAMA, Masahiko TAKAHASHI, and Katsumi KIMURA**

A tunable vacuum ultraviolet (VUV) laser should be powerful especially in the experiments of two-color (1 + 1) resonant ionization for studying highly excited states including autoionizing states of molecules and molecular complexes in the gas phase. The purpose of this work is to design and construct several heat pipe ovens of metal vapor (such as Hg and Mg) to produce intense VUV laser sources which can be useful for photoelectron spectroscopy. One of the heat pipes constructed here is shown schematically in Figure 1, consisting of the double heat pipe structure to make the metal vapor homogeneous. With such a heat pipe oven, we have produced tunable VUV laser radiation with the energy of $2\omega_1 + \omega_2$ by means of a four-wave sum mixing technique by focusing two kinds of strong visible and UV laser beams (ω_1, ω_2) on the same position inside the metal vapor tube. Ion-current measurements in the region 115-168 nm are possible with these heat pipe ovens. The maximum intensity was roughly estimated to be 7 μjoule/pulse at 155 nm.

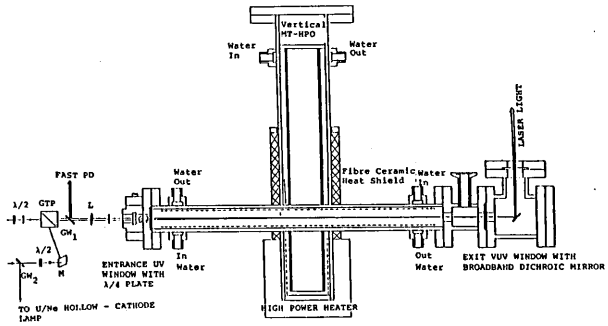

Figure 1. Magnesium heat pipe oven and optical arrangement.

IV-J-6 Application of Tunable VUV Laser Produced with Mg Vapor. (1 + 1) Resonant Photoionization and Photoelectron Spectra due to the Excited $F^2\Delta$ State of NO

Katsuhiko OKUYAMA, Masahiko TAKAHASHI, Ivo PLAZIBAT *(Univ. of Split, Yugoslavia)*, **and Katsumi KIMURA**

In the present work, a heat pipe oven of Mg vapor (IV-J-5) was used for the first time to measure ion-current spectra and photoelectron spectra which are originated from (1 + 1) resonant photoionization of NO via the Rydberg $F^2\Delta$ state at the $v' = 1$ vibrational level. The ion-current spectrum obtained here in the region 155.2–155.6 nm is shown by spectrum (a) in Figure 1, indicating many rotational peaks. Spectrum (b) in Figute 1 is the photoelectron spectrum obtained here at 155.37 nm (indicated by an arrow on the ion-current spectrum), showing a single photoelectron

peak at 0.67 eV. This indicates that the resulting ionic state is the $v^+ = 1$ vibrational level of $NO^+(X)$ produced by $\Delta v = 0$ selection rule.

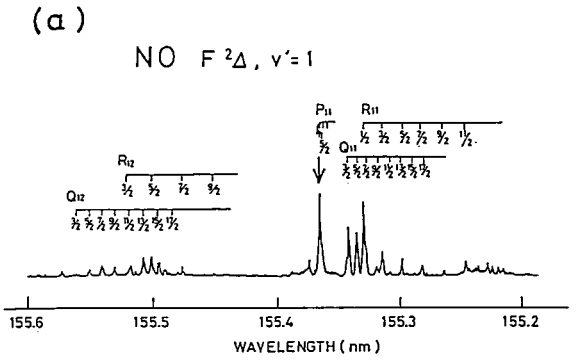

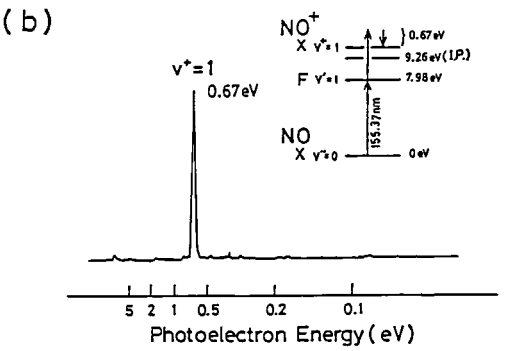

Figure 1. The ion-current spectrum (a) and photoelectron spectrum (b), obtained by two-color photoionization of NO via the Rydberg F $^2\Delta$ state.

IV–K Synchrotron Radiation Researches of Molecules and Molecular Clusters: Photoionization and Photoelectron Spectroscopy

The use of the 750-MeV electron storage ring (UVSOR) of this Institute for photoionization and photoelectron spectroscopy in the gas phase is attractive for studying higher electronic states and various ionic states of molecules and molecular clusters, because of its continuous character of the radiation in the whole VUV region. The synchrotron radiation studies in this project have been carried out with a molecular-beam photoionization apparatus on Beam Line BL2B2.

IV-K-1 Determination of the C-H Bond Dissociation Energies of Ethylene and Acetylene by Observation of the Threshold Energies of H^+ Formation by Synchrotron Radiation

Haruo SHIROMARU, Yohji ACHIBA *(Tokyo Metro. Univ.)*, **Katsumi KIMURA, and Yuan T. LEE** *(Univ. of Calf., Berkeley, U.S.A.)*

[*J. Phys. Chem.*, **91**, 17 (1987)]

The C-H bond dissociation energies D_0(R-H) of ethylene (C_2H_4) and acetylene (C_2H_2) are among some of the most important quantities in chemistry which need to be accurately determined. Acetylene is especially important in the area of combustion, and has received a great deal of attention in recent years. So far, several different values have been reported for the C-H bond dissociation energies of ethylene and acetylene, showing some scatters to a considerable extent. In most of these studies, the C-H bond dissociation energies D_0(R-H) of given hydrocarbons (RH) have been determined from the measurements of the threshould energy of the R^+ formation in the dissociative ionization.

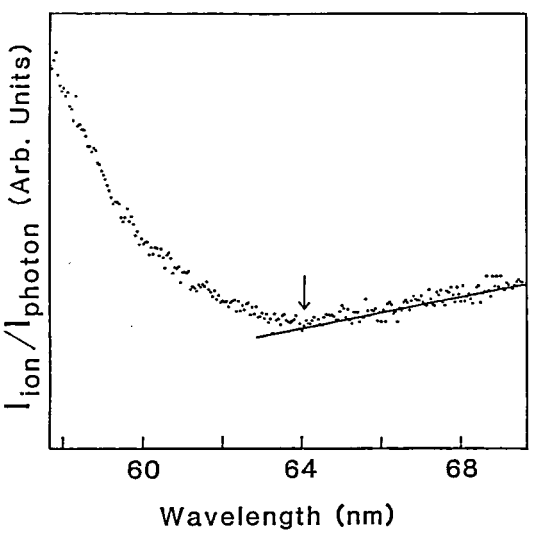

Figure 1. The efficiency curve of H^+ formation in the process $C_2H_2 + h\nu \rightarrow C_2H + H^+ + e^-$, observed by synchrotron radiation through the helium filter gas at 0.1 Torr. The onset of H^+ formation is indicated by an arrow.

In the present work, using synchrotron radiation we have deduced the C-H bond dissociation energy D_0(R-H) by measuring the threshold energy of H^+ formation in the process

$$RH + h\nu \rightarrow R + H^+ + e^-$$

in the wavelength region 58–70 nm. Subtracting the ionization potential of hydrogen atom (13.598 eV) from the observed threshold energies, we have deduced values of 5.06 ± 0.05 eV and 5.75 ± 0.05 eV for the C-H bond dissociation energies D_0(R-H) of ethylene and acetylene, respectively.

IV-K-2 Synchrotron Radiation Measurements of Appearance Potentials for $(H_2O)_2^+$, $(H_2O)_3^+$, $(H_2O)_2H^+$ and $(H_2O)_3H^+$ in Supersonic Jets

Haruo SHIROMARU, Hisanori SHINOHARA, Nobuaki WASHIDA *(Nat'l. Inst. Environ. Stud. and IMS)*, **Hee-Soo YOO** *(Chungbuk Nat'l. Univ.)*, **and Katsmi KIMURA**

[*Chem. Phys. Letters*, **141**, 7 (1987)]

The photoionization of water clusters $(H_2O)_n$ is shown by the reaction $[(H_2O)_n^+]^*_\nu \rightarrow (H_2O)_{n-k}H^+ + OH + (k\text{-}1)H_2O$, where ν represents the vertically ionized point. The absence of unprotonated cluster ions (except for the water dimer ion) is consistently explained in terms of poor Franck-Condon overlaps between the neutral and the ionic states whose potential minima are largely displaced from each other. From pure water clusters the ions $(H_2O)_n^+$ ($n > 2$) have not been observed by photoionization. Recently, using mixed water clusters, Shinohara et al.[1] have observed various unprotonated cluster ions $(H_2O)_n^+$ by using ArI lines.

In the present work, using a water-argon binary mixture in supersonic jets, we have determined the appearance potentials for the unprotonated trimer ion and the protonated dimer and trimer ions by synchrotron radiation for the first time. The appearance potentials for producing $(H_2O)_2^+$, $(H_2O)_3^+$, $(H_2O)_2H^+$ and $(H_2O)_3H^+$ are 10.87 ± 0.06, 10.92 ± 0.04, 11.18 ± 0.02, and 11.10 ± 0.02 eV, respectively.

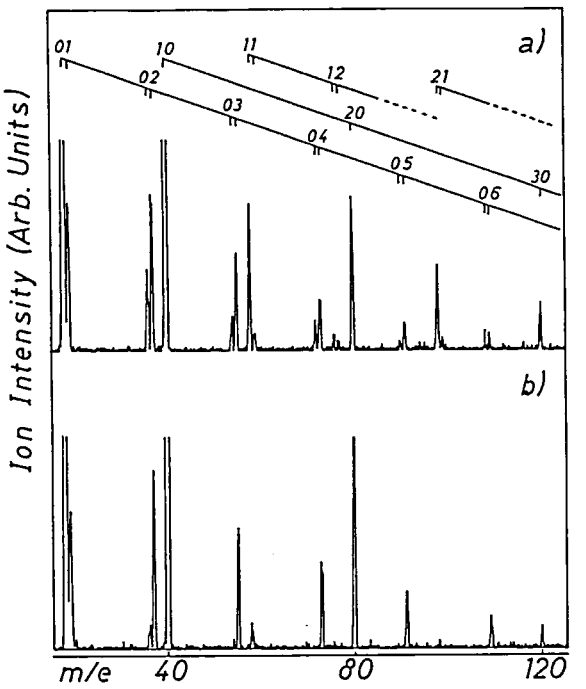

Figure 1. Photoionization mass spectra obtained by synchrotron radiation at 85 nm for a water-Ar binary mixture in a supersonic jet at stagnation pressures of (a) 7.0 atm and (b) 4.0 atm. The numbers "*mn*" on the peaks indicate $Ar_m(H_2O)_n^+$ and $Ar_m(H_2O)_nH^+$, and the numbers "*m*0" indicate Ar_m^+.

Reference

1) H. Shinohara, N. Nishi and N. Washida, *J. Chem. Phys.*, **84**, 5561 (1986).

IV–L Production, Characterization, and Spectroscopic Studies of Molecular Complexes and Clusters

There are several techniques to investigate physics and chemistry of molecular complexes and clusters. One of the most powerful techniques for producing such weakly bound complexes is the supersonic expansion of a high pressure gas through a small nozzle hole, by which one can produce a very large numbers of exotic molecules. However, characterization of such complexes is hard because of its weak bonding character.

In this project we have applied laser induced fluorescence spectroscopy combined with a nanosecond time resolved fluorescence technique to study the dynamics of electronically excited rare gas clusters and solvated molecules of substituted anthracenes produced in a free jet expansion. In the course of the present project we have realized it to be important to fully understand the relaxation dynamics of electronically excited states of isolated molecules.

IV-L Excess-energy Insensitive Fluorescence Decay of Jet Cooled 9,10-Dicyanoanthracene

Satoshi HIRAYAMA *(Kyoto Inst. of Tech.)*, **Fujio TANAKA** *(Univ. of Osaka Prefecture)*, **and Kosuke SHOBATAKE**

[*Chem. Phys. Lett.*, **140**, 447 (1987)]

The fluorescence decays of jet-cooled 9,10-dicyanoanthracene (DCNA) were found to follow single exponentials with the lifetimes which were of the order of 21 ns and were hardly dependent on the excess excitation energy up to 3000 cm^{-1}. Even at 4307 cm^{-1} the decrease in the lifetime was no more than 25%. Complexation with Ar, Xe and ethanol did not alter the dacay feature. Partially cooled states yielded the same lifetime as the supercooled states, making a marked contrast to 9-cyanoanthracene and 9,10-dichloroanthracene.

IV–M Molecular Beam Studies of Chemical Reaction Dynamics

In this project we investigate dynamics of (1) chemical reactions involving reactive species such as N, B, O, and C atoms, (2) dissociative excitation transfer reactions and excimer formations reactions involving metastable rare gas atoms, and (3) molecule-molecule reactions, using a crossed molecular beams technique. For the production of supersonic beams of reactive species used for the reactions (1) and (2), an arc-heated nozzle beam has been used. For the molecular beam chemiluminescence experiments described in the following first three studies, a molecular beam chemistry apparatus-II (MBC-II) with fluorescence detection was used. For the study of molecule-molecule reactions a crossed molecular beam apparatus (MBC-I) with a rotatable mass spectrometer detector was used.

IV-M-1 Deuterium Isotope Effect on the Cross Section for the Dissociative Excitation Process: Ar ($^3P_{0,2}$) + CH_3CN, $CD_3CN \rightarrow$ Ar + CH_3, CD_3 + $CN(B^2\Sigma^+)$

Kiyohiko TABAYASHI and Kosuke SHOBATAKE

[*J. Chem. Phys.*, **87**, 2404 (1987)]

The dissociative excitation of acetonitrile by collision with metastable Ar* has been studied via the absolute cross section over the collision energy range 0.5–2.0 eV. The magnitude of the cross section for CH_3CN/Ar^* lies around 1.7 $Å^2$ and its dependence on collision energy is slightly negative over the energy range studied. For CD_3CN/Ar^* system, in contrast, enhancement of the cross section is prominent at lower energies (by a factor ~ 2), and it shows negative dependence on collision energy also. A comparison of our cross section with total quenching cross section (~ 160$Å^2$) gives an estimate of the low branching fraction

for this process. The results are quite parallel to those of VUV photodissociation and support the conclusion that the dissociative excitation is competitive with other fast exit channels. Fast H elimination from acetonitrile has been postulated as the major exit channel to account for the gross feature of the reaction product. This would explain both the low yield of CN(B) and observed kinetic isotope effect. The negative energy dependence observed for both system indicates that the first collision-induced excitation step is caused by the long-range attractive potential between the reactants.

IV-M-2 Chemiluminescence and Energy Distributions of NO($B^2\Pi$) and NO ($A^2\Sigma^+$) Produced in the Crossed-Beam Reaction of N(^2D, ^2P) with N_2O

Kiyohiko TABAYASHI and Kosuke SHOBATAKE

Chemiluminescent reaction of N(^2D, ^2P) with N_2O has been studied under the collision energies between 0.5 and 2.0 eV. Figure 1 shows a typical product emission spectrum recorded for the lower-energy collisions ($0.5 \leqq E \leqq 1.1$ eV) using TOF energy selection technique. In addition to NO($B^2\Pi$ - $X^2\Pi$) transition comparable intensities of NO($A^2\Sigma^+$ - $X^2\Pi$) band emission are observed. The results show a clear contrast to those obtained at thermal energies, where the formation of NO($A^2\Sigma^+$) is of negligible importance, and indicate the presence of a potential barrier on the particular reaction surface.

The vibrational and rotational distribution in the product NO ($B^2\Pi$) and NO($A^2\Sigma^+$) have been analyzed by computer modeling of the emission spectra. Comparison of a computer generated spectrum with the observed is also shown in Figure 1. The analysis showed that the V/R distribution of NO($B^2\Pi$) are close to the statistical, whereas those of NO($A^2\Sigma^+$) deviate from the statistical distributions. The average branching ratio for these chemiluminescent reactions was found to be NO($A^2\Sigma^+$)/NO($B^2\Pi$) = 0.2 over the collision energies 0.5–1.1 eV and decrease as the collision energy increases above 1.0 eV.

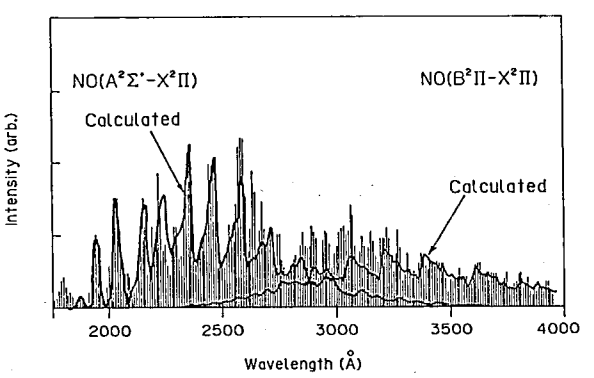

Figure 1. Experimental and calculated bands of NO($B^2\Pi$) and NO($A^2\Sigma^+$) for N(^2D, ^2P) + N_2O collisions. Chemiluminescence by collisions of $0.5 \leqq E \leqq 1.1$ eV is recorded.

IV-M-3 A Supersonic Atomic Oxygen Beam Source for Crossed Molecular Beam Experiments

Kiyohiko TABAYASHI and Kosuke SHOBATAKE

One of reactive species, atomic oxygen, is of particular importance in combustion and upper atmospheric chemistry, and availability of a high intensity O beam source is then a primary requirement in conducting crossed-beam reactive scattering experiments. Our previous approach[1] for generating atomic nitrogen beam was based on dissociation of molecular nitrogen by arc-discharge heating between electrodes prior to nozzle expansion. The disadvantage of using the same source for producing an atomic oxygen beam is to cause rapid corrosion of metal electrodes at high temperatures. Therefore the earliear version of our arc-heater has been modified by mounting a long nozzle channel where oxygen gas can be admixed into a hot argon flow downstream of the discharge region to allow thermal dissociation.

Figure 1 shows a typical TOF spectrum recorded by injection of 5% O_2/Ar gas into the nozzle channel (ℓ = 15 mm). The beam parameters, calculated by fitting the spectrum to the theoretical nozzle beam velocity distribution function are described in the footnote. The fractional dissociation was $\geqq 0.60$, which lead to an O beam flux of $\sim 10^{17}$ atom/sr/sec. The degree of dissociation was found to depend on the power input to the discharging Ar gas, the length of nozzle channel ℓ, and the diluent gas for O_2 admixture. The source is also applicable for the production of other non-condensible atom beams, such as N and H, with much smaller fractions of electronically excited metastable species.

Reference
1) K. Tabayashi, S. Ohshima, and K. Shobatake, *Rarefied Gas Dynamics*, **14**, 635 (1984).

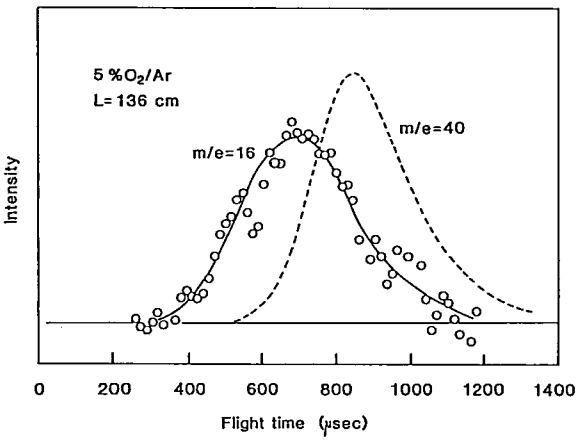

Figure 1. A typical TOF spectrum of O atom beam. The beam parameters are; speed ratio s = 2.9, average parallel velocity $\bar{v}$ = 1.6 × 10^5 cm/sec, and average translational energy $\bar{E}$ = 0.31 eV. The broken line represents a TOF spectrum of the main Ar flow.

IV-M-4 Reactive Scattering of F_2 plus C_6H_6, C_6D_6 in Crossed Molecular Beams

Ye WEN, J. Robb GROVER *(Brookhaven Natl. Lab. and IMS)*, **Yan T. LEE** *(Univ. of Calif., Berkeley and IMS)*, **Kiyohiko TABAYASHI, and Kosuke SHOBATAKE**

Angular distributions and relative total cross sections were measured for products of the title reactions

$$C_6X_6 + F_2 \rightarrow C_6X_6F + F, \quad (X = H, D)$$

at relative collision energies 15–33 kcal/mol using molecular beam chemistry apparatus MBC-I.[1] The conspicuous product is the "ipso"-fluorocyclohexadienyl radical C_6X_6F at M/e = 97[1] for X = H and at M/e = 103 for X = D, which display a rather narrow peak at the laboratory center-of-mass angle at all collision energies studied. This means that the reaction proceeds preferentially by a statistical (unimolecular decay), or largely statistical, mechanism. From careful analysis of F_2 + C_6H_6 data the onset of the reaction was determined to be 13.9 kcal/mol. Figure 1 shows the c.m. collision energy dependence of reactive cross section for F_2 + C_6D_6 reaction measured at the peak position of the angular distribution in the collision energy range 15–33 kcal/mol. The feature above the threshold to 25 kcal/mol is very similar to the one obtained for C_6H_6 reaction. Further, one finds a decrease in the cross section above 27.5 kcal/mol, at which a new reactive channel C_6D_5F + H + F is expected to open as the result of unimolecular decomposition of the vibrationally excited ipso-C_6D_6F radical.

Reference
1) J. R. Grover, Y. T. Lee, and K. Shobatake, *IMS Annual Review* 1986, pp. 98.

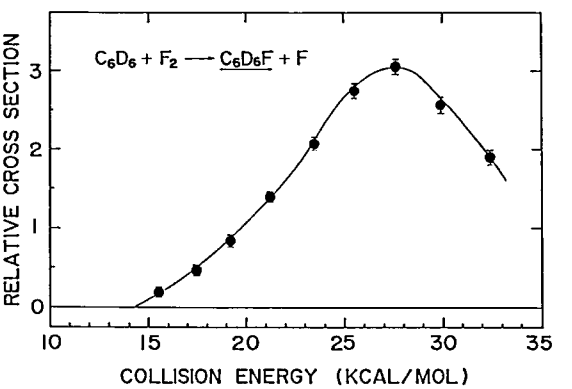

Figure 1. Dependence on c.m. collision energy of the relative cross section for the production of C_6D_6F (M/e = 103) from the reaction of F_2 with C_6D_6 at nominal c.m. collision energies 15–33 kcal/mol.

IV–N Vacuum UV Photochemistry of Molecules and Clusters

Photochemistry by vacuum UV (VUV) light has recently become a very active field owing to the rapid progress in and the relatively easy access to the VUV light sources such as synchrotron orbital radiation (SOR) and VUV laser as well as conventional atomic resonance lines. In the present project we seek to obtain more detailed information about, 1) photodissociation dynamics of simple molecules, 2) production of emitting species from highly excited molecules, and 3) excited states of clusters formed in a supersonic free-jet and chemical reactions from those states, applying direct absorption and fluorescence spectroscopy by means of the tunable VUV light from SOR.

IV-N-1 Vacuum Ultraviolet Fluorescence Excitation Spectrum of I_2

Atsunari HIRAYA and Kosuke SHOBATAKE, Robert J. DONOVAN *(Univ. of Edinburgh)*, **and A. HOPKIRK** *(Daresbury Lab.)*

[*J. Chem. Phys.* in press]

Both absorption and fluorescence excitation spectra were recorded simultaneously using continuously tunable SOR light. At long wavelength (176—210 nm) the fluorescence excitation spectrum is dominated by the $D(0_u^+)$ ion-pair state. Several dips are observed in the fluorescence excitation spectrum in this region as shown in Figure 1. The origin of the dips which coincident with the vibrational structure in the C_6 Rydberg absorption system is attributed to an *intramolecular* nonradiative transitions from the D ion-pair state to the predissociative C_6 Rydberg states. A fairly large and important contribution of hot-band excitations to these dips are suggested. In addition to this type of perturbation, an intense Rydberg system, observed between 149–151 nm, is found to be perturbed by the $F(0_u^+)$ and $F'(0_u^+)$ ion-pair states which give rise to emission in the ultraviolet region.

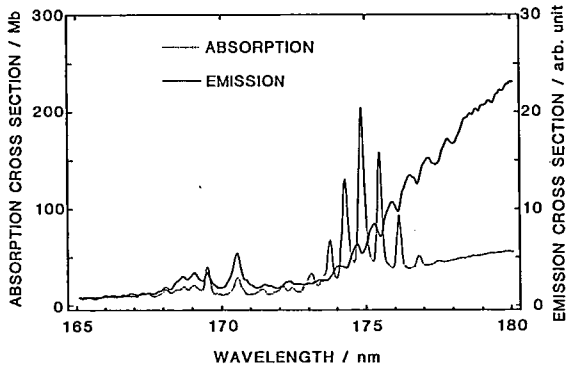

Figure 1. Absorption and fluorescence excitation spectra of I_2 in the wave length range 165–180 nm.

IV-N-2 VUV Photochemistry of $CHFCl_2$ and $CHFBr_2$, Absorption Spectra and CHF ($\tilde{A}^1A''$) Radical Formation

Toshio IBUKI *(Kyoto Univ.)*, **Atsunari HIRAYA, and Kosuke SHOBATAKE**

Absorption and emission excitation spectra of $CHFCl_2$ and $CHFBr_2$ were measured in the wavelength region of 106–200 nm using synchrotron radiation as a light source. The observed bands were assigned as the Rydberg transitions of the outer shell orbitals. In the vacuum ultraviolet photolyses of $CHFCl_2$ and $CHFBr_2$ diffuse emission bands of CHF ($\tilde{A}^1A'' \rightarrow \tilde{X}^1A'$) were observed in the region of 350–700 nm. The 2_0^n(n = 0–4) vibrational progression and 2_1^0 transition were identified. The radiative lifetime of the $\tilde{A}^1A''$ state was determined to be 2.57 ± 0.16 μs. In the photodecomposition of $CHFCl_2$ excited CClF ($\tilde{A}^1A''$) radical with a lifetime of 644 ± 15 ns was also detected.

IV-N-3 Construction of a Supersonic Free-Jet Apparatus for Absorption and Fluorescence Spectroscopy of Supercooled Molecules and Molecular Complexes Using UVSOR as a Light Source

Kosuke SHOBATAKE, Atsunari HIRAYA, and Kiyohiko TABAYASHI

A supersonic free-jet apparatus for absorption spectroscopy and fluorescence spectroscopy of molecules, molecular complexes, and clusters in vacuum UV (VUV) region has been constructed on a beam line BL2A of UVSOR. Figure 1 shows a schematic view of the apparatus. The vacuum chamber is evacuated through a liquid nitrogen trap by an oil diffusion pump (Varian VHS-10, 5000 ℓ/s) backed by a mechanical booster pump (ULVAC YM600-AS, 600 m^3/h). The vacuum chamber is, at present, isolated by a LiF window from 1 m Seya monochromator. The liquid nitrogen trap can be isolated by the upper and the lower gate valves, and can be evacuated through a chemical trap. This isolatable liquid nitrogen trap enables us to use corrosive and toxic gas samples. Sample gas, vaporized from the solid or liquid state at an appropriate temperature, is expanded into the chamber with or without carrier gas through a pulsed valve. The monochromatized SOR light crosses the free-jet and is monitored by a combination of sodium salicylate and photomultiplier tube (PMT). Fluorescence is observed by a PMT perpendicular to both the incident light and free-jet stream line. Photon signals of transmitted light are counted by two counters enabled by two gates, one corresponding to the free-jet on and the other to the free-jet off. In this manner, reliable absorbance can be obtained regardless of the fluctua-

tions of incident light intensity. So far direct absorption and emission excitation spectra are successfully measured for H_2O, D_2O, N_2O, Xe (Xe_2, Xe_n), I_2, and I_2/Xe mixture.

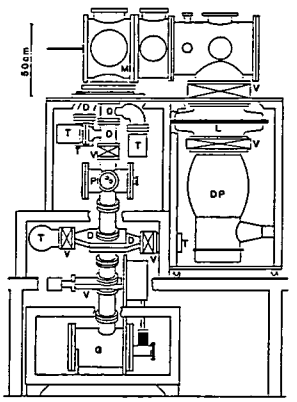

Figure 1. A schematic view of a supersonic free-jet apparatus. From top to down, M: main chamber; V: shutoff valve; D: differential pumping port; T: turbomolecular pump; L: liquid nitrogen trap; P: post-mirror chamber; DP: oil diffusion pump; G: grating chamber.

IV-N-4 VUV Absorption and Fluorescence Excitation Spectra of Jet-cooled I_2

Atsunari HIRAYA, Kosuke SHOBATAKE, and Robert J. DONOVAN *(Univ. of Endiburgh)*

Direct absorption spectrum and fluorescence excitation spectrum of I_2 seeded in a supersonic free jet of He have been measured simultaneously in the wavelength region of 174.5–193 nm as shown in Figure 1 (a). Comparing with the spectra (b) obtained for room temperature vapor, vibrational cooling of I_2 molecules in the free jet is indicated by i) the decrease in intensities of vibrational hot-bands in the C_6 Rydberg system, ii) the narrowing of the vibrational envelopes in the D ion-pair system. Comparing these spectra one can conclude, for the fluorescence dips in D ion-pair system, as follows: 1) The dip at 185 nm, which appears only in vapor phase spectra, does not result from any perturbations but from an overlap of Franck-Condon patterns of each transitions from v" = 0, 1, 2, ... in ground state. 2) The dip at 182.5 nm, observed for both spectra, should result from the crossing of a dissociative potential curve with that of D ion-pair state. 3) For the dips at 174–178 nm, which fade out for the spectrum in jet, a fairly large contribution of hot-band transitions to the D ion-pair state is found. These findings confirm our previous proposal that an isoenergetic perturbation between vibrational levels of the C_6 Rydberg state and those of D ion-pair state is the origin for the dips at 174–178 nm.

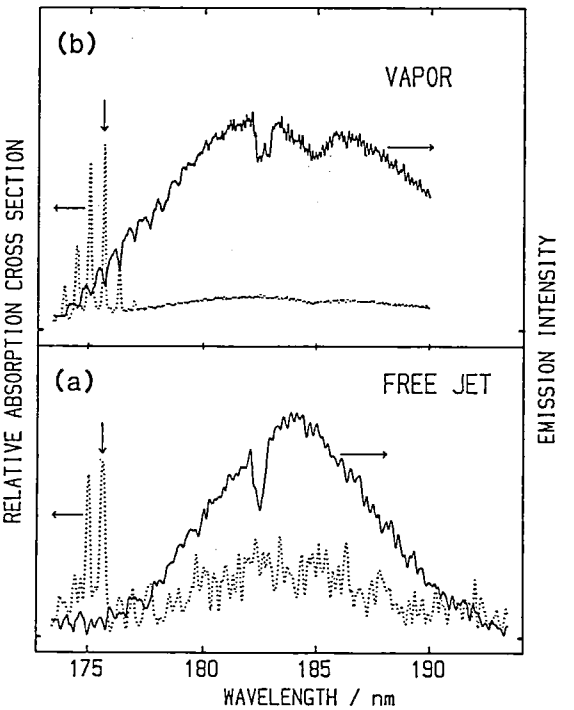

Figure 1. Absorption and fluorescence excitation spectra of I_2 in a supersonic free-jet (a), and in a gass cell (b).

IV-N-5 VUV Absorption and Fluorescence Excitation Spectra of Xe Dimers and Clusters in a Free Jet

Atsunari HIRAYA and Kosuke SHOBATAKE

Although the electronic structure of rare gas dimers have been extensively studied, the interaction potential surfaces of the rare gas clusters are not well known, especially in the electronically excited states. As the first step of the studies on rare gas clusters, direct absorption and fluorescence (λ_f > 180 nm) excitation spectra in the VUV region have been measured in a free jet of Xe. Figure 1 shows the spectra measured under several stagnation pressures in the wavelength region near the first allowed atomic line ($^3P_1$, 146.96 nm). The absorption bands at 146.4 nm and 148.2 nm (in the spectrum at 400 torr) are due to the transitions

to the 1_u and 0_u^+ excited states of Xe dimer, respectively, both of which correlate to $^3P_1 + {}^1S_0$. Under higher pressure conditions, the strong and broad absorption feature with maximum at 147.8 nm becomes apparent. A cubic pressure dependence of the absorbance at 147.8 nm is found. In the fluorescence excitation spectra, the contributions of Xe ($\lambda_f \simeq 147$ nm) and Xe dimer ($\lambda > 180$ nm) should be small since fluorescence is monitored at longer wavelengths than 180 nm. Although the fluorescence spectra of Xe clusters are not known, they should appear in the longer wavelength range than that of dimer. Therefore, it is expected that the present fluorescence excitation spectra represent the excitation function of the cluster(s) formed. In conclusion, the absorption band which extends from 144 nm to 151 nm with maximum at 147.8 nm was assigned as cluster band(s). The location of this cluster band is in good agreement with the lowest absorption peak at 148.3 nm in solid Xe.

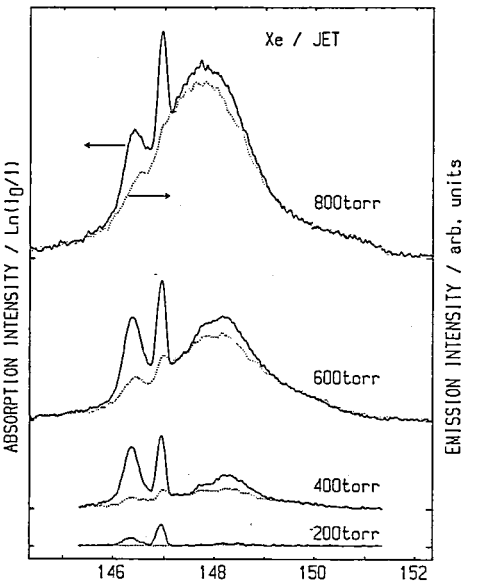

Figure 1. Absorption and fluorescence excitation spectra measured in a supersonic free-jet of Xe at several stagnation pressures.

IV–O Synchrotron Orbital Radiation-Assisted Surface Reactions

Synchrotron orbital radiation (SOR) is a still new light beam source from the view point of promoting chemical reactions on solid surfaces although lithography of the resist materials by means of SOR has been known for about a decade. We have initiated the title project in order to explore the possibilities of promoting surface reactions or making new types of thin films using SOR, and furthermore to understand the mechanisms of photochemical reactions which occur on solid surfaces. In the early stage of this research project we will concentrate our efforts on SOR-assisted etching reaction of some solid surfaces and chemical vapor deposition for forming various thin films.

IV-O-1 Construction of an Apparatus for SOR-Assisted Surface Reaction Studies

Nobuo HAYASAKA, Atsunari HIRAYA, and Kosuke SHOBATAKE

We have constructed an apparatus to study photochemical surface reactions using UVSOR as a light source. Figure 1 is a schematic of the apparatus installed on beam line BL8A. It consists of three chambers, a reaction chamber (RC) and the first (DPC-1) and the second differential pumping chamber (DPC-2). The neighboring chambers are connected to each other via a channel. Each DPC is pumped by a turbomolecular pump (TP) and a liq. N_2 cryopump as well. A thin metal filter fitted between DPC-2 and the beam line chamber serves as a filter to select the wavelength range of the irradiated light and also as a window to prevent reactive gas from going into the beam line.

Solid samples are held on a sample mainpulator in the reaction chamber, the base pressure of which is 1.0×10^{-9} Torr. After the gate value under the RC is closed, sample gas is constantly flowed upon the solid surface through a thin tube. Even when the pressure of sample gases condensable with liq. N_2 is raised to about 0.5 Torr in the reaction chamber, the pressures in the first and the second DPC's reach only 5.0×10^{-5} and 1.2×10^{-8} Torr, respectively. When SOR filtered through a Ti foil 500 Å thick which is transparent mostly in the extreme vacuum region 1–20 nm is admitted into the RC filled with Cl_2 gas, a light bluish-green, cylindrical glow marked the light's path.

The degree of reactivity is measured either by the depth of the etched solid surface or by the thickness of the deposited film per irradiated light.

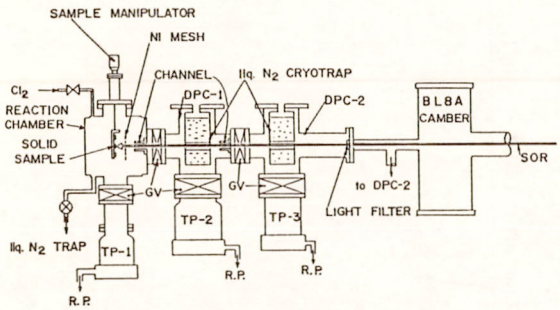

Figure 1. Apparatus used for photochemical surface reaction studies. See the text for explanations except for R.P.: rotary pump, GV: gate valve.

IV-O-2 Synchrotron Radiation-Assisted Etching of Silicon Surface

Nobuo HAYASAKA, Atsunari HIRAYA, and Kosuke SHOBATAKE

[*Jpn. J. Appl. Phys.* **26**, L1110-1112 (1987)]

The photo-assisted etching of heavily phosphorous-doped polycrystalline silicon (n^+ poly-silicon) by chlorine was studied using synchrotron radiation from UVSOR as an extreme UV light source. For the present experiment a SOR surface experimental apparatus with only one differential pumping chamber was used. Transparent light through a Ti foil of 500 Å was irradiated on a n^+ poly-silicon surface. Since the formation of Cl^+ ions was identified from the emission spectrum of the glow marked in the light's path, a rectangularly netted Ni mesh (M) with 64% transmittance was positioned 0.6 cm upstream from the Si sample. The quantum yield for the removal of the Si atoms at a chlorine pressure of 0.3 Torr was found to be about 0.5% photon^{-1} using the Ti-filtered light, which is mostly in th soft x-ray region, 1–20 nm.

Negative bias applied to the Si crystal was found to increase the etch rate. A micrograph of the silicon surface photo-etched for 230 mA hr irradiation at a 75 volt bias voltage and 0.3 Torr Cl_2 gas pressure is illlustrated in Figure 1, the etch depth of which was measured to be 900 ± 100 Å, corresponding to the quantum yield = 1.0%.

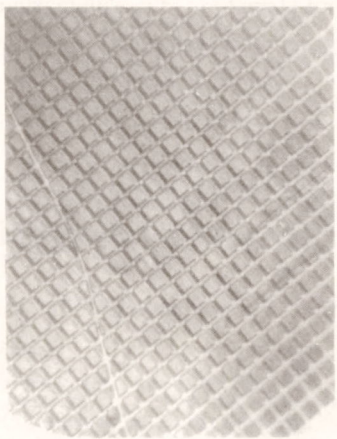

Figure 1. Micrograph of a Si surface obtained by photo-assisted etching by Cl_2 gas at 0.3 Torr using SR with a Ti filter 500 Å thick. The rectangular lines are due to nickel mesh of 20 μm used for an application of negative bias (at 75 V) to the Si sample. The etch depth was measured to be 900 ± 100 Å.

IV–P Black Phosphorus

Black phosphorus is a layered structure semiconductor. We have prepared iodine intercalated compounds of black phosphorus and revealed their metallic character. Recently, inclusion or alloying of silicon, germanium, or gallium to black phosphorus has been undertaken.

IV-P-1 Electrical Properties of Black Phosphorus-Silicon Compounds

Yusei MARUYAMA, Ichimin SHIROTANI *(Muroran Inst. of Technology and IMS)*, **and Toshifumi NISHII** *(Mitsubishi Peterochemical Co. Ltd.)*

Black phosphorus-silicon compounds have been prepared by inclusion of silicon in the course of single crystal preparation of black phosphorus, in the bismuth flux cell or in the high pressure cell. The inclusion efficiency is very low for both cases, and the structure is not known yet. The electrical resistivity becomes a little

lower after inclusion, at most one order, and the temperature dependence of it also changes especially at low temperatures. Several needle-like crystals obtained by bismuth-flux method showed a definite drop in the resistivity around 1.5 K with decreasing temperature. The confirmation of this resistivity drop and the high-pressure effect for the resistivity are now under way.

IV–Q Ultra-Thin Organic Multi-Layers Films Prepared by Molecular Beam Epitaxy Technique

As a strategy for preparation of new types of organic materials, we have undertaken to prepare ultra-thin organic multi-layers films with "MBE" technique. We are expecting new types of charge transfer compounds and/or intercalation compounds (hybrid compounds), and also the realization of novel two-dimensional conductivity in such materials.

IV-Q-1 Ultra-Thin Organic Layers Prepared by Molecular Beam Epitaxy Technique

Hajime HOSHI, Yusei MARUYAMA, and Tamotsu INABE

An ultra-high vacuum MBE system for organic materials has been constructed. TCNQ or TTF-TCNQ has been deposited on silicon, KCl, or saphire single crystals, and the epitaxial structures have been examined mainly with a SEM. The surface conditions of the substrate may be very crucial to the epitaxial growth of the film.

IV-Q-2 Preparation and Charge Carrier Drift Mobility Measurement of Evaporated μ-Bridged Metallophthalocyanine Polymer Films

Anthony John DANN *(Univ. of Nottingham and IMS)*, **Hajime HOSHI, Tamotsu INABE, Martin Richard WILLIS** *(Univ. of Nottingham)*, **and Yusei MARUYAMA**

In collaboration with Dr. M. R. Willis in the University of Nottingham, we have started to study the electronic properties of evaporated μ-bridged (-F-) metallo(Al)phthalocyanine polymer films. The films are prepared with the use of our MBE system or a conventional evaporation system, and ion (iodine) implantation to the films is carried out in the University of Surrey. The films are characterized by a variety of techniques including SEM, ESCA, X-ray diffraction and optical/I.R. spectroscopy. Charge carrier drift mobilities of the films are measured by a surface-type time-of-flight method.

IV–R Preparation and Characterization of Metal Oxide High Temperature Superconductor Films

After the discovery of new high temperature superconductors, La-Ba-Cu-O and Y-Ba-Cu-O, a lot of works including film preparation have been carried out. We also have started to prepare thin films of such superconductors by a sputtering method with the purpose of searching out new compositions, structures and elements for high temperature superconductivity.

IV-R-1 Preaparation and Characterization of Y-Ba-Cu-O Thin Films

Yoichiro KAWAI *(Toyota Motor Corp. and IMS)*, **Toshifumi TERUI** *(Muroran Inst. of Technology and IMS)* **and Yusei MARUYAMA**

We have been trying to prepare Y-Ba-Cu-O thin films with an rf high-rate sputtering machine. Sputtering conditions are quite crucial to get highly conductive films, and especially the composition and the heat treatment of the sputtering target are essentially important in the case of one target sputtering. We are now searching out the best target composition and other sputtering conditions, such as sputtering power, gas pressure or its ratio ($Ar+O_2$), materials of the substrate or its temperature, and so on. Characterization of the obtained films is carried out with X-ray diffraction and ICP analysis.

IV–S Synthesis and Electrical Properties of Organic Conductors

Our research activities are focused on the synthesis and characterization of new type of organic conductors mainly based on AzaTCNQ and OCNAQ, whose structures are shown below.

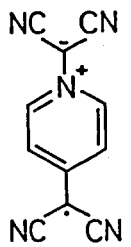

AzaTCNQ

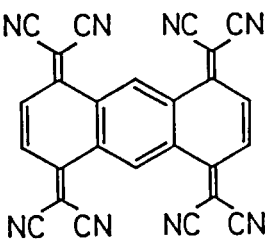

OCNAQ

IV-S-1 Crystal Structures and Electronic Properties of Organic Conductors Based on AzaTCNQ

Hatsumi URAYANA *(ISSP, Univ. of Tokyo)*, **Tamotsu INABE, Takehiko MORI, Yusei MARUYAMA, and Gunzi SAITO** *(ISSP, Univ. of Tokyo)*

AzaTCNQ (4-dicyanomethylenepyridinium dicyanomethylide) is employed as an organic acceptor to form new organic conductors with a TTF family such as TTF, TMTTF, TMTSF, HMTTF, and DBTTF. Among them, TMTTF and TMTSF give 2:1 single crystals and the latter affords the most conductive complex which shows the metallic character down to 150 K, observed by the measurements of the thermoelectric power and the ESR spectra. The crystal structure analysis indicates that only TMTSF molecules stack to form one-dimensional conduction pathways, while AzaTCNQ molecules are arranged side-by-side and oriented almost perpendicular to the donor molecules. The orientational disorder of the nitrogen atoms of AzaTCNQ molecules may be associated with a weak temperature dependence of the electrical conductivity.

IV-S-2 A Twin-TCNQ-type Acceptor: Synthesis of 11,11,12,12,13,13,14,14-Octacyano-1,4:5,8-anthradiquinotetramethane and the Structure of Its (1:1) Tetraethylammonium Salt

Tsutomu MITSUHASHI *(Univ. of Tokyo)*, **Midori GOTO** *(Nat. Chem. Lab. for Industry)*, **Kazumasa HONDA** *(Nat. Chem. Lab. for Industry)*, **Yusei MARUYAMA, Tadashi SUGAWARA** *(Univ. of Tokyo)*, **Tamotsu INABE, and Tokuko WATANABE** *(Univ. of the Air)*

[*J. Chem. Soc., Chem. Commun.*, **1987**, 810]

Bromination of octahydroanthracene with N-bromosuccinimide (NBS) followed by dicyanomethylation with excess of $NaCH(CN)_2$ followed by repetition of the successive bromination-dehydrobromination procedure gives the title compound (20%), the structure of which has been confirmed by X-ray analysis of its monoanionic semiconductor Et_4N salt.

IV-S-3 Organic Conductors Based on OCNAQ (11,11,12,12,13,13,14,14-Octacyano-1,4:5,8-anthradiquinotetramethane)

Tamotsu INABE, Tsutomu MITSUHASHI *(Univ. of Tokyo)*, **and Yusei MARUYAMA**

Several new electrically conductive OCNAQ complexes with organic donors have been prepared. The metallic behavior of TTF and TTT complexes is observed in conductivity measurements. The thermoelectric power measurements show that both compounds are semimetallic.

IV-S-4 Crystal Structure and Electrical Properties of $(TTT)_2OCNAQ(DMF)$

Tamotsu INABE, Tsutomu MITSUHASHI *(Univ. of Tokyo)*, **and Yusei MARUYAMA**

Solvent included single crystals of $(TTT)_2OCNAQ(DMF)$, where TTT is tetrathiatetracene and DMF is *N,N*-dimethylformamide, have been prepared electrochemically. The TTT molecules stack one-dimensionally while the OCNAQ molecules turn their plane parallel to the TTT columns as shown in Figure 1. There are some short contacts between the S atoms of TTT and the N atoms of OCNAQ. The crystal is metallic above 300 K, and the small anisotropy of conduction ($\sigma_{//c}/\sigma_{\perp c} \sim 30$) suggests the existence of intercolumnar interactions.

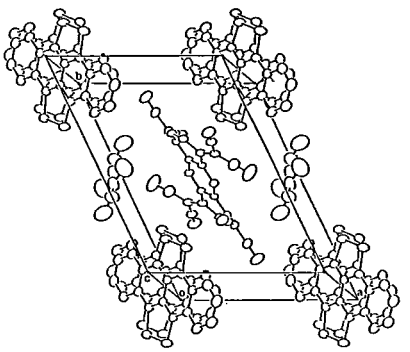

Figure 1. Crystal structure of $(TTT)_2OCNAQ(DMF)$.

IV–T Synthesis and Characterization of Proton-Transfer/ Charge-Transfer System

Hydrogen bonded system, in which proton transfer is coupled to the π-electron configurational change, is subjected to the studies. In such a system, there are two kinds of chemical species which are interconvertible by the proton transfer. Molecule itself can be utilized as memory divices or switching devices. Furthermore, if the intermolecular interaction is sufficiently strong in the crystalline state, the proton transfer is expected to largely modulate the solid state properties, especially the coupling between the electronic properties and proton motion is expected. To investigate the possibility mentioned above, compounds which have fundamental skeleton of salicylideneaniline have been synthesized. Some of them studied in detail are shown below.

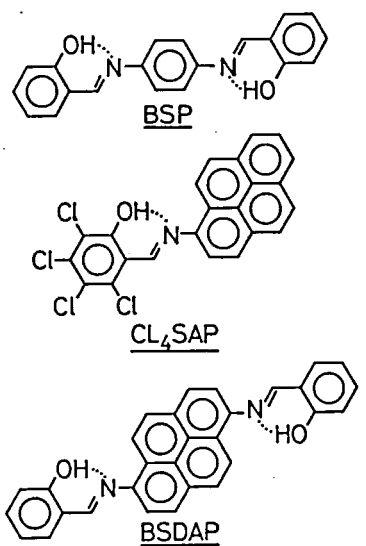

IV-T-1 Structure and Optical Properties of a Thermochromic Schiff Base. Thermally Induced Intramolecular Proton Transfer in *N,N'*-Bis(salicylidene)-*p*-phenylenediamine Crystals

Naomi HOSHINO, Tamotsu INABE, Tadaoki MITANI, and Yusei MARUYAMA

A thermochromic derivative of salicylideneaniline, *N,N'*-bis(salicylidene)-*p*-phenylenediamine (BSP), has been prepared and subjected to structural and optical studies in the crystalline state. The X-ray crystallographic analysis shows that the molecules are planar and stacked in parallel fashion to form one-dimensional

columns. The interplanar spacing is found to be quite small, suggesting the existence of intermolecular charge transfer interaction. The molecules contain fairly short O-H···N hydrogen bonds, the strength of which is manifested in an OH stretching absorption band in the infrared region showing considerable broadening and low-frequency shift. The BSP crystals are remarkably thermochromic and visible absorption and emission spectral changes with temperature have been interpreted in terms of intramolecular proton transfer from hydroxyl oxygen to imine nitrogen through O-H···N hydrogen bond. Emission spectra have also been examined under high pressures.

IV-T-2 Intra/Intermolecular Charge Transfer System Induced by Intramolecular Proton Transfer; *N*-Tetrachlorosalicylidene-1-aminopyrene (CL_4SAP)

Tamotsu INABE, Naomi HOSHINO, Tadaoki MITANI, and Yusei MARUYAMA

The title compound, which has a specific feature of intramolecular proton transfer through the hydrogen bond, has been synthesized. The molecule also consists of donor and acceptor portions, and the structural study reveals the existence of intermolecular charge transfer interaction in the solids. Single crystal infrared spectral as well as the crystallographic studies show that fairly strong hydrogen bond is formed in this material.

IV-T-3 Intramolecular Hydrogen Bonded System; *N,N'*-Bis(salicylidene)-1,6-diaminopyrene (BSDAP). Its Exceptional Properties among Salicylideneaniline Derivatives

Naomi HOSHINO, Tamotsu INABE, Tadaoki MITANI, and Yusei MARUYAMA

The title compound has been synthesized as a member of intramolecular proton transfer system. Although it has a fundamental skeleton of salicylideneaniline, the chromic behavior has not been observed. The structural study reveals the non-flat structure of BSDAP. The intramolecular hydrogen bond is not weak, but the deformed structure which is fixed in the crystal makes unable to transfer the proton.

IV-T-4 Studies of Proton-Transfer/Charge-Transfer Complexes

Tamotsu INABE, Naomi HOSHINO, Tadaoki MITANI, and Yusei MARUYAMA

Some salicylideneaniline derivatives have been employed as a donor component to form charge transfer complexes with TCNQ derivatives. This is the first example of the charge transfer complexes which include the intramolecular proton transfer system. Among the complexes obtained two compounds, (I) and (II), have been studied structurally. In both compounds the donor and acceptor molecules form mixed-stack structure, but the composition is different from each other; 1:2 for (I) and 2:1 for (II). The specific feature is appeared in the hydrogen bonded part of the donor molecule in both complexes. Namely the proton which should be bound to the hydroxyl oxygen in the single component crystals is located near the center of hydrogen bond or rather close to the imine nitrogen upon formation of complex. This indicates that the position of proton is quite sensitive to the electronic states of system, suggesting the possibility of the coupling between the electronic properties and proton motion, which is desirable situation for this project.

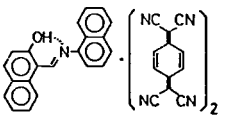

(I)

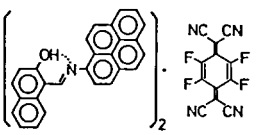

(II)

IV–U High-T_c Oxide Superconductors

Until Bednorz and Müller published their historical discovery of high-T_c oxide superconductors, various conductive oxides had been studied here with a motive force to find new type superconductors or high-T_c superconductors. After their discovery, various kinds of experimental studies have been carried out to clarify what kind of differences cause the large difference between the T_c-values of newly found high-T_c oxides and other oxides which were studied here. Search for similar high-T_c superconductors have also been carried out. Here, single crystals of $(La_{1-x}M_x)_2CuO_{4-\delta}$ (M = Sr and Ba) have been first synthesized and the large anisotropy of the transport properties have been experimentally shown. $LnBa_2Cu_3O_{7-\delta}$ with various magnetic lanthanide atoms Ln was discovered and first reported here. Reported results of these works are briefly shown below.

IV-U-1 X-Ray Analysis on Structural Transition in Magnéli Phase Mo_nO_{3n-1} I. Superlattice structure in Mo_9O_{26}

Masashige ONODA and Masatoshi SATO

[to be submitted to *J. Solid State Chem.*]

Structural study by four-circle X-ray diffraction have been carried out for Magnéli phase molybdenum oxide Mo_9O_{26}, which undergoes the transition to the commensurate phase at about 400 K. The real crystal structure with superlattice reflections and the average one with the assumption of zero intensity for all superlattice reflections, which approximately describes the structure above 500 K, are determined. Full-matrix least-squares refinement give the final values of ($R(F)$ = 0.041 and $R_w(F)$ = 0.071 for the real structure on 2805 independent reflections and $R(F)$ = 0.026 and $R_w(F)$ = 0.050 for the average one on 2264 independent reflections. The condensed mode at the transition is found to have a similar character to that of the M_3-mode of the pseude-cubic lattice of MoO_6 octahedra. The structural transition is found to be associated with the charge-density-wave formation by the application of Zachariasen's bond length-bond strength relation to the Mo-O bonds for the real and average structures.

IV-U-2 X-Ray Analysis on Structural Transition in Magnéli Phase Mo_nO_{3n-1} II. Superlattice structure in $(Mo_{0.88}W_{0.12})_{10}O_{29}$

Masashige ONODA and Masatoshi SATO

[to be submitted to *J. Solid State Chem.*]

Structural study by four-circle X-ray diffraction have been carried out for Magnéli phase molybdenum oxide $Mo_{0.88}W_{0.12})_{10}O_{29}$. The present compound undergoes the transition to the commensurate phase at about 612 K which is higher than those of other members of Magnéli phase oxides, Mo_8O_{23} and Mo_9O_{26}. The real crystal structure with superlattice relfections and the average one with the assumption of zero intensity for all superlattice reflections are solved and refined to $R(F)$ = 0.061 and $R_w(F)$ = 0.073 on 2568 independent reflections, and $R(F)$ = 0.048 and $R_w(F)$ = 0.061 on 2221 independent ones, respectively. It is found that the condensed mode at the transition is mainly described by the inhomogeneous rotations of MoO_6 octahedra and the transition is associated with the charge-density-wave formation. A correlation between the transition temperature and the conduction electron number density in the present compound series is pointed out.

IV-U-3 Structural Transitions in Mo_nO_{3n-1} (n = 9 and 10)

Masatoshi SATO, Masashige ONODA, and Yuji MATSUDA

[*J. Phys.*, **C20** (1987)]

Resistivity measurements and structural studies have been carried out for Magnéli phase molybedenum oxides, Mo_9O_{26} and $(Mo_{0.88}W_{0.12})_{10}O_{29}$. Resistivities of both compounds are quite anisotropic and for Mo_9O_{26} the temperature dependence is very similar to that of

Mo_8O_{23} which was reported previously. The resistivity of $(Mo_{0.88}W_{0.12})O_{29}$ behaves as a semiconductor. Both compounds undergo the structural transitions above room temperature to the commensurate phase. The condensed modes are readily shown to have a character of M_3-like one of the pseudo cubic lattice of MoO_6 octahedra. The valence orderings take place at the transitions similarly to the case of Mo_8O_{23}, although the M_3-like rotational mode of the octahedra, at first sight, does not seem to couple to the charge density wave. The transition temperature or the electron-phonon coupling becomes larger as the conduction electron number density ($2/n$ per Mo atom) becomes smaller for the present Magnéli phase compounds.

IV-U-4 Localization and Superconductivity in $Li_{0.9}Mo_6O_{17}$

Masatoshi SATO, Yuji MATSUDA, and Hidetoshi FUKUYAMA* *(*Institute for Solid State Phys., Tokyo Univ.)*

[*J. Phys.*, **C20**, L137 (1987)]

By use of the physical parameters extracted from the previous and the present experimental studies, the phenomena of sharp resistivity rise with decreasing temperature and the subsequent onset of superconductivity at low temperature found in $Li_{0.9}Mo_6O_{17}$ are explained by the electron-electron interaction effect within the weak-localisation regime. The compound can be considered to be a microscopically random material which exhibits two conflicting phenomena, superconductivity and electron localisation.

IV-U-5 Electron Tunneling Study on Superconductivity of $Li_{0.9}Mo_6O_{17}$

Toshikagu EKINO*, Jun AKIMITSU*, Yuji MATSUDA, and Masatoshi SATO *(*Aoyama-Gakuin Univ.)*

[*Solid State Commun.*, **63**, 41 (1987)]

Quasiparticle tunneling measurement has been carried out for a single crystal of $(Li_{0.65}Na_{0.35})_{0.9}Mo_6O_{17}$ through the point contact with Al electrode. The observed energy gap is consistent with the BCS value and the shape of the tunneling density-of-states confirms the intrinsic origin of the occurrence of the superconductivity in the present compound. The result supports the idea that the same electron system exhibits two conflicting phenomena, the superconductivity and the sharp resistivity upturn above T_c with decreasing temperature.

IV-U-6 Superconductivity of La-M-Cu-O System (M = Ba, Sr and Ca)

Masatoshi SATO, Syoichi HOSOYA*, Shin-ichi SHAMOTO, Masashige ONODA, Ken-ichi IMAEDA, and Hiroo INOKUCHI *(*Institute for Materials Research, Tohoku Univ.)*

[*Solid State Commun.*, **62**, 85 (1987)]

Superconductivity of the compounds of La-M-Cu-O system with K_2NiF_4 type structure has been studied. For the sintered compounds with M = Ba, Sr and Ca, the highest onset transition temperatures, T_{ci}, estimated from resistivity measurement are about 36.9 K, 43.0 K and 23.5 K, respectively and the highest temperatures where the resistivity vanishes, T_{cf}, are about 27.8 K, 34.0 K and 15.5 K, respectively. Almost complete Meissner effect has been confirmed by low frequency ac susceptibility measurement. Crystals of the compounds with M = Ba and Sr have been prepared. As the result of the preliminary experiment for a crystal with Ba, it is found that T_{cf} of the crystal is higher than any one of the sintered specimens with M = Ba, while the T_{ci} of the crystal is nearly the same as the highest one of the sintered specimens.

IV-U-7 Electron Tunneling Study of High-T_c Superconductor, La-Sr-Cu-O System

Toshikazu EKINO+, Jun AKIMITSU+, Masatoshi SATO, and Syoichi HOSOYA* *(*Institute for Mateirals Research, Tohoku Univ., +Aoyama-Gakuin Univ.)*

[*Solid State Commun.*, **62**, 535 (1987)]

Electron tunneling experiment on novel superconductor La-Sr-Cu-O system with the transition temperature of about 35 K has been carried out by point contact

method. The observed electronic density of states is smeared out compared with the BCS one. The energy gap seems to be larger than 3.52 kT_c expected by BCS theory. Based on these results, the superconducting properties of the system are discussed.

IV-U-8 Anisotropy of the Superconducting Critical Magnetic Field H_{c2} of La-M-Cu-O System (M = Sr and Ba)

Shin-ichi SHAMOTO, Masashige ONODA, Masatoshi SATO, and Syoichi HOSOYA* *(*Institute for Materials Research, Tohoku Univ.)*

[*Solid State Commun.*, **62**, 479 (1987)]

Preliminary measurement of the superconducting critical magnetic field H_{c2} of La-M-Cu-O system (M = Sr and Ba) with layered perovskite structure has been carried out. The results show a quite large anisotropy of H_{c2} indicating that the present system has a two dimensional character of the electron transport. The measured conductivities seem to be consistent with the values estimated from the observed H_{c2} by use of an ideal two dimensional band with free electron mass.

IV-U-9 Pressure Effect on Superconductiviting Transition Temperature of La-Sr-Cu-O System

Masatoshi SATO, Masashige ONODA, Shin-ichi SHAMOTO, Syoichi HOSOYA*, Yuji MATSUDA, and Yusei MARUYAMA *(*Institute for Materials Research, Tohoku Univ.)*

[*Chem. Lett.*, 1039 (1987)]

Effect of pressure on the superconducting transition temperature of La-Sr-Cu-O system has been studied up to 5.9 kbar with the use of a conventional clamp cell method. The transition temperature T_c where the resistivity vanishes increases linearly in response to the applied pressure p within the observed range, namely dT_c/dp = 0.2 K/kbar, and the onset temperature of the superconductivity seems to increase more sensitively with the pressure.

IV-U-10 High-T_c Superconductivity in New Oxide Systems

Syoichi HOSOYA*, Shin-ichi SHAMOTO, Masashige ONODA, and Masatoshi SATO *(*Institute for Materials Research, Tohoku Univ.)*

[*Jpn. J. Appl. Phys.*, **26**, L325 (1987)]

Superconducting transitions have been observed by resistivity measurements for several specimens of L-M-Cu-O system with L being Yb, Lu, Y, La and the mixture of Yb and La, and M being Ba and mixture of Ba and Sr. The onset transition temperature T_c becomes very close to 100 K. Since Yb-Ba-Cu-O and Lu-Ba-Cu-O have almost the same transition temperatures (T_c > 90 K), the magnetic moment of Yb atoms does not seem to destroy the superconductivity in the present system. This suggests that the superconductivity occurs in certain parts of the system which are, at least, far from the Yb atom sites. Therefore M-Cu-O or Cu-O system may have an essential role in the occurrence of the superconductivity.

IV-U-11 High-T_c Superconductivity in New Oxide Systems II

Syoichi HOSOYA*, Shin-ichi SHAMOTO, Masashige ONODA, and Masatoshi SATO *(*Institute for Materials Research, Tohoku Univ.)*

[*Jpn. J. Appl. Phys.*, **26**, L456 (1987)]

Superconducting transitions observed by resistivity measurements for several new systems of L-M-Cu-O, where L = Tm, Er, Ho, Dy, Eu and Lu, and M = Ba are reported. Although all of the elements L except for Lu have magnetic moment, the transition temperature T_c is as high as almost 100 K. This is suggestive that the M-Cu-O or Cu-O system has an essential role for the high-T_c superconductivity.

IV-U-12 Superconductivity of La-M-Cu-O System (M = Ba, Sr and Ca)

Masatoshi SATO and Syoichi HOSOYA* *(*Institute for Materials Research, Tohoku Univ.)*

[Proc. IUPAC CHEMRAWN VI World Conf. on Adv. Materials for Innovations in Energy, Transportation and Communications]

Superconducting properties of La-M-Cu-O (M = Ba, Sr and Ca) system with K_2NiF_4 type structure have been studied by using sintered specimens and single crystals. We have discovered more than ten new compounds with very high transition temperatures $T_c <$ 100 K. These compounds contains lanthanide atoms with magnetic moment as one of the main components, which acts as the disturbance for the electrons to form Cooper pairs. Possible explanations of the present findings are given.

IV-U-13 Crystal Structures of $(La_{1-x}M_x)_2CuO_{4-\delta}$ (M = Sr and Ba)

Masashige ONODA, Shin-ichi SHAMOTO, Masatoshi SATO, and Syoichi HOSOYA* *(*Institute for Materials Research, Tohoku Univ.)*

[*Jpn. J. Appl. Phys.*, **26**, L363 (1987)]

Structure determinations of $(La_{1-x}Sr_x)_2CuO_{4-\delta}$ and $(La_{1-x}Ba_x)_2CuO_{4-\delta}$ ($x \simeq 0.075$) are carried out by single crystal X-ray diffraction. The former is tetragonal with space group *I4/mmm*, while the latter is orthorhombic with *Pccn*. Both compounds have the K_2NiF_4-type layered perovskite structures formed by the linkage of CuO_6 octahedra. The orthorhombic distortion in the compound with Ba is found to be mainly described by the rotation of CuO_6 octahedra which corresponds to the R_{25} mode of cubic perovskite lattice.

IV-U-14 Effect of Vaccum Annealing on the Superconducting Transition Temperature of La-Sr-Cu-O System

Shin-ichi SHAMOTO, Syoichi HOSOYA*, Masashige ONODA, and Masatoshi SATO *(*Institute for Materials Research, Tohoku Univ.)*

[*Jpn. J. Appl. Phys.*, **26**, L493 (1987)]

Effect of vacuum annealing on the superconducting transition temperature T_c of the ceramic superconductor La-Sr-Cu-O system with K_2NiF_4 type structure has been studied. For a constant annealing time, the resistivity-increase and the T_c-decrease become larger for higher annealing temperatures. This may be qualitatively understood as the result of introduction of oxygen vacancies at their sites in the basal plane of CuO_6 octahedra which are parallel to the (001) plane of the tetragonal cell.

IV-U-15 Raman Study of High-T_c Superconductors $(La_{1-x}Sr_x)_2CuO_4$

Shinji SUGAI*, Masatoshi SATO, and Syoichi HOSOYA$^+$ *(*Department of Phys. Osaka Unvi., $^+$Institute for Materials Research, Tohoku Univ.)*

[*Jpn. J. Appl. Phys.*, **26**, L495 (1987)]

Lattice vibrations in high T_c superconductors $(La_{1-x}Sr_x)_2CuO_4$ are investigated by Raman scattering using single crystals. In La_2CuO_4 the 664 and 153 cm^{-1} peaks are resonantly enhanced at low temperatures. The enhancement is caused by the electronic transition spanning the quasi-square Fermi surface to the nesting directions. The 664 cm^{-1} mode is assigned to the planar breathing mode which strongly interacts with electrons at the Fermi level and the 796 cm^{-1} mode in $(La_{0.925}Sr_{0.075})_2CuO_4$ is tentatively assigned to the axial breathing mode.

IV-U-16 Ultraviolet Photoemission Study of High-T_c Superconductor $(La_{1-x}Sr_x)_2CuO_{4-\delta}$

Takashi TAKAHASHI*, Fumihiko MAEDA*, Syoichi HOSOYA$^+$ and Masatoshi SATO *(*Department of Phys. Tohoku Univ. $^+$Institute for Materials Research, Tohoku Univ.)*

[*Jpn. J. Appl. Phys.*, **26**, L349 (1987)]

Ultraviolet photoemission spectra of high-T_c superconductor $(La_{1-x}Sr_x)_2CuO_{4-\delta}$ ($x = 0.075$ and $\delta \leqq 0.04$) are presented. The experimental result was compared with the band calculations of La_2CuO_4 by Mattheiss and Takegahara *et al.* It was found that as regards the valence-band width (about 7 eV) the experiment and the calculations are in good agreement with each other, but the position of the calculated valence bands

contributed mainly by weakly bonding Cu(3d)-O(2p) states are shiftd toward the lower binding energy by about 1 eV with respect to the experiment. The possible origins for this discrepancy were discussed.

IV-U-17 High-T_c Superconductivity in New Oxide Systems and Their X-Ray Diffraction Study

Shin-ichi SHAMOTO, Masashige ONODA, Masatoshi SATO, and Syoichi HOSOYA* *(*Institute for Materials Research, Tohoku Univ.)*

[*Jpn. J. Appl. Phys.*, **26**, L642 (1987)]

Resistivity measurements for Ln-Ba-Cu-O systems with Ln being lanthanide atoms have been carried out. In addition to the previously reported systems with Ln = Lu, Yb, Tm, Er, Ho, Dy and Eu, we have discovered the high-T_c superconductivity in the systems with Ln = Nd, Sm and Gd. Preliminary results of X-ray powder diffraction study are given and the superconductivity is discussed in relation to them.

IV-U-18 Crystal Structures of $YBa_2Cu_3O_x$ and $LnBa_2Cu_3O_x$ (Ln = Ho and Dy)

Masashige ONODA, Shin-ichi SHAMOTO, Masatoshi SATO, and Syoichi HOSOYA* *(*Institute for Materials Research, Tohoku Univ.)*

[*Jpn. J. Appl. Phys.*, **26**, L876 (1987)]

Structure determinations of $YBa_2Cu_3O_x$ and $LnBa_2Cu_3O_x$ (Ln = Ho and Dy) are carried out by single crystal X-ray diffraction. The x values obtained in the present analyses are about 6.0, 6.0 and 6.25 for Y, Ho and Dy compounds, respectively and they have tetragonal structure with space group *P4/mmm*. The structures are perovskite-related ones with the c axis triplicated due to the ordering of Ba and Y or Ln. All oxygen atom sites around Y or Ln atoms in the c plane are vacant. Almost all oxygen atom sites in the layers which contain the Cu(1) sites (*4/mmm*) are also vacant. The present $YBa_2Cu_3O_6$ crystal is found to be a semiconductor, which indicates the importance of the oxygen number for the occurrence of superconductivity in Y-Ba-Cu-O and Ln-Ba-Cu-O systems.

IV-U-19 High-T_c Superconductivity in Ln-Ba-Cu-O System (Ln-Lanthanide Atoms)

Masatoshi SATO, Syoichi HOSOYA, Shin-ichi SHAMOTO, and Masashige ONODA

[*Jpn. J. Appl. Phys.*, **26**, S26-3, 1025 (1987)]

High-T_c superconductivity has been discovered for Ln-Ba-Cu-O systems with Ln = Lu, Yb, Tm, Er, Ho, Dy, Gd, Eu, Sm and Nd. The transition temperatures T_c are as high as that of the Y-Ba-Cu-O system, although almost all Ln atoms carry magnetic moments. The insensitivity of the T_c-values seems to be understood by the consideration of their structures, where the superconducting electrons are within the layers of Ba-Cu-O systems separated by the layers of Ln atoms.

IV-U-20 Structural Study of $(La_{1-x}M_x)_2CuO_{4-\delta}$ by X-Ray Four Circle Diffraction

Masashige ONODA, Shin-ichi SHAMOTO, Masatoshi SATO, and Syoichi HOSOYA* *(*Institute for Materials Research, Tohoku Univ.)*

[*Jpn. J. Appl. Phys.*, **26**, S26-3, 1049 (1987)]

Full structure determinations of $(La_{1-x}M_x)_2CuO_{4-\delta}$ (M = Sr and Ba), La_2CuO_4 and $M'Ba_2Cu_3O_{7-\delta}$ (M' = Y, Ho and Dy) are carried out by X-ray four circle diffraction. The structures of $(La_{1-x}M_x)_2CuO_{4-\delta}$ crystal specimens ($x \simeq 0.075$ and $\delta \simeq 0$) which exhibit superconductivity are K_2NiF_4-type ones with CuO_6 ochtahedra. The Sr compound is tetragonal (*I4/mmm*) and the Ba compound is orthorhombic (*Pccn*) characterized by the rotation of CuO_6. This rotation is different from that observed in La_2CuO_4. All the present specimens of $M'Ba_2Cu_3O_{7-\delta}$, which are found to be semiconducting, are tetragonal with *P4/mmm* and the δ values are close to 1.0. Their structures are perovskite-related ones with the c axis triplicated due to the ordering of Ba and Y (Ho and Dy).

IV-U-21 Anisotropy of the Superconducting Critical Magnetic Field H_{c2} of La-M-Cu-O System (M = Sr and Ba)

Shin-ichi SHAMOTO, Masashige ONODA, Masatoshi SATO, and Syoichi HOSOYA* *(*Institute for Materials Research, Tohoku Univ.)*

[*Jpn. J. Appl. Phys.*, **26**, S26-3, 1131 (1987)]

Results of experimental studies on single crystals of high-T_c oxide superconductors are presented. The anisotropy of the superconducting critical magnetic field H_{c2} of $(La_{1-x}M_x)_2CuO_{4-\delta}$ (M = Ba and Sr and $x \sim 0.075$) indicates that the ratio of the conductivities along the directions within and perpendicular to the c plane, $\sigma_{\parallel}/\sigma_{\perp}$, is of the order of 10^2. The results show the direct evidence of the two dimensional character of the electron transport. The thermoelectric power of the same crystal of $(La_{1-x}Sr_x)_2CuO_{4-\delta}$ is also shown. Brief comments on the crystal preparation are presented.

IV-U-22 Magnetic Properties of La_2CuO_4 Single Crystals

Kenji FUKUDA, Masatoshi SATO, Shin-ichi SHAMOTO, Masashige ONODA, and Syoichi HOSOYA* *(*Institute for Materials Research, Tohoku Univ.)*

[*Solid State Commun.*, **63**, 811 (1987)]

Magnetic susceptibility χ of La_2CuO_4 crystals have been measured with external magnetic field perpendicular to and within the c plane. A kind of ordering or condensation of the spin system with the spin direction parallel to the c axis has been found although it is difficult to consistently explain all of the observed behaviors. Even above the ordering temperature (~250 K), uniaxial anisotropy of χ has also been observed.

IV-U-23 Photoelectron Spectroscopy of High-T_c Superconductor $(La_{1-x}Sr_x)_2CuO_{4-\delta}$

Takashi TAKAHASHI*, Fumihiko MAEDA*, Tsuneaki MIYAHARA, Syoichi HOSOYA$^+$ and Masatoshi SATO** *(*Department of Phys. Tohoku Univ., **National Laboratory for High Energy Phys., $^+$Institute for Materials Research, Tohoku Univ.)*

[*Jpn. J. Appl. Phys.*, **26**, S26-3, 1013 (1987)]

Electronic structure and chemical state of high-T_c superconductor $(La_{1-x}Sr_x)_2CuO_{4-\delta}$ ($x = 0.075$ and δ 0.04) were studied by photoelectron spectroscopy. Resonant photoemission with synchrotron radiation showed that the copper atom in the La-Sr-Cu-O system is mostly divalent. The experimental results were compared with the band calculations performed for La_2CuO_4.

IV-U-24 Studies of High-T_c Oxide Superconductors

Masatoshi SATO, Syoichi HOSOYA*, Kenji FUKUDA, Masafumi SERA, Masashige ONODA, Shin-ichi SHAMOTO, Kunihiko ODA, and Hiroumi UNOKI**** *(*Institute for Materials Research, Tohoku Univ., **Electro-Technical Laboratory)*

[*Physica.* **B** to be published]

Recent results of experimental studies on high-T_c oxide superconductors are presented. Anisotropy and temperature dependence of magnetic susceptibility χ of La_2CuO_2 do not seem to easily be explained by a simple antiferromagnetic spin ordering with the spin direction within the CuO layers. Moreover with increasing magnetic field perpendicular to the layers, χ exhibits sudden increase below T_N. The tunneling study revealed that the energy gap value of $YBa_2Cu_3O_y$ is consistent with BCS theory and any additional structure has not been observed in the present tunneling spectra.

IV-U-25 Single Crystal Studies and Electron Tunneling of $(La_{1-x}M_x)_2CuO_{4-\delta}$ (M = Ba and Sr)

Masatoshi SATO, Shin-ichi SHAMOTO, Masashige ONODA, Masafumi SERA, Kenji FUKUDA, Syoichi HOSOYA*, Jun AKIMITSU$^+$, Toshikazu EKINO$^+$ *(*Institute for Materials Research, Tohoku Univ., $^+$Aoyama-Gakuin Univ.)*

[Proc. Int. Workshop on Novel Mechanisms of Superconductivity 1987 Berkeley, Plenum Press]

Various kinds of works on single crystal specimens of high-T_c oxide superconductors and their electron tunneling experiment carried out at IMS group are reviewed. Various superconducting and normal state properties of the high-T_c superconductors are discussed

in order to find out what differences cause the large difference of the T_c-values between the newly found oxides and other oxides.

IV-U-26 Crystal Preparation of $(La_{1-x}M_x)_2CuO_{4-\delta}$ (M = Sr and Ba) and Discovery of Magnetic Superconductors Ln-Ba-Cu-O Systems (Ln = Lanthanide Atoms)

Syoichi HOSOYA*, Shin-ichi SHAMOTO, Masashige ONODA and Masatoshi SATO *(*Institute for Materials Research, Tohoku Univ.)*

[Proc. Int. Workshop on Novel Mechanisms of Superconductivity, 1987 Berkeley, Plenum Press]

Single crystals of high-T_c oxide superconductors are first successfully prepared at IMS. This paper presents the method to prepare single crystals. It also presents the convenient way to find the unknown superconducting substances.

IV-U-27 Single Crystal X-Ray Diffraction Study of $(La_{1-x}M_x)_2CuO_{4-\delta}$ (M = Sr and Ba), $La_2CuO_{4-\delta}$ and $LnBa_2Cu_3O_{7-\delta}$ (Ln = Y, Dy and Ho) Systems

Masashige ONODA, Shin-ichi SHAMOTO, Masatoshi SATO, and Syoichi HOSOYA* *(*Institute for Materials Research, Tohoku Univ.)*

[Proc. Int. Workshop on Novel Mechanisms of Superconductivity 1987 Berkeley, Plenum Press]

Almost all results of the structural analyses of the high-T_c superconductors obtained at IMS mainly by X-ray four circle diffraction are reviewed. The relationship between the structural characteristics and the oxygen vacancies can easily be understood.

IV-U-28 Optical-Reflectance Study of the Single Crystal Superconductor $(La_{1-x}Sr_x)_2CuO_4$

Tsunehara KOIDE*, Hirohito FUKUTANI, Atsushi FUJIMORI$^+$, Riichiro SUZUKI**, Tetsuo SHIDARA*, Takeshi TAKAHASHI^{++}, Syoichi HOSOYA$^\#$, and Masatoshi SATO** *(*National Laboratory for High Energy Physics, **Tsukuba Univ., $^+$National Institute for Research in Inorganic Materials, $^{++}$Department of Phys. Tohoku Univ., $^\#$Institute for Materials Research, Tohoku Univ.)*

[Proc. Int. Workshop on Novel Mechanisms of Superconductivity, 1987 Berkeley, Plenum Press]

The reflectance in the energy range from 0.55 eV to 6.0 eV is reported for a single crystal $(La_{1-x}Sr_x)_2CuO_4$. The spectrum is Kramers-Kronig analyzed to obtain the dielectric function and the related functions. The result is discussed with reference to the electronic properties of the compound.

IV-U-29 Synchrotron-Radiation Photoemission Study of High-T_c Superconductor $YBa_2Cu_3O_{7-\delta}$

Takashi TAKAHASHI*, Fumihiko MAEDA*, Hiroshi ARAI*, Hiroshi KATAYAMA-YOSHIDA*, Yutaka OKABE*, Takashi SUZUKI*, Syoichi HOSOYA, Atsushi FUJIMORI$^+$, Tetsuo SHIDARA^{++}, Masashige ONODA, Shin-ichi SHAMOTO and Masatoshi SATO** **(Department of Phys. Tohoku Univ., **Institute for Materials Research, Tohoku Univ., $^+$National Institute for Research in Inorganic Material, $^{++}$National Laboratory for High Energy Phys.)*

[*Phys. Rev.*, **B** to be published]

Photoemission measurement has been performed for high-T_c superconductor $YBa_2Cu_3O_{6.85}$ by the use of synchrotron radiation of 20–110 eV. It was found that the valence band is shifted by 1.1 to 1.6 eV toward higher binding energy relative to the band calculation. The effective intra-atomic Coulomb energy between d electrons (U_{dd}) was evaluated from the energy position of the valence-band satellite due to the two-hole-bound state: U_{dd} = 5–6 eV, which is comparable to the valence-band width (W = 6–7 eV). This strongly suggests that electron correlation plays a key role in characterizing the electronic properties of this oxide superconductor.

IV-U-30 Superconducting Phase in $La_{3-x}Ba_{3+x}Cu_6O_y$ System

Masashige ONODA, Kenji FUKUDA, Masafumi SERA, and Masatoshi SATO

[*Solid State Commun.*, **64**, 1225 (1987)]

The superconducting phase in the $La_{3-x}Ba_{3+x}Cu_6O_y$ system are investigated by X-ray diffraction and by measurements of electrical resistivity, magnetic susceptibility and Hall coefficient. A bulk superconductivity in this system is observed only in the vicinity of $x = 1.0$ and its phase is essentially similar to that of the typical high-T_c compound $YBa_2Cu_3O_{7-\delta}$.

IV-U-31 Raman and Infrared Studies of Oxide Superconductors $(La_{1-x}M_x)_2CuO_4$

Shinji SUGAI*, Masatoshi SATO, Syoichi HOSOYA, Shin-ichi UCHIDA+, Hidenori TAKAGI+, Koichi KITAZAWA+ and Shoji TANAKA+** *(*Department of Phys. Osaka Univ., **Institute for Materials Research, Tohoku Univ., +Tokyo Univ.)*

[*Jpn. J. Appl. Phys.*, **26**, S26-3, 1003 (1987)]

Raman and infrared studies of lattice vibrations new superconductors $(La_{1-x}M_x)_2CuO_4$ are presented. The 664 cm^{-1} mode which shows resonant enhancement in La_2CuO_4 is assigned to the planar breathing mode which strongly interacts with electrons at E_F. This resonant scattering is produced by the electronic transition spanning the quasi-square Fermi surface to the nesting directions. In the spectra of Im(ε) a strong peak appears at 246 cm^{-1} on substituting Sr for La. It is suggested that this mode is related to the electronic transition.

IV-U-32 Photoelectron Spectroscopy of $LnBa_2Cu_3O_{7-\delta}$ (Ln = Y and Sm)

Takashi TAKAHASHI*, Fumihiko MAEDA*, Hiroshi ARAI*, Hiroshi KATAYAMA-YOSHIDA*, Yutaka OKABE*, Takashi SUZUKI*, Yuji TAKAKUWA*, Syoichi HOSOYA#, Atsushi FUJIMORI, Tsuneaki MIYAHARA+, Tsuneharu KOIDE+, Tetsuo SHIDARA+, Masatoshi SATO, Shin-ichi SHAMOTO and Masashige ONODA** *(*Department of Phys., Tohoku Univ. #Institute for Materials Research, Tohoku Univ., **National Institute for Research in Inorganic Materials, +National Laboratory for High Energy Phys.)*

[*Physica* **B** to be published]

Photoelectron spectroscopy was performed for the high-T_c superconductor $LnBa_2Cu_3O_{7-\delta}$ (Ln = Y, Sm) with synchrotron radiation of 20–140 eV as well as the He I (21.2 eV) and Mg Kα (1253.6 eV) lines. The sample was prepared by sintering pressed pellet in air and/or oxygen atmosphere. In the photoemission measurements, the sample was scraped by a diamond file in the spectrometer to obtain the fresh surface. The sample was kept at low temperature (about −110 to −180°C) to prevent the removal of oxygen atoms from the sample surface into vacuum.

The results obtianed are;

(1) the observed valence band is shifted by 1–2 eV toward the high binding-energy side compared with the band calculation by Mattheiss and Hamann while the band width (6–7 eV) shows a fairly good agreement between the two,

(2) the observed density of states at the Fermi level is very small compared with the band calculation,

(3) the 4f level in $SmBa_2Cu_3O_{7-\delta}$ is observed around 8 eV in binding energy, which shows the trivalent state of Sm,

(4) the copper atom in $LnBa_2Cu_3O_{7-\delta}$ (Ln = Y, Sm) is mostly divalent which was determined from the energy position of the valence band satellite due to the two-hole bound state, and

(5) the intra-atomic Coulomb energy between d electrons (U_{dd}) was directly estimated from the valence-band satellite and is about 5 eV, which is comparable to the valence-band width (6–7 eV). This suggests that the electron correlation plays an important role in featuring the electronic structure of this high-T_c superconductor.

RESEARCH ACTIVITIES V
Department of Applied Molecular Science

V-A High-Spin Organic Molecules

Through-bond and through-space topological considerations have been employed successfully in these laboratories for design and construction of high-spin organic molecules. Introduction of heteroatoms in the alternant non-Kekulé hydrocarbons was now found to be only a minor perturbation. Model experiments have shown that poly(acetylene) and poly(diacetylene) main chains are effective in aligning spins residing on the side chains. A quintet porphyrin derivative has been prepared for constructing high-spin molecular aggregates.

V-A-1 (3-Nitrenophenyl)methylene: a Ground State Quintet Molecule having Both Carbenic and Nitrenic Atoms

Hideyuki TUKADA *(Univ. of Tokyo)*, **Kiyoshi MUTAI** *(Univ. of Tokyo)*, **and Hiizu IWAMURA**

[*J. Chem. Soc., Chem. Commun.*, 1159 (1987)]

The ground state spin multiplicity of the title nitrenocarbene (**1**) cannot be predicted straightforwardly because the non-bonding molecular orbitals are far from degenerate. Difference in the electronegativity of carbon and nitrogen might stabilize a zwitterionic singlet or triplet state.

Irradiation of freshly sublimed (3-azidophenyl)diazomethane in 2-MTHF at 18 K produced material exhibiting a set of ESR signals due to a quintet species together with a signal characteristic of the *X*, *Y* transition of a triplet nitrene (Figure 1).

The observed resonance fields, in particular the signal at 0.7295 T assigned to the *Z*-transition of $\Delta m=1$ for a quintet, were best reproduced by a third-order perturbation calculation[1] with $|D|=0.124$ cm^{-1} and $|E|=0.002$ cm^{-1}. The intensities of all signals appearing below 0.8 T obeyed the Curie law in the temperature range 17-69 K, indicating that the quintet is the ground state of **1**.

Ground state spin multiplicities of alternant non-Kekulé molecules appear to be less sensitive to the splitting of energy levels of NBMOs due to replacement with heteroatoms. The results may point the way to the construction of high-spin molecules by combination of various open-shell centers.

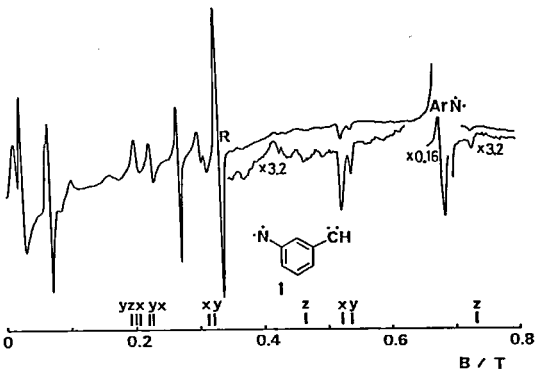

Figure 1. ESR spectrum (9.33149 GHz) of **1** obtained by uv irradiation in 2-MTHF at 22 K. R and ArN denote doublet and triplet impurities, respectively.

References

1) K. Itoh, Abstracts, 6th ESR Symposium of the Chemical Society of Japan, Kyoto, Japan, 1967, p.117.

V-A-2 Exchange Interaction between Two Triplet Phenylnitrene Moieties Linked with a 1,3-Butadiyne Unit

Shigeru MURATA and Hiizu IWAMURA

As models for the monomers of poly(diphenyldiacetylenes) that have radical centers in the side chain, *m,p'*- and *m,m'*-bis(nitrenophenyl)diacetylenes have been generated. Both isomers have two π-non-bonding molecular orbitals,[1] but only the former is non-disjoint.[2]

When the *m,p'*-diazido precursor was photolyzed in 2-MTHF at 18 K, an ESR fine structure (Figure 1) was obtained that followed the Curie law. The *m,m'* isomer showed very weak signals due to the quintet state that

grew in as the temperature was raised from 18 to 30 K. In good agreement with theory, only the *m,p'* isomer is in the ground quintet state. Solid state head-to-tail polymerization of a diphenyldiacetylene carrying the radical centers at the *m,p'* positions is predicted to give the corresponding high-spin polymer.

Attempts are in progress to prepare high-spin polymers based on these molecular design and model experiments.

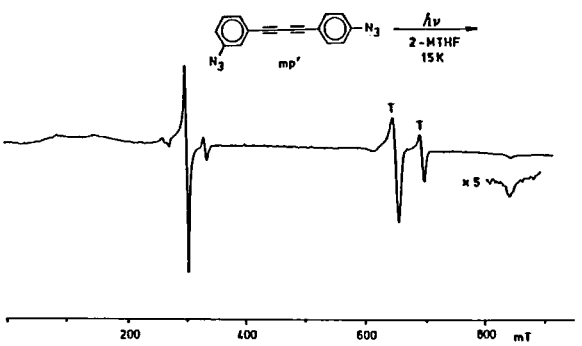

Figure 1. ESR spectrum due to *m,p'*-bis(nitrenophenyl)-diacetylene in the quintet state. Signals denoted T are due to triplet mononitrene impurities.

References

1) H.C. Longuet-Higgins, *J. Chem. Phys.*, **18**, 265 (1950).
2) W.T. Borden and E.R. Davidson, *J. Am. Chem. Soc.*, **99**, 4587 (1977).

V-A-3 Exchange Interaction of Electron Spins in Tetraphenylporphyrins and Its Metal Complexes Carrying Carbenic Centers in the Phenyl Rings

Noboru KOGA and Hiizu IWAMURA

A series of tetraphenylporphyrin (TPP) derivatives carrying one or more α-diazobenzyl groups have been prepared and photolyzed at cryogenic temperature to study the exchange interaction between the triplet carbene centers on the TPP ring system by means of their absorption and ESR spectra.

The mono-(α-diazobenzyl) derivative showed signals ($|D|$=0.404 and $|E|$=0.0192 cm^{-1}) characteristic of a triplet diphenylcarbnene. Two isomeric bisdiazo compounds (*syn* and *anti*) showed signals due to quintet states at 250 and 400 mT as well as the triplet signals. The temperature dependence of the quintet signals was quite contrasting between the two isomers; it obeyed Curie law in the *syn* isomer, whereas a curved plot that has a maximum at temperature lower than 20 K was observed in the *anti* isomer. Similar results were obtained in the corresponding zinc complexes of the diazo compounds. It is concluded that the two open-shell centers at the para positions of the phenyl groups in TPP may interact ferromagnetically when they are located in the *syn* dispositions.

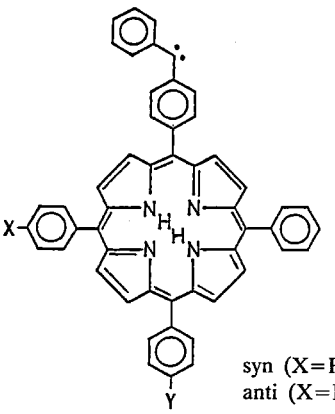

syn (X=PhC̈, Y=H)
anti (X=H, Y=PhC̈)

V-A-4 Exchange Interaction between Two Diphenylcarbene Units Incorporated in [3.3] Paracyclophane Skeleton

Akira IZUOKA, Shigeru MURATA, Tadashi SUGAWARA, Hiizu IWAMURA, Teruo SHINMYOZU *(Kyushu Univ.)*, **and Takahiko INAZU** *(Kyushu Univ.)*

In a previous paper,[1] we have shown that isomeric bis(phenylmethylenyl)[2.2]paracyclophanes serve as good models for studying the effect of stacking orientation on the resultant intermolecular spin alignment in molecular assemblies. In order to exclude the possible contribution of through-bond interaction via two ethano bridges in these model compounds, we have prepared the corresponding [3.3]paracyclophane derivatives.

Photolysis of the pseudoortho-didiazo precursor in a 2-MTHF matrix at 18 K gave an ESR spectrum characteristic of a quintet species (Figure 1). From the parallel results between the two series, it is concluded that the through-space exchange interaction is the major mechanism for realizing the ferromagnetic spin alignment between the two molecular moieties.

Interestingly, our preliminary results show that effective exchange integral J between the two facing

benzene rings is greater by 140~165% for the [3.3]-paracyclophane than the [2.2]paracyclophane.

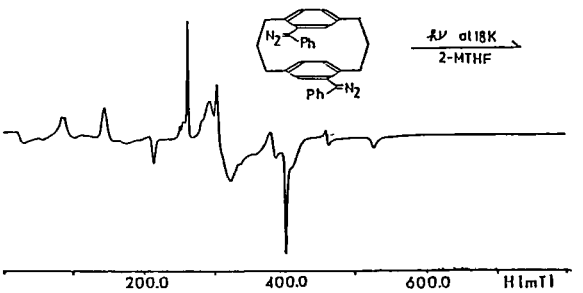

Figure 1. ESR fine structures due to quintet pseudoorthodicarbeno[3.3]paracyclophane

Reference

1) A. Izuoka, S. Murata, T. Sugawara, and H. Iwamura, *J. Am. Chem. Soc.*, **109**, 2631 (1987); *IMS Ann. Rev.*, 110 (1986).

V-A-5 Intermolecular Magnetic Interaction in the Crystal of Bis(*p*-decyloxyphenyl) Nitroxide

Tadashi SUGAWARA, Akira IZUOKA, Shigeru MURATA, Hiizu IWAMURA, Nobuo KURIKI *(Nagoya Univ.)*, **Makoto KIMURA** *(Nagoya Univ.)*, **and Yasuhiko SAWAKI** *(Nagoya Univ.)*

[*Mol. Cryst. Liq. Cryst.* in press]

Irradiation of polycrystalline bis(*p*-octylphenyl)-diazomethane at cryogenic temperature gives rise to the clusters of the corresponding triplet carbene molecules with ferromagnetic interaction which extends over several molecules on an average at 2 K.[1)]

Encouraged with this observation, we have synthesized an analogous nitroxide (**1**) that is persistent at ambient temperature, and measured the magnetic susceptibility of its polycrystalline sample in the temperature range 2~110 K by means of a Faraday-type magnetic balance system.

An antiferromagnetic inter-radical interaction with the Weiss temperature of –10 K was observed (Figure 1). When the external magnetic field higher than 3.6 T was applied at 2.1 K, the magnetization of the samples increased nonlinearly due to a spin-flopping mechanism. The result is in startling contrast to that of the above diphenylcarbene counterpart. Estimated weaker interaction between the spin-containing benzene rings is considered to be responsible for the lack of ferromagnetic interaction.

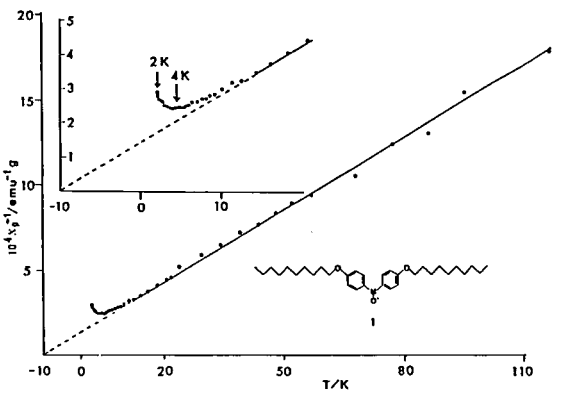

Figure 1. Temperature dependence of the reciprocal paramagnetic susceptibility of nitroxide **1**.

Reference

1) T. Sugawara, S. Murata, K. Kimura, and H. Iwamura, *J. Am. Chem. Soc.*, **107**, 5293 (1985).

V-B Stereochemical Consequences of the Non-bonded Interactions in Overcrowded Molecules

Studies of disrotatory coupling of the internal rotational degrees of freedom in double rotor molecules Tp_2X have been extended to X = S, revealing the role of central atoms X on the tightness of the molecular bevel gears.

V-B-1 Correlation of the Two Torsional Degrees of Freedom About the Bonds Connecting the Bridgehead Carbons to the Sulfur Atom in Bis(9-triptycyl) Sulfide

Yuzo KAWADA *(Ibaraki Univ.)*, **Joji ISHIKAWA** *(Ibaraki Univ.)*, **Hiroshi YAMAZAKI** *(Ibaraki Univ.)*, **Gen KOGA** *(Ibaraki Univ.)*, **Shigeru MURATA, and Hiizu IWAMURA**

[*Tetrahedron Lett.*, **28**, 445 (1987)]

Most of the known methods for the preparation of aliphatic sulfides are not applicable to Tp_2S (Tp = 9-triptycyls)(**1**) since the alpha carbons are both bridgehead. Pyrolytic extrusion of sulfur dioxide took place smoothly from the corresponding thiosulfonates $TpSSO_2Tp$ as in Scheme 1. When Tp = 2-chloro-9-triptycyl, the meso and dl isomers (**1'**) were obtained as separate microcrystalline plates by gel permeation chromatography. It is concluded that a pair of torsional motions about the C-S bonds in this sulfide are in strict gearing and requires a barrier of 29.3 ± 0.3 kcal/mol for gear slippage.

Scheme 1

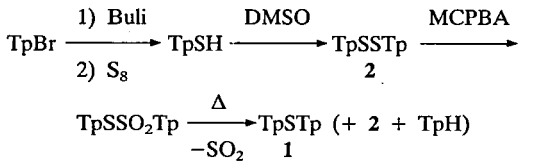

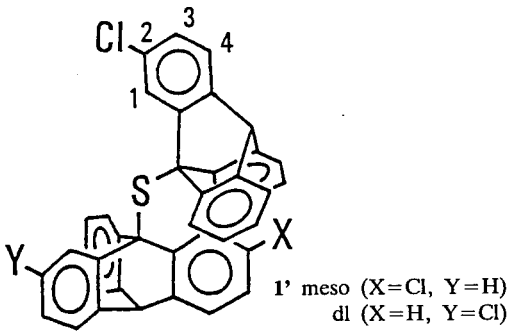

1' meso (X=Cl, Y=H)
dl (X=H, Y=Cl)

V-B-2 The Heights of Barriers to Gear-Slippage in Tp_2X Derivatives

Yuzo KAWADA *(Ibaraki Univ.)* **and Hiizu IWAMURA**

An experimental estimate of the energy requirement for gear slippage has been obtained by a study of the rates of interconversion of meso and dl phase isomers (diastereomerization). The results are collected in Table 1. With the exception of the silane, data for which were obtained by variable-temperature ^1H NMR measurements, the tabulated information was obtained by monitoring dl/meso isomer ratios as a function of time using high boiling solvents and temperature intervals ranging from 61~132°C for the sulfide to 220~330°C for the ethers. Reaction kinetics were all strictly first-order. The log *A* values are consistent with unimolecular processes.

The decrease in barrier height is primarily a consequence of the increase in C-X bond length; as a result the Tp groups are pushed further apart, the gear system is loosened up, and slippage becomes easier. The high barrier height of the sulfide is rather exceptional. The small C-S-C angle, as compared to C-Si-C, evidently plays an important role in tightening the gear system and elevating the gear slippage barrier.

We would like to point out that the values of these barrier heights are lower limits for the linearization energy of the ether and the sulfide.

Table 1. Activation Parameters for Gear-Slippage Processes: Diastereomerization of Tp_2X Derivatives

substitution pattern[a] X	2	3	E_a[b] (kcal mol^{-1})	Log *A*	*K* (DL/meso)
CH_2	Cl	H	32.2±0.1	12.1±0.1	1.65±0.01
CH_2	H	Cl	33.1±0.2	12.2±0.1	1.86±0.01
O	Cl	H	42.0±0.5	12.3±0.2	1.90±0.03
O	H	Cl	43.2±0.3	12.5±0.1	1.89±0.01
NH	Cl	H	39.1±0.5	12.4±0.2	1.82±0.01
SiH_2	Cl	H	21.1±0.4	13.9±0.2	2.08±0.02
S	Cl	H	29.3±0.3	12.2±0.2	1.73±0.01

[a]Numbers refer to positions on the ring. [b]Arrhenius activation energy for the process DL → meso.

References

1) *IMS Ann. Rev.*, 107 (1980); 111 (1981); 87 (1982); 113 (1983); 110 (1984); 110 (1985); 112 (1986).

V-C Oxidation Reaction Mechanisms and New Reactive Intermediates

Whereas thermal and photochemical decomposition of diazo compounds to give the corresponding triplet carbenes is well established, it is only of recent date that the electrochemical counterpart became the subject of interest. We have been able to establish that there are two different electronic structures, i.e., σ- and π-radical cations, depending on the substituents of diazo compounds. The scope of the photochemical cleavage of 1-pyrenylmethyl esters has been clarified.

V-C-1 Electron Spin Resonance Study on the σ- and π-Radical Cations Formed by One-Electron Oxidation of Aryldiazomethanes

Katsuya ISHIGURO *(Nagoya Univ.)*, **Yasuhiko SAWAKI** *(Nagoya Univ.)*, **Akira IZUOKA, Tadashi SUGAWARA, and Hiizu IWAMURA**

[*J. Am. Chem. Soc.*, **109**, 2530 (1987)

When the electrolytic oxidation was carried out in CH_2Cl_2 containing 0.1 M n-Bu_4NBF_4 at −70~−90°C, diphenyldiazomethanes and methylphenyldiazomethane showed ESR spectra characteristic of the σ-radical of $PhRCN_2^+$ (**1**, R=Ph or CH_3).[1] Under similar conditions, *tert*-butylphenyldiazoemthanes showed quite different ESR hyperfine structures (Figure 1). The results are interpreted in terms of the hither-to elusive π-radical structures (**2**). The bulky *tert*-butyl group introduced at the α-carbon may disfavor the sterically more demanding bent σ-radical structure and the less hindered linear structure with the π-radical character is considered to become a more favorable species.

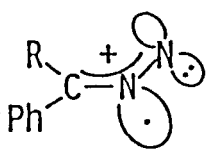

1

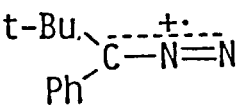

2

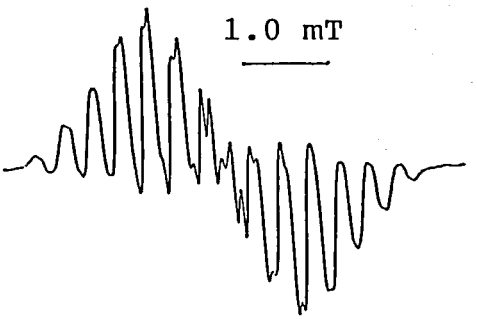

Figure 1. ESR spectrum observed during the electrochemical oxidation of *p*-MeC_6H_4(*tert*-Bu)CN_2 at −90°C in CH_2Cl_2, and simulated by parameters: g=2.0017, a_{N1}=0.35, a_{N2}=0.47, a_{H1}=0.35 (2H), a_{H2}=0.08 (2H), a_{H3}=0.67 (3H) mT.

Reference

1) *IMS Ann. Rev.*, 113 (1986).

V-C-2 Diazomethane Radical Cations as Dipolarophiles in the Dimeric Olefin Formation from Diazo Compounds

Katsuya ISHIGURO *(Nagoya Univ.)*, **Yasuhiko SAWAKI** *(Nagoya Univ.)*, **and Hiizu IWAMURA**

[*Chemistry Lett.*, 1853 (1987)]

Diazomethanes are known to form the corresponding dimeric olefins when subjected to one-electron oxidation. As we noted earlier,[1] one of the most interesting features of these reactions is the formation of *cis*-stilbene in preference to the thermodynamically more stable *trans* isomer from phenyldiazomethane (**1**). Since the parent diazo compounds serve as typical 1,3-dipoles and the corresponding radical cations are electron defficient species, we propose as a mechanism for the stereospecific dimerization a secondary orbital interaction between the two phenyl rings in the face-to-face cycloaddition to form the radical cation of 5,6-dihydro-1,2,3,4-tetrazine (**2**). As shown in Scheme

1, the orbital coefficients of the HOMO of the diazo compound and the LUMO of the radical cation match nicely to stabilize the transition state.

Scheme 1

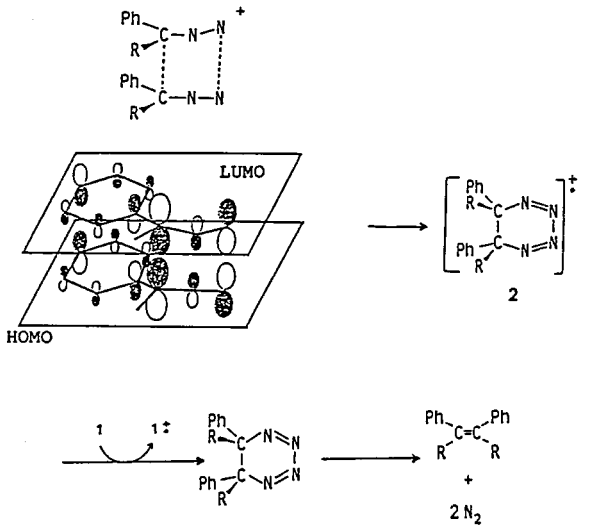

Reference

1) Y. Sawaki, K. Ishiguro, and M. Kimura, *Tetrahedron Lett.*, **25**, 1367 (1984).

V-C-3 A Novel Electrooxidative Methoxylation of Cyanomethly Sulfides

Makoto KIMURA *(Nagoya Univ.)*, **Kazuhiro KOIE** *(Nagoya Univ.)*, **Shinichi MATSUBARA** *(Nagoya Univ.)*, **Yasuhiko SAWAKI** *(Nagoya Univ.)*, **and Hiizu IWAMURA**

[*J. Chem. Soc., Chem. Commun.*, 122 (1987)]

We have found that alkylthioacetonitriles (**1**) give novel α-methoxylated sulfides (**2**) by electrolysis in methanol using toluene-*p*-sulfonic acid as the supporting electrolyte:

$$\underset{(1)}{PSCH_2CN} \xrightarrow[TsOH\cdot H_2O]{-e \text{ in MeOH}} \underset{(2)}{RSCH(OMe)CN} \quad (1)$$

In a typical procedure, a solution of **1** in methanol containing 2 mmol of TsOH was electrolyzed at a constant current of 0.2 A in an undivided cell using Pt electrodes (1×3 cm^2). After an appropriate amount of electricity had been passed for the consumption of >95% of **1**, the electrolyzed solution was concentrated and the residue chromatographed on SiO_2 or distilled to give **2**.

CV measurements showed that radical cations of **1** are formed at potentials higher than ca. 0.5 eV than those of simple sulfides. Electrolysis of the deuteriated sulfide *t*-$BuSCD_2CN$ resulted in methoxylation without any deuterium exchange. Therefore a pathway involving Pummerer-type intermediates (Eq. 2) is suggested.

$$\mathbf{1} \xrightarrow{-e} RS\overset{+}{C}H_2CN \xrightarrow[-e]{-H^+} \left[RS{=}CHCN \leftrightarrow RS{-}\overset{+}{C}HCN \right] \xrightarrow[-H^+]{MeOH} \mathbf{2} \quad (2)$$

V-C-4 Photoreactivity of 1-Pyrenylmethyl Esters. Dependence on the Structure of the Carboxylic Acid Moieties and the Nature of the Excited States

Michiko IWAMURA *(Toho Univ.)*, **Kazuko TOKUDA** *(Toho Unvi.)*, **Noboru KOGA, and Hiizu IWAMURA**

[*Chemistry Lett.*, 1729 (1987)]

The photolysis of the 1-pyrenylmethyl esters (**1**) of typical carboxylic acids in methanol leads to nearly complete recovery of the starting carboxylic acids along with formation of methyl 1-pyrenylmethyl ether (**2**) under mild and neutral conditions.[1] We have now found that 1-pyrenylmethyl 1-naphthoate (**1a**) and 9-anthracenecarboxylate (**1b**) are inert to the photolysis under these conditions.

The photo-reactive esters showed fluorescence spectra characteristic of the pyrene chromophore and had long fluorescence lifetime in methanol ($\tau_f \geq 100$ ns). Both fluorescence quantum yield and τ_f were strongly solvent-dependent in **1a** (Table 1). Only a broad structureless fluorescence band was observed at 480 nm for **1b**. It is concluded that the formation of both non-radiative and radiative intramolecular exciplex formation interfere with the photolytic reactions.

Table 1. Quantum Yields and Lifetimes of Fluorescence of 1-Pyrenylmethyl 1-Naphthoate in Various Solvents

Solvent (Dielectric constant)	Φ_f	τ_f/ns
Methanol (32.6)	0.001	0.85
Isobutyl alcohol (17.5)	0.012	2.8
Tetrahydrofuran (7.6)	0.017	3.9
Di-isobutyl ether (3.1)	0.087	60
Iso-Octane (2.1)	0.36	170

Reference

1) M. Iwamura, T. Ishikawa, Y. Koyama, K. Sakuma, and H. Iwamura, *Tetrahedron Lett.*, **28**, 679 (1987).

V-D Synthesis and Properties of a Novel Type Transition Metal Oxide Clusters

Clusters are expected to serve as a bridge between atoms in molecules and those in more extended arrays. Metal carbonyl and metal-sulfer clusters have been mainly studied in connection with metal surfaces (or gaseous metal atoms) and active centers of enzymes such as a Fe_4S_4 unit in ferredoxine and $Mo_xFe_xS_z$ unit in nitrogenase, respectively.

Recently, we have successfully synthesized a new type of metal oxide clusters containing organometallic groups and polyoxoanions, which will be possible models for metal oxide surfaces bound to oranometallic species as catalysts for a variety of hydrocarbon transformations. In addition, the clusters will open up a new field in which low-valent transition metal chemistry and high-valent transition metal chemistry are fused together.

V-D-1 Synthesis of an Organometallic Oxide Cluster Having a Triple-cubane core structure: $[M(C_5Me_5)M'O_4]_4$ (M=Rh and Ir, M'=Mo and W)

Yoshihito HAYASHI[1] and Kiyoshi ISOBE

The titled complexes were prepared by the reactions of $[MCp^*Cl_2]_2$ (M=Rh and Ir, $Cp^*=C_5Me_5$: pentamethylcyclopentadienyl) with $Na_2M'O_4\cdot 2H_2O$ (M'=Mo, W) in water adjusted to an appropriate pH. The complexes were characterized by

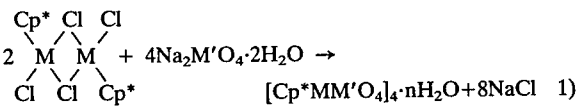

the elemental analyses, molecular weight measurements, and IR and NMR (^1H, ^{13}C, ^{17}O (Figure 1), ^{95}Mo, ^{103}Rh, ^{183}W) spectroscopies. They have a common molecular formula as $[M'(C_5Me_5)M'O_4]_4\cdot nH_2O$ (**1**: M=Rh, M'=Mo, **2**: M=Rh, M'=W, **3**: M=Ir, M'=Mo, **4**: M=Ir, M'=W, n=0~2; the water of crystallization are easily lost under vacuum at room temperature.) and are soluble in general organic solvents. Rhodium complexes are also soluble in water.

The oxidation states of the four Mo's and Rh's in the $Rh_4Mo_4O_{16}$ core were found to be Mo^{VI} and Rh^{III}, respectively by means of the ESCA technique (binding energies of $Mo3d_{5/2}$: 231.4 eV, Rh $3d_{5/2}$: 308.8 eV).

Reference

1) IMS graduate student from Osaka City University for 1987.

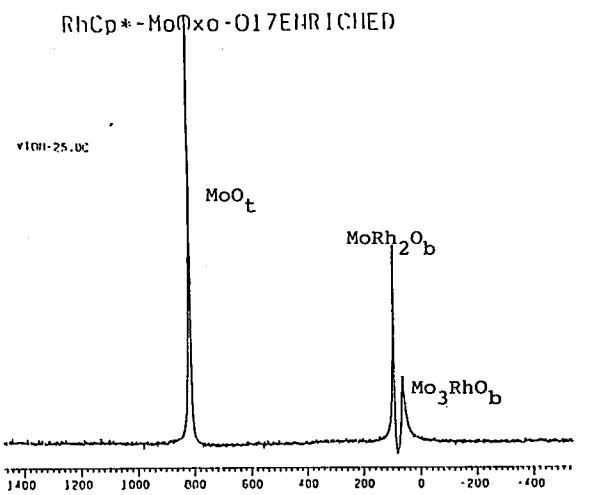

Figure 1. ^{17}O NMR spectrum of $[Rh(C_5Me_5)MoO_4]_4$ in $CDCl_3$.

V-D-2 Crystal and Molecular Structure of $[RhC_p^*MoO_4]_4 \cdot 2H_2O$

Yoshihito HAYASHI[1], Koshiro TORIUMI, and Kiyoshi ISOBE

It is essential to determine the molecular structure of $[RhCp^*MoO_4]_4 \cdot 2H_2O$ for an understanding and development of this organometallic oxide cluster chemistry. The crystals of $[RhCp^*MoO_4]_4 \cdot 2H_2O$ **1** were grown from CH_2Cl_2-C_6H_5Me system. The red crystal of **1** was used for X-ray measurement. Crystal data are: cubic, space group $I\bar{4}3d$, a=25.285(2) Å, Z=12, D_m=2.07, D_x=2.05 g cm^{-3}, μ (Mo Kα)=14.8 cm^{-1}. Intensity data were collected on an automated four-circle diffractometer with graphite-monochromated Mo Kα radiation in the $2\theta \leqq 60°$ range. The structure was solved by a direct method MULTAN 78 and refined by a block-diagonal least-squares technique. The current R value is 0.045 for 1274 reflections. As shown in Figure 1, the molecular structure of **1** has a novel triple cubane framework consisting of two $Rh_2Mo_2O_8$ cores, and has symmetry of S_4. Each Mo and Rh atom has a distorted octahedral coordination: a Mo atom is surrounded by two terminal O atoms (O_t) and four bridging O atoms (O_b; one $MoRh_2O$ and three Mo_3RhO) and a Rh atom by three O_b atoms (two $MoRh_2O$, one Mo_3RhO) and a Cp* ring, respectively. Important bond distances and angles are given in the caption of Figure 1.

Reference

1) IMS graduate student from Osaka City University for 1987.

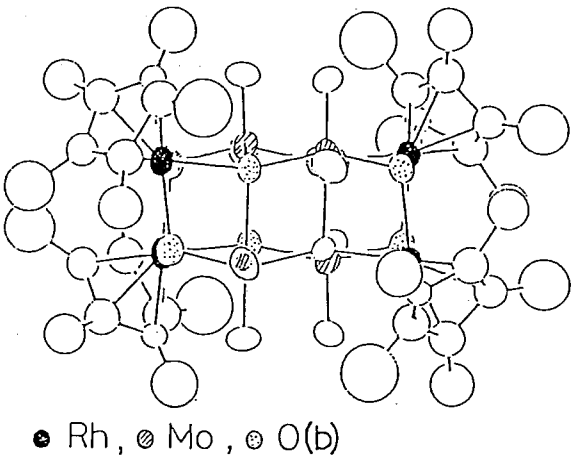

Figure 1. Molecular structure of the oxide cluster $[Rh(C_5Me_5)MoO_4]_4$. Important bond lengths (Å) and angles (deg) are given with e.s.d.'s in parentheses: Rh-O, 2.088(8), 2.132(9); Mo-O_t, 1.691(8), 1.712(8); Mo-O_b, 1.968(8), 1.906(8), 2.341(8); O_t-Mo-O_t, 102.6(5); O_b-Mo-O_b, 144.1(4).

V-E Photochemistry of Mo-Mo and Mo-C bonds

Various photolyses have been used to prepare many organometallic compounds as a most useful synthetic technique. Most of them, however, are still left in a relative absence of mechanistic information. A few exceptions are the phtolyses of metal carbonyls with metal-metal single bond and metal-alkyl bond, for example, $(CO)_3CpMo$-$MoCp(CO)_3$ and $(CO)_3CpMo$-$CH_2C_6H_5$, respectively.

We are applying the photochemistry of Mo-Mo and Mo-C bonds to the important redox reactions in inorganic chemistry and to formation of valuable and reactive intermediates for organic synthesis, respectively.

V-E-1 Comparative Studies of the Photochemical and Thermal Reactivities of the Molybdenum-Molybdenum Single Bond in $[Mo_2(\eta^5$-$C_5H_5)_2(CO)_6]$ and Triple Bond in $[Mo_2(\eta^5$-$C_5H_5)_2(CO)_4]$ towards Nitrite and Nitrate

Kiyoshi ISOBE, Shinji KIMURA *(Osaka City Univ.)*, **and Yukio NAKAMURA** *(Osaka City Univ.)*

[*J. Organometal. Chem.* in press]

Complex $[Mo_2(C_5H_5)_2(CO)_6]$ **1** shows characteristic uv-visible absorption bands in the region 350~550 nm: λ_{max}385 (ε 17700, σ-σ* transition of the Mo-Mo bond) and 505 nm (ε 1650, dπ-σ* transition of the Mo-Mo bond). The irradiation of **1** at the σ-σ* or dπ-σ* transition in the presence of $NaNO_2$ in MeOH-THF gave $[Mo(\eta^5$-$C_5H_5)(CO)_2NO]$ and several oxo complexes including $[\{Mo(\eta^5$-$C_5H_5)(O)_2\}_2O]$ in good yields with a significant decrease in the optical densities over the region of 350 to 420 nm. The disappearance of

1 was conveniently monitored by spectroscopy (Figure 1). The qunatum yields for the disapperance of **1** in the reaction with NO_2^- depend on the nitrite concentration, thus suggesting participation of the metal-radical intermediate in the reduction of nitrite.

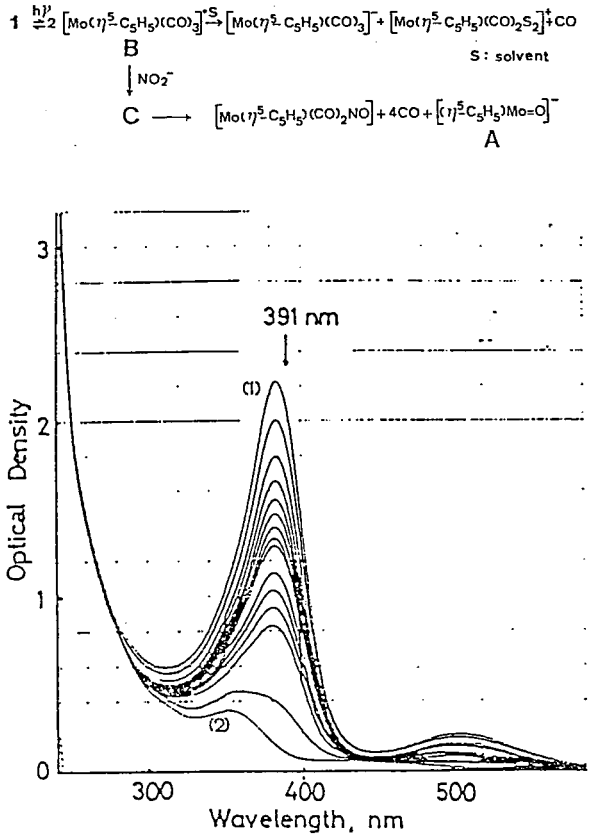

Figure 1. Changes in spectral absorption of **1** in MeOH-THF containing $NaNO_2$ with time on irradiation at 391 nm at 25°C. Curves (1) and (2) represent the spectra after irradiation for 0 and 45 min, respectively. The initial concentrations of the starting complex and $NaNO_2$ were 0.13 and 7.3 mmol dm^{-3}, respectively.

V-E-2 Synthesis and Photochemical Behavior of μ-*p*-Xylene-α,α′-diyldimolybdenum(II) Complex

Kiyoshi ISOBE, Shozo TERO-KUBOTA, Hisao TANAKA *(Osaka City Univ.)*, **Yukio NAKAMURA** *(Osaka City Univ.)*, **Seichi OKEYA** *(Wakayama Univ.)*, **and Kazuo SAITO**

[*J. Organometal. Chem.* **329**, C21 (1987)]

Reaction of $Na[MoCp(CO)_3]$ (Cp=η^5-cyclopentadienyl) with α,α′-dibromo-*p*-xylene afforded $[\{MoCp(CO)_3\}_2(\mu\text{-}CH_2C_6H_4CH_2\text{-}p)]$ which reacts with PMe_2Ph to give a mono-acyl, and then finally a bis-acyl complex.

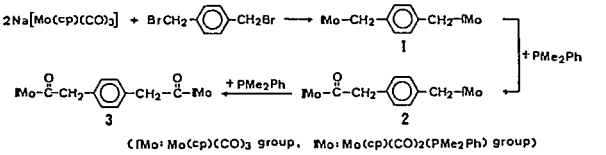

Photolysis of the μ-*p*-xylene-α,α′-diyl complex induces homolytic cleavage of the Mo-C bond to produce radical intermediates, which are converted, *via* *p*-quinodimethane, to *p*-xylene and its polymers.

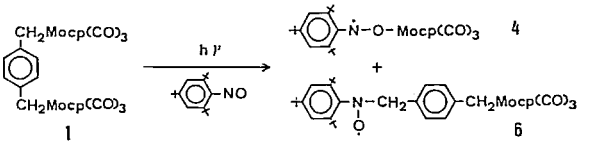

V-F One-Dimensional Halogen-Bridged Metal-Complexes

In the past ten years, crystal structures and solid state properties of the halogen-bridged one-dimensional mixed-valence compounds have been extensively studied for the Pt^{II}-Pt^{IV} and Pd^{II}-Pd^{IV} systems, and further for the hetero-metal systems of Ni^{II}-Pt^{IV} and Pd^{II}-Pt^{IV} [See *IMS Ann. Rev.*, 115 (1986)]. Their characteristic physical and chemical properties such as the charge transfer excitation and luminescence spectra accompanying the large Stokes shift were well interpreted in temrs of the strong electron-phonon coupling in the quasi-one-dimensional systems.

Recently, we succeeded in the synthesis of a new type of halogen-bridged one-dimensional compounds having interesting physical properties. In the novel Ni^{III}-Ni^{III} compound formulated as $Ni(R,R\text{-chxn})_2Br\cdot Br_2$, the bridging Br atom was sit at the midpoint of the Ni atoms. From the detailed analyses of the crystal structure, and the magnetic and optical properties, the SDW state of the linear chain structure was expected.

V-F-1 Crystal Structure and Magnetic Properties of Halogen-Bridged One-Dimensional Ni^{III}-Ni^{III} compound, $Ni(R,R\text{-chxn})_2Br\cdot Br_2$

Koshiro TORIUMI, Masahiro YAMASHITA *(Nagoya Univ.)*, **Shunji BANDOW, and Yuki FUJII** *(Ibaraki Univ.)*

Physical and chemical properties of halogen-bridged one-dimensional compounds are highly dependent on a position of the bridging halogen atom. For an understanding of the electronic structure of the title compound, crystal structure analysis and magnetic susceptibility measurements were carried out. Crystallographic data are: orthorhombic, I222, Z=2; at 25°C, a=23.587(5), b=5.161(2), c=7.121(1) Å, V=866.8(4) $Å^3$, R=0.035 for 1043 reflections; at −152°C, a=23.501(4), b=5.157(1), c=7.090(1) Å, V=859.3(3) $Å^3$, R=0.037 for 1261. The crystal structure is isomorphous with that of the halogen-bridged Pt^{II}-Pt^{IV} mixed-valence compound of $[Pt(R,R\text{-chxn})_2][PtCl_2(R,R\text{-chxn})_2]Cl_4$. The bridging Br atom in the Ni compound is, however, located at the midpoint of the nickel atoms. This indicates that all the nickel atoms are crystallographically and chemically equivalent, and $Ni(R,R\text{-chxn})_2Br\cdot Br_2$ can be regarded as the Ni^{III}-Ni^{III} compound.

Magnetic susceptibility measurements for the single crystal samples were carried out by the Faraday method in the range of 2.5-300 K. A temperature independent diamagnetic susceptibility was observed, which suggested the strong antiferromagnetic interaction between the Ni^{III} atoms on the linear chain. These results as well as the observed optical properties strongly suggest the SDW state in this quasi-one-dimensional system.

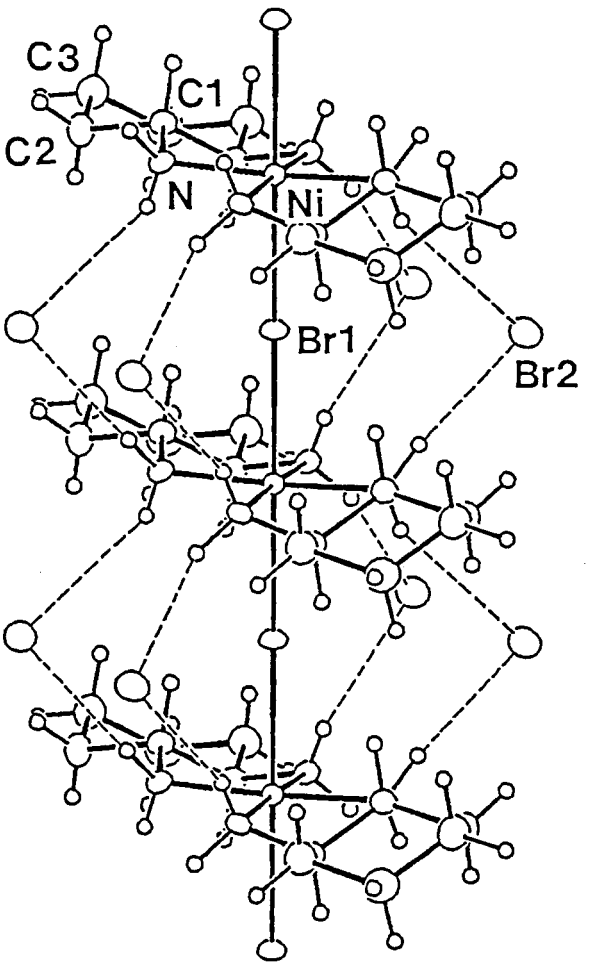

Figure 1. Portion of the inifinite chain along the b axis with surrounding Br^- ions. The dashed lines correspond to hydrogen bonds.

V-F-2 Crystal Structure of $[Ni^{III}Br_2([14]aneN_4)]ClO_4$

Koshiro TORIUMI and Masahiro YAMASHITA *(Nagoya Univ.)*

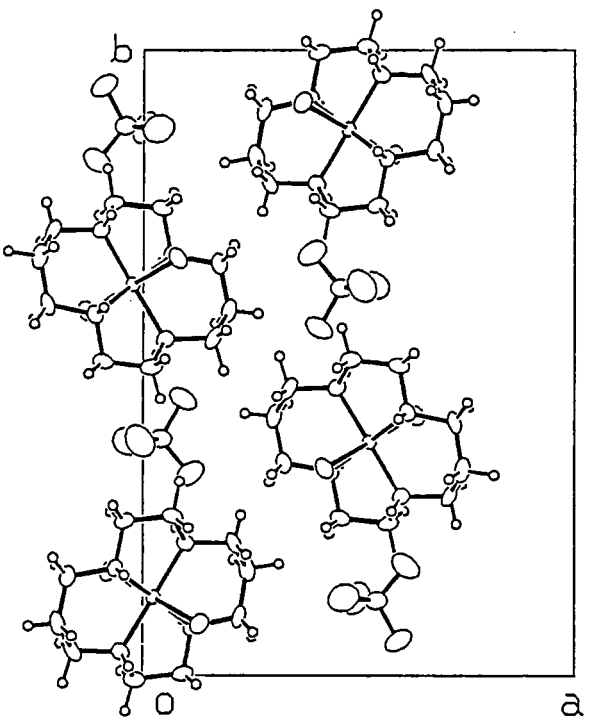

Figure 1. A perspective view of the crystal structure of $[NiBr_2([14]aneN_4)]ClO_4$.

In order to compare the Ni^{III}-Br distance along the linear chain structure of $Ni(R,R\text{-chxn})_2Br\cdot Br_2$ with that of a discrete Ni^{III} compound, the crystal structure analysis of the title compound has been made at 25°C. Crystallographic data are: orthorhombic, $P2_12_12_1$, Z=4, a=13.282(2), b=19.451(4), c=6.745(1) Å, V=1742.6(5) $Å^3$, R=0.042 for 3663 reflections. The Ni atom is surrounded octahedrally by a square planar array of four nitrogen atoms of the macrocyclic ligand and two Br atoms occupying the axial positions. The average Ni^{III}-N and Ni^{III}-Br distances are 1.971(7) and 2.616(1) Å, respectively. The Ni-Br distance (2.580(1) Å) in the chain compound of $Ni(R,R\text{-chxn})_2Br\cdot Br_2$ is significantly shorter than the observed value for the discrete Ni^{III} complex. This result confirms the Ni^{III}-Ni^{III} structure of $Ni(R,R\text{-chxn})_2Br\cdot Br_2$, in which the bridging Br atom is not deviated from the center of two nickel atoms.

V-G Crystallographic Study of Iron(III) Spin-Crossover Complexes

A number of spin crossover iron complexes have so far been reported. Recently, some N_4O_2 type ferric complexes were found to show exceptionally rapid spin interconversion rate (10^{-8} sec) between high-spin($^6A_{1g}$) and low-spin($^2T_{2g}$) states in a solid. It should be considered that the inter- and intramolecular interactions can be responsible for such a rapid spin flipping phenomenon. X-ray craystallographic study was applied to clarify which interactons can cause such a rapid spin flippng rate.

V-G-1 Temperature Dependence of Structures in Spin Crossover Ferric Complex, $[Fe(acpa)_2](BPh_4)$

Hiroki OSHIO, Koshiro TORIUMI, Yonezo MAEDA *(Kyushu Univ.)*, **and Yoshimasa TAKASHIMA** *(Kyushu Univ.)*

The crystallographic approach at various temperatures (311 K, 247 K, 202 K, and 120 K) was applied to the spin crossover ferric complex, $[Fe(acpa)_2](BPh_4)$, which shows a rapid spin flipping phenomenon. Crystal data are: triclinic, $P\bar{1}$, Z=2; a=12.982(3), b=13.592(2), c=11.701(3)Å, α=92.87(1), β=101.77(2), γ=98.74(1)°, V=2006.2(7)$Å^3$, at 311 K; a=12.784(3), b=13.290(4), c=11.776(4)Å, α=93.35(3), β=102.29(2), γ=98.37(2)°, V=1939.0(9) $Å^3$ at 120 K. The average bond distance changes corresponding to the spin transition are ΔFe-O=0.029(2), ΔFe-N*=0.115(2) and ΔFe-N**=0.097(2) Å (N* and N** stand for the nitrogen atom of pyridine and imine moiety, respectively). On the other hand, the changes of bond distance for $[Fe(acpa)_2](PF_6)$, which shows smaller spin flipping rate than $[Fe(acpa)_2](BPh_4)$, are ΔFe-O=0.050(2), ΔFe-N*=0.164(2), and ΔFe-N**=0.140(2)Å [See *IMS Ann. Rev.*, 118 (1986)]. These results suggested that the smaller bond distance changes accompanied by the spin transition makes the activation energy from low- to high-spin states smaller and this enhances the faster spin flipping phenomena in this system.

V-H Cycloaddition Mechanisms and Novel Open-Shell Reactive Intermediates

The striking difference between the photoreaction of barbaralone with chloroanil and that with benzophenone is the formation of the [6+2] cycloadduct in the former photoreaction. A mechanism was investigated by laser flash photolyses of both systems in various solvents. By combination of experimental results with those of flash photolyses, it was proposed that the radical ion pair of a novel bis-homoaromatic barbaralone radical cation and chloranil anion radical is responsible for the [6+2] cycloaddition reaction.

V-H-1 Cycloaddition Reactions of Bis-Homoaromatic Barbaralone Radical Cations with Chloranil and Benzophenone

Tsutomu MIYASHI *(Tohoku Univ. and IMS)*, **Akinori KONNO, Toshio MUKAI** *(Tohoku Univ.)*, **Noboru KOGA, and Hiizu IWAMURA**

Irradiation of barbaralone (**1**) with chloranil (CA) gave two adducts (**2**) and (**3**) in bezene or dichloromethane, but not formed in the more polar acetonitrile. In contrast, similar irradiation with benzophenone(BP) in benzene or acetonitrile gave **4**.[1] Laser flash photolyses revealed that **1** efficiently quenched CA triplet (510 nm) with $k_q=4\times10^9M^{-1}S^{-1}$ in acetonitrile, generating $CA^{-\cdot}$ (410 nm) or with $k_q=1.3\times10^9M^{-1}S^{-1}$ in benzene and benzophenone triplet (520 nm) with $k_q=1.9\times10^8M^{-1}S^{-1}$ in acetonitrile. The value observed for BP is much larger than that expected from an electron transfer quenching. Those results suggest that similar type adducts **2** and **4** are formed through triplet exciplexes, whereas the ion pair of bis-homoaromatic $\mathbf{1}^{+\cdot}$ and $CA^{-\cdot}$ gives **3** before dissociation. The electron transfer induced cycloaddition with CA at the C_4-D_6 positions of **1** is compatible with results of CIDNP experiments.[2]

References

1) K. Kurabayashi and T. Mukai, *J. Chem. Soc., Chem. Commun.*, 1016 (1972)
2) H.D. Roth and C.J. Abelt, *J. Am. Chem. Soc.*, **108**, 2013 (1986). T. Miyashi, Y. Takahashi, A. Konno, T. Mukai, H.D. Roth, M.L. Schilling, C.J. Abelt, *J. Am. Chem. Soc.*, submitted. H.D. Roth, M.L. Schilling, C.J. Abelt, T. Miyashi, Y. Takahashi, A. Konno, T. Mukai, H.D. Roth, M.L. Schilling, C.J. Abelt, *J. Am. Chem. Soc.*, submitted.

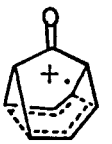

$1^{+\cdot}$

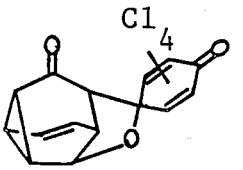

2

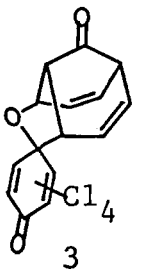

3

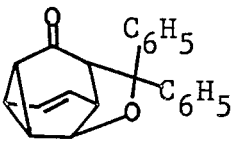

4

RESEARCH ACTIVITIES VI
Coordination Chemistry Laboratories

VI-A Synthesis, Structure, and Properties of Polynuclear Metal Complexes

Novel type binuclear and polynuclear metal complexes have been synthesized by use of organic binucleating ligands. The complexes obtained show interesting physical and chemical properties which could not be observed for mononuclear complexes.

VI-A-1 Crystal and Molecular Structure of $[Cu_2(taec)X]$ $(ClO_4)_3 \cdot nH_2O$(taec = *N*, *N'*, *N''*, *N'''*-Tetrakis (2-aminoethyl)-1, 4, 8, 11-tetraazacyclotetradecane; X = I, F, NO_2, and CH_3COO; n = 0,1, or 2). Effect of Incorporation of an Anion X on the Structure of the Complex Cation

Masahiro MIKURIYA, Sigeo KIDA, and Ichiro MURASE *(Kyushu Univ.)*

[*Bull. Chem. Soc. Jpn.*, **60**, 1681 (1987)]

The crystal structure of four binuclear copper(II) complexes of taec, $[Cu_2(taec)I](ClO_4)_3$(**1**), $[Cu_2(taec)F](ClO_4)_3 \cdot H_2O$(**2**), $[Cu_2(taec)(NO_2)](ClO_4)_3$(**3**), and $[Cu_2(taec)(CH_3COO)](ClO_4)_3 \cdot 2H_2O$(**4**) were determined by single-crystal X-ray analysis. In all the compelxes except for **4** adopt similar structures, where I^-, F^-, or NO_2^- is incorporated into the "cavity" of $[Cu_2(taec)]^{4+}$ as a bridging group. The structure of **4** is different from those of **1**, **2**, and **3**. In **4**, one of the oxygen atoms of acetate ion coordinates to one of the copper ions at the apical site and the other oxygen ocuupies an in-plane coordination site of the other copper ion. The structural effect of incorporation of ananion, X, into $[Cu_2(taec)]^{4+}$ was discussed on the basis of the crystal structures.

VI-A-2 Crystal and Molecular Structure of a Novel Mixed-spin Binuclear Nickel(II) Complex with *N*, *N'*, *N''*, *N'''*-Tetrakis (2-aminoethyl)-1, 4, 8, 11-tetraazacyclotetradecane

Masahiro MIKURIYA, Sigeo KIDA, and Ichiro MURASE *(Kyushu Univ.)*

[*J. Chem. Soc., Dalton trans.*, **1987**, 1261]

The crystal structure of $[Ni_2(taec)Cl]Cl_3 \cdot H_2O$ was determined by the single-crystal X-ray diffraction method. The $[Ni_2(taec)Cl]^{3+}$ cation has a novel binuclear structure in which one of the nickel ions is coordinated by a square-planar N_4 donor set and the other by a distorted square-pyramidal N_4Cl donor set.

VI-A-3 Crystal and Molecular Structure of a Thiolate-Bridged Binuclear Nickel(II) Complex, $[Ni_2\{SCH(CH_2CH_2NH_2)_2\}_2]Br_2$

Masahiro MIKURIYA, Sigeo KIDA, and Ichiro MURASE *(Kyushu Univ.)*

[*Bull. Chem. Soc. Jpn.*, **60**, 1180 (1986)]

The crystal structure of bis[μ-(1, 5-dimino-3-pentanethiolato)-N, N', μ-S-]dinickel(II) bromide was determined by the single-crystal X-ray diffraction method. The complex has a thiolate-bridged binuclear structure, with a dihedral angle 145.2° between the two coordination planes.

VI-A-4 Synthesis and Characterization of a Dinuclear Manganese(II, III) Mixed Valence Complex with the Dinucleating Ligand, L-py, 2, 6,-Bis{bis(2-pyridylmethyl)aminomethyl}-4-methylphenol

Masatatsu SUZUKI *(Kanazawa Univ.)*, **Shuji MURATA** *(Kanazawa Univ.)*, **Akira UEHARA** *(Kanazawa Univ.)*, **and Sigeo KIDA**

[*Chem. Lett*, **1987**, 281]

A novel dinuclear manganese(II,III) mixed valence complex, $[Mn_2(L\text{-}py)(CH_3COO)_2](ClO_4)_2\cdot H_2O$, was prepared by reaction of equimolar amounts of $Mn(ClO_4)_2\cdot 6H_2O$ and $Mn(dmso)_6(ClO_4)_3$ with HL-py, CH_3COOH and $(C_2H_5)_3N$ in methanol. Cyclic voltammogram in acetonitrile showed two quasi reversible waves at 0.47 V and 1.02 V (vs. SCE), which are assigned to the redox reactions of Mn(II,III)/Mn(II, II) and Mn(III,III)/Mn(II,III), respectively.

VI-A-5 Synthesis and Characterization of Dinuclear Iron(II, II) and Iron(II, III) Complexes with a Dinucleating Ligand, 2, 6-Bis[bis(2-pyridylmethyl)aminomethyl]-4-methyl-phenolate(1-)

Masatatsu Suzuki *(Kanazawa Univ.)*, **Akira UEHARA** *(Kanazawa Univ.)*, **Hiroki OSHIO, Kazutoyo ENDO** *(Tokyo Metropolitan Univ.)*, **Makoto YANAGA** *(Tokyo Metropolitan Univ.)*, **Sigeo KIDA, and Kazuo SAITO**

[*Submitted to Bull. Chem. Soc. Jpn.*]

Dinuclear iron(II, II) complexes, $[Fe_2(L\text{-}py)(RCOO)_2]ClO_4\cdot nH_2O$ (R=CH_3(1a) and R=C_6H_5(2a)), and two types of dinuclear mixed valence iron(II, III) complexes $[Fe_2(L\text{-}py)(RCOO)_2](BF_4)_2\cdot nH_2O$ (R=CH_3(1b) and R=C_6H_5 (2b)) and $[Fe_2(L\text{-}py)\text{-}(CH_3COO)(OH)](BF_4)_2\cdot 2H_2O$ (3) were prepared. Only one of two iron(II) ions in the iron(II, II) complexes are easily oxidized with molecular oxygen in methanol to form the mixed valence complexes, $[Fe_2(L\text{-}py)(RCOO)_2](BF_4)_2\cdot nH_2O$, which were characterized by chemical analysis and Mössbauer measurements. Magnetic susceptibility measurements over the temperature range 80~300 K revealed that high spin iron(II) and iron(III) ions are antiferromagnetically coupled with spin exchange coupling constants ($J=-3\sim-8$ cm^{-1}). The complexes exhibited an ESR signal with $g_{av}=1.7$ near liquid nitrogen temperature. Such an ESR signal arises from an antiferromagnetically spin-coupled high-spin iron(II, III) dimer. An intervalence charge transfer transition was observed in the region 700~8500 cm^{-1}. The electron delocalization parameter α is estimated to be ca. 0.08, which corresponds to the class II mixed valence type. Cyclic voltammorgram of the complex 2b in acetonitrile showed reversible couples at +0.05 and +0.73 V (vs. SCE), which were assigned to the redox reactions of Fe(II, III)/Fe(II, II) and Fe(III, III)/Fe(II, III), respectively. The comproportionation constants of 1b and 2b at 20°C are 1.6×10^{12} and 5.0×10^{11}, respectively, implying that the present mixed valence complexes are significantly stabilized.

VI-A-6 Cobalt(II) and μ-Oxodiiron(III, IV) Complexes of Salen Analog with Aromatic Thioether Pendant Group, *N, N'*-Disalicylidene-2-methyl-4-(2-methylthiophenyl)-1, 2-butanediamine

Kaoru HORIUCHI*, Masayuki KOIKAWA*, Shichiro BABA*, Hisashi OKAWA*, Yonezo MAEDA*, Hiroki OSHIO, and Sigeo KIDA *(*Kyushu Univ.)*

[*Submitted to Inorg. Chim. Acta*]

A pentadentate salen analog containing a thioether group in the pendant tail, N, N'-disalicylidene-2-methyl-4-(2-methylthiophenyl)-1,2-butanediamine, has been synthesized. The cobalt(II) complex of this ligand retains a planar configuration of the pendant group at room temperature but adopts a square-pyramidal configuration with the thioether at the apex near liquid nitrogen temperature. The iron complex obtained with this ligand is shown to be a μ-oxodiiron(III, IV) complex comprised of high-spin iron(III) and low-spin iron(IV), based on cryomagnetic data (80~300 K), ESR, and Mossbower spectra. An antiferromagnetic interaction operates between the metal ions ($J=-13.0$ cm^{-1}).

VI-A-7 Synthesis and Properties of One-dimensional Heterometal Assemblies [Au(TPP)] [M(mnt)$_2$] (M=Ni, Pt, Au)

Zhuang JIN ZHONG*, Hisashi OKAWA*, Ryozo AOKI*, and Sigeo KIDA *(*Kyushu Univ.)*

[*Submitted to Inorg. Chim. Acta*]

Metal complexes of the type [Au(TPP)][M(mnt)$_2$] (M = Ni, Pt, Au; TPP=tetraphenylporphyrinate ion; mnt = maleonitriledithiolate ion) have been synthesized and characterized. They were presumed to be discrete one-dimensional assemblies based on magnetic, ESR, visible spectral and conductometric investigations. Electric conductivities of the complexes could be expressed by the equation $\sigma = \sigma_0 \exp(-E/kT)$ in the temperature range 303~373 K. The paramagnetic Au-Ni and Au-Pt complexes showed higher electric conductivities and lower activation energies compared with the diamagnetic Au-Au complex, suggesting that the unpaired electron plays an important role in electric conduction of the former complexes.

VI-B Noncovalent Interactions in Metal Complexes

In the previous papers of this series it was shown that the intramolecular interligand interaction gives rise to a stereospecific formation of a geometrical and/or optical isomer in some complexes with ligands possesing a hydrophobic pendant group. This is a further study of this series.

VI-B-1 Proton NMR Spectroscopic Investigation on Stereoselectivity in Cobalt(III) Complexes of Various 3-Substituted 1-Phenyl-1,3-propanediones

Michio NAKAMURA *(Kyushu Univ.)*, **Hisashi OKAWA** *(Kyushu Univ.)*, **Tasuku ITO, Masako KATO, and Sigeo KIDA**

[*Bull. Chem. Soc. Jpn.*, **60**, 539 (1987)]

1:3-Cobalt(III) complexes of 3-substituted 1-phenyl-1, 3-propanediones (C_6H_5-CO-CH_2-CO-R) have been synthesized and stereoselectivities were studied with 400 MHz proton NMR spectroscopy. When the substituent (R) was ethyl, propyl, isopropyl, or isobutyl, the complexes were obtained in a mixture of fac and mer isomers with the fac/mer ratio of 1/3, demonstrating statistical distribution. When the substituent was *t*-butoxymethyl or cyclohexyloxymethyl the fac isomer was predominantly formed. The stereoselectivity in the geometrical isomer formation of the complexes was ascribed to the interligand CH/π-interaction occuring between the R group and the phenyl ring. The stereo-selectivities of the complexes Co(*l*-moba-X)$_3$ (*l*-moba-X$^-$ = 4-(*l*-mentyloxy)-1-(p-X-phenyl)-1,3-butanedionate ion; X=H, Br, CH_3) were also examined by means of ^{1}H NMR spectroscopy and compared with the CD spectral result previously reported.

VI-C Thermodynamic and Structural Studies of Metal Complexes in Solution

Complexation of metal ions has been extensively investigated in water by using various techniques. However, our knowledge on the complexation of metal ions in nonaqueous solvents is still limited. Reliable enthalpies and entropies of formation of metal complexes in nonaqueous solvents have not been obtained even in simple metal-halide systems. We constructed a precise titration calorimetry system to study complex formation equilibria in nonaqueous solution.

VI-C-1 Calorimetric and Spectrophotometric Studies of Bromo Complexes of Copper (II) in *N*, *N*-Dimethylformamide

Shin-ichi ISHIGURO, Kazuhiko OZUTUMI, László NAGY, and Hitoshi OHTAKI* *(*Tokyo Institute of Technology)*

[*Bull. Chem. Soc. Jpn.*, **60**, 1691 (1987)]

Complexation of Cu(II) with Br^- ions has been studied by calorimetry and spectrophotometry in DMF containing 0.16 mol dm^{-3} $(C_2H_5)_4NClO_4$, 1 mol dm^{-3} $LiClO_4$, and 1 mol dm^{-3} NH_4ClO_4 as constant ionic media at 25°C. Calorimetric titration curves obtained in each solution were well explained in terms of formation of $[CuBr_n]^{(2-n)+}$ (n = 1-4) and their formation constants, enthalpies and entropies were determined. Electronic spectra of individual copper(II) bromo complexes were also determined in these DMF solutions. The complexation of Cu(II) with Br^- ions is considerably weaker in the $LiClO_4$ than in the $(C_2H_5)_4NClO_4$ and is still weakened in the NH_4ClO_4 solution owing to the formation of LiBr and NH_4Br ion pairs in the relevant solutions. The stepwise enthalpy and entropy values suggest that the coordination structure about copper(II) ion changes from octahedral to tetrahedral at the formation of $[CuBr_3]^-$.

VI-C-2 Calorimetric and Spectrophotometric Studies of Ternary Copper(II) Complexes with Bromide Ions and 2,2'-Bipyridil in *N*,*N*-Dimethylformamide

Shin-ichi ISHIGURO, László NAGY*, and Hitoshi OHTAKI* *(*Tokyo Institute of Technology)*

[*Bull. Chem. Soc. Jpn.*, **60**, 2053 (1987)]

Mixed ligand complexation of Cu(II) with Br^- ions and 2,2'-bipyridil(bpy) has been calorimetrically studied in DMF containing 0.16 mol dm^{-3} $(C_2H_5)_4NClO_4$ at 25°C. Complexation of the metal ion with 2,2'-bipyridil has been also studied in the same solution. The calorimetric titration curves were satisfactorily explained in terms of formation of the $[CuBr_p(bpy)_q]^{(2-p)+}$ (denoted as (1pq)) complexes such as (111), (121) and (121), and their formation constants and enthalpies were determined. These mixed ligand complexes are quite stable and yielded to a large extent in the DMF solution. Electronic spectra of these complexes have been measured in DMF over the range 400~1500 nm. The thermodynamic quantities and electronic spectra of the complexes suggested the five coordinate $[Cu(bpy)_2(dmf)]^{2+}$ and $[CuBr(bpy)_2]^+$ complexes in DMF as well as in crystal.

VI-C-3 A Calorimetric Study of Ternary Zinc (II) Complexes with Chloride Ions and 2,2'-Bipyridil in *N*,*N*-Dimethylformamide

Shin-ichi ISHIGURO, László NAGY*, and Hitoshi OHTAKI* *(*Tokyo Institute of Technology)*

[*Bull. Chem. Soc. Jpn.*, **60**, 2865 (1987)]

Formation equilibria of ternary Zn(II) complexes with Cl^- ions and 2,2'-bipyridil (bpy) have been calorimetrically studied in DMF containing 0.4 mol dm^{-3} $(C_2H_5)_4NClO_4$ as a constant ionic medium at 25°C. Formation of binary (2,2'-bipyridil)zinc(II) complexes has also been explored. The calorimetric data were satisfactorily explained in terms of formation of the ternary $[ZnCl(bpy)]^+$ and $[ZnCl_2(bpy)]$ complexes together with the binary $[Zn(bpy)_n]^{2+}$ (n=1-3) ones, and their formation constants and enthalpies were

determined. The ternary complexes are not so favorably formed in DMF. It is suggested that both $[ZnCl(bpy)]^+$ and $[ZnCl_2(bpy)]$ complexes have the four-coordinate tetrahedral structure in DMF.

VI-C-4 Calorimetric and Spectrophotometric Studies of Chloro Complexes of Manganese(II) and Cobalt(II) Ions in *N*, *N*-Dimethylformamide

Shin-ichi ISHIGURO, Kazuhiko OZUTSUMI, and Hitoshi OHTAKI* *(*Tokyo Institute of Technology)*

[*J. Chem. Soc. Faraday Trans. 1*, in press]

Formation of chloro complexes of manganese(II) and cobalt(II) ions has been calorimetrically and spectrophotometrically studied in DMF containing 0.4 mol dm^{-3} $(C_2H_5)_4NClO_4$ as a constant ionic medium at 25°C. Calorimetric data obtained in each system were explained in terms of the formation of $[MCl_n]^{(2-n)+}$ (n = 1-4 and M = Mn or Co), and their formation constants, enthalpies and entropies were determined. As to the cobalt(II) chloride complexes, their formation constants, together with their individual electronic spectra, were also determined by using spectrophotometric data. The thermodynamic quantities of formation the chloro complexes of these metal ions are compared with those of Ni(II), Cu(II) and Zn(II) ions.

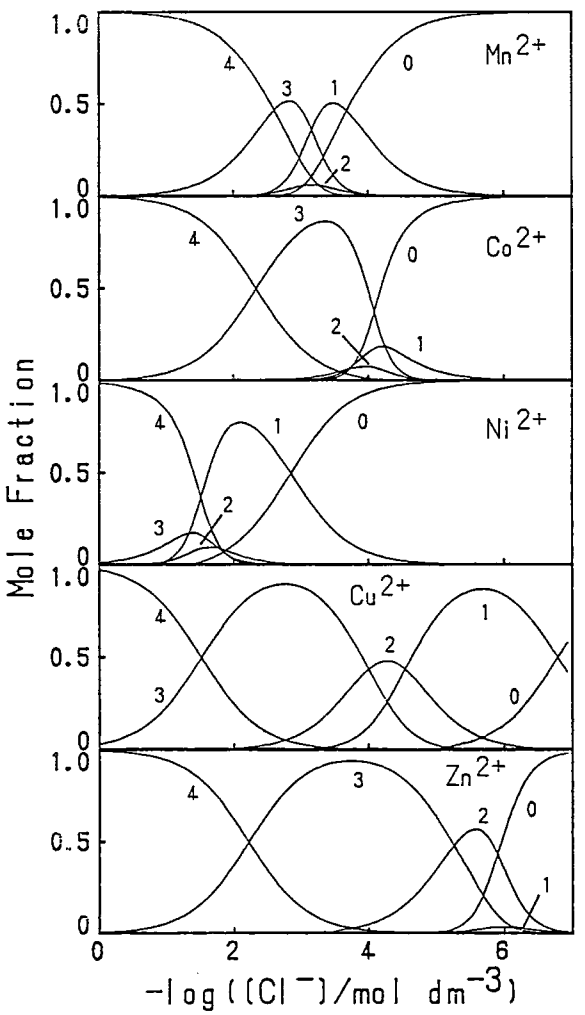

Figure 1. Distribution of the chloro complexes of transition metal(II) ions in DMF. The numbers represent n within the $[MCl_n]^{(2-n)+}$ complex.

VI-C-5 A Calorimetric Study of Thiocyanato Complexes of Cobalt(II) Ion in Micellar Solutions of a Nonionic Surfactant

Shin-ichi ISHIGURO, Takeshi SOTOBAYASHI*, Keiichi SATOH*, and Kazuo SAITO *(*Niigata Univ.)*

[*Inorg. Chem.*, in press]

Complex formation equilibria between cobalt(II) and thiocyanate ions have been studied calorimetrically in an aqueous solution and in micellar solutions of a nonionic surfactant Triton X-100 containing 0.5 mol dm^{-3} $MClO_4$ (M = Li, Na and NH_4) as constant ionic media at 25°C. Calorimetric data were well explained in terms of the formation of $[Co(NCS)]^+$ and $[Co(NCS)_2]$, and of $[Co(NCS)]^+$, $[Co(NCS)_2]$ and $[Co(NCS)_4]^{2-}$, in water and in micellar solutions, respectively. The formation of $[Co(NCS)_3]^-$ was found to be practically negligible in any of the solutions examined. The formation constant and enthalpy of formation of $[Co(NCS)_4]^{2-}$ change with the concentration of the surfactant and with the ionic media in the micellar solutions, while those of $[Co(NCS)]^+$ remain practically constant. It is suggested that the $[Co(NCS)]^+$ complex is formed only in the aqueous phase, while $[Co(NCS)_4]^{2-}$ extensively in micelles as ion pairs.

VI-C-6 An X-Ray Diffraction Study on the Structure of Solvated Cadmium(II) Ion in *N*, *N*-Dimethylformamide and Tetrathiocyanatocadmate(II) Complex in *N*, *N*-Dimethylformamide and Dimethyl Sulfoxide

Kazuhiko OZUTSUMI, Toshiyuki TAKAMUKU*, Shin-ichi ISHIGURO, and Hitoshi OHTAKI* *(*Tokyo Institute of Technology)*

The structure of the solvated cadmium(II) ion in *N*, *N*-dimethylformamide (DMF) and the tetrathiocyanatocadmate(II) complex in *N*, *N*-dimethylformamide and dimethyl sulfoxide (DMSO) has been determined by means of X-ray diffraction at 25°C. The radial distribution curve for the cadmium(II) perchlorate DMF solution was well explained in terms of the presence of the octahedral $[Cd(dmf)_6]^{2+}$ complex with the Cd-O bond length of 229.6(3) pm. The Cd-O distance within the $[Cd(dmf)_6]^{2+}$ is the same as that within the $[Cd(dmso)_6]^{2+}$ in DMSO and the $[Cd(H_2O)_6]^{2+}$ in H_2O. In DMF solution containing the tetrathiocyanatocadmate(II) complex as the predominant species, the complex has a tetrahedral structure and is described as $[Cd(SCN)(NCS)_3]^{2+}$. In DMSO solution, on the other hand, the tetrathiocyanatocadmate(II) complex has a five-coordination (trigonal bipyramidal or square pyramidal) structure with and additional DMSO molecule and is described as $[Cd(SCN)(NCS)_3(dmso)]^{2-}$. The coordination structure of the complexes in DMF and DMSO is different from that found in aqueous solution, which is described as $[Cd(SCN)_2(NCS)_2]^{2-}$.

VI-D Structure and Properties of Hexamolybdenum Cluster Complexes with Mixed Capping Ligands

Kazuo SAITO and Yoichi SAKAKI* *(*Tohoku Univ.)*

[*Pure and Appld. Chem.*, **59**, (1987)]

Molybdenum gives octahedral Mo_6 clusters which are capped by 8 η^3-halide ions e.g. $Mo_6Cl_8^{4+}$. They have 6 terminal halides and $(Mo_6Cl_8)Cl_6^{2-}$ is soluble in water and luminescent, but are oxidized or reduced with great difficulties. When capped by 8 η^3-chalocogenides, however, $Mo_6S_8^{4-}$ cluster anion is very easily oxidized and gives with a variety of non-stoichiometric compounds such as Chévrel-type compounds. We intended to synthesize mixed capping ligand complexes such as $[(Mo_6Cl_7Se)Cl_6]^{3-}$ (Mo_6 in 12 + state) and $[(Mo_6Cl_6Se_2)Cl_6]^{4-}$ and obtained single crystals of the compounds in Table 1, in which Mo_6 moiety is not only in 12+, but also in 13+ and 14+ state. Their X-ray crystal structure was determined, and the redox potential measured by cyclic voltammetry.

Introduction of selenide as capping ligand does not change the bond distances in the cluster, even when the oxidation state of Mo_6 moiety was changed. On the other hand, the change in redox potential is very remarkable. (Table 2) It appears as if the electrons in Mo_6 core are delocalized and the ease of electron transfer is changed remarkably on the introduction of softer chalcogenide in place of halide.

Table 1. Structural data of hexamolybdenum cluster complexes with mixed capping lignads and terminal chloride.

Compounds	Mo_6	I	SG	Mo-Mo	Mo-X_b	Mo-Cl_t
1. $Cs_3[(Mo_6Cl_7S)Cl_6].H_2O$	+12		$P\bar{1}$	2.609 (2)	2.478 (2)	2.467 (6)
2. $Cs_3[(Mo_6Cl_7Se)Cl_6].H_2O$	+12		$P\bar{1}$	2.612 (2)	2.500 (2)	2.473 (6)
3. $Cs_4[(Mo_6Cl_6Se_2)Cl_6].H_2O$	+12	A	$P6_3/mcm$	2.612 (8)	2.515 (6)	2.481 (7)
4. $Cs_4[(Mo_6Cl_6Se_2)Cl_6].H_2O$	+12	B	$P6_3/mcm$	2.603 (7)	2.506 (6)	2.472 (7)
5. $Cs_3[(Mo_6Cl_6Se_2)Cl_6].H_2O$	+13	B	$P\bar{1}$	2.641 (8)	2.523 (6)	2.481 (15)
6. $Cs_2[(Mo_6Cl_6Se_2)Cl_6].9H_2O$	+14	A	Pm3m	2.622 (4)	2.518 (6)	2.516 (10)
7. $Cs_2[(Mo_6Cl_6S_2)Cl_6].9H_2O$	+14	M	Pm3m	2.618 (8)	2.480 (5)	2.490 (10)
8. $(pyH)_3[(Mo_6Cl_7S)Cl_6]$	+12		$P2_1/c$	2.604 (2)	2.473 (4)	2.454 (4)

Mo_6: formal charge number of Mo_6 cluster. I: isomers, see text, M, mixture. SG: space group pyH: pyridinium ion.

Table 2. Electrode potential of hexamolybdenum cluster complexes with mixed capping ligands and terminal halide.

Complexes [a]	+14/+13 [b]	+13/+12 [b]	+12/+11 [b]
1. $[(Mo_6Cl_8)Cl_6]^{2-}$	irrev. [c]	+1.56 [c]	−1.53 [c]
2. $[(Mo_6Br_8)Br_6]^{2-}$	—	+1.38	<−1.7
3. $[(Mo_6Cl_7S)Cl_6]^{3-}$	>+1.4	+0.69	<−1.7
4. $[(Mo_6Cl_7S)Br_6]^{3-}$	>+1.4	+0.74	<−1.7
5. $[(Mo_6Cl_7Se)Cl_6]^{3-}$	>+1.4	+0.64	<−1.7
6. $[(Mo_6Br_6S)Cl_6]^{3-}$	>+1.3	+0.55	<−1.7
7. $[(Mo_6Cl_6S_2)Cl_6]^{4-}$ (A)	+0.51	−0.24	<−1.7

In acetonitrile, against Ag/Ag^+ (0.1 M $AgNO_3$) electrode, working electrode, glassy carbon; counter electrode, platinum; in $(C_4H_9)_4NClO_4$ (0.1 M)

a) Complexes in the form of $(C_4H_9)_4N^+$ salt, charges are of the Mo_6 (12+) state.

b) Charge numbers are those of Mo_6 clusters.

c) Potential data are converted into those against S.C.E., V.

VI-E Pressure Effect on Rates for Solvent Substitution and Electron Transfer of Metal Complexes in Solution

Solvent exchange and electron transfer processes on metal complexes are the fundamental phenomena in solution and dynamic studies on such processes are very important for elucidating the mechanism. The activation volume, $\Delta V^{\ddagger}$, has proved to be particularly diagnostic of activation mode. Therefore, we have measured rates for solvent substitution and electron transfer of metal complexes under high pressures.

VI-E-1 Variable Pressure and Temperature Nuclear Magnetic Resonance Study of Solvent Exchange on Manganese(II) Ion in *N*, *N*-Dimethylformamide. Influenece of Solvent Molecular Size on Solvent Exchange Mechanism

Masao ISHII*, Shigenobu FUNAHASHI *(Nagoya Univ. and IMS)*, **and Motoharu TANAKA*** *(*Nagoya Univ.)*

[*Chem. Lett.* 871 (1987)]

The solvent exchange rates for manganese(II) ion in DMF have been measured at various temperatures and pressures by the oxygen-17 NMR line-broadening method. For the high-pressure experiments, a multinuclear NMR probe has been built which fits into the wide-bore of the 6.34 Tesla superconducting magnet. The pressure vessel has been tested up to 350 MPa. Activation parameters for the solvent exchange were determined to be $k=(2.7\pm0.2)\times10^6 s^{-1}$ at 25.0°C, $\Delta H^{\ddagger}=35.8\pm0.6$ kJ mol^{-1}, $\Delta S^{\ddagger}=-2\pm2$ J $mol^{-1}K^{-1}$, and $\Delta V^{\ddagger}=1.6\pm0.5$ cm^3mol^{-1}. The small but positive activation volume points to an interchange mechanism operative in the exchange process, and this is attributed to the bulkiness of DMF.

VI-E-2 Kinetics of Imidazole Addition to the Axial Site of the Iron(II) Complex of 2, 3, 9, 10-Tetraphenyl-1, 4, 8, 11-tetraaza-1, 3, 8, 10-cyclotetradecatetraene in Dimethyl Sulfoxide. Evidence for a Dissociative-Interchange Mechanism

Shigenobu FUNAHASHI *(Nagoya Univ. and IMS)*, **Naotaka UCHIYAMA*, Masao ISHII*, and Motoharu TANAKA*** *(*Nagoya Univ.)*

[*Inorg. Chim. Acta*, **128**, 169 (1987)]

The axial adduct formation of the iron(II) complex of 2, 3, 9, 10-tetraphenyl-1, 4, 8, 11-tetraaza-1, 3, 8, 10-cyclotetradecatetraene (L) with imidazole in dimethyl sulfoxide has been investigated spectrophotometrically at various temperatures and pressures. In the presence of a large excess of imidazole the reaction with the two phases has been observed. The first faster reaction is the formation of the monoimidazole complex of FeL^{2+}, and the second slower reaction corresponds to the formation of the bisimidazole complex. Activation parameters are as follows: for the first step with k_1 (25.0°C)$=(6.8\pm0.2)\times10^5$ mol^{-1} kg s^{-1}, $\Delta H^{\ddagger}_1=47.5\pm4.9$ kJ mol^{-1}, $\Delta S^{\ddagger}_1=26\pm16$ J K^{-1} mol^{-1}, and

$\Delta V^{\ddagger}_1$ (30.0°C)=27.2±1.5 cm^3 mol^{-1}; for the second step with k_2 (25.0°C)=26.8±0.8 mol^{-1} kg s^{-1}, $\Delta H^{\ddagger}_2$ 91.6±0.8 kJ mol^{-1}, $\Delta S^{\ddagger}_2$=90±3 J K^{-1} mol^{-1}, and $\Delta V^{\ddagger}_2$ (35.0°C)=21.8±0.9 cm^3mol^{-1}. The large positive activation volumes strongly indicate a dissociative character of the activation process.

VI-E-3 Ligand Isotopic Exchange Kinetics of Tris(acetylacetonato)aluminium(III) under Atmospheric and Elevated Pressures

Akira NAGASAWA*, Hiroaki KIDO*, Tomoko HATTORI*, and Kazuo SAITO *(*Tohoku Univ.)*

[*Inorg. Chem.*, **25** 4330 (1986)]

The rate of ligand exchange of this complex in acetylacetone is expressed by $R=(k_1+k_2[H_2O])[Al(acac)_3]$ at 14 to 50°C and under 0 to 237 MPa. The $\Delta H^{\ddagger}$, $\Delta S^{\ddagger}$ and $\Delta V^{\ddagger}$ and 85 ± 5 and 79 ± 7 kJ mol^{-1}, −38±18 and −34±14 J $K^{-1}mol^{-1}$, and +10±2 and +5±1 cm^3mol^{-1}, respectively for k_1 and k_2. An interchange mechanism to form an intermediate containing both $acac^-$ and Hacac as unidentate ligand or water molecule was proposed.

VI-E-4 A Kinetic Study of Pressure Effect upon an Outersphere Electron Transfer Reaction Involving Free Radicals

Masahiro EBIHARA, Yoichi SASAKI*, Shozo TEROKUBOTA, and Kazuo SAITO *(*Tohoku Univ.)*

[*Bull. Chem. Soc. Jpn.*, **60**, 391 (1987)]

Volume of activation for the redox reaction between $[(en)_2\text{-}Co^{III}(\mu\text{-}NH_2,\mu\text{-}O_2^{(-)})Co^{III}(en)_2]^{4+}$ (en ethylenediamine) and 2, 2, 6, 6-tetramethyl-1-piperidinyloxyl radical is zero. This result endorses our previous discussion that the changes in solvation and in intrinsic volume of reactants are respectively responsible for determining the precursor and transition state.

VI-E-5 Large Positive Activation Volume (+38 cm^3mol^{-1}) for the Intra-molecular Electron Transfer Reaction from Iron(II) to Cobalt(III) in (μ-pyrazine-*N*, *N'*-) (pentamminecobalt(III))pentacyanoiron(II) in Aqueous Solution.

Yoichi SASAKI*, Takayuki NINOMIYA*, Akira NAGASAWA*, Kaoru ENDO*, and Kazuo SAITO *(*Tohoku Univ.)*

[*Inorg. Chem.*, **26** 2164 (1987)]

The title reaction gave $\Delta V^{\ddagger}$ of +38 cm^3mol^{-1} at pH 5.0 and I=0.10 M, at 25°C under 0.1 to 70 MPa. The first order rate constant changes with the change in added electrolytes, $\Delta V^{\ddagger}$, $\Delta H^{\ddagger}$ (130 k $Jmol^{-1}$) and $\Delta S^{\ddagger}$(+165 J $K^{-1}mol^{-1}$) remain unchanged. The $\Delta V^{\ddagger}$ cannot be interpreted by the intrinsic volume change (< 20 cm^3mol^{-1}) and electrorestriction of the solvation sphere (< 6.5 cm^3mol^{-1}). Contribution of hydrogen-bonded water molecules around the ligand is suggested.

VI-E-6 Ligand Isotopic Exchange of *cis*-Bis(acetylacetonato)-dioxomolybdenum(VI) in Acetylacetone

Akira NAGASAWA*, Hideaki K. TANAKA*, Masayuki MIYOSHI*, and Kazuo SAITO* *(*Tohoku Univ.)*

[*Inorg. Chem.*, **26**, (1987)]

Kinetic studies by the isotopic labelling method with ^{14}C disclosed that the rate law is expressed by $(k_1 + k_2[H_2O])$[complex] the k_1 and k_2 being 1.05 × $10^{-3}s^{-1}$ and 8.27 × $10^{-3}M^{-1}s^{-1}$, respectively at 25°C. Application of pressure up to 92 MPa resulted in no change in rate, thus indicating $\Delta V^{\ddagger}$ is 0 cm^3mol^{-1}. An associative interchange mechanism was suggested on the basis of large negative $\Delta S^{\ddagger}$ values (−86 and −71 J $mol^{-1}K^{-1}$ for k_1 and k_2, respectively).

VI-F Stereoselective Oxygenation of Thioethers with Organic Hydroperoxide in the Presence of Schiff Base Complexes of Oxovanadium(IV) in Solution

Kiyohiko NAKAJIMA, Kazuo SAITO, Masaaki KOJIMA*, and Junnosuke FUJITA* *(*Nagoya Univ.)*

Oxovanadium(IV) complex of *N*-salicylidene-*R*-aminocarboxylates (terdentate ligand) catalyses the oxygenation of methyl phenylthioether with tert-butyl hydroperoxide in dichloromethane to give (*R*)-methyl phenyl sulfoxide with an enantiomeric excess of 10~15%. A plausible precursor for the catalytically active intermediate was isolated in crystalline state as a mixture of two binuclear complexes in which two vanadium(V) atoms are bridged by oxygen at cis-site to the terminal oxide. These species have a common structure in which the terdentate ligand and bridging oxygen occupy the basal sites. The bridge is decomposed by methanol and alkyl hydroperoxides to give *cis*(oxo, methoxo) and *cis*(oxo, alkylperoxo) species, respectively. UV absorption spectrometry suggests that the latter is the catalytically active species.

VI-G Synthesis of Octahedral Tungsten Cluster Chloro Complexes with Trialkylphosphines and Their Conversion to η^1-Ethyl Derivatives

Taro SAITO *(Osaka Univ. and IMS)*, **Shozo TERO** *(Tohoku Univ. and IMS)*, **and Hiroki OSHIO**

[*Inorg. Chem.*, **26**, 1362 (1987)]

Hexanuclear tungsten cluster chloro complexes coordinated with two trialkylphosphines were prepared and the structure of trans-$[(W_6Cl_8)Cl_4(PBu_3)_2]$ was determined. The complex crystallizes in the monoclinic space group C2/c with a = 29.045(15) Å, b =10.326(3) Å, c = 21.485(9) Å, ß =135.33(2)°, and Z = 4. The two tributylphosphines are coordinated to the trans positions of the octahedral tungsten cluster core with eight face-bridging and four terminal chlorines. Selected bond distances are W–W = 2.626 Å, W–Cl^t = 2.413 Å, W–Cl^b =2.496 Å, and W–P = 2.581 Å. The diethyl and triethyl cluster complexes all-trans-$[(W_6Cl_8)Cl_2(C_2H_5)_2(PR_3)_2]$ (R = n–C_4H_9, n–C_5H_{11}) and trans, mer-$[(W_6Cl_8)Cl(C_2H_5)_3(PR_3)_2]$ were synthesized by the reaction of the chloro clusters with triethylaluminum. In the solid state these ethyl cluster complexes are heat- and air-stable. However, the solutions are very sensitive to visible light and homolysis of the W–C bonds occurs under a short period of irradiation.

VI-H Time-Resolved ESR Study on the Non-Phosphorescent Triplet States

Shozo TERO *(Tohoku Univ. and IMS)*, **Hiroki OSHIO, and Kouto MIGITA** *(Yamaguchi Univ.)*

It is well known that UV-irradiation of free Schiff base generates enolimine form via intramolecular proton transfer from the S_1 state of the ketoamine form. However, there has been little study on the electronic structure of the T_1 state of the enolimine because of the non-phosphorescence. Using time-resolved ESR technique, we detected transient ESR signal due to T_1 state of the enolimine form of N-alkylsalicylideneimines in toluene glassy matrix at 77 K. Nitrogen laser (Molectron UV-24) was used as a light source. Zfs parameters of $|D| = 0.071$ and $|E| = 0.013$ cm^{-1} were determined. The absolute D value obtained is smaller than that of the corresponding Zn complex.

Quadridentate Schiff base complex of cadmium, Cd(Salphen), emits no phosphorescence probably owing to

heavy atom effect. Although no ESR signal due to the triplet state of the complex was observed upon continuous irradiation, transient ESR spectrum was clearly measured with N_2 laser pulse photolysis. The spin polarization pattern is completely different from that of Zn(Salphen), that is AAAE/AEE, where A is enhanced absorption and E is emission of microwave. It was shown that the absolute D value slightly decreases with increasing atomic number of the coordinated metal. Present study suggests that spinorbit coupling interaction affects markedly ISC anisotropy as well as phosphorescence lifetime while it shows minor effect on zfs parameters in this system.

VI-I Properties of Rare Earth Salts of Rhodium-Boron Clusters

Platinum metal ions and boron give characteristic clusters such as $Rh_4B_4^{3-}$ and Rh_3B^{3-}, and their rare earth salts provide various interesting properties.

VI-I-1 Heterogeneous Olefin Hydrogenation Catalysis of Metal Cluster Compounds Consisting of Rhodium-boron Cluster Anion and Rare Earth Cations

Kazuo SAITO, Akira NAKAMURA *(Osaka Univ.)*, **Humihiko TAKEI, and Bateer WANG**

[*J. Catal.*, **106**, 292 (1987)]

$TbRh_4B_4$ and $PrRh_3B$, with rock salt structure between Tb^{3+} and $Rh_4B_4^{3-}$ and Perovskite structure, respectively, catalyse the hydrogenation of olefins in benzene under atmospheric pressure and at room temperature. The catalytic action is accompanied by a small change in lattice constants of the solid, but the original dimension is restored on the treatment of the used powder with olefins in benzene. There is marked selectivity that the double bond at 1-position is preferably hydrogenated. On repeated use of the powder the apparent catalytic activity increases presumably owing to the decrease in grain size. It appears as if the chemically adsorbed hydrogen in the solid is active towards the hydrogenation.

VI-I-2 Studies on Solide-Solution Systems Er(Rh, M)$_3$B, (M = Pd, Pt), with Perovskite Structure

Humihiko TAKEI and Hiroyuki TAKEYA *(Univ. of Tokyo)*

[*J. Less-Common Metals*, **134**, 263 (1987)]

The solid-solution systems Er(Rh, M)$_3$B, (M=Pd, Pt) have been investigated by X-ray diffraction and X-ray photoelectron spectroscopy analyses. The samples were prepared with an arc-melting furnace in the argon atmosphere and annealed at 1250°C. The stability field of perovskite structure was determined by changing the composition of substituent metal M and boron. In some cases, boron defect at the octahedral (body-centered) position occurred dependent on the particular substution ratio of M to Rh. The results can not be explained by the stacking of the constituent atoms but by the concept of valence electron concentration (VED) per unit cell, which is calculated from the sum of valence electrons in each atom in the unit cell. The high stability of these perovskites is governed by the VEC value from 31.0 to 34.4.[1)]

The state analyses of these systems were performed using an X-ray photoelectron spectroscopy equipment (ESCALAB MkII, VG Co.). The results indicated that Er and B are positively charged, whereas Rh is negative, as shown in Figure 1. These facts lead to the conclusion that borons as well as erbium atoms tender their valence electrons to Rh or M at the face-centered position to strenghten the Rh-Rh or Rh-M bonds in the octahedral (Rh, M)$_6$B sublattice.

RESEARCH ACTIVITIES VII
Computer Center

VII–A Theoretical Investigatigations of Metallo-porphyrins by the Ab Initio SCF MO Method

Metal complexes are interesting polyatomic systems because of their complicated electronic structure and their catalytic functions. Metalloporphyrins are prominently important as an active center of energy conversion processes in biological systems. In this project the electronic structure and the fundamental functions are studied for several complexes by using the *ab initio* SCF MO program JAMOL3 and a newly developed MCSCF program JASON2.

VII-A-1 *Ab initio* MO Study on Fe Out-of-Plane Displacement and Fe-Ligand Vibration in Five-Coordinate Fe-Porphyrin

Minoru SAITO *(Nagoya Univ. and IMS)* **and Hiroshi KASHIWAGI**

[Int. J. Quant. Chem. Symp. 21 661 (1987)]

Ab initio SCF MO calculations were carried out for fluoro(porphinato)iron(III)[FePF]. Potential curves as functions of the Fe out-of-plane displacement and Fe-F bond distance were calculated for the ground state (ferric high-spin state). The moleucular structure of FeP and potential energy curves for the iron displacement(Fe-Ct) and Fe-F distance are shown in Fig. 1. By using these curves, the equilibrium iron displacement, Fe-F distance, and frequency of the Fe-F stretching mode were evaluated. The values evaluated (0.45 Å, 1.85 Å, and 656 cm^{-1}) are in good agreement with the experimental values (0.47 Å, 1.792 Å, and 606 cm^{-1}, respectively). In this mode, an amplitude of the F atom is 2.58 times larger than that of the Fe atom. Another mode corresponds to the out-of-plane motion of the Fe-F moiety and has the frequency of 194 cm^{-1}.

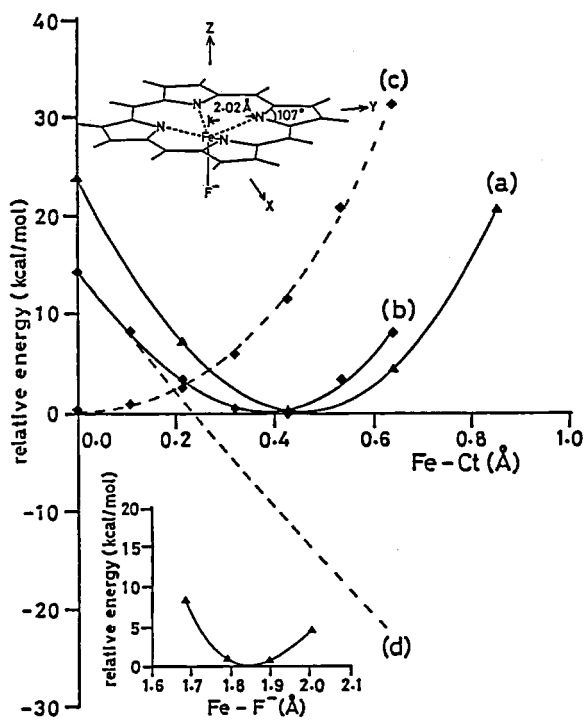

Figure 1. (a) The potential energy curve as a function of the out-of-plane displacement of the Fe atom for FePF. (b) This curve was composed from the curves (c) and (d). (c) The Fe-Ct potential curve for the ferric high-spin state of FeP. (d) The potential curve for the Coulomb repulsion between four porphine nytrogens and F^- estimated by the point charge approximation. The FePF molecular structure used in the present calculations and potential energy curve as a function of the Fe-F distance in FePF are also shown in this figure.

The Fe-Ct potential curve(Fig. 1 (a)) is similar to a potential curve(Fig. 1 (b)) which was obtained by adding a potential curve for the Coulomb repulsion between the four porphine nitrogens and F^- ion (Fig. 1 (d)) to a Fe-Ct potential curve for the ferric high-spin state of FeP (Fig. 1 (c)). Therefore, the Fe out-of-plane displacement is caused mainly by the Coulomb repulsion between porphine nitrogens and the fluorine anion.

VII-A-2 *Ab initio* RHF and CASSCF studies on Fe-O bond in high-valent iron-oxo-porphyrins

Shigeyoshi YAMAMOTO, Junji TERAOKA* and Hiroshi KASHIWAGI *(*: Osaka-city University)*

[*J. Chem. Phys.*, in press]

The electronic structure of the Fe-O bond in highly oxidized iron porphyrins was elucidated by RHF and CASSCF (complete active space SCF) calculations on a neutral complex FeP(py)O (P = porphine, py = pyridine), which is a model of peroxidase compound II. Its molecular geometry is given in Figure 1. Equilibrium distance and stretching frequency of Fe-O were calculated to be 1.66 Å and 890 cm^{-1}, respectively, from the potential energy curves obtained by CASSCF. The calculated bond length 1.66 Å is close to the value of 1.64 Å obtained by EXAFS for HRP-II (horse radish peroxidase compound II). Furthermore, Mössbauer spectrum parameters (quadrupole splitting, isomer shift, asymmetry parameter and direction of the principal axis of the electric field gradient tensor) and spin density were evaluated. They are in good agreement with experiments on ferryl-oxo porphyrin compounds. It is revealed that the electronic structure of the Fe-O bond is equivalent to that of the elongated O_2 molecule.

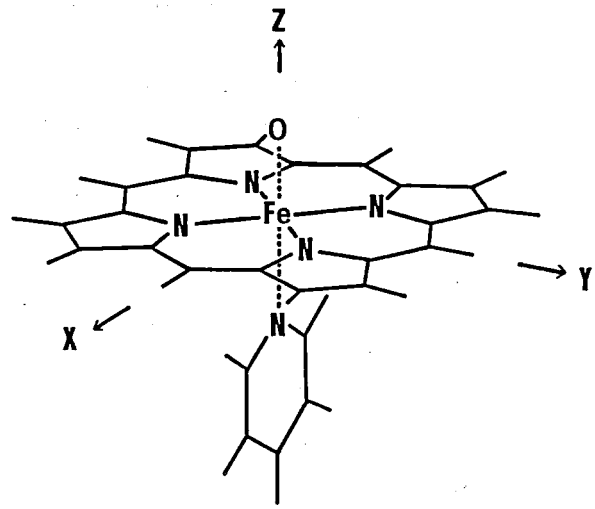

Figure 1. Geometry assumed for FeP(py)O. The pyridine molecule lies in the xz plane.

Chemical Materials Center

VII–B Synthesis, Structure, and Reactions of New Organometallic Compounds

Reactions of organometallic compounds usually proceed in a stepwise manner involving unit reactions such as oxidative addition, migratory insertion, rearrangement, reductive elimination, etc. The study on such basic reactions of organometallic compounds is directly relevant to an understanding of the reaction mechanisms of synthetically important catalyses such as olefin oligomerization, cyclocoupling, metathesis, and so on and may also provide the basis for developments of new efficient catalyst systems. We have been studying synthesis, characterization, and reactions of new organometallic compounds of both early and later transition metals. Especially interested is the chemistry of metallacyclic compounds and transition metal-olefin complexes.

VII-B-1 First η^1-Acyltitanium Complexes Prepared by the Reaction of 2-Titana-1-oxacyclopentanes with Carbon Monoxide

Kazushi MASHIMA, Hiroshi HARAGUCHI,* Akira OHYOSHI,* and Hidemasa TAKAYA *(*Kumamoto Univ.)*

The chemistry of metallacyclic compounds has been of much interest because of their importance as intermediates in various metal-assisted organic reactions. Reactions of metallacycles with carbon monoxide have been extensively investigated. Information on the mechanism of carbonylation, however, has been limited probably because of thermal and/or kinetic

instability of intermediates.[1] We have found that introduction of an electronegative atom adjacent to titanium stabilizes the intermediary acyltitanium complexes.

2-Titana-1-oxacyclopentanes **1** in toluene reacted smoothly with atmospheric pressure of carbon monoxide at 20 °C. Initial orange color of the solution changed deep purple, from which purple crystals of **2** were isolated after recrystallization from hexane at −80 °C. Extrusion of carbon monoxide, the reverse reaction of eq 1, was not observed even under reduced pressure. The molecular structure of **2c** was established by a single-crystal *X*-ray diffraction method (Figure 1). The Ti–O(10) bond distance (3.039(3) Å) in **2c** is in sharp contrast with the metal-oxygen bond distances (2.167–2.47 Å) in η^2-acyl transition metal complexes, and is comparable with that (3.121(4) Å) of the η^1-nickel complex, indicating that **2c** has a novel η^1-acyltitanium structure. The acyl derivatives of early transiton metals usually have η^2-structures. To our knowledge this provides the first example of η^1-acyltitanium complexes.

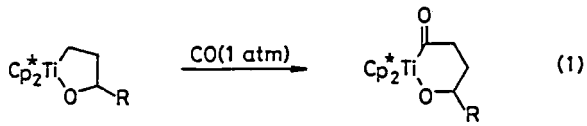

1

2

a: R = CH_3
b: R = C_2H_5
c: R = $CH(CH_3)_2$

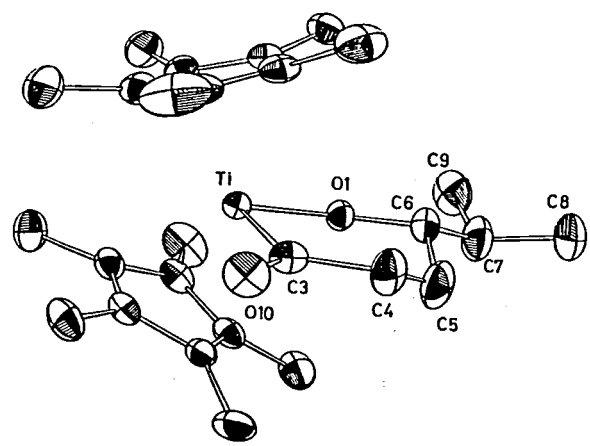

Figure 1. The ORTEP drawing of the complex **2c** with the atom numbering scheme. All hydrogen atoms are omitted for simplicity.

Reference

1) K. Mashima and H. Takaya, *Organometallics*, **4**, 1464 (1985).

VII-B-2 New Convenient Synthesis of Lanthanide–Cyclooctatetraene Complexes: *X*-Ray Crystal Structure of CeI(COT)(THF)$_3$

Kazushi MASHIMA and Hidemasa TAKAYA

Recently the organometallic compounds of lantanide and actinide series have been of great interest. Lanthanide–COT complexes (COT = cyclooctatetraene) have mostly been prepared by the reaction of lanthanide halides with dianion derived from COT. We found an alternative, convenient route to this class of compounds, which enables us to prepare various lanthanide–COT complexes in good yields.

Lanthanide complexes having the formula LnI(COT)(solvent)$_3$ have been prepared by the direct reaction of lanthanide metal with COT in THF in the presence of stoichiometric amount of iodine. For example, treatment of cerium metal with COT and iodine at 50 °C for 48 h afforded CeI(COT)(THF)$_3$ (**1**) as pale yellow crystalline solids in 85% yield (eq 1). The single-crystal *X*-ray diffraction method revealed that the complex **1** is monomeric and has three THF coordinated to the central Ce as shown in Figure 1. Similary, COT complexes of La, Sm, etc. have been synthesized in good yields.

$$\mathrm{Ce} + \mathrm{COT} \xrightarrow[\mathrm{THF}]{\mathrm{I_2}} \underset{\mathbf{1}}{\mathrm{CeI(COT)(THF)_3}} \quad (1)$$

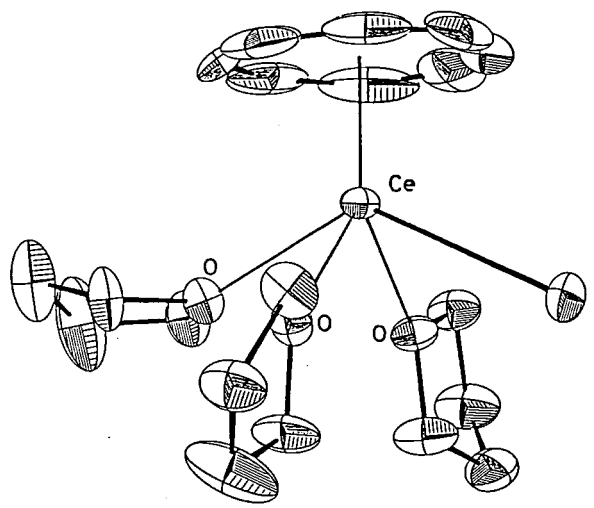

Figure 1. The ORTEP drawing of the complex **1** with the atom numbering scheme. All hydrogen atoms are omitted for simplicity.

VII–C Synthesis of New Chiral Diphosphines and Their Use in Homogeneous Asymmetric Catalysis

The molecular designing and synthesis of new effective chiral ligands are the most important requirements for developing synthetically useful asymmetric catalysis. Our attention has been focussed on the subjects of developments of new effective homogeneous asymmetric catalysis, elucidation of the reaction mechanisms, and explication of the factors controlling the asymmetric induction.

VII-C-1 BINAP-Ruthenium(II) Dicarboxylate Complexes: New Highly Efficient Catalysts for Asymmetric Olefin Hydrogenations

Tetsuo OHTA, Hidemasa TAKAYA, and Ryoji NOYORI *(Nagoya Univ.)*

[*Inorg. Chem.* in press]

We have prepared the mononuclear BINAP-ruthenium(II) complexes, $Ru(OCOR)_2$[(*R*)- or (*S*)-2,2'-bis(diarylphosphino)-1,1'-binaphthyl] [(*R*)-**1** or (*S*)-**1**]. The crystal structure of Λ-(*S*)-**1b** has been determined by single-crystal *X*-ray analysis and compared with that of Rh[(*R*)-binap](norbornadiene)ClO_4, which revealed interesting characteristics of the complex **1**. The absolute configurations of the complexes **1a** and **1c** were substantiated by comparing CD spectrum of Λ-(*S*)-**1b** with those of (*S*)-**1a**, (*R*)-**1a**, and (*R*)-**1c** (Figure 1). These BINAP-Ru complexes serve as highly efficient catalysts for asymmetric hydrogenations of various enamides,[1] α-acylaminoacrylic acids, α, β- and β, γ-unsaturated carboxylic acids, allylic and homoallylic alcohols,[2] and α-amino ketones, etc. In all cases, the Ru complexes are much superior to the corresponding Rh complexes and are now becoming one of the most efficient catalysts for asymmetric hydrogenations.

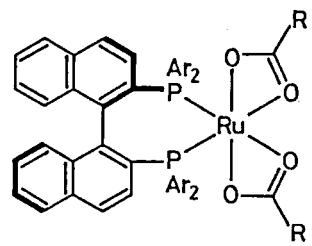

Δ–(*R*)–1

a: R = CH_3, Ar = C_6H_5

b: R = $(CH_3)_3C$, Ar = C_6H_5

c: R = CH_3, Ar = *p*–$CH_3C_6H_4$

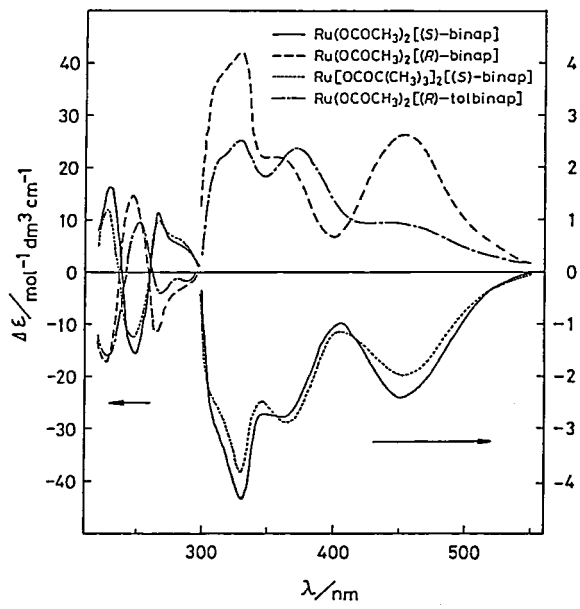

Figure 1. Circular dichroism spectra of $Ru(OCOCH_3)_2$[(*S*)-binap], $Ru(OCOCH_3)_2$[(*R*)-binap], $Ru[OCOC(CH_3)_3]_2$[(*S*)-binap], and $Ru(OCOCH_3)_2$[(*R*)-tolbinap] in dichloromethane ($5.2\text{-}7.5 \times 10^{-5}$ *M*).

References

1) R. Noyori, M. Ohta, Yi Hsiao, M. Kitamura, T. Ohta, and H. Takaya, *J. Am. Chem. Soc.*, **108**, 7117 (1986).
2) H. Takaya, T. Ohta, N. Sayo, H. Kumobayashi, S. Akutagawa, S. Inoue, I. Kasahara, and R. Noyori, *J. Am. Chem. Soc.*, **109**, 1596 (1987).

VII-C-2 Asymmetric Hydrogenation of Unsaturated Carboxylic Acids Catalyzed by BINAP-Ruthenium(II) Complexes

Tetsuo OHTA, Hidemasa TAKAYA *(IMS)*, **Masato KITAMURA, Katsunori NAGAI, Ryoji NOYORI** *(Nagoya Univ.)*

[*J. Org. Chem.*, **52**, 3174 (1987)]

Rhodium(I) complexes bearing certain chiral phosphine ligands catalyze highly enantioselective hydrogenation of α-acyaminoacrylic acids or their esters. The extensive, systematic study led to the conclusion that the double-bond geometry and the presence of the α-acylamino group are obrigatorily important for the high efficiency. Without the amide or related groups, any of the catalyst systems designed so far were unable to give high enantiomeric excesses. To our knowledge, only exceptional substrate is itaconic acid, an unsaturated dicarboxylic acid. We have found that asymmetric hydrogenation of α,β-unsaturated carboxylic acids **1** in methanol containing a catalytic amount of $Ru(OCOCH_3)_2$[(*R*)- or (*S*)-2,2'-bis(diarylphosphino)-1,1'-binaphthyl] (aryl = phenyl, *p*-tolyl, *p*-anisyl) affords the corresponding saturated products **2** in high enantiomeric excesses and in quantitative yield. This catalysis provides the first successful example of a high degree of enantioselective hydrogenation of acrylic acids without α-acylamino directing group. β,γ-Unsaturated carboxylic acids were also hydrogenated with high enantioselectivity. Factors controlling the stereoselectivity are discussed. The wide utility has been demonstrated by asymmetric synthesis of (*S*)-2-[2-(6-methoxynaphthyl)]propionic acid [(*S*)-naproxen] (**3**), (3*S*,4*S*)-3-[(1*R*)-1-*t*-butyldimethylsiloxyethyl]-4-[(1*R*)-1-carboxyethyl]azetidin-2-one (**4**) (synthetic precursor of 1-methylcarbapenems), 2-methylbutyrolactone (**5**), 3-methylbutyrolactone (**6**), 3-methylvalerolactone (**7**), etc.

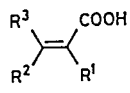

1

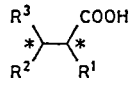

2

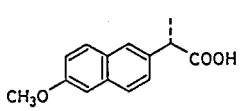

3

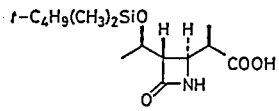

4

5

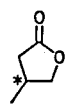

6

7

VII-C-3 Asymmetric Hydrogenation of β-Keto Carboxylic Esters. Practical, Purely Chemical Access to β-Hydroxy Esters in High Enantiomeric Purity

Ryoji NOYORI, Takeshi OHKUMA, Masato KITAMURA *(Nagoya Univ.)*, **Hidemasa TAKAYA** *(IMS)*, **Noboru SAYO, Hidenori KUMOBAYASHI, and Susumu AKUTAGAWA** *(Takasago Internat. Corp.)*

[*J. Am. Chem. Soc.*, **109**, 5856 (1987)]

Optically active β-hydroxy carboxylic esters are an extremely important class of compounds for natural product synthesis. Access to such compounds has so far relied mainly on biological or biochemical transformations. Asymmetric hydrogenation of the keto esters is an alternative complementary methodology, and the purely chemical means should allow even easier control of the chiral outcome at will, giving both antipodes with equal ease. However, the practical chemical processes have not sufficiently been exploited. We have found that the BINAP-Ru complexes formed from $Ru(OCOCH_3)_2$[(*R*)- or (*S*)-binap] and HX (X = Cl, Br, of I) in 1:2 ratio, as well as $Ru_2Cl_4(binap)_2(C_2H_5)_3N$, serve as excellent catalysts for the enantioselective hydrogenation of a wide range of β-keto carboxylic esters (eq 1). Homogeneous hydrogenation using a substrate to catalyst mole ratio of >1000 proceeds smoothly in methanol under an initial hydrogen pressure of 50 to 100 atm to give the corresponding β-hydroxy esters in nearly quantitative yield and with exceptionally high (up to 100%) enantioselectivity. The efficiency of the chemical chiral multiplication rivals or is even superior to that of biological conversion. The transition metal catalyzed reaction is clean and operationally simple, and it can be conducted with high (up to 50%) substrate concentration.

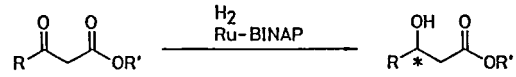

(1)

VII-C-4 Homogeneous Asymmetric Hydrogenation of Functionalized Ketones

Masato KITAMURA, Takeshi OHKUMA, Shin-ichi INOUE *(Nagoya Univ.)*, **Noboru SAYO, Hidenori KUMOBAYASHI, Susumu AKUTAGAWA** *(Takasago Internat. Corp.)*, **Tetsuo OHTA, Hidemasa TAKAYA** *(IMS)*, **and Ryoji NOYORI** *(Nagoya Univ.)*

[*J. Am. Chem. Soc.*, in press]

Under the influence of the (*R*)- or (*S*)-BINAP-based Ru(II) complexes (BINAP = 2,2'-bis(diphenylphosphino)-1,1'-binaphthyl), a wide range of functionalized ketones are hydrogenated in a highly enantioselective and predictable manner. The hydrogenation proceeds smoothly in alcoholic media at room temperature with initial hydrogen pressure of 40-100 atm. The substrate to catalyst mole ratio ranges from 230 to 2200. Ru complexes of the type RuX_2(binap) (X = halogen, empirical formula), Ru_2Cl_4(binap)$_2$ $N(C_2H_5)_3$, or Ru(OCOR)$_2$(binap) are employable as catalysts, depending on the substrates. The general sense of the asymmetric induction, illustrated in eq 1 and eq 2, suggests that the key factor in the stereodifferentiation is the simultaneous coordination of the carbonyl oxygen and heteroatom, X or Y (C = nonstereogenic sp^2- or sp^3 hybridized carbon), to the Ru atom making a five- and six-membered chelate ring, respectively. Various functionalities including dialkylamino, hydroxyl, alkoxyl, siloxyl, keto, alkoxycarbonyl, alkylthiocarbonyl, dialkylaminocarbonyl, caboxyl, etc., can act as the efficient directive group. Neighboring halogen atoms also affect strongly the stereochemical outcome. Certain α- and β-diketones are hydrogenated to give isomeric diols by double stereodifferentiation. Relative importance of efficacy of the catalyst/carbonyl chirality transfer and effect of the initially created stereogenic center is highly dependent on the ketonic substrates.

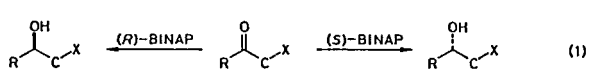

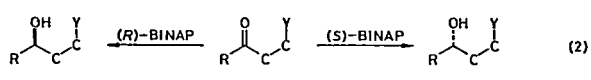

VII-C-5 General Asymmetric Synthesis of Benzomorphans and Morphinans via Enantioselective Hydrogenation

Masato KITAMURA, Yi HSIAO, Ryoji NOYORI *(Nagoya Univ.)*, **and Hidemasa TAKAYA**

[*Tetrahedron Lett.*, **28**, 4829 (1987)]

Naturally occurring morphine (**1**) is important as an analgesic but exhibits undesired addicting side effect. The structural modification can overcome this problem to a considerable extent. Described herein is the asymmetric synthesis of artificial morphines **2** and **3** and their enantiomers utilizing the recently discovered enantioselective hydrogenation of enamides[1] as key step.

Homogeneous hydrogenation of **4a** in methanol with Ru(OCOCF$_3$)$_2$[(*R*)-tolbinap] (25°C, H_2 100 atm, 120 h) afforded (*R*)-**5a** in 98% ee and in 98%-yield which was converted to (*R*)-**6a** by the treatment with 2 N NaOH at 80°C. These compounds, (*R*)-**5a** and (*R*)-**6a**, are useful intermediates for synthesis of (-)-metazocine (**2a**), (-)-pentazocine (**2b**), (-)-cyclazocine (**2c**), (-)-phenazocine (**2d**), etc. This method has been successfully extended to the enantioselective synthesis of dextromethorphan (**3a**), and extremely important bronchodilating agent. Asymmetric synthesis of (*S*)-**5b** from **4b** was accomplished in 97% ee which was then converted to **3a**. In addition, (*S*)-**6b** derived from (*S*)-**5b** acts as an intermediate leading to dextrorphan (**3b**), and anticough agent. Thus, the new procedure is general and efficient and allows flexible synthesis of both enantiomers of artificial morphine-based analgesics.

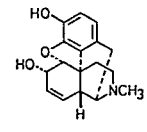

1

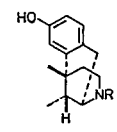

2a, R = CH3
2b, R = CH2CH=C(CH3)2
2c, R = cyclopropylmethyl
2d, R = CH2CH2C6H5

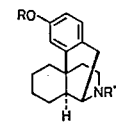

3a, R = R' = CH3
3b, R = H; R' = CH3

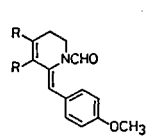

4a, R = CH3
4b, R—R = (CH2)4

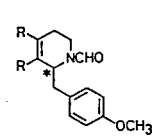

5a, R = CH3
5b, R—R = (CH2)4

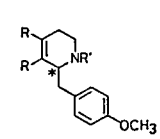

6a, R = CH3; R' = H
6b, R—R = (CH2)4; R' = H

Reference

1) R. Noyori, M. Ohta, Yi Hsiao, M. Kitamura, T. Ohta, and H. Takaya, *J. Am. Chem. Soc.*, **108**, 7117 (1986).

VII-C-6 Kinetic Resolution of 4-Hydroxy-2-cyclopentenone by Rhodium-catalyzed Asymmetric Isomerization

Masato KITAMURA, Kenji MANABE, Ryoji NOYORI *(Nagoya Univ.)*, **and Hidemasa TAKAYA**

[*Tetrahedron Lett.*, **28**, 4719 (1987)]

(*R*)-4-Hydroxy-2-cyclopentenone [(*R*)-**1**] is a key chiral building block in our three-component coupling prostaglandin synthesis. This compound has been obtained by various ways. We describe here a new convenient synthesis of optically pure (*R*)-**1** by the chemical kinetic resolution of (±)-**1** based on a new transition metal-catalyzed asymmetric 1,3-hydrogen migration. When racemic **1** was exposed to the (*R*)-BINAP-Rh^+ complex, (*R*)-**4**[1,2] the *S* enantiomer was converted more readily to the diketone **3** via **2**. The asymmetric isomerization in THF at 0°C afforded k_{fast}/k_{slow} = 5:1 discrimination, providing a convenient method for resolution of readily accessible (±)-**1** to give the important *R* enantiomer. The reaction with 0.5 mol% of (*R*)-**4** gave (*R*)-**1** in 91% ee at 72% conversion, and the extremely high crystallinity of **3** allowed easy separation of (*R*)-**1** from the reaction mixture. The enantiomerically pure enone was obtained by conversion to the crystalline *O*-silyl derivative, (*R*)-**5**.

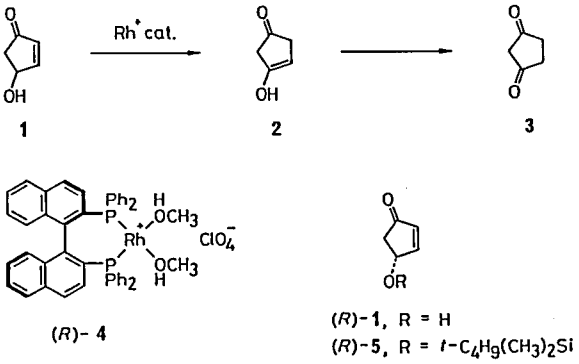

Reference

1) A. Miyashita, H. Takaya, T. Souchi, and R. Noyori, *Tetrahedron*, **40**, 1245 (1984).
2) H. Takaya, K. Mashima, K. Koyano, M. Yagi, H. Kumobayashi, T. Taketomi, S. Akutagawa, and R. Noyori, *J. Org. Chem.*, **51**, 629 (1986).

Instrumental Center

VII–D Excitation-Energy Transport in Organized Molecular Assemblies

Long-distance excitation energy transfer (Förster type) has been studied with interfacial surfaces, monomolecular layer and multilayers such as Langmuir-Blodgett films and semiconductor surfaces. Kinetics of the energy transfer under restricted geometries of molecular organization, i.e., two-dimensional and stacking multilayers (Figure 1), is investigated by means of a picosecond time-resolved fluorescence spectrophotometer.[1] The focus has been directed to (1) fundamentals of kinetics for the sequential energy migration and collection in multilayered architectures and (2) development of new molecular devices capable of spatially controlling and switching of photonic-energy transport.

Reference
1) I. Yamazaki, N. Tamai, H. Kume, H. Tsuchiya and K. Oba, *Rev. Sci. Instrum.*, **56**, 1187 (1985).

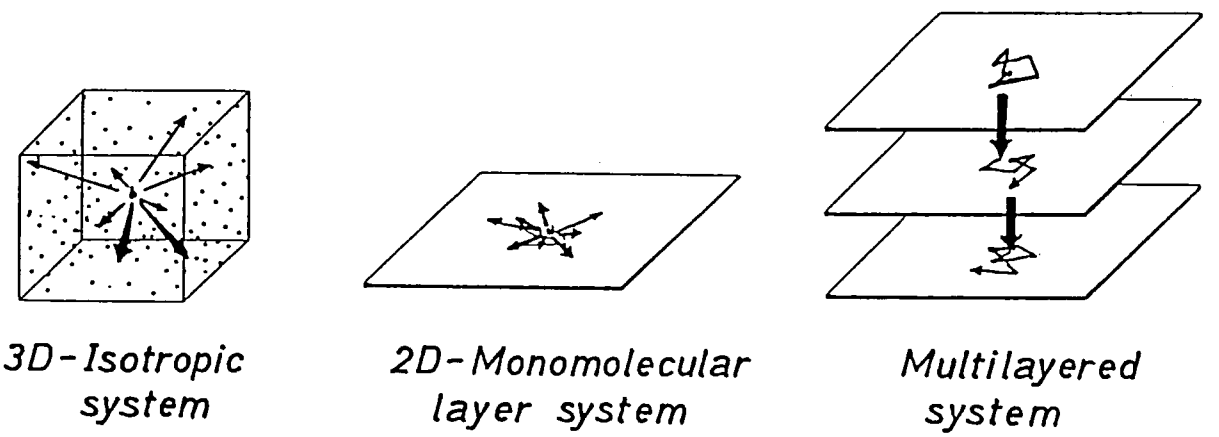

Figure 1. Schematic illustration of the molecular system where the Förster-type long range excitation transfer takes places; (a) 3D isotropic system in which acceptor molecules are distributed randomly and uniformly; (b) 2D monomolecular layer system of LB monolayer film; (c) Stacking monomolecuar layers in which the excitation is transferred from the outer surface to the inner layer.

VII-D-1 A Comparative Study on Ultrafast Photonic Energy Transport in Biological Antenna and Artificial LB Multilayer Films

Iwao YAMAZAKI, Naoto TAMAI, and Tomoko YAMAZAKI

Ultrafast photonic energy transport has been studied with a biological antenna and an artificial Langmuir-Blodgett (LB) multilayer, by means of a picosecond time-resolved fluorescence spectroscopy. In the phycobilin-chlorophyll system of red and blue-green algae, fluorescence bands were observed successively from various pigments, in the order of PE-PC-APC-Chl *a*. The spectral change occurs in the time range of 0-400 ps. Overall time behaviors are compared with an artificial analogue of the LB multilayer films containing different types of cyanine dyes as energy donor and acceptor. Similarly rapid excitation energy transport can be seen. In both two cases, the sequential behavior in the fluorescence is characterized by rapid rise in the acceptor but much slower decay in the donor. Such a sequential energy transport can be fitted to the equation of $\exp(-2kt^{1/2})$ type rather than $\exp(-3kt^{1/3})$ type.

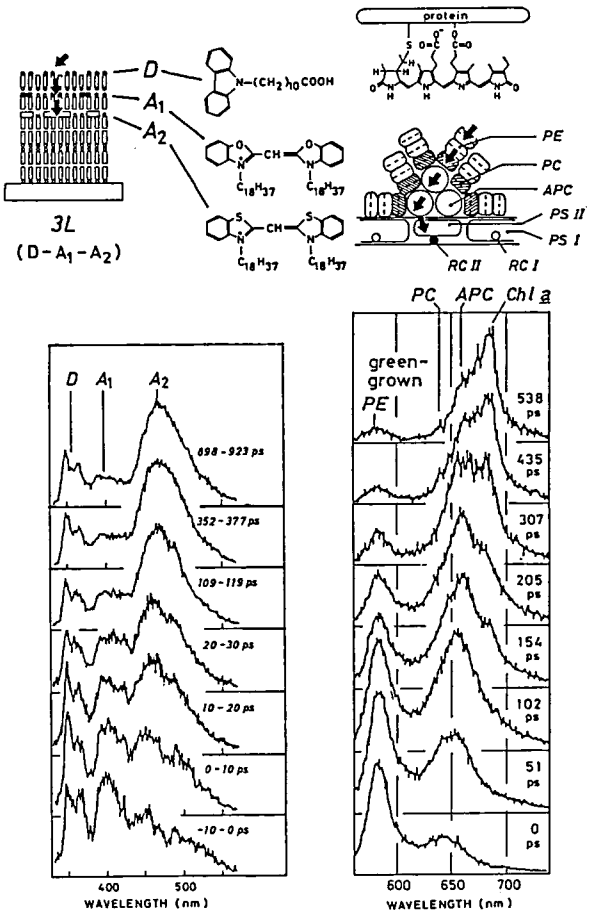

Figure 1. Time-resolved fluorescence spectra of the LB multilayer film and the biological photosynthetic antenna (a blue-green algae, F. diplosiphon). The structures of the LB film and the biological antenna are shown above.

VII-D-2 Interlayer Excitation-Energy Transfer in Stacking Langmuir-Blodgett Multilayer Films

Naoto TAMAI, Tomoko YAMAZAKI, and Iwao YAMAZAKI

The Förster type excitation energy transfer between stacking LB multilayers has been studied with a picosecond time-resolved fluorescence spectrophotometer. LB films consisting of energy donor (D) and acceptor (A_1 and A_2) were deposited on quartz plates with different numbers of acceptor layers. As the number of acceptor layers increase, effeciency of energy transfer from D layer increases from 56 % in D-A_1 to 73 % in D-4A_1. Figure 1 shows fluorescence dacay curves of D with different numbers of A_1 layers. Fluorescence decay curves can be analyzed by the equation

$$\varrho(t) = \exp[-t/\tau_D - \gamma(t/\tau_D)^{\beta}]$$

In D-4A_1 system, apparent fractal dimension was obtained to be 2.34 and 2.0 in D-A_1 system. On going from D-A_1 to D-4A_1 systems, distribution of acceptors will be changed from two-dimensional to three-dimensional nature. In the case of D-A_1 -A_2 multilayers, the energy transfer D-A_1 is enhanced in transfer rate and in transfer efficiency.

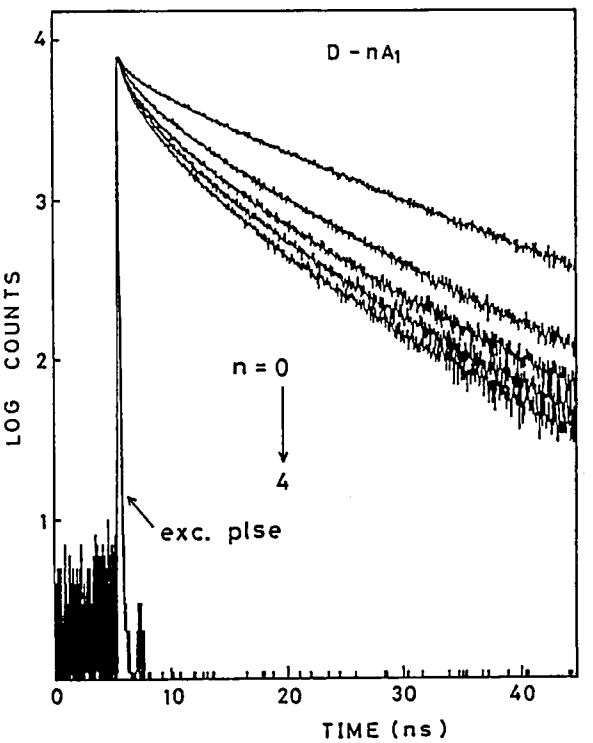

Figure 1. Fluorescence decay curves of donor in carbazole-oxacyanine LB multilayer films as a function of number of acceptor layers.

VII-D-3 Excitation Energy Migration in Langmuir-Blodgett Monomolecular Layer

Naoto TAMAI, Tomoko YAMAZAKI, Hirosi MATSUO *(Yamaguci W. Univ.)*, **and Iwao YAMAZAKI**

Picosecond time-resolved fluorescence spectra and their decay curves have been measured for dye chromophores in Langmuir-Blodgett (LB) monomolecular film with different concentrations of chromophore;

rhodamine B. Figure 1 shows time-resolved fluorescence spectra. In the short time region (0-100 ps), the peak position of fluorescence band is 573 nm, but it red-shifts gradually with time: 580 nm after 10 ns. Similar spectral shift was observed for higher concentrations. In higher concentrations, another fluorescence band can be seen at longer wavelength in short time region which might be recognized as originating from aggregated species. These results show that energy levels of electronically excited state of rhodamine B at different sites are broadened inhomogeneously in a LB monolayer. Migration of the excitation energy within a LB monolayer from site to site causes time-dependent spectral shift. Fluorescence decay curves for various concentrations can be analyzed in terms of an equation of two-dimensional excitation energy migration and trapping.[1)]

Reference

1) N. Tamai, T. Yamazaki and I. Yamazaki, *J. Phys. Chem.*, **91**, 841 (1987).

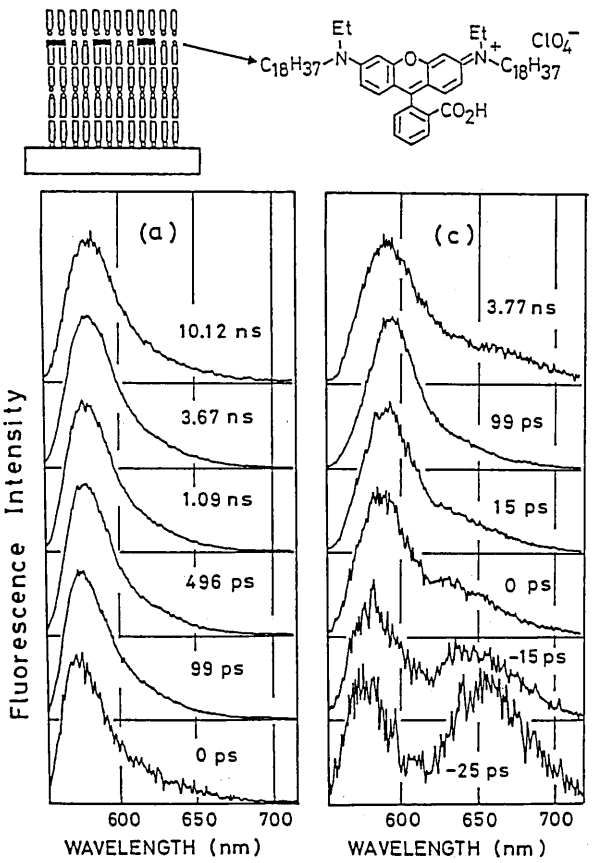

Figure 1. Time-resolved fluorescence spectra for LB monolayers of N, N′ -dioctadecylrhodamine B. Concentrations are 1.02 (a) and 34.1 mol% (b), Delay times after exciting pulse are indicated in the figure.

VII-D-4 Excited State Interactions of Dyes Adsorbed on Semiconductor Surfaces

Silvia M.B. COSTA *(Instituto Superior Tecnico, Portugal and IMS)*, **Naoto TAMAI, Tomoko YAMAZAKI and Iwao YAMAZAKI**

Semiconductor electrodes modified by incorporation of dyes at the surface exhibit photocurrents with quantum yields lower than 10^{-2}. Fluorescence measurements have shown that photophysical processes such as energy transfer occurring between the photoexcited dye and the semiconductor can be highly competitive.[1)] The systems were prepared depositing, by evaporation or vacuum deposition (10^{-5} Torr) with controlled thickness, several dyes:tetraphenylporphyrin (TPP), zinc tetraphenylporphyrin (ZnTPP), tetramethylpyridil-porphyrin iodide ($TMePyP^{4+}$) and rhodamine B on glasses covered by tin oxide (SnO_2) or indium oxide/tin oxide (ITO). The fluorescence decays could be analyzed with two or three exponentials (Fig. 1) and in samples of dyes deposited on ITO and SnO_2 a much shorter component is observed, which is attributed to electron transfer from the excited dye to the n-type semiconductor. As a first approximation, if the order of rate constant is measured from the shorter component it is found that $k^{SnO_2} > k^{ITO}$ as would be anticipated. The formation of aggregates is also found and confirmed by time-resolved emission spectra with large spectral changes at longer times. The results will be discussed in terms of different trapping sites and electron injection into the semiconductors.

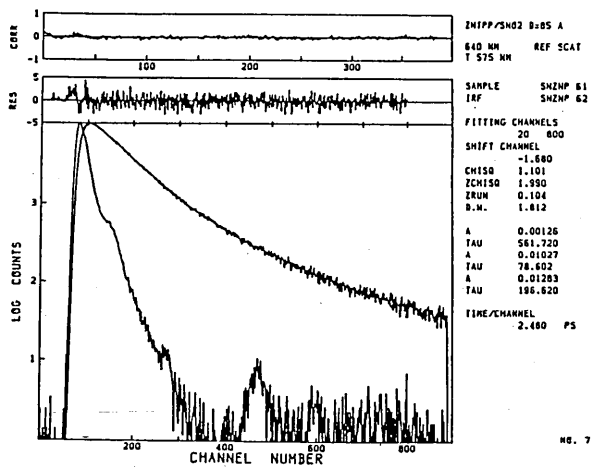

Figure 1. Representative examples of fluorescence decay curve and its analysis for ZnTPP deposited (d = 85 Å) on a quartz substrate covered with SnO_2.

Reference
1) S. M. B. Costa, M. I. C. Ferreira, R. I. P. C. Pereira and T. M. S. Ribeiro, *Abstract of XI IUPAC Symposium on Photochemistry, Lisbon* (1986) p. 479.

VII–E Picosecond Time-Resolved Fluorescence Spectroscopy on Photophysical Processes in Organized Molecular Assemblies

In ordered molecular assemblies such as polymers and Langmuir-Blodgett films, one can expect to observe new aspects of photochemical and photophysical processes because one-dimensional polymers or uniform thin layers with the two-dimensional order might show configurational and dynamical behaviors quite different from those of homogeneous solution. In this research project, excimer formation and photochemical reaction in the highly anisotropic media are investigated by means of a picosecond time-resolved fluorescence spectroscopy.

VII-E-1 Time-Resolved Fluorescence Studies on Langmuir-Blodgett Films with UVSOR

Naoto TAMAI, Takaya YAMANAKA, Tomoko YAMAZAKI, Tadaoki MITANI and Iwao YAMAZAKI

A VUV pulsed light from UVSOR, the synchrotron orbital facility in IMS, was applied to Langmuir-Blodgett films and polystyrene films containing benzene chromophore, 15-phenylpentadecanoic acid (PPA). Irradiating LB films with VUV light ranging from 170 to 220 nm from a Seya-Namioka monochromator,[1] we measured time-resolved fluorescence spectra by means of a time-correlated, single-photon counting system. The LB film shows only a monomer-like fluorescence with a peak at 283 nm, while the polystyrene film shows an excimer fluorescence with a peak at 325 nm. The fluorescence decay curve of LB film is approximately single-exponential, with a lifetime of 26 ns which is close to the value of PPA in n-hexane. Figure 1 shows the excitation-energy dependence of fluorescence quantum yield (Φ_F). We can see a behavior similar to the third-channel relaxation characteristics: As the excitation energy is increased, Φ_F value is decreased sharply at 240 nm in polystyrene and 200 nm in LB film. The Φ_F value is recovered in higher energy region, indicating that the S_1 state or the excimer state is produced through a benzene CT state in high energy excitation.[2]

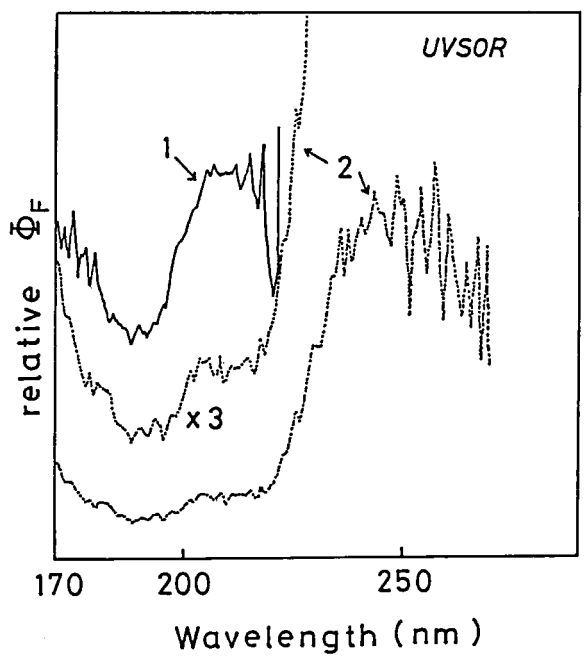

Figure 1. Plots of the fluorescence quantum yields of LB film of PPA (1) and polystyrene film (2) against excitation wavelength.

Reference
1) T. Yamanaka, M. Suzui, T. Horigome, T. Mitani and I. Yamazaki, *Ann. Rev. IMS*, **138** (1985).
2) F. P. Schwarz and M. Mautoner, *Chem. Phys. Lett.*, **85**, 239 (1982).

VII-E-2 Photochromic Reaction by Tautomerism in Langmuir-Blodgett Films

Takahide MINAMI *(Kao Co. and IMS)*, **Naoto TAMAI, Takaya YAMANAKA, Tomoko YAMAZAKI and Iwao YAMAZAKI**

Primary process of the photochromic reaction by tautomerism has been studied with 1-octadecyl-3,3-

dimethyl-6-nitrospiro[2H-1-benzopyran-2,2-indoline] (SSP) in Langmuir-Blodgett films which were prepared in a mixed film with stearic acid, arachidic acid and tripalmitine. It is known that SSP is changed to merocyanine-type compound (SMC) by UV-light irradiation, and SMC is converted to SSP by visible light irradiation or heating. When SSP in LB films were excited at 360 nm UV light, two fluorescence bands were observed; one has a maximum at 660 nm, and the other has a very weak maximum at 530 nm. We assigned them to the fluorescence band of SMC and its precursor, so-called X, respectively. Figure 1 shows the fluorescence decay curves of SSP LB films. It is suggested that the rigidity surrounding SSP molecules is an important factor to determine the rate of photoconversion from SMC to SSP.

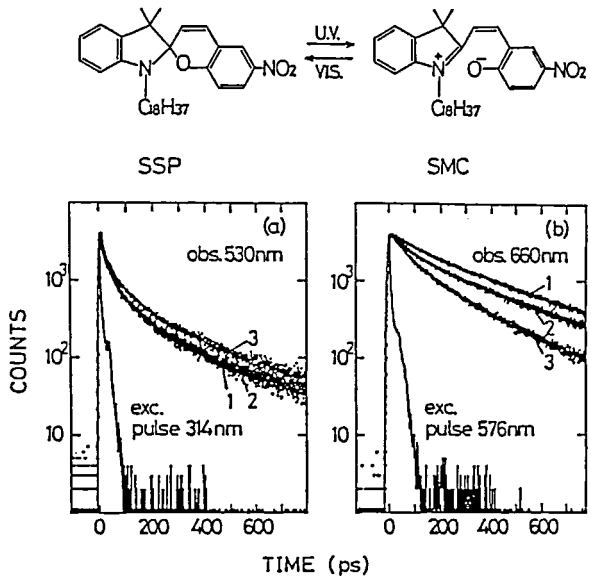

Figure 1. Fluorescence decay curves of SSP in LB films mixed with stearic acid (1), arachidic acid (2) and tripalmitine (3). Wavelength of excited laser pulse (λ_{exc}) and observed fluorescence (λ_{em}) are 314 nm and 530 nm, respectively. (b) λ_{exc} is 576 nm and λ_{em} is 660 nm.

VII-E-3 Molecular Association of pyrene in Langmuir-Blodgett Films

Katsuhiro SUMI, Naoto TAMAI, Tomoko YAMAZAKI and Iwao YAMAZAKI

Molecular association of chromophoric pyrene has been studied with the Langmuir-Blodgett (LB) films. It was found in our previous study[1] that pyrene chromophores in LB films form two types of excimers; one is a sandwich-type, two-center excimer (E_2) which form through a weakly-coupled dimer, and the other is a one-center type (E_1) which appears in the initial time region after pulsed excitation.[2] The present study is concerned with the fluorescence quantum yields (Φ_F) of excimers in LB films consisting of Py16 and fatty acids having different length of alkyl chains. Figure 1 shows plots of the ratio of Φ_F of excimer to monomer fluorescence as a function of PHA concentration. The relative position of pyrene chromophore to the fatty acid is also shown schematically in the figure. In Py16-Pal and Py16-Ara, Φ_F of excimer is significantly higher in four layer than in two layers. In Py12-Ara, Φ_F of excimer is comparable between four and two layers, indicating that an interlayer interaction acts through adjacent layers. On the other hand, in 4Py6-Ara where the interlayer interaction is impossible, Φ_F is significantly decreased.

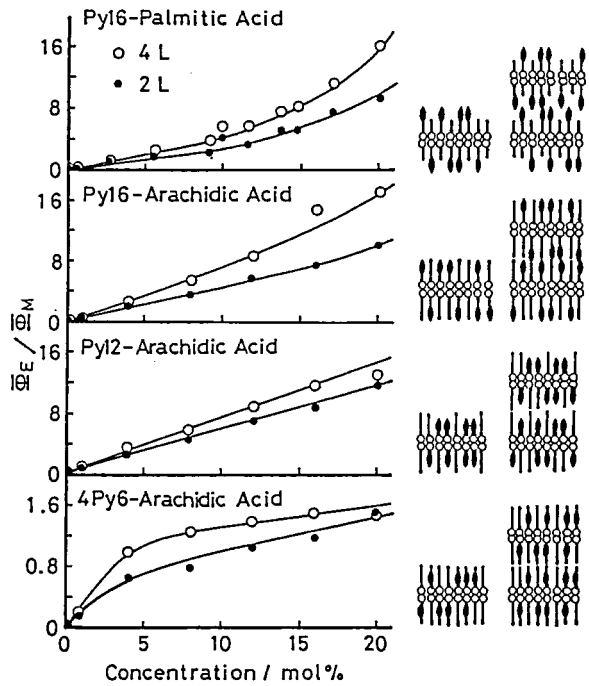

Figure 1. Plots of the fluorescence quantum yield ratio of excimer to monomer upon the concentration of pyrene compounds. Py16, Py12 and 4Py6 represent pyrenehexadecanoic acid, pyrenedodecanoic acid and butylpyrenehexanoic acid, respectively. The relative position of pyrene ring to the fatty acid is shown schematically in the right side.

Reference

1) T. Yamazaki, N. Tamai and I. Yamazaki, *Chem. Phys. Lett.*, **124**, 326 (1986).

2) I. Yamazaki, N. Tamai and T. Yamazaki, *J. Phys. Chem.*, **91**, 3572 (1987).

VII-E-4 Free-, Quasi-Free and Self-Trapped Exciton Luminescence in Anthracene Crystal

Atsuo MATSUI, Ken-ichi MIZUNO *(Konan Univ.)*, **Michihiro KOBAYASI** *(Osaka Univ.)*, **Naoto TAMAI, Tomoko YAMAZAKI and Iwao YAMAZAKI**

When free excitons are introduced into a crystal in which the exciton-phonon coupling is strong, they relax to the self-trapped-exciton state by thermally activated surmounting over or tunneling through the adiabatic potential-energy barrier, the so-called ST barrier existing between the free- and self-trapped-exciton luminescence associated with radiative annihilation of self-trapped excitons. In addition to self-trapped-exciton liminescence one often observes luminescence due to radiative annihilation of free excitons.[1] In the present study, ordinary liminescence (277-4.6 K), time-resolved luminescence (300 and 87 K), absorption and luminescence spectra under pressure (0–40 GPa at 1.5 K) have been measured. At higher temperatures, quasi-free and self-trapped excitons coexist, while at reduced temperature below about 6 K only free excitons exist. Applying pressure at 1.5 K coexistence of free- and self-trapped excitons is achieved. The exciton-phonon coupling constant $g < 1$ at ambient pressure increases to $g > 1$ with pressure.

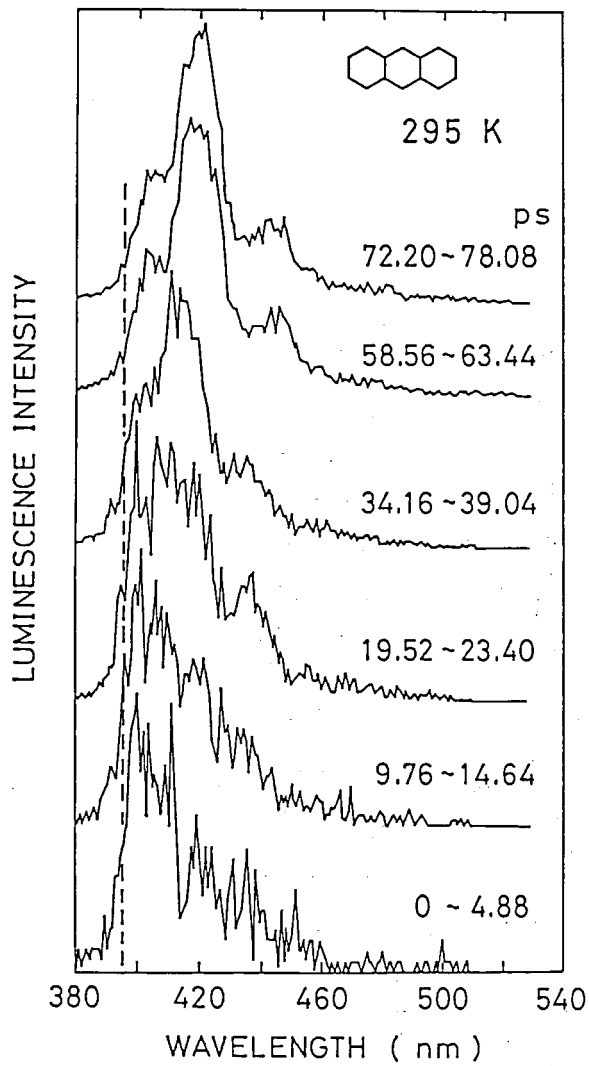

Figure 1. Time-resolved luminescence spectra of anthracene crystal at room temperature. Excitation wavelength is 365 nm. Each spectrum is corrected for the instrumental sensitivity and normalized at the maximum intensity.

Reference

1) A. Matsui, K. Mizuno, N. Tamai and I. Yamazaki, *Chem. Phys.*, **113**, 111 (1987).

VII-E-5 Excimer Formation in Pyrene Labeled Hydroxypropyl Cellulose in Water

Francoise M. WINNIK *(Xerox Res. Center of Canada)*, **Mitchell A. WINNIK** *(Univ. Toronto)*, **Shigeo TAZUKE** *(Tokyo Inst. Tech.)* **and Iwao YAMAZAKI**

Excimer formation of pyrene chromophores in an aqueous solution of hydroxypropyl cellulose has been studied with a picosecond time-resolved fluorescence spectrophotometer. The time-resolved spectra show two types of broad structureless fluorescence bands at (1) 420 nm in a short time region (0–7 ns) and (2) 470 nm in the time region after 50 ns. The latter is the well-known sandwich-type pyrene excimer, and the other is assumed to be a one-center-type excimer similar to those observed in several other molecular assemblies such as LB films,[1] vapor-deposited films,[2,3] and single crystals.[4] This is the first report on the detection of such excimers in a dilute polymer solution.

Reference

1) T. Yamazaki, N. Tamai and I. Yamazaki, *Chem. Phys. Lett.*, **124**, 326 (1986); I. Yamazaki, N. Tamai and T. Yamazaki, *J. Phys. Chem.*, **91**, 3572 (1987).
2) M. Mitsuya, Y. Taniguchi, N. Tamai, I. Yamazaki and H. Masuhara, *Thin Solid Films*, **129**, L45 (1985).

3) A. Itaya, T. Kawamura, H. Masuhara, Y. Taniguchi, M. Mitsuya, H. Uraki, K. Kano and S. Hashimoto, *Chem. Lett.*, 1541 (1986).

4) A. Matsui, K. Mizuno and H. Nishimura, *J. Phys. Soc. Jpn.*, **53**, 2818 (1984).

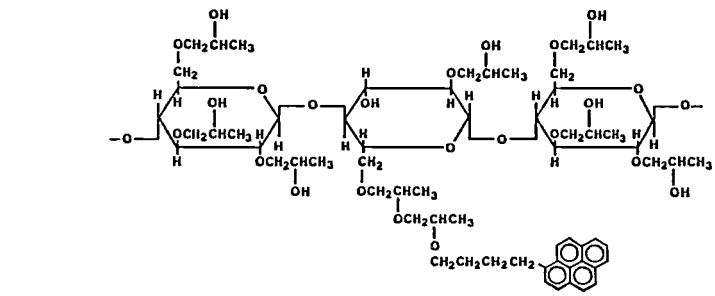

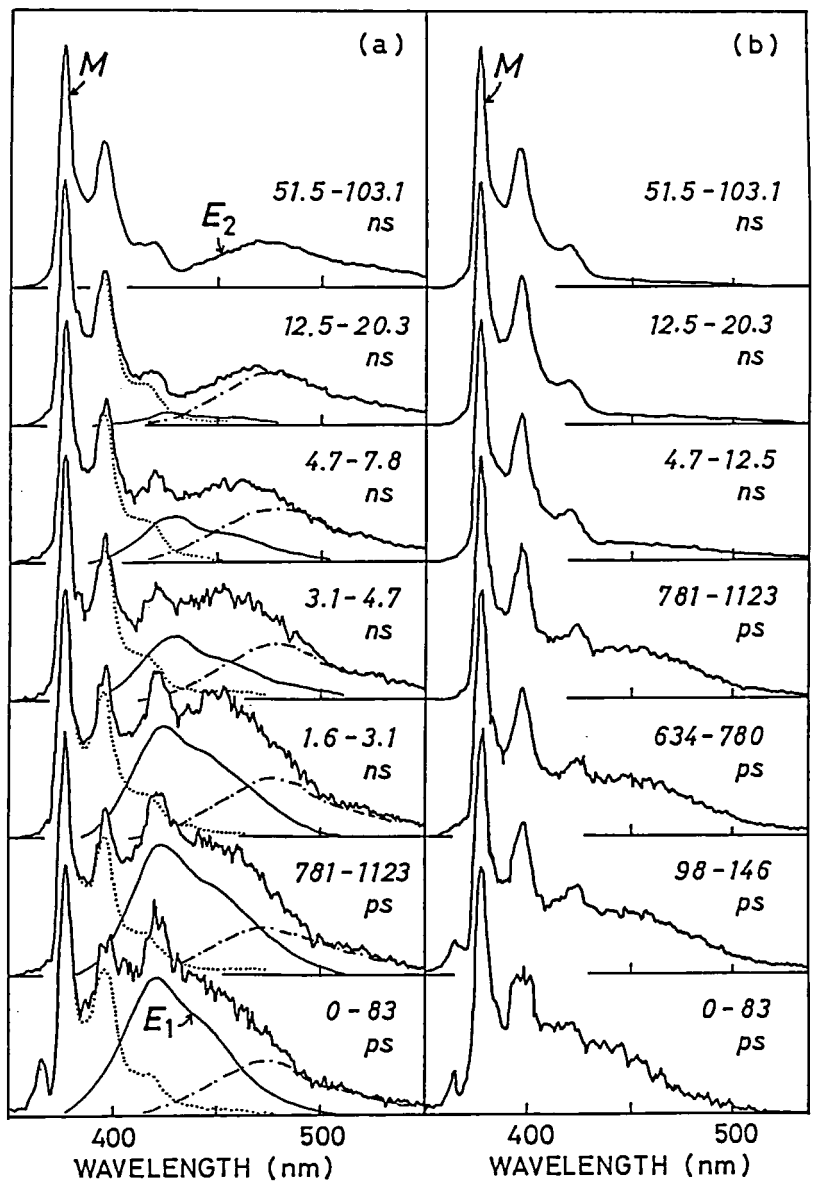

Figure 1. Time-resolved fluorescence spectra of pyrene-labeled hydroxypropyl cellulose, HPC-Py/56 (a) and HPC-Py/438 (b), in water. The excitation wavelength is 324 nm. The time zero corresponds to the time in which the excitation laser pulse reaches maximum intensity. The spectrum analysis into component was made by assuming three components, one monomer M and two excimers E_1 and E_2.

VII–F Photonic Energy Transport and Primary Reaction in Biological Photoreceptors

Primary processes in biological photoreceptors such as photosynthetic pigments and phytochrome are characterized by highly efficient absorption and subsequent transfer of photo-excitation energy to the reaction centers. These ultrafast processes of the energy transport and the primary photochemical reaction have studied on the basis of picosecond time-resolved fluorescence spectroscopy.

VII-F-1 Comparative Study of Photoconversion of Phytochrome Isolated from Oats and Peas

Pill-SOON SONG *(Texas Tech Univ.)*, **Satoru TOKUTOMI** *(NIBB)*, **Masaki FURUYA** *(NIBB)*, **Naoto TAMAI and Iwao YAMAZAKI**

To characterize the nature of primary photoprocesses of phytochrome which serves as the red-far red reversible photoreceptor for photomorphogenesis in plants, the fluorescence lifetimes and time-resolved spectra (Figure 1) of phytochrome have been investigated. The photoconversion kinetics of two kinds of phytochromes isolated from oat (Avena sativa L.) and pea are compared. The fluorescence decay of both phytochromes from oat and pea exhibited approximately two components; one with lifetimes in the range of 50–70 ps and the other with 1.1–1.2 ns in phosphate buffer with or without 40–67 % glycerol. However, relative amplitudes of these decay components were found to be strongly viscosity dependent. These results have been interpreted in terms of primary reaction from the excited singlet state of phytochrome, yielding a photoreversible intermediate whose rates of formation and decay were apparently viscosity-dependent. Further, the viscosity dependence is consistent with the Song's model for the conformational changes of the chromophore and its apoprotein environment. Oat and pea phytochromes exhibit difference in the reaction kinetics; the pea phytochrome undergoes the photoconversion acompanying conformational change of appoprotein environment larger than the oat phytochrome.

References

1) P. S. Song, N. Tamai and I. Yamazaki, *Biophys. J.*, **49**, 645 (1986).

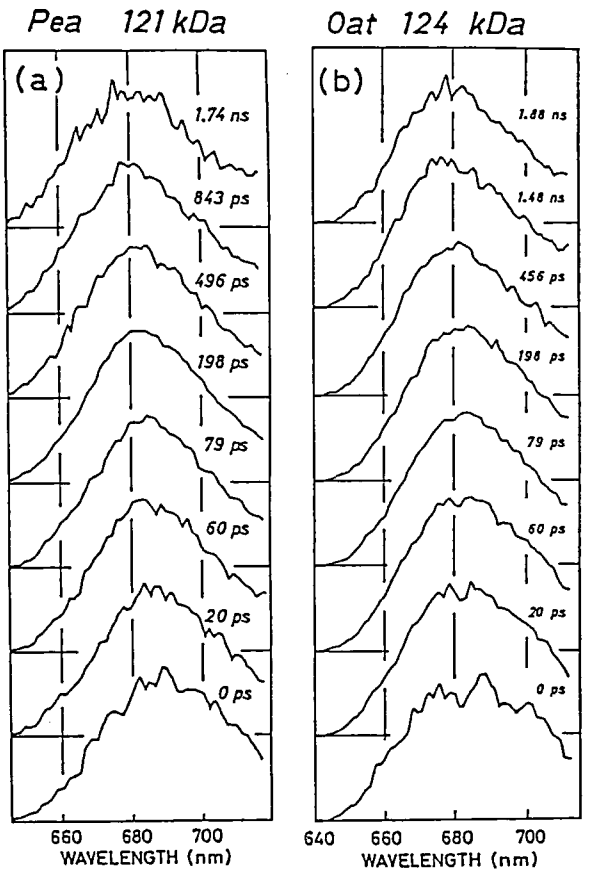

Figure 1. Time-resolved fluorescence spectra of phytochromes of (a) 121 kDa from pea and (b) 124 kDa from oat (Avena sativa L.), in 64–67 % glycerol. The excitation wavelength is 637 nm.

VII-F-2 Picosecond Time-Resolved Fluorescence Spectroscopy on Sequential Energy Transport in Phycobilin Antenna Systems

Yoshihiko FUJITA, Akio MURAKAMI, Mamoru MIMURO *(NIBB)*, **Naoto TAMAI, Tomoko YAMAZAKI and Iwao YAMAZAKI**

Photosynthetic light haversting antenna system in

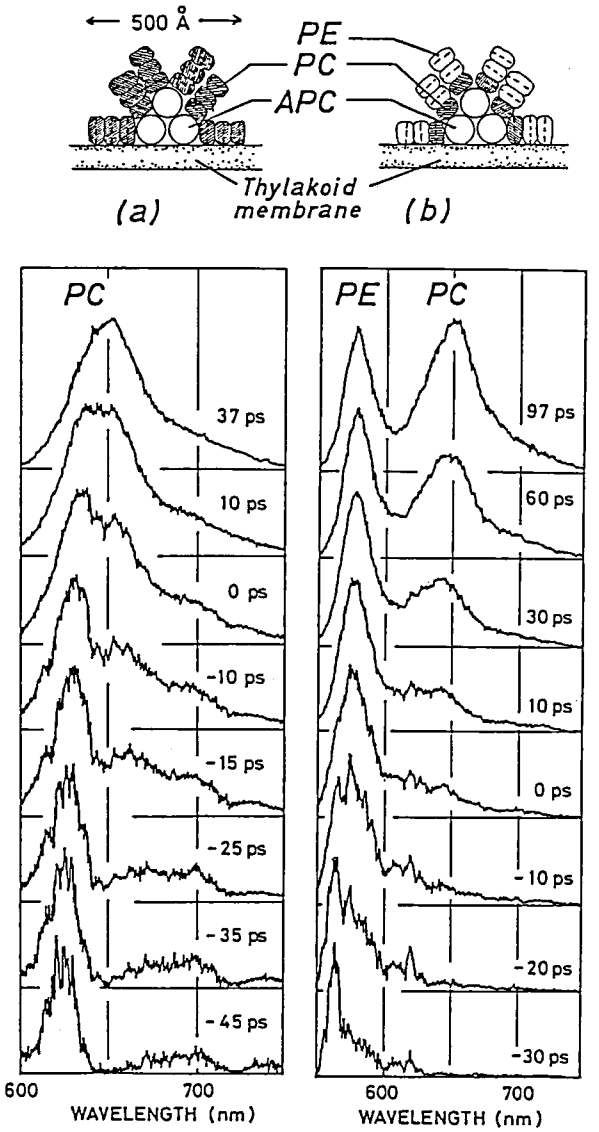

Figure 1. Time-resolved fluorescence spectra of Synecocystis sp.; (a) PE-less cells and (b) PE-rich cells. Schematic illustration of stacking pigment proteins for respective types are shown above. Each spectrum is normalized at its peak intensity.

algae consists of several kinds of phycobiliporteins and chlorophyll. In our previous study,[1,2] it was found that excitation energy absorbed at outer surface of the phycobilisome is transferred to the reaction center sequentially through several phycobiliproteins. The present study is directed toward observing excitation energy transport within a phycobiliprotein trimer or tetramer by means of a picosecond time-resolved fluorescence spectrophotometer which was recently improved in time resolution (FWHM of an instrumental response function is 19 ps) by the use of a microchannel-plate photomultiplier of 6-micron channels. Figure 1 shows the time-resolved fluorescence spectra of blue-green algae, Synecocistis sp. (PCC 6714), PC-cells and PE-cells. It can been seen that in the short time region (−30–0 ps) the fluorescence bands is shifted from 560 nm to 575 nm in PE-cells and from 625 nm to 635 nm in PC-cells. This means that the excitation migrates within a phycobiliprotein trimer, i.e., phycoerythrin in PE-cells and phycocyanin in PC-cells.

Reference

1) I. Yamazaki, M. Mimuro, T. Murao, T. Yamazaki, K. Yoshihara and Y. Fujita, *Photochem. Photobiol.*, **39**, 233 (1984).
2) M. Mimuro, I. Yamazaki, T. Yamazaki and Y. Fujita, *Photochem. Photobiol.*, **41**, 597 (1985).

VII–G Investigations of CT Complexes in Reticulate Doped Polymers by XPS Spectroscopy

J. K. JESZKA *(Polish Academy of Sciences and IMS)*, **Keisaku KIMURA, A. TRACZ** *(Polish Academy of Sciences)*, **Hiroo INOKUCHI, and M. KRYSZEWSKI** *(Polish Academy of Sciences)*

[*Material Science*, **VIII**, 103 (1987)]

Charge transfer complexes in reticulate doped surface conductive and bulk conductive polymers were investigated by XPS method. It was found that in the case of the surface conductive system polycarbonate+TTF-TCNQ the concentration of the CT complex in the surface layer is enhanced as compared with the average concentration and its XPS spectrum is similar to that reported for crystalline TTF-TCNQ. In bulk conductive films the CT complex concentration was found to be different on the upper and lower surface of the film and the ratio of neutral to charged TCNQ was different in the films with different morphology of the conductive network.

VII–H Study of Metal Fine Particles Prepared by Gas Evaporation Technique

The physical properties of fine particles, the sizes of which are less than ten nm, are affected by the quantum size effect, by the surface effect and by a fluctuation of a thermodynamical properties due to low dimensionality. These effects were studied as functions of metal species, organic liquids and preparation techniques.

VII-H-1 Quantum Size Effect observed in Ultrafine Magnesium Particles

Keisaku KIMURA and Shunji BANDOW

[*Phys. Rev. B*, in press]

The static magnetic susceptibilities of ultrafine Mg particles were measured as a function of particle diameter in the temperature range from 2 to 240 K. The temperature-independent paramagnetism enhancement was observed and found to be inversely proportional to the cube of particle size, revealing for the first time a direct evidence for the zero-dimensional magnetism in small metal particle. The importance of the electronic state of corner atoms of a particle is suggested for this zero-dimensionality. It was also suggested that this enhanced paramagnetism exhibits a phase transition at 150 K.

The marked decrease in magnetic susceptibility at low temperature with the onset of moderate increase in intermediate temperature has been analyzed in terms of the quantum size effect. We first clarify experimentally the energy-level statistics of small metals by the combination of Poisson and orthogonal distributions. The effect of surface irregularity is discussed with the aid of Tanaka's formulas, which indicates that the surface of small particles are not rough. This is inconsistent with commonly accepted assumptions.

Reference

1) S. Tanaka and S. Sugano, *Phys. Rev.*, **B34**, 740 (1986).

VII-H-2 Conduction Electron Spin Resonance of Magnesium Ultrafine Particles: Surface Irregularity

Shunji BANDOW and Keisaku KIMURA

The surface irregularity of metallic ultrafine particle (UFP) was hitherto believed very large. Hence the energy level statistics of UFPs were considered to follow the random matrices theory (RMT). According to RMT, a sharp ESR signal (line width is several gausses) must be observed when the average diameter of UFPs become smaller thatn ca. 10 nm. In the present experiments, however, we could not detect such sharp ESR spectrum originating from the conduction electrons (see Fig. 1 A, B). This finding is probably against the assumption that the surface of UFP is very irregular. When the surface of UFPs is smooth, the energy level statistics follows the Brody distribution rather than the function expected from RMT according to Tanaka's theory.[1] In other words, the correlation between states of different spins is lost in the case of UPF with small surface irregularity. Taking account of Tanaka's theory, the ESR line becomes broader with smaller the surface irregularity, because the phase memory time becomes short as disappearing the correlation between states. When the surface becomes more regular, finally an ESR spectrum can not be

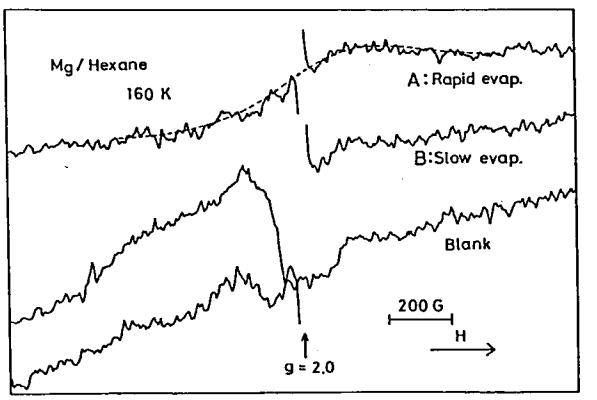

Figure 1. ESR spectra of Mg ultrafine particles. The sharp ESR signal at $g = 2.0$ is an exogeneous signal due to O^-_2 ion. The surface of particles is considered to be smooth for a slowly evaporated sample than for a rapidly evaporated one. Only in a rapidly evaporated sample, a very braod ESR spectrum with line width ca. 1200 G was detected. This spectrum is probably due to the conduction electrons.

detected because of the reduction of susceptibility. The findings of the present experiments are therefore consistent with the assumption on the regularity of the surface of UFPs. The surface of the UFP is therefore not rough enough. It seems more smooth.

Reference
1) S. Tanaka and S. Sugano, *Phys. Rev,*, **B34**, 740 (1986).

VII-H-3 Measurement of the Spin Relaxation Time of Zinc Ultrafine Particles using the Spin Probe Method

Shunji BANDOW and Keisaku KIMURA

It is difficult to detect CESR (conduction electron spin resonsnce) in many metallic ultrafine particles (UFPs), because of the inadequacy of resonance conditions due to the shape of the Fermi surface and the surface irregularity of UFPs. However we found that it is possible to obtain the information on the conduction electrons through the ESR active spins locating on the UFP surface that interact with the conduction electrons. Spin probes were prepared as follows: Zn metal in the crucible is evaporated in the He atmosphere with the mixture of N_2 and O_2 (air ratio) using the matrix isolation technique. In this sample, the ESR spectrum is observed near $g = 1.97$. The origin of the ESR is regarded as the Zn^+ ion which is located at the ZnO part of UFP surface. This Zn^+ ion interacts with conduction electrons. The microwave energy absorved by Zn^+ ion flows to conduction electrons and finally to phonon system. The energy flow rate of metallic UFPs were quantitatively measured giving the longitudinal relaxation time T_1 by the use of saturation method. The results, shown in Fig. 1, indicate that all T_1 of different size samples have an exponential temperature dependence below ca. 10 K. These findings are explained by the quantum size effect on the phonon energy dispersion. When the particle size is reduced, a low energy phonon is cut off and the energy transfer from a spin system to phonon system is prevented.

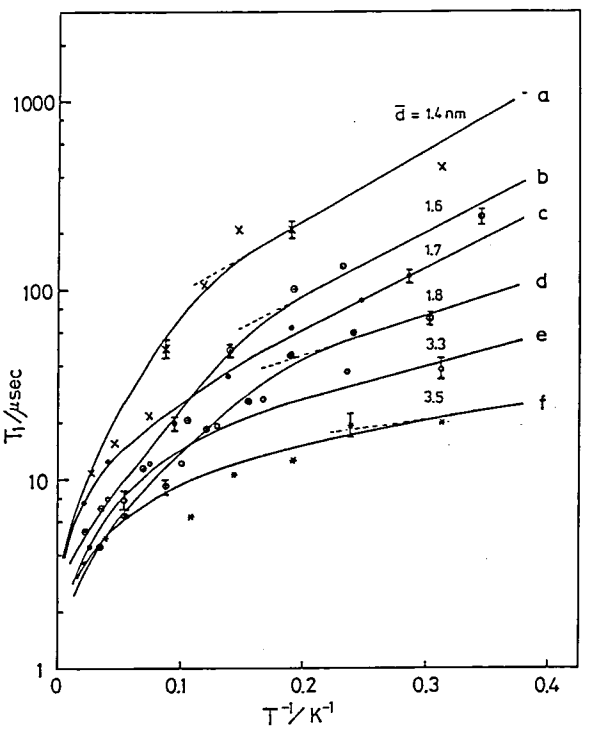

Figure 1. Temperature dependence of the longitudinal relaxation time of ESR of Zn UFPs with different particle sizes. $\bar{d}$ is the diameter at the maximum size distribution.

VII-H-4 Characterization of the Particle Contact between Zinc Ultrafine Particles

Shunji BANDOW and Keisaku KIMURA

Many problems remains unclarified in the physical properties of UFPs, such as the contact between particles, surface irregularity and size distribution of particles. First we focus on the contact problem and examined the state of UFPs using the ESR with changing the degree of particle contact. A sample was prepared by the matrix isolation method. The ESR active spin was produced on the surface of a particle by the reported method (VII-H-3 in this review). Acetone was used for the matrix, because it is easy to control the degree of particle contact. A sample is dispersed (flocculation) soon after the sample preparation in the Zn/Acetone colloidal system. After several hours, however, UFPs precipitate (precipitation) and are considered to contact with each other. ESR spectra in both conditions are shown in Fig. 1. From this figure, we found that the line width of a precipitated sample is more broader than that of flocculated one. This phenomenon is explained as follows: Wave functions locating at each UFP spread over UFPs when UFPs were precipitated. Due to the particle contact, the

energy level spacing δ near the Fermi energy becomes smaller than δ of an isolated UFP. Therefore the energy level mismatch between the Zn^+ level and the quantized conduction electron level becomes small and then the electron jumping rate between these levels becomes large. Hence the line width of a precipitated sample becomes broad according to the lifetime broadening.

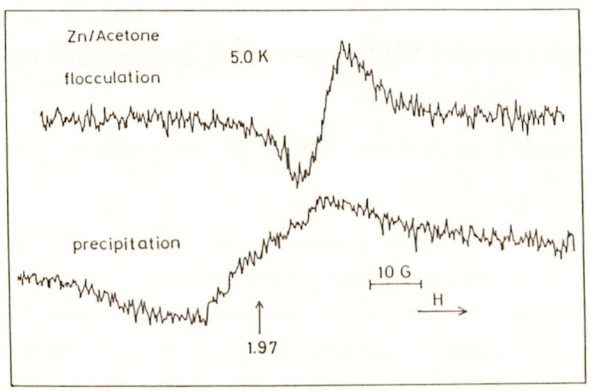

Figure 1. ESR spectra of the colloidal system of Zn/Acetone with different degree of condensation. Flocculation represents that particles are well separated and precipitation represents that particles are considered to contact with each other.

VII-H-5 Formation of Stable Colloid Dispersions of Metal Fine Particles – Detergent Complex in Organic Liquids

Naoki SATOH *(Kao Corporation and IMS)*, **and Keisaku KIMURA**

Stable Colloid dispersions of metal fine particle (MFP) are of great importance not only from the stand point of physical or chemical interests but also from applications of MFP. We report here a versatile method to obtain stable MFP colloid dispersions in organic liquid (even poor dispersibility for MFP[1]) using a small amount of detergent. The gas flow-cold trap method developed by the present author[2] was improved to introduce detergent solutions of organic liquid on frozen matrix of MFP/organic liquid under an Ar gas atmosphere. After the introduction of detergent solution, ultrasonic wave was irradiated to the system until melting of the matrix was completed. We show the TEM pictures of dried a) Au/dioctadecyl dimethylammonium chloride/c-hexane dispersion by the method described above and b) Au/c-hexane dispersion by a conventional method without a detergent or an ultrasonic treatment. The effectiveness of this method is clear from these pictures.

References

1) K. Kimura and S. Bandow, *IMS Ann. Rev.*, **142** (1986)
2) K. Kimura and S. Bandow, *Bull. Chem. Soc. Jpn.*, **56**, 3578 (1983)

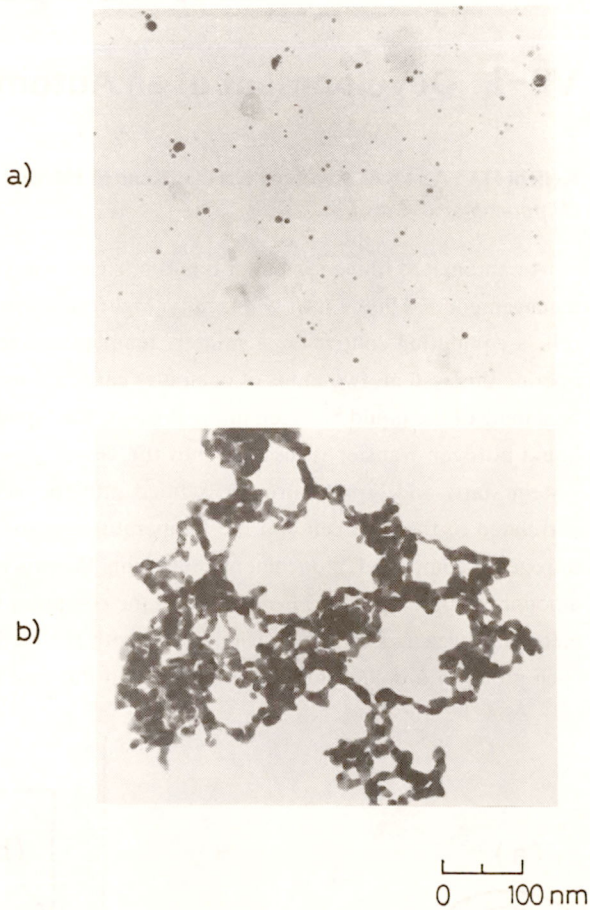

Figure 1. TEM pictures of dried a) Au/DOAC/hexane stable colloid dispersion and b) Au/hexane unstable dispersion

VII-H-6 Zero-dimensionality in a finite system

Keisaku KIMURA

Many physical quantities are normally size independent and expressed as a bulk value. While in small size materials often called clusters or ultrafine particles, some physical quantities deviate from their bulk values and the terminology, size effect, is used to express the cause of the deviation and to imply the contributions of both the surface and volume effects. In small subst-

ances, the edge atom plays an important role in detemining the functions and the properties of the materials. Moreover, in these finite systems, the ratio of the number of atoms at the surface, edge and corner to the volume changes with different size dependence and their effects develop at different stages of size. There are many examples of such size dependent quantites. The concept of "zero-dimensionality" and of "dimensional effect" are presented and applied to many kind of finite systems.

Low-Temperature Center

VII–I Development of an Automated Liquid Nitrogen Filling System

Keiichi HAYASAKA, Kiyonori KATO, Kenichi IMAEDA, Toshiaki ENOKI, Hiroo INOKUCHI, and Yoshinobu ITO
(Nippon Sanso Co. Ltd.)

An automated filling system of liquid nitrogen was developed for saving time, efficient utilization and simplified management of a liquid nitrogen facility. Figure 1 shows the system developed by our group, which consists of a load cell, a computing controller, a printer, temperature sensor, automatic high pressue valves and safety valves. To operate this system, two kinds of computer cards are used for an user and a liquid nitrogen vessel (10-250 1). At the beginning of the liquid nitrogen filling process, the liquid nitrogen vessel is put on the load cell and a flexible tube for liquid nitrogen transfer is inserted into the vessel. Inserting these two cards and pushing a start button make the system start, and liquid nitrogen is filled into the vessel through automatic operation of the valves which are correlated to the load cell and the temperature sensor by the computer system. After the filling process of liquid nitrogen is completed, a document concerning the process (user name, date, time, group name of the user and filled amount of liquid nitrogen) is recorded in the computer system. The user can recognize the end of the process by an electronic buzzer. The system is equipped with the memories for recording the amounts of liquid nitrogen used for each group in a day, a month and a year. In the case of emergency, the system can be operated with a buttery.

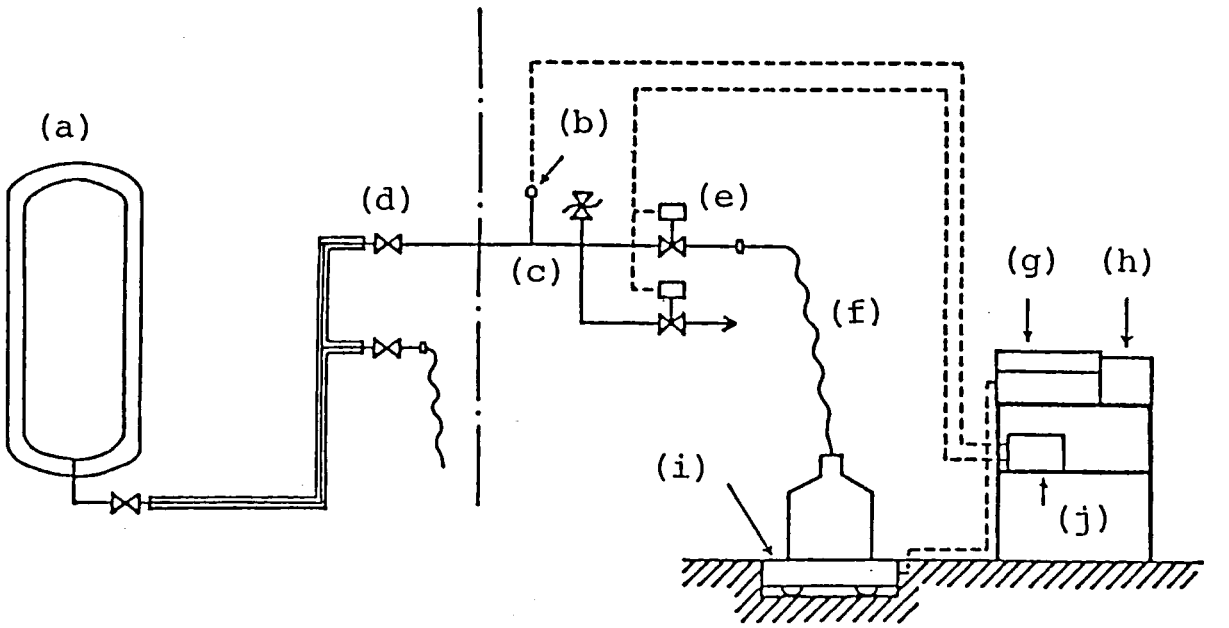

Figure 1. Automated liquid nitrogen filling system: (a) liquid nitrogen container (3000 1), (b) temperature sensor, (c) safty valve, (d) liquid nitrogen vessel (10-250 1), (e) automatic high pressure value, (f) flexible transfer tube, (g) computer, (h) printer, (i) load cell, (j) thermometer.

In our institute, about 70000 l of liquid nitrogen is comsumed by about 100 users in a year. The efficiency of the liquid nitrogen facility has been enhanced by using this automated system.

VII–J Alkali Metal-Hydrogen-Graphite Ternary Intercalation Compounds

Graphite-alkali metal intercalation compounds absorb hydrogen chemisorptively, leading to the occlusion of hydrogen in intercalant layers. The introduction of hydrogen gives effects on the electronic and lattice properties of the compounds due to the strong electron affinity of hydrogen and the occupation of the sites by hydrogen species in the intercalated layers. We investigate the properties of the alkali metal-hydrogen-graphite ternary intercalation compounds by means of electrical resistivity, thermoelectric power, ESR and proton-NMR.

VII-J-1 Novel Electronic Structure of the Hydrogen-Potassium-Graphite Ternary Intercalation Componds

Toshiaki ENOKI, Kenichi IMAEDA, Hiroo INOKUCHI, and Mizuka SANO *(Kumamoto University)*

[*Phys. Rev.*, **B35**, 9399 (1987)]

Thermoelectric power and resistivity experiments give evidence for the coexistence of a large electron and a small hole band in hydrogen-potassium-graphite ternary intercalation compounds consisting of ionic K-H-K sandwich intercalants between metallic graphite sheet. Potassium acts as a donor to graphite, while hydrogen plays the role of an acceptor due to its strong electron affinity. This novel electronic structure, as shown in Fig. 1, is accomplished through the cooperation of potassium and hydrogen in a charge transfer process in addition to delocalization effects associated with conduction electrons.

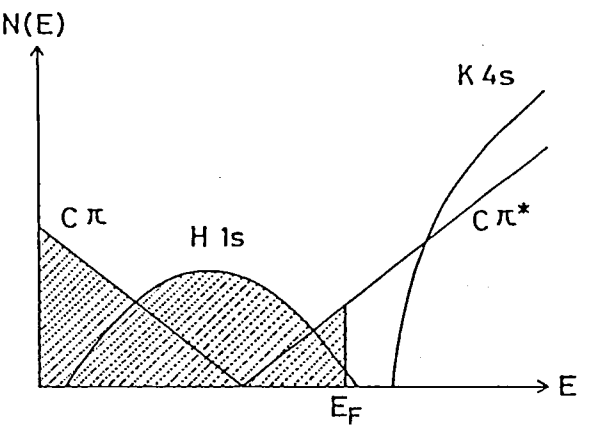

Figure 1. The electronic structure of the KH-GIC's consisting of the graphite π, π*, potassium 4s, and hydrogen 1s bands. For simplicity, position of the K 4s level is shown to shift up well above E_F in this figure, though the level can be slightly degenerate at E_F depending on stage number in the actual case.

Equipment Development Center

VII–K Optical Study of Quasi-1D Charge-Transfer Complexes

VII-K-1 Electric Conductivity and Phase Diagram of a Mixed-stack Charge-transfer Crystal: Tetrathiafulvalene-p-chloranil

Tadaoki MITANI, Yoshio KANEKO*, Seiji TANUMA*, Yoshinori TOKURA*, Takao KODA*, and Gunji SAITO* *(*Univ. of Tokyo)*

[*Phys. Rev.*, **B35**, 427 (1987)]

The electric conductivity has been measured on the mixed-stack charge-transfer crystal tetrathiafulvalene (TTF)-p-chloranil as a function of temperature ($T > 30$ K) and pressure ($P < 11$ kbar). On the basis of the experimental results, a P-T phase diagram is presented for the charge-transfer state in TTF-p-chloranil.

VII-K-2 Optical Reflectivity Spectra of the Mixed-stack Organic Charge-transfer Crystal TTF-p-chloranil under Hydrostatic Pressure

Yoshio KANEKO*, Seiji TANUMA*, Yoshinori TOKURA*, Takao KODA*, Tadaoki MITANI, and Gunji SAITO* *(*Univ. of Tokyo)*

[*Phys. Rev.*, **B35**, 8024 (1987)]

Optical reflectivity spectra have been measured on single crystals of TTF-p-chloranil under hydrostatic pressure up to 11 kbar. From the characteristic behavior under pressure, it is concluded that TTF-p-chloranil crystals undergo a gradual pressure-induced N-I transition in an intermediate region from 0 to 10 kbar, in contrast with a first-order temperature-induced N-I transition. In this pressure range, both quasi-neutral and quasi-ionic molecular domains coexist in the lattice, until a discontinuous transition to a dimerized ionic phase occurs at about 11 kbar.

VII-K-3 Photoconductivity and Photo-induced ESR in the Mixed-charge Transfer TTF-p-chloranil Single Crystals

Tadaoki MITANI and Gunji SAITO *(Univ. of Tokyo)*

[*Synth. Metals*, **19**, 515 (1987)]

From our recent investigation of the neutral-to-ionic (N-I) phase transition in TTF-p-chloranil crystals, it has bee demonstrated that collective excitations of ionic (or neutral) molecules play an essential role in the optical, electrical and magnetic properties near the N-I phase transition. A possibility of photo-generation of such a collective excitation of molecules as the mobile NI domain wall or soliton-like (and antisoliton-like) defects is confirmed by temperature-dependences of the photoconductivity and the photo-induced ESR.

VII-K-4 A New Phase Transition Assoxiated with Electron- and Proton-transfer in Mixed-stack Charge-transfer Quinhydrone Crystals

Tadaoki MITANI, Gunji SAITO*, and Hatsumi URAYAMA* *(*Univ. of Tokyo)*

In quinhydrone charge-transfer (CT) crystals, which have a similar crystal structure to TTF-p-chloranil complex except for the presence of the inter-chain hydrogen-bonding between donor-acceptor molecules, a new phase transition has been discovered as a results of the application of hydrostatic pressure. This effect is rather similar to the N-I phase transition but exhibits striking changes in the absorption spectrum of the O-H vibrational mode as well as the CT exciton. The pressure-induced changes in the spectra of the O−H and C=O vibrations (see Fig. 1) and the CT exciton are accounted for by the effect of the electron- and proton-transfer, taking account of the phonon-assisted proton tunneling in the hydrogen bonding.

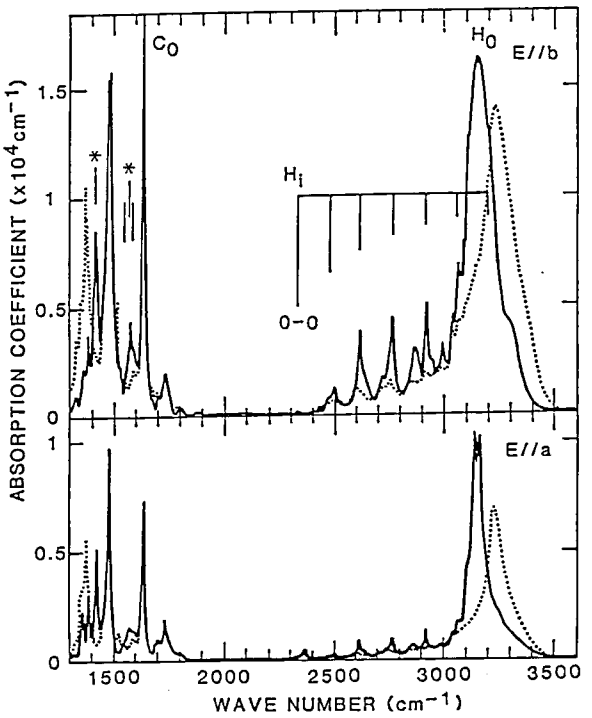

Figure 1. Polarized IR absorption spectra of a quinhydrone single crystal parallel (lower part) and perpendicular (upper part) to the CT axis at 10 K (solid lines) and 300 K (broken lines). The structures of the O−H stretching mode (H_0 and H_i) and the C=O stretching mode (C_0) show characteristic changes near the "electron- and proton-transfer" phase transition.

VII-K-5 Study of Binuclear Halogen-Bridged Platinum Complexes

Yoshiki WADA, Tadaoki MITANI, Masahiro YAMASHITA *(Nagoya Univ.)*, **and Koshiro TORIUMI**

Single crystals of binuclear halogen-bridged platinum complexes, $K_4[Pt_2(pop)_4X_2]2H_2O$;X=Cl, Br and I, and $Pt_2(CH_3CS_2)_4I$, have been investigated by polarized reflectivity, Raman scattering, magnetic susceptibility, and conductivity measuements. The halogen-dependences of these experimental results, which are closely correlated to those of mixed-valence mononuclear platinum analogues, $[PtA_2][PtX_2A_2](ClO_4)_4$ (A stands for a ligand molecule), have been accounted for on the basis of the extended Peierls-Hubbard model, introducing the distortion energy due to relative displacements of adjacement platinum atoms in addition to the distortion energy of halogen ions.

VII−L Optical Spin Orientation in Condensed Matter and Spectroscopic Measurements Using a Novel Optical Gating Technique

VII-L-1 Laser-Induced Transient Magnetization in Diamagnetic Transition Metal Complexes

Yoshihiro TAKAGI

Optically induced magnetization has been directly observed in single-and poly-crystals and aqueous solutions of transition metal complexes at room temperature in an external magnetic field. A linearly polarized second harmonic of a mode-locked Nd:YAG laser was focused on the sample. The induced magnetization was detected with a pick-up coil. Table 1 shows materials in which the magnetization was observed. We reported previously (see Ann. Rev. 1985, VII-M) two different mechanisms of the magnetization: ground-state magnetization in paramagnetic materials irradiated with a circularly polarized light and magnetization in photo-excited triplet state of diamagnetic molecules in external magnetic field. In the present experiment a circularly polarized light also induces the magnetization in the absence of magnetic field for materials listed in Table 1 as well as the linearly polarized light in the presence of magnetic field. These materials thus include both two mechanisms of magnetization. For the latter mechanism we remember that the materials in Table 1 can form polymer. If a dymer is formed, a triplet state may exist in the higher energy side depending on J-value. If we assume a fast intersystem crossing from an excited singlet state to this triplet state, a magnetization would be created. The polarity of the signal, i.e. the direction of magnetization, depends on materials as shown in Table 1. This must be due to difference of the structure of the zero-field splitting. Relexation time of the magnetization was observed with a high time resolu-

tion. Copper acetate showed a relaxation time different from that in the magnetization in the paramagnetic ground state. Detailed description is in preparation.

Table I. Materials in which laser-induced magnetization was observed.

Material	Solvent	Excitation Wavelength	Signal Polarity
(Liquid)			
$Cr_2(SO_4)_3$	H_2O	532 nm	–
$Cr(HCOO)_3$	Methanol	"	–
$Cr(CH_3COO)_3$	H_2O	"	–
$NH_4Fe(SO_4)_2{\cdot}4H_2O$	"	"	+
$Fe(NO_3)_3{\cdot}9H_2O$	"	"	+
$FeCl_3{\cdot}6H_2O$	"	"	–
Iron Ammonium Citrate $(NH_4)_3Fe(C_2O_4)_3$	"	"	+
$Fe_2(SO_4)_3{\cdot}xH_2O$	"	"	+
Cu Acetyl Acetonate	CH_3COOH	532, 1064 nm	+
$Cu(CH_3COO)_2$	"	" "	+
(Single Crystal)			
Fe Alum	–	532 nm	+
(Powder)			
$CuCl_2$ (Anhyd$_1$)	–	"	–
$Cu(CH_3COO)_2$ (Anhyd$_1$)	–	"	–
Cr Acetyl Acetonate	–	"	–

VII-L-2 Observation of a Macroscopic Fluctuation in Optical Parametric Generation

Yoshihiro TAKAGI

Macroscopic fluctuation in the output power is a well known phenomena in nonlinear optical processes such as superfluorescence of dye and stimulated Raman scattering pumped by a strong laser light. Distribution of the power fluctuation reflects the statistics of the quantum noise when the amplification gain is relatively low. Raymer et al.[1] showed the photon statistics of the stimulated Raman process gives an exponential distribution (100% fluctuation) that means an initiation of the process being due to quantum noise.

We observed a macroscopic fluctuation in optical parametric generation (OPG). A single crystal of KDP was pumped by a fourth-harmonic of a mode-locked Nd:YAG laser. At a high pump power, the noncollinear phase matching allows a very broad spatially resolved spectral distribution in the output of OPG. We found in a monochromator output a number of sharp spikes along both the wavelength and the vertical (along the slit) axes that correspond to the logitudinal and transverse modes respectively. The position of the spikes changed shot to shot in quite a random manner. The monochromator output was monitored by a SIT camera and the image was on-line processed by a computer. Figure 1 shows a typical example of the output energy distributions with a relatively low and high pump power. At the low pump power a clear exponential form is seen while at high power the distribution concentrates arround its average value. This result is quite similar to that of Raymer et al.. They obtained the same result in a hydrogen Raman scattering under the single-mode condition using thousands of laser shots, whereas we needed only one laser shot under the multi-mode condition. Detail will be reported soon.

Reference

1) I. A. walmsley and M. G. Raymer, Phys. Rev. Lett., **28**, 962 (1983).

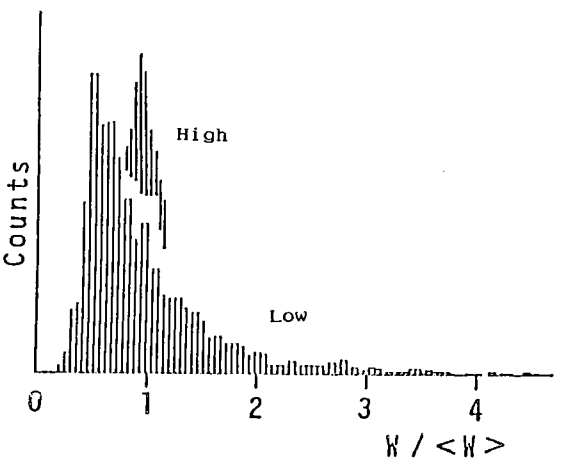

Figure 1. Photon counting distributions of optical parametric emission.

VII-M Development of Experimental Devices

VII-M-1 High-power Opertaion of a Simple Oscillator-Amplifier Nd:YAG Laser as a Picosecond Widely Tunable Light Source

Yoshihiro TAKAGI, Kazuo HAYAKAWA, Hisashi YOSHIDA, Toshio HORIGOME, Norio OKADA, Mitsukazu SUZUI, Shinji KATO, Nobuo MIZUTANI, Masaaki NAGATA, and Tadaoki MITANI

We designed a simple home-built mode-locked Nd:YAG laser system as a picosecond tunable light source (see Ann. Rev., 1986, VII-M-1). In order to operate in a wide tunability range the system includes various nonlinear optical processes such as harmonic generation, optical parametric generation, stimulated Raman scattering, and sum and difference frequency mixings. We have achieved a highly stable laser oscillation in a passively mode-locked Nd:YAG laser (less than 10% shot-to-shot fluctuation) by carefully controlling the temperature and concentration of the saturable dye solution and also by high repetetion rate firing (30 Hz). Further stabilization by an active-passive mode locking is in preparation. The output beam has a stable TEM_{00} Mode without the use of an aperture in the resonator. The oscillator output energy of the whole pulse train was about 3mJ and no optical damage was found for several months operation. After a single-pulse selector using a Klytron-switched Pockels cell, the beam was passed through two amplifiers and a quarter-wave plate and then retro-reflected to be amplified twice more by the same amplifiers. The output was taken out with a double plate thin film polarizer between the oscillator and the first amplifier. No effect at the oscillator due to the backward propagation was found. Each amplifier gain was about three.

We are trying to obtain higher intensity at the YAG fundamental for the use of pump source of an optical parametric generator and a tunable dye laser (ultrashort cavity dye laser).

VII-M-2 Production of 30-Channels Floating Power Supply by Using Automatic Printed-Circuit Milling Machine

Hisashi YOSHIDA and Kazuo HAYAKAWA

As a first product of the automatic printed-circuit milling-machine system (LPKF-J. Seebach Co.), which was settled in the Equipment Development Center last year, a newly designed power supply to control the electrostatic lenses for improvement of the mass spectrometer used in TEPSICO II (installed in the UVSOR facility) has been produced. This Milling machine is composed of CAD and CAM systems, which serve for fine electric circuit and artwork designs and milling processing of printed circuits. A combination of these sytems allows us to make many printed-circuits in a short time with a high reliability, and also easily to revise printed circuits after testing their abilities. In the case of producing the power supply, we could resolve the problem associated with the instability of the circuit in changing the range of floating DC amplifier, and improve the stability of DC outputs of 30 channels for a balanced operation of the channels.

Ultraviolet Synchrotron Orbital Radiation Facility

VII–N Construction of UVSOR Light Source

VII-N-1 Longitudinal Active Damping System for UVSOR Storage Ring

Toshio KASUGA, Masami HASUMOTO, Toshio KINOSHITA, and Hiroto YONEHARA

A longitudinal coupled-bunch instability had already observed when the routine operation of the UVSOR storage ring was started. It was also found that a coupling element of the instability was the RF acceleration cavity. The instability deteriorates beam quality; the increased energy spread due to the instability enlarges the horizontal beam size thorugh the non-zero energy dispersion function, and the time structure of electron bunches is agitated. A longitudinal active damping system was installed in the ring for suppression of the instability. The system consists of sixteen independent feedback loops; each of them corrects energy deviation of a certain bunch in sixteen bunches individually. Figure 1 shows the effect of the system. The phase oscillation (the trace **a** in Fugure 1 is widended by the instability) is completely suppressed (**b** in Figure 1).

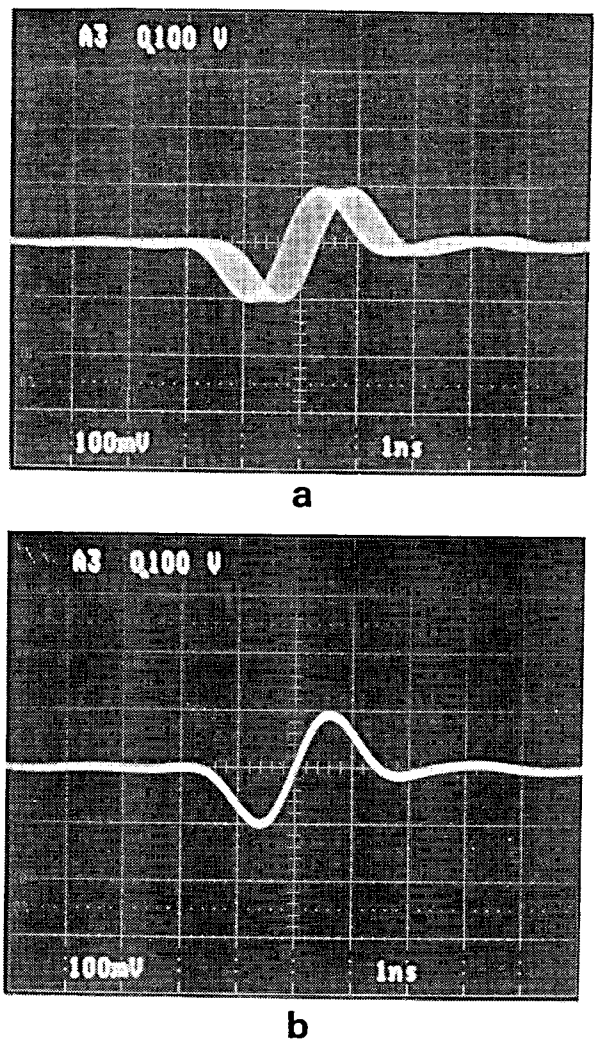

Figure 1. Synchrotron oscillation due to the coupled-bunch instability (a) is completely suppressed with the feedback system (b).

VII-N-2 Tune Shifts due to UVSOR Wiggler

Hiroto YONEHARA, Toshio KASUGA, Toshio KINOSHITA, and Masami HASUMOTO

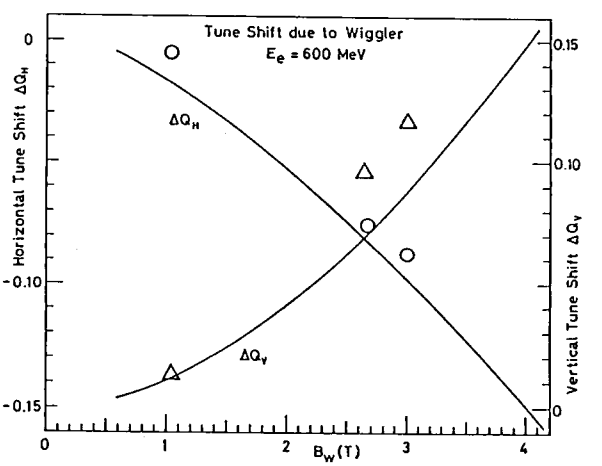

Figure 1. Tune shift due to UVSOR wiggler excitation at the electron energy of 600 Mev.
Abscissa is the wiggler field strength B_W in Tesla. Solid lines show the horizontal and vertical tune shifts, ΔQ_H and ΔQ_V, which are expected from the sextupole components of UVSOR wiggler field. Circles and triangles show the observed horizontal and vertical values.

A superconducting wiggler was installed in the UVSOR storage ring, which has 3 magnetic poles and the maximum field is 4 T. Since the width of the wiggler coil is finite, the quadratic term of the radial distribution of the magnetic field is not negligible. The measured coefficients of the term at the field of 2 T and 4 T are 130 m^{-2} and 90 m^{-2} respectively. The horizontal and vertical tune shift, ΔQ_H and ΔQ_V, due to the wiggler, are estimated as shown in Figure 1. And the tune shifts of the beam at the beam energy of 600 MeV were observed with the RF knockout methods and the actual tune shifts are also shown in Figure 1. The observed values are in good agreement with the expected ones. These tune shifts depend on the beam energy and the wiggler field strength, and can be corrected with the trim coils of the quadrupole magnets. A correction system of the tune shifts due to the wiggler field is now under construction.

VII–O Development of Measurement Systems for UVSOR

VII-O-1 Construction of a 1 m Seya-Namioka Monochromator for BL1B

O. MATSUDO, E. NAKAMURA, J. YAMAZAKI, K. SAKAI, K. FUKUI, E. ISHIGURO *(Osaka City Univ.)*, **and M. WATANABE**

At BL1B a 1 m Seya-Namioka monochromator was installed. It is used for both solid state and gas phase experiments. Figure 1 shows the side view of the monochromator. Synchrotron radiation is gathered by a pre-mirror M_1 and deflected vertically upward by 40°. The light which passes through the entrance slit S_1 irradiates one of three gratings G, the groove densities of which are 600/mm, 1200/mm and 2400/mm. The monochromatized light passing through the exit slit S_2 is deflected by one of two post-mirrors M_2 so that its axis lies on horizontal plane, and is focussed at the sample position Q. The surface of one of the post-mirrors is coated with gold and the surface of the other, aluminum. The beam size at Q is less than 3 mm × 2 mm (W × H). The monochromator was designed to be usable under ultrahigh vacuum. The grating chamber is evacuated by a 500 l/s sputter ion pump and a titanium sublimation pump. At present the pressure is 1×10^{-8} Torr. With the entrance and exit slits with 100 μm width, the resolution of less than 2 Å is achieved by the use of 1200/mm grating.

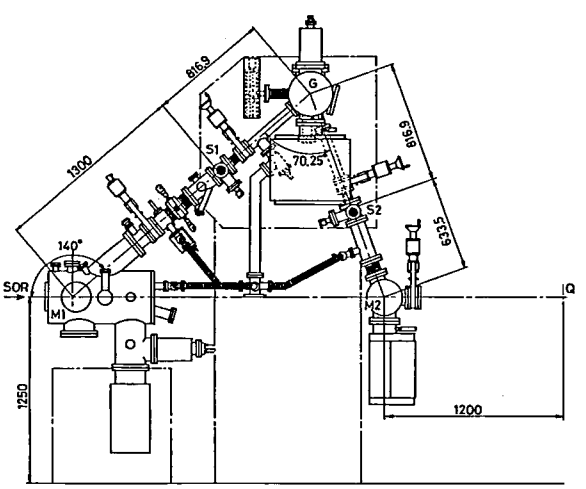

Figure 1. Side view of BL1B equipped with a 1 m Seya-Namioka Monochromator.

VII-O-2 Luminescence Observation System at BL3A1

M. WATANABE, T. DEGUCHI[a)], H. FUJII[b)], M. FUJITA[c)], K. FUKUI, E. ISHIGURO[b)], T. KATO[d)], O. MATSUDO, T. MIYANAGA[e)], T. MOMOSE[d)], I. MUNRO[f)], H. NAKAGAWA[a)], E. NAKAMURA, K. SAKAI, M. SUZUI and J. YAMAZAKI (a) *Fukui Univ.*, b) *Osaka City Univ.*, c) *Marine Safety Academy*, d) *Kyoto Univ.*, e) *Wakayama Univ.* and f) *Daresbury Lab.)*

The beam line BL3A1 utilizes the undulator radiation as the quasi-monochromatic light. One of the main experiments at BL3A1 is observation of luminescence from solids, which can be observed only by the use of intense exciting light in VUV. The first harmonic of the undulator radiation is used to excite the solids. The higher harmonic radiation is cut by thin film filters. The wavelength is chosen by changing the gap of the undulator. Figure 1 show the plan view of the luminesc-

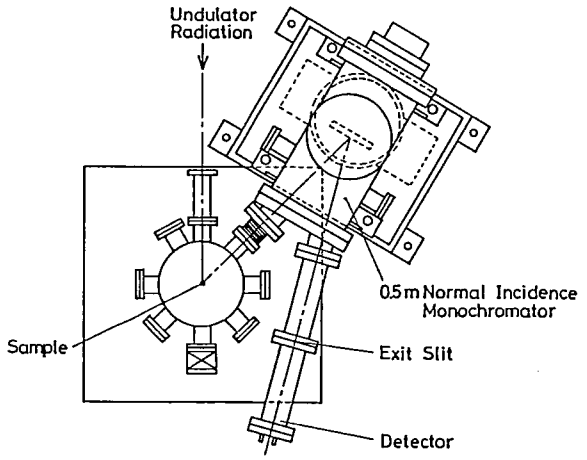

Figure 1. Plan view of luminescence observation system at BL3A1.

ence observation system at BL3A1. The undulator radiation is focussed by a pre-mirror on the sample through a pin-hole with a diameter of 1 mm. The monochromator which analyzes the luminescence is a 0.5 m normal incidence VUV monochromator without an entrance slit. The source point of the luminescence acts as the entrance slit. The groove density of the grating is 1200/mm and its ruled area is 100 mm × 100 mm. The sample can be cooled down to 35 K. At present, this system is used to observe the luminescence from ionic and organic solids.

VII–P Researches by the Use of UVSOR

Researches of IMS staff other than UVSOR staff are reported at some other place in this issue. Details of al researches preformed by inside and outside users will be reported in UVSOR Activity Report 1987.

VII-P-1 Soft X-Ray Absorption Studies by a Two Crystal Monochromator in BL7A

Shun-ichi NAOÉ *(Kanazawa Univ. and IMS.)*, **Tokuo MATSUKAWA** *(Osaka Univ.)*, **and Takatoshi MURATA** *(Kyoto Univ. of Education)*

Soft X-ray absorption spectra were measured mainly for the K edge of light elements of various compounds by a two crystal monochromator.[1] The elements studied were Na, Mg, Si, P, Cl and K. In the wavelength region between 14 Å to 6 Å, a Beryl crystal has excellent properties as a monochromating crystal to measure the spectra with high resolution. Characteristic spectra of core excitons, XANES and EXAFS were obtained for Na halides, Mg halides and mixtures of Na-K halide. At wavelangths below 7 Å, InSb crystal was used. Si glass and KCl have been measured. The K edge of K (at about 3.4 Å) in KCl was measured for the case of the short wavelength limit in UVSOR facilities, as shown in Figure 1. Its resolving power is a little less than that of the previous report.[2] Using Ge as a monochromating crystal, a high resolution will be attained.

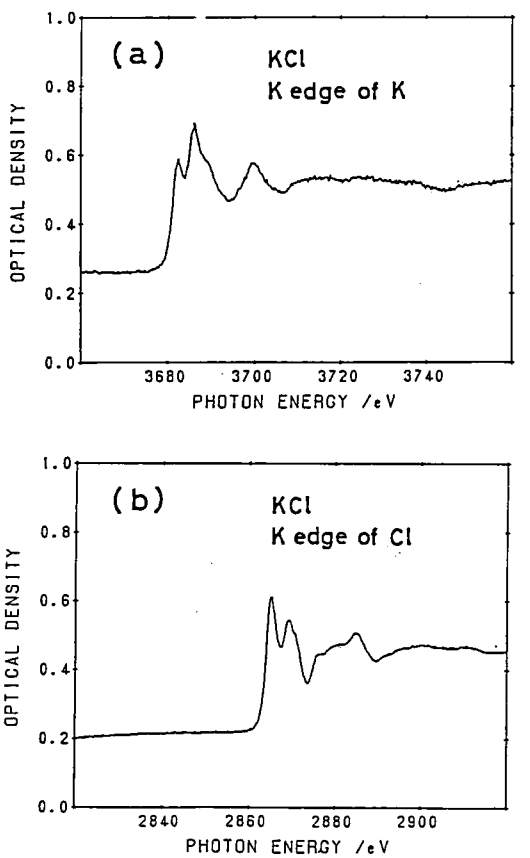

Figure 1. Absorption spectra of a thin film of KCl on a collodion substrate. The electron energy of the storage ring is 750 MeV. (a) The K edge structure of K. (b) That of Cl.

References

1) T. MURATA, T. MATSUKAWA, M. MORI, M. OBASHI, S. NAOÉ, H. TERAUCHI, Y. NISHIHATA, O. MATSUDO and J. YAMAZAKI, *J. Phys.* (France), **47**, C8-135 (1986).
2) L.G. PARRATT and E.L. JOSSEM, *Phys. Rev.*, **97**, 916 (1955).

RESEARCH FACILITIES

For the sake of brevity of the present issue are included only the newly installed facilities and the activities since September 1986. Concerning the activities and facilities before September 1986, please refer to IMS Annual Review (1978～1986).

Computer Center

A supercomputer HITAC S-810/10 and a general purpose computer HITAC M-680H, which were introduced in the December 1986, are running well. The maximum speed of S-810 is 315 MFLOPS. S-810 has 128 mega byte main memory and 1 giga byte extended storage. The CPU speed of M-680H is about 14 MFLOPS and it has 64 mega byte main memory. Both computers can access 85 giga byte disk memory and optical disk memory whose maximum content is 86 giga byte. Two kinds of high speed IO facilities are equipped. Although the extended storage is used only for working files, it is 88 times as fast as usual disk. The other is a parallel IO disk set which consists of 16 channels for each computer and 40 giga byte disk memory. Its observed speed is 46 times as fast as usual disk speed. The computer system can be accessed from every place in Japan through the telephone line and DDX network. In the campus of IMS, an optical fiber local area network supports high speed data transfer.

The computers are used not only by the research staff at IMS but also by the staff at nearby National Institutes as well as by scientists outside the Institutes in the related fields. The number of project groups was 234 consisting of 637 users in March 1987. In the twelve month period ending March 1987, 289915 jobs were processed with 3422 hours of CPU time on M-680H and 4002 hours on S-810.

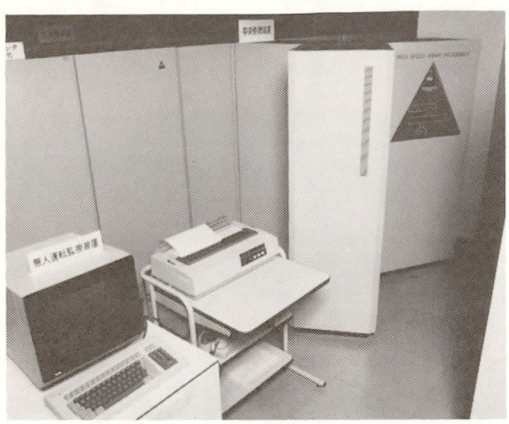

Supercomputer HITAC S-810/10

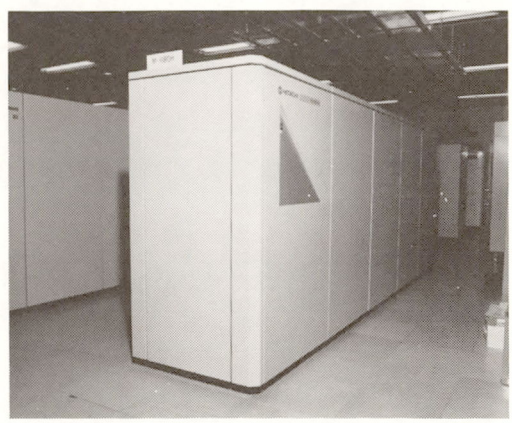

General purpose computer HITAC M-680H

Chemical Materials Center

The Chemical Materials Center plays an important role in the synthesis and purification of chemical substances in IMS. The scientists and technical associates of this facility support other people in IMS to carry out the above works. Upon request, technicians carry out elemental and mass spectrometric analyses of new compounds prepared at IMS. They also carry out their own researches on synthesis of new interesting compounds, developments of new selective chemical transformations, elucidation of reaction mechanisms, and application of new methodologies developed in IMS to the analysis of chemical substances and reactions. Parts of the scientific activities are presented in the Section VII.

Instrument Center

For the efficient use of instruments, the Center is equipped with various types of instruments for general use.[1] Two instruments have been newly installed in 1987.

1) **Excimer Laser and Dye Laser** (Lambda Physik EMG401, FL3000)
The excimer laser generates a pulse with pulse energy of 44 mJ/pulse at 308 nm (XeCl) and with repetition rate up to 500 Hz. Coupled with the excimer laser, the dye laser is operated in the tuning ranges of 315–970 nm in fundamentals and 217–360 nm in frequency doubling.

2) **SQUID Magnetometer**–VTS 905
Magnetic susceptibility can be measured with the magnetic field up to 50 kOe in the temperature range of 3K–380K. The resolution of the field is about 0.1 Oe and 10 Oe for the field regions less then 1 kOe and higher than 1 kOe, respectively. The maximum sensitivity is 10^{-8} emu.

Reference
1) *List of Instruments*, No.**6**, IMS Instrument Center (1986).

Low Temperature Center

The amount of liquid helium supplied in 1986 was about 15,000 l with the increase by 3,000 l compared with the last year. In order to cope with the increasing demand of liquid helium, a new liquefier with 150 l/h capacity will be introduced at the end of this fiscal year. All other facilities corresponding to this liquefier will also be equipped in the next fiscal year, and the new system will start to work within that year.

Mr. Shuji Nakane, a technical associate, has been employed as a new member of the staff in the center since April 1, 1987.

Equipment Development Center

A number of research instruments have been designed and constructed by use of the mechanical, electric and glass-blowing technologies available at this Facility. Representative instruments developed during this fiscal year of 1986 are listed below.

- o SOR Surface Experimental Apparatus
- o Discharge Flow Cell for REMPI Measurements
- o Flowing Afterglow Cell for LIF Measurements of Molecular Ions
- o Supersonic Ion Jet Apparatus
- o Carbon Cluster Vaporizing Source
- o Heat Pipe Oven for Coherent Tunable VUV Light Generation
- o Helium-Cryostat for Clean-Surface Optical-Measurements
- o 2.2m Constant Deviation Grating Incidence Monocromator
- o High Intensity Pulsed Xenon Lamp Driver
- o Single Pulse Selecter for Pulsed YAG Laser
- o Power Supply for Pulsed YAG Laser
- o Pulse Molecular Beam Driver
- o Interface for OMA2

- 3-Channels peak Holder Circuit
- Electrolysis cell for ESR
- Rere-Gas Resonance Lamp
- Thin Test Tube for X-ray Diffraction Measurements

Ultraviolet Synchrotron Orbital Radiation Facility

The UVSOR light source is usually operated at an electron energy of 750 MeV with an initial current of 100 mA. Single bunch operation has been performed with a frequency of 1 week per 2 months. The coupled-bunch instability has been suppressed successfully by a newly developed feedback system. Two beam lines have been opened to users. One is BL1B equipped with a 1 m Seya-Namioka monochromator and the other is BL8B1 equipped with a 2.2 m Rowland-circle grazing incidence monochromator. The Institute of Plasma Physics, Nagoya University provided BL5B with a plane grating monochromator for the calibration of plasma diagnostic devices. A users' meeting and a workshop on beam dynamics were held in December. The Activity Report 1986 has been published in this April.

SPECIAL RESEARCH PROJECTS

IMS has special research projects supported by national funds. Tthree projects presently in progress are:

(1) Development and evaluation of molecular synergistic systems and their application to chemical energy conversion (1985–1990).

(2) Fundamental research of molecular devices (1985–1990).

(3) Molecular science of primordial chemical evolution (1982–1987).

These projects are being carried out with close collaboration between research divisions and facilities. Collaborators from outside also make important contributions. Research fellows join these projects. The results in 1986 are reviewed in this report.

(1) Development and Evaluation of Molecular Synergistic Systems and their Application to Chemical Energy Conversion

Picosecond Dynamics of Excitation-Energy Transport in Multilayered Molecular Architectures

Iwao YAMAZAKI, Naoto TAMAI, and Tomoko YAMAZAKI

Dynamics of two- and three-dimensional excitation energy transports are investigated by means of a picosecond time-resolved fluorescence spectrophotometer with some biological and artificial multilayered architechtures: Langmuir-Blodgett multilayer films and photosynthetic antenna pigment systems. In the multilayer systems in which several monolayers containing different chromophores are stacked, the light energy absorbed by the outer surface is transferred sequentially among the layers, and finally trapped at the reaction center. During this course of the energy transfer, fluorescence is emitted from each layer, and is used as a probe for investigating kinetics of the sequential energy transport.

One can prepare stacking multilayer having a molecular architecture analogous to the so-called "antenna pigment" system in the photosynthetic organisms, particularly, the accessary pigment system in blue-green and red algae, in which different kinds of phycobiliproteins are stacked like the artificial multilayers. The results have been presented in the *International Conference on Luminescence* (ICL 87) held in Beijing, China (August 17–21, 1987). The final goal of our study is to develop a electrooptic device in molecular scale that controls the light energy transport in the two- and three-dimensional architectures.

Synthesis of Highly Functional Transition Metal Complexes and Their Use in Catalytic Reactions

Hidemasa TAKAYA*, Tetsuo OHTA, and Kazushi MASHIMA

Homogeneous asymmetric hydrogenation with transition metal complexes possessing chiral di-*tert*-phosphine ligands provides a powerful tool for chemical multiplication of chirality. So far the highly stereoselective reactions have been achieved mainly by the Rh(I)-based complexes. We have synthesized new mononuclear Ru(II) complexes containing axially dissymmetric (*R*)- or (*S*)-2,2′-bis(diphenylphosphino)-1,1′-binaphthyl [(*R*)- or (*S*)-BINAP] and its derivatives. These complexes exhibit very high catalytic activity and enantioselectivity in hydrogenation of a wide range of substrates such as enamides, α-acylaminoacrylic acids, alkyl- and aryl-substituted acrylic acids, α,β-unsaturated carboxylic acids, allylic and homoallylic alcohols, α-amino ketones, etc. The Ru complexes are in many cases superior to the corresponding Rh complexes, and are now becoming one of the most useful catalysts in this field. Parts of these results are presented in the Section VII-C.

Dynamical Molecular Structure and Control of Reactive Molecules

Eizi HIROTA*, Chikashi YAMADA, Yasuki ENDO, Kentarou KAWAGUCHI, Hideto KANAMORI, Masatoshi KAJITA, and Robert F. CURL *(Rice Univ. and IMS)*

Infrared laser kinetic spectroscopy combined with excimer laser photolysis has been applied to the acetylene photolysis at 193 nm (II-A-19, II-A-24) and also to the photolysis of some Cl-containing molecules (II-A-16). A similar method has been developed in the millimeter- and submillimeter-wave regions and has been employed to determine the branching ratio for the O+acetylene reaction (II-A-22). It has also been used to generate SO in the $a^1\Delta$ state from Cl_2SO (II-A-14).

A molecular-beam apparatus is being constructed to directly observe infrared transitions of transient species generated by excimer-laser photolysis at the exit of the nozzle. In a preliminary experiment SO radicals generated from SO_2 were observed, but the rotational temperature was close to room temperature.

Construction of Coherent VUV Light Source with Narrow Bandwidth, High Intensity and Wide Tunability

Norio MORITA and Keiichi SATO

Coherent vacuum ultraviolet light source is an attractive and powerful tool for the study of highly excited states of atoms and molecules with high resolution. We have been constructing this light source, in which the VUV light is generated by four-wave mixing in a gaseous medium. We mainly utilize a scheme of two-photon resonant four-wave difference mixing with 4p–5p two-photon resonance of Kr atom, because the difference mixing is less restricted by the phase-matching condition. The UV input light (216 nm) resonant with this transition can be generated with high efficiency by using a recently devised non-linear crystal, β-BaB_2O_4. The fundamental light for this UV light is produced by four-stage amplification of a single mode cw dye laser in order to obtain as narrow bandwidth as possible. While we usually use a pulsed dye laser as the other input light for the mixing, we prepare another cw dye laser with an amplifier chain. This scheme is expected to generate 120–200 nm VUV light with high intensity and uniform tunability. As a preliminary result, we have generated coherent VUV light at around 140 nm with high efficiency by using the above scheme with Kr atom. Farther improvement and measurements are in progress.

Construction of an Efficient Spectrometer for X-ray Raman Scattering Study

Kazuyuki TOHJI and Yasuo UDAGAWA

In order to detect very weak x-ray inelastic scattering (X-ray Raman Scattering), an efficient x-ray spectrometer shown in Figure 1 was constructed. It makes use of a curved and bent crystal and a position sensitive detector (PSPC), and is similar to the one described by Pattison et al[1]. A Johansson type Ge(333) crystal with Rowland radius of 320 mm is positioned about 100 mm from the sample, to which Cu $K_{\alpha 1}$ line from a rotating anode x-ray generator is focused. The sample is placed in a defocused position relative to the analyzer crystal. The scattered radiation from the sample is brought to a focus at a distance of 485 mm from the analyzer crystal. At this position a PSPC was placed at the focal plane and serves to detect as well as to locate the scattered photons.

With this optics the efficiency improved by about 10 times and the resolution is doubled when compared

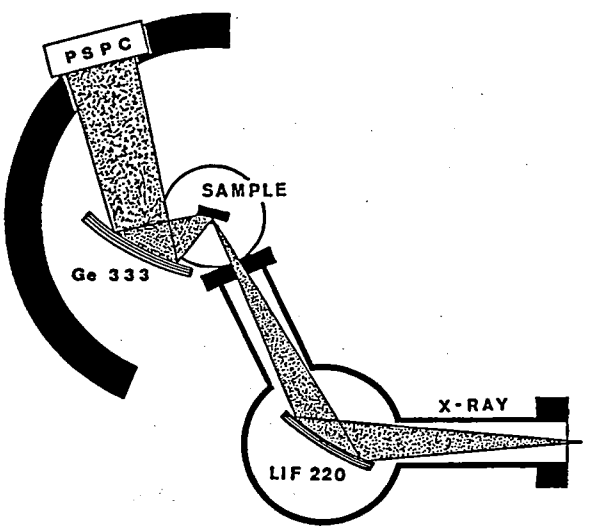

Figure 1. A schematic diagram of the spectrometer based on a Johansson cut and bent Ge(333) crystal and PSPC.

with the previously employed system based on a plane crystal and solid state detector (SSD). It is expected to obtain fine structure of X-ray Raman spectra with this spectrometer within several days.

Reference
1) P. Pattison, H.J. Bleif, and J.R. Schneider, J. Phys. *E:Sci. Instrum.* **14**, 95 (1981).

Excited-State Photoelectron Spectroscopy for Studying Photophysical and Photochemical Behaviors of Molecules and van der Waals Complexes in Supersonic Jets

Katsumi KIMURA, Katsuhiko OKUYAMA, and Masahiko TAKAHASHI

Excited-state photoelectron spectroscopy combining a UV/visible pulse laser technique and a supersonic molecular beam technique has been developed in this Institute since 1980 (IMS Annual Review, 1980–86). This method has made it possible to study dynamic behavior of excited-state species which include nonradiative electronic states. Photoelectron spectra originating from various molecular excited states have been investigated from photophysical and photochemical points of view. The information deduced from excited-state photoelectron spectra have been found to be unique and important.

In this project, with this technique we have being studying not only single molecules but also van der Waals molecules (or molecular clusters) produced in supersonic jets, and we have demonstrated some typical applications in the following several subjects: (1) ionization selectivity, (2) autoionization, (3) intramolecular vibrational redistribution, (4) photodissociation, and (5) excited states of van der Waals molecules.

Construction of a Femtosecond Laser System for the Research of Ultrafast Molecular Processes

Hiromi OKAMOTO, Yoshihiro TAKAGI, and Keitaro YOSHIHARA

Recent development in laser technique enables us to obtain coherent light pulses in the femtosecond time domain. The time scale corresponds to the period of a molecular vibration (100 fs = 333 cm^{-1}, for example). Any kind of chemical intermediate is therefore time-resolvable in principle. We are constructing a frequency tunable, high peak power femtosecond laser system and related detection equipments. The second harmonic of a CW mode-locked Nd:YAG laser (532 nm, average power 700 mW, pulse width 70 ps, repetition rate 83 MHz) excites a dye laser. We adopt a recently developed linear-cavity hybridly mode-locked dye laser, which produces frequency tunable ultrashort pulses without an extra-cavity dispersion-compensation element[1]. In the present stage the pulse width of less than 2 ps is achieved without saturable absorber. Several devices are developed to stabilize the laser output energy and pulse width. Construction of an amplifier excited by copper-vapor laser is under way.

Reference
1) M.D. Dawson, T.F. Boggess, D.W. Garvey and A.L. Smirl, *Opt. Commun.*, **60**, 79 (1986).

Photoinduced Electron Transfer on Semiconductor Surfaces

Masahiro HIRAMOTO, Kazuhito HASHIMOTO, and Tadayoshi SAKATA

Relating with semiconductor photoelectrode processes, electrochemical properties of several kinds of semiconductor electrodes with a pn-junction have been investigated. For a pn-Si electrode, whose surface is composed of a thin p-layer, it was proved that the electrons are injected from the inside n-layer into the surface p-layer with almost 100% efficiency. Due to the injection, hydrogen was evolved vigorously from the p-Si surface. This result indicates that a pn-Si/electrolyte junction works as electrochemical transistor.

The ultramicrostructured electrode systems with the scale of nm orders have been prepared and the vertical sections of the multilayered thin films have been applied to electrochemical reactions. For this type of electrode, supporting electrolyte is not necessary for the electrochemical reaction due to the very short distance between electrodes. It was also confirmed that this new electrode can work in the gas phase and in several cases at low temperatures.

Luminescence decays of $Ru(bpy)_3^{2+}$ and $Ru(bpz)_3^{2+}$ adsorbed on powdered oxide semiconductors were measured in vacuo. Electron transfer rates from the excited state of the Ru(II) complexes to semiconductors were evaluated from the decay curves. The electron transfer rate increased monotonically with increasing the energy gap between the oxidation potential of the excited dye and the bottom of the conduction band.

External Magnetic Field Effects upon Chemical Reactions

Hisaharu HAYASHI *(Inst. of Phys. and Chem. Res.)*, **Hirochika SAKURAGI** *(Univ. of Tsukuba and IMS)*, **Ryoichi NAKAGAKI, Haruo ABE** *(Inst. of Phys. and Chem. Res. and IMS)*, **Yoshio FUKUDA and Saburo NAGAKURA**

In the present research project, we have studied the magnetic field effects on inter- and intra-molecular photo-induced electron transfer reactions involving a radical pair and a biradical as reaction intermediates. The magnetic field affects conspicuously the relative yield between the escape and cage products, Φ(escape)/Φ(cage), in the photoreactions of some bichromophoric species containing electron donor and acceptor moieties. Thus, the magnetic field effects have some potential for application, *e.g.* control of reaction yields. We have also examined the mechanism for magnetic quenching of CS_2 fluorescence in the gas phase. External magnetic field effects have been used as an excellent probe for elucidating the reaction mechanism, and the magnetic field cotnrol of reaction yields is currently in progress in our laboratory.

Molecular Beams Study of Dynamics of Molecule-Molecule Reactions

J. Robb GROVER *(Brookhaven Natl. Lab. and IMS)*, **Yuan T. LEE** *(Univ. of California, Berkeley and IMS)*, **Ye WEN, Kiyohiko TABAYASHI, and Kosuke SHOBATAKE**

Dynamics of chemical reactions involving atoms or radicals has been studied very extensively for the last 25 years. In contrast the dynamics of molecule-molecule reactions has not been studied as extensively as atom-molecule reactions, although reactions involving only stable molecules as reagents somethimes play very important roles in, for example, organic synthesis. In the present project we seek to clarify the dynamics of molecule-molecule reactions from the view point that they are the extension of molecular interactions on van der Waals potential surfaces.

The reactions of F_2 with C_6H_6 and C_6D_6 have been studied on a Molecular Beam Chemistry apparatus-I (MBC-I) using a crossed molecular beam technique. Preliminary results have been reported in IMS Annual Review 1986, pp. 98–99. In the fiscal year of 1986 a closed-loop helium cryostat was installed to cool the apertures for two crossing beams so that the mass spectrometer detector sees only a cold surface kept at 20K. Installing the He cryostat along with a liquid nitrogen cooled cold shield in the ionizer chamber of the mass spectrometer detector, the background of scattered species went down by one order of magnitude at higher masses above m/e = 90. The results are briefly presented in the Research Activities IV-M-4 of the present issue.

(2) Fundamental Research of Molecular Devices

Research of Co-operative Phenomena of Electron- and Proton-Transfer in Charge-Transfer Crystals

Tadaoki MITANI

In order to elucidate the fundamental aspect of the co-operative phenomena of the electron- and proton-transfer in solids, quinhydrone charge-transfer crystals, which have a prototype of the 2-dimensional (2D) proton lattice, have been investigated by optical spectroscopy in a wide frequency range from the far infrared to ultraviolet region. A new phase transition associated with the order-disorder of the 2D proton lattice has been discovered as a result of application of hydrostatic pressure (see VII-K-4). This provides a unique opportunity for studying the dynamics of the electron-proton interaction in solids. In fact, this phase transition exhibits striking changes in the absorption spectra of the charge-transfer exciton as well as the O-H stretching vibrational mode. The temperature- and pressure-induced changes of the ir spectra can be accounted for in terms of the proton tunneling through a barrier of the H-bonded double-well potential. These characteristic features suggest the possibility of the formation of protonic domain walls or soliton-like kinks in the proton-electron-transfered state. Such a new type of elementary excitations in solids allows us to expand the subject of this research to design of a new molecular function in charge-transfer complexes.

High-T_c Superconductors

Masatoshi SATO, Masashige ONODA, Shin-ichi SHAMOTO, Syoichi HOSOYA* *(Institute for Materials Research, Tohoku Univ.)*, **Masafumi SERA, Kenji FUKUDA, and Shinji KONDOH**

Last one year was a fantastic period for people who had been studying on superconductivity, because the historical discovery of high-T_c oxides was perfomed by Bednorz and Müller. We had also been, at that time, studying various conductive oxides with the motive force to find new type superconductors or high-T_c superconductors. Actually, the structural characteristics of $Li_{0.9}Mo_6O_{17}$, the superconductivity of which we studied are very similar to the high-T_c oxides. Immediately after the first paper by Bednorz and Müller appeared, the work on the high-T_c materials was started by all of our group members. No distinction can be made between our usual activities and the special research project. Therefore, please refer Research Activities IV-V.

Fabrication of Novel Organic Molecular Assemblies with the Use of Molecular Beam Epitaxy Technique

Yusei MARUYAMA, Hajime HOSHI, and Tamotsu INABE

In order to prepare new materials which could be useful for molecular devices elements, we have started to design and fabricate ultra-thin organic multi-layered systems. As the first candidate for this strategy, we have chosen a combination of charge transfer donor and acceptor molecules, e.g. TTF and TCNQ. Sequence of donor and acceptor in the order of monomolecular thickness in each may result in new structure material which presumably realize new properties. There are many experimetal difficulties to obtain a significant size of highly organized 2-dimensional thin-layers. Epitaxial growth deposition of well-regulated molecular beams is now undertaken for TCNQ and TTF-TCNQ. We have found out that the surface condition of a substrate is very crucial to the epitaxial growth of the films. We are now trying to get larger size of 2-dimensional area with homogeneous epitaxy.

Coupled Proton and Electron Transfer in the Crystals of Salicylideneaniline Derivatives and their Complexes

Tamotsu INABE, Naomi HOSHINO, Tadaoki MITANI, and Yusei MARUYAMA

Salicylideneanilines are known to show chromic behavior in solids by proton transfer accompanying

π-electron configurational change. By strengthening the intermolecular interaction the physical properties of molecular assemblies are expected to be influenced, especially the electronic properties are expected to be coupled with the proton motion. In order to study the possibility many compounds have been prepared and the results of structural and optical studies are presented in Section IV-T.

Molecular Fastener for Molecular Devices

Takehiko MORI, Ichimin SHIROTANI, Yusei MARUYAMA, and Hiroo INOKUCHI

A series of uncapped TTF derivatives, TXC_n-TYF (X, Y = S, Se, and Te) have been studied as a novel type of organic semiconductors (see also IV-B). These organic solids realize moderately high conductivity ($>10^{-5}$ S cm^{-1}) and quite large mobility (28 $cm^2V^{-1}s^{-1}$) without forming charge-transfer complexes. The peculiar stacking of the TTF skeletons accompanied by the close interaction of the uniformly oriented side chains, which we call "molecular fastener" and "atomic wire" effects, induces these intriguing properties.

Resonance Raman Study on Cytochrome c_3 (2)

A.L. VERMA, K. KIMURA, A. NAKAMURA, T. YAGI, H. INOKUCHI and T. KITAGAWA

Cytochrome c_3 is an electron carrier protein of a sulfate reducing bacteria and contains four hemes in a single polypeptide. A thin film of anhydrous cytochrome c_3 on a quartz plate containing a trace amount of hydrogenase was shown to exhibit the semiconductor-type electric conductivity, and the size of an electric resistance of its reduced form is ca. 10^{-10} times as large as that of the oxidized form. It is the aim of this project to elucidate what kinds of structural changes upon reduction of the heme oxidation state are related to the electric conductivity. At the first step we investigated visible resonance Raman spectra of cytochrome c_3 in a solution and compared them with those of a horse cytochrome *c*, which shows the conductivity similar to that of the oxidized cytochrome c_3 in both oxidized and reduced states. For the hydrogenase-catalyzed reduction of cytochrome c_3 with hydrogen, we have detected five distinct reduction states. This suggested that all four hemes in the protein are non-equivalent and have dissimilar redox properties. Observation of well defined Raman peaks due to individual hemes in the partially reduced state at the expected positions indicates that either the intramolecular- or intermolecular electron exchange between arbitrary two hemes is slower than the time scale of the resonance Raman process. Splitting of Raman lines were observed in the intermediate redox states of cytochrome c_3 but not in the fully oxidized and fully reduced states. Complete photoreduction was observed for cytochrome *c* upon the blue excitation but it occurred partially for cytochrom c_3. A similar experiment for a thin film prepared on a quartz plate and UV resonance Raman spectra of cytochrome c_3 in a solution are also under investigation.

An On-Line Controlled Spectrophotometric Titration System for Studying Complex Formation Reactions of Metal Ions in Solution

Shin-ichi ISHIGURO

A variety of methods have been developed for the determination of stability constants of metal complexes in solution. The spectrophotometric titration is one of the useful and widespread techniques. This method can be applied for such metal systems that no suitable electrole for potentiometry is available. In order to evaluate stability costatants of a metal-ligand system, a large number of electronic spectra have to be measured in solutions with varying compositions of the metal to ligands. For this purpose, an on-line data aquisition system using PC-9801VM has been developed. To evaluate stability constants a set of absorbance data at given 50 wavelengths over the range measured are treated with the least-squares program developed in our laboratory. Electronic spectra of individual metal complexes are simultaneously determined together with the stability constants.

Synthesis of Novel Binuclear Transition Metal Complexes and their Structure, and Physical and Chemical Properties

Sigeo KIDA, Masahiro MIKURIYA, Eiji ASATO, and Makoto HANDA

The octadentate ligand, N,N′,N″,N‴-{tetrakis (amino-ethyl)-1, 4, 8, 11-tetraaza}cyclotetradecane (=taec), reacts with various bivalent transition metal ions forming binuclear complexes which show interesting molecular structures and chemical behaviors, because of its complex chelate ring arrangement.

Crystal structures of a series of complexes with the general formula $[Cu_2(taec)X](ClO_4)_3$ were determined by X-ray diffraction method, where X=I, F, NO_2, CH_3COO, N_3, and NCO. In all the complexes except for the case of $X=CH_3COO$ the anion X is incorporated into the cavity of the $[Cu_2(taec)]^{4+}$ and coordinates to axial sites of both copper ions, where N_3^- and NCO^- coordinate in an end-on fashion, and NO_2^- with the nitrogen. In the case of $X=CH_3COO$ one of the oxygen atoms of acetate ion coordinate to one of the copper ion at the apical site and the other oxygen occupies an in-plane coordination site of the copper ion.

The structure of $[Cu_2(taec)(NCS)_2](ClO_4)_2 \cdot H_2O$ is unique. The coordination mode of taec is the trans III form different from the above complexes. Each copper ion is coordinated by NCS^- nitrogen.

$Cr_2(taec)X_4$(X=Cl,Br) were prepared by the reaction of chromium(II) acetate and taec in methanol under argon atmosphere. This compounds are stable in dry air in spite of the fact that chromium(II) compounds are generally very sensitive to the air. This should be attributed to the steric effect of taec ligand which hinders the six-coordination of chromium (III).

(3) Molecular Science of Primordial Chemical Evolution

Molecular Aggregation of Hydrophilic Compounds in Hot Water

Nobuyuki NISHI and Kazunori YAMAMOTO

At the stage of the primordial chemical evolution *on the earth*, volcanic heat is the most probable energy source causing chemical reactions in a submarine environment. Nevertheless, a question comes that hot water may just scatter or diffuse organic molecules into infinite amount of sea water. In this respect, any laboratory simulation may be not at all persuasible. It is now highly necessary to investigate how dissolved molecules associate and give rise to chemical reactions in aqueous systems. The new method we developed isolates molecular complexes or associates as clusters from solutions through adiabatic expansion of liquid jets. Mass-spectroscopic analyses of the cluster beams made it possible to measure the equilibrium constants and enthalpy changes of the association processes. A systematic analysis of more than 15 solute species gave the following important results. Hydrophobic solute species tend to associate or oligomerize at lower temperatures due to large enthalpy decrease of the association processes. At high liquid temperatures, homogeneity of solute-solvent mixing becomes higher so that active water molecules dissociate the complexes forming hydrated solution monomers. Hydrophilic solute species, such as urea, N-methylformamide, or formic acid showed unexpected behavior with increasing temperature. At low temperatures, homogeneity of the solutions is rather good, although the average size of each monomer-hydrate varies. Temperature increase gained inhomogeneity of the solutions producing hydrated solute-oligomers. This general trend for hydrophilic molecules strongly suggests that, in hot water, amino acids, peptides, or some other prebiotic molecules exist in the form of oligomers or complexes and their association is accelerated by the hot water molecules.

Studies of Ion-Molecule Reactions Relevant to the Interstellar Synthesis of Molecules

Inosuke KOYANO, Shinzo SUZUKI, and Teruhiko OGATA *(Shizuoka Univ.)*

As a part of our experimental contribution toward the gas phase ion-molecule reaction model for the formation of interstellar molecules, we have studied the formation of the $C_3H_3^+$ ions by both unimolecular decomposition of the three isomeric $C_3H_4^+$ ions and bimolecular reactions between $C_3H_4^+$ and C_3H_4 (see also Research Activities IV-F-4). $C_3H_3^+$ is a key ion in the model, since it is believed to be the precursor of the recently observed unique interstellar hydrocarbon C_3H_2(cyclopropenylidene). The structure, heats of formation, and reactivity of $C_3H_3^+$ have long been a controversial issue. So far we have found that the $C_3H_3^+$ ions produced by bimolecular reactions have a much smaller heat of formation than and behave quite differently from those produced by unimolecular decompositions.

OKAZAKI CONFERENCES

"Okazaki Conferences" are principal symposia at IMS, which are held on the subjects related to the "Special Research Projects." They are held two or three times a year, with a moderate number of participants around 50, including several invited foreign speakers. The formal language for the conference is English. Outlines of the twenty-seventh to twenty-nineth conferences are as follows.

The Twenty-seventh Okazaki Conference

High Spin Molecules and Spin Alignment
(September 8–10, 1986)

Organizers: K. Itoh *(Osaka City Univ.)* **and H. Iwamura** *(IMS)*
Invited Speakers: D.J. Klein *(Texas A & M Univ.)*, **A.A. Ovchinnikov** *(USSR Academy of Sciences)*, **and W. Weltner, Jr.** *(Univ. of Florida)*

The electron spins in molecules and molecular assemblies have strong tendencies to form antiparallel pairs as dictated by Pauli's exclusion principle. Therefore special molecular designs are necessary to construct high spin molecules and align very many spins in parallel in assemblies of open-shell molecules. Since this is the best area where one can look for interesting magnetic properties from molecular materials, a marked advance has been made of recent years in various laboratories including those of the organizers of this meeting.

About fifty active scientists consisting of chemists, physicists and theoreticians participated in the meeting where seventeen talks were presented.

Prof. Klein discussed the valence bond theory predicting correctly the spin-multiplicity of the conju-

gated molecules in the ground state. The advantage was pointed out over the Longuet-Higgins' molecular orbital theory of NBMO and the advanced MO theory by Davidson and Borden. Prof. Weltner reported the matrix-isolated Cu_5, Mn_5 (S = 25/2) and other reactive intermediates such as C_4–C_9. Prof. Ovchinnikov presented a design and construction of molecular ferromagnets based on organic polymers. He proposed a new concept of transfer of spins; as long as the exchange interaction is strong in the main conjugated chain, those between the radical sites and the main chain can be very small. A number of other talks were focussed on poly(*m*-phenylenecarbenes) that had been pioneered by Japanese chemists in the nineteen sixties.

As Prof. Ovchinnikov has predicted exquisitely, this meeting will be memorized as the fisrst of a number of forthcoming international conferences of this kind that deal with molecular magnets.

The 28th Okazaki Conference

Solid State Chemistry with VUV Synchrotron Radiation

(February 5–7, 1987)

Organizers: H. Inokuchi *(IMS)*, **M. Watanabe** *(IMS)* **and K. Seki** *(Hiroshima Univ.)*
Invited Speakers: V. Saile *(HASYLAB)*, **I. Munro** *(Daresbury Lab.)*, **J. Klein** *(Strasbourg Univ.)*, **F.C. Brown** *(Illinois Univ.)*, **R. Stockbauer** *(NBS)* **and T.K. Sham** *(BNL)*

The principal topic was the interaction of VUV photons with bulk materials as an approach to the production of new materials with VUV photons. Much of the oscillator strength of materials lies in VUV, resulting in a major interaction between photons and materials in the VUV range. That is, many photoche-

mical, photophysical and even photobiological changes can be produced in that region and there is therefore the possibility to produce quite new materials using VUV photons. The topics were spectroscopy, photoelectron spectroscopy, time resolved spectroscopy, self-trapped exciton, defect formation, photodesorption, photofragmentation, photochemistry in solids and prospective projects.

Although solid state chemistry is a rather new field in association with synchrotron radiation research, the full and intensive discussions made us feel sure that the Conference has been a milestone in considering the production of new materials with VUV photons. A total number of 25 talks were presented, including 6 invited lectures. The programme, the collected abstracts and the list of participants are presented in UVSOR Activity Report 1986.

The Twenty-nineth Okazaki Conference

Molecular Aspects for Ion-Ion and Ion-Solvent Interactions in Solution

(May 26–28, 1987)

Organizers: H. Ohtaki *(Tokyo Inst. Tech.)*, **K. Saito** *(IMS)* **and S. Ishiguro** *(IMS)*
Invited Speakers: G.W. Neilson *(Univ. Bristol)*, **P.J. Rossky** *(Univ. Texas at Austin)*, **J.M.G.Barthel** *(Univ. Regensburg)* **and Y. Ducommun** *(Univ. Lausanne)*

The aim of this conference was to discuss ion-ion and ion-solvent interactions in solution on the basis of the microscopic structure of liquids, the solvated ions and complexes. The main subjects were (1) Structure of liquids, solvated ions and complexes studied by the diffraction methods. (2) Theoretical approaches to ion-solvent and solvent-solvent interactions. (3) Transport properties of ions and molecules. (4) Reaction equilibria and kinetics. The number of presentation including four invited lectures was 19 and about 80 people participated.

JOINT STUDIES PROGRAMS

As one of the important functions of an inter-university research institution, IMS undertakes joint studies programs for which funds are available to cover research expenses as well as travel and living expenses of individuals. The proposals from domestic scientists are reviewed and controlled by the inter-university committee. The programs are carried out under one of five categories:

1) Joint Studies on special projects (a special project of significant relevance to the advancement of molecular science can be carried out by a team of several groups of scientists).
2) Research Symposia (on timely topics in collaboration with both outside and IMS scientists).
3) Cooperative Research (carried out in collaboration with both outside and IMS scientists).
4) Use of Facility (the Computer Center, Instrument Center and other research facilities at IMS are open to all researchers throughout the country).
5) Joint studies programs using UVSOR facilities.
   a) Special Project, b) Cooperative Research, c) Use of UVSOR Facility.

In the fiscal year 1986, numbers of joint studies programs accepted amounted to 4, 9, 154 and 211 for categories 1)–4), respectively and 4, 24 and 59 for 5a)–5c), respectively.

1) Special Projects

Near Infrared Raman Spectroscopy of Doped Polyacetylene

Coordinators: **Jiro TANAKA** *(Nagoya University)*
Teizo KITAGAWA *(Department of Molecular Structure)*
Iwao YAMAZAKI *(Instrument Center)*

Raman spectra of alkaline metal doped polyacetylene were studied at various levels of doping for $(CHM_y)_x$ and $(CDM_y)_x$, M = Na and K, with y = 0–0.18. Several steps in the doping process can be recognized in changes of the Raman spectra; the initial Raman lines remain for y = 0–0.06 but change completely into a new pattern at y = 0.13. Raman and ESR spectra of alkaline metal doped β-carotene were measured as a model study of the alkaline metal doping of polyacetylene. The correlation of these spectra together with the ab initio SCF MO calculation on model compounds show that a heavily alkaline metal doped poly-acetylene chain does not have a uniform bond length structure but is composed of a charged soliton structure connected by a uniform chain. The new Raman bands were assigned based on this structure, implying that a bond alternation still exist in the metallic state of alkaline metal doped polyacetylene.

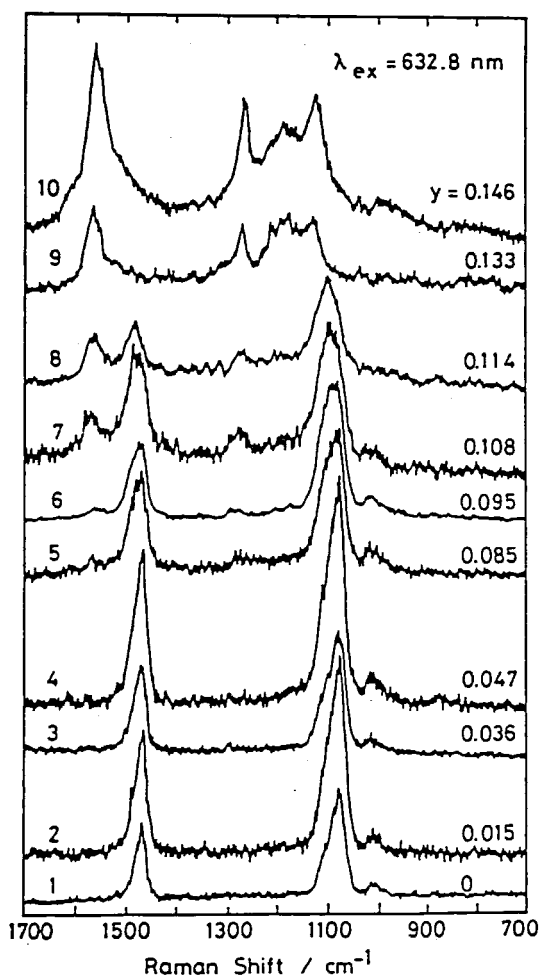

Figure 1. Raman spectra of thin *trans*-$(CH)_x$ film doped with Na; the composition is shown by the value of *y* value in $(CHNa_y)_x$

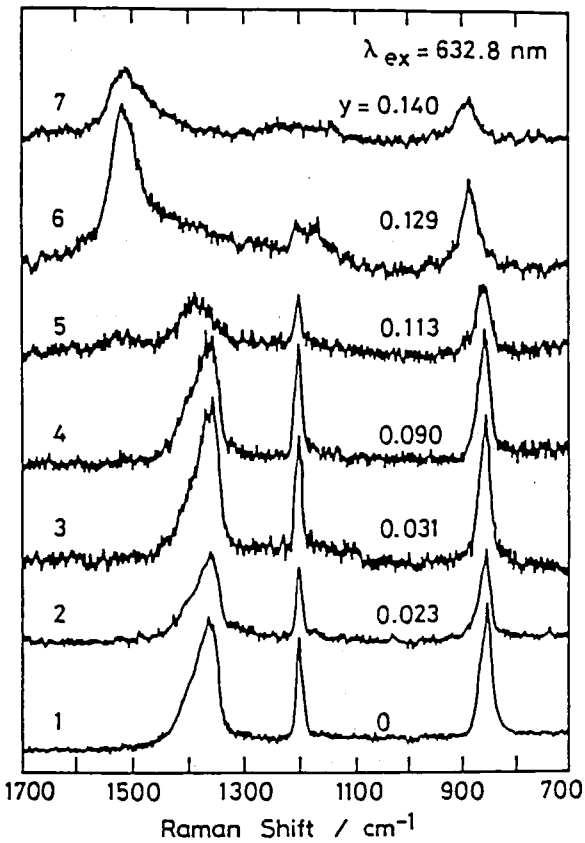

Figure 2. Raman spectra of *trans*-$(CD)_x$ film doped with Na. The content of Na is shown by y valued in the figure.

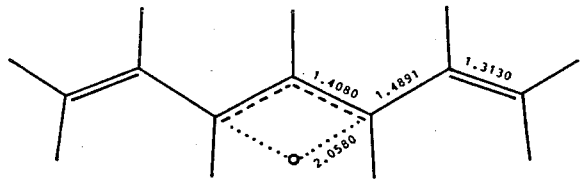

Figure 3. A model of charged soliton structure, C_7H_9LI, estimated by ab initio SCF MO calculation.

Cooperators: Masaaki Shimizu, Chizuko Tanaka, Masashi Tanaka and Kimihiko Hirao *(Nagoya University)*, Takayoshi Kobayashi *(University of Tokyo and IMS)*

References

1) J. Tanaka, Y. Saito, M. Shimizu, C. Tanaka and M. Tanaka, *Bull. Chem. Soc. Jpn.*, **60**, 1595 (1987).
2) C. Tanaka, J. Tanaka and K. Hirao, *Synth. Metals*, **17**, 19 (1987).

Molecular Mechanism of the Electron and Proton Transfers by Proteins and Their Coupling

Teizo KITAGAWA and Takashi OGURA *(Department of Molecular Dynamics)*, **Akio MAEDA** *(Kyoto University)*, **Nobuhito SONE** *(Jichi Medical School)*, **Yutaka ORII** *(Kyoto University)*, **Kohki OHONO** *(Jichi Medical School)*, **Hideo AKUTSU** *(Yokohama National University)* **and Masamitsu FUTAI** *(Osaka University)*

The vectorial proton translocation across the membrane against the concentration-gradient is known to be essential to production of biological energy but its molecular mechanism remains to be solved. This project aims to elucidate a mechanism of the proton translocation by proteins for three representative cases; 1) the electron-driven proton pump, 2) the light-driven proton pump, 3) a passive proton translocation. The first system is seen in the respiratory chain of aerobic organisms and out of three pumping sites, we pick up only site-III where cytochrome *c* oxidase pumps protons when electron are transferred to molecular oxygen. The electron transfer between two heme groups in this enzyme and the reduction mechanism of molecular oxygen have been investigated mainly with transient resonance Raman spectroscopy. For this experiment we constructed an artificial cardiovascular system which can regenerate enzymes to measure their spectra repeatedly. The timing of the proton translocation induced by the electron transfer will be determined by using photoreduction of the enzyme and the time-resolved fluorescence spectra for which the instruments have been completed recently. Drs. Ogura, Sone, and Orii are involved in this subject. The second system is seen in light-harvesting bacteria and we pick up two examples; one is bacteriorhodopsin which involves cis-trans isomerization of the retinal Schiff base and the subsequent proton transfer from the Schiff base to the protein moiety, and the other is a chromatophore which creates the pH gradient upon light illumination. Drs. Maeda, Ogura, and Ohno are involved in the former problem and our group at IMS has observed transient resonance Raman spectra with the pump-probe technique, while Dr. Akutsu treats the latter problem. The third system intends to study a molecular mechanism of the H^+-ATPase, which catalyzes the formation of ATP from ADP and P_i upon the proton translocation. Drs. Futai, Sone and Ohno are involved in this project.

Magnetic Field Effects upon Dynaimic Behavior of Excited Species

Coordinators: **Hisaharu HAYASHI** *(Inst. of Phys. and Chem. Res.)*, **Noboru MATAGA** *(Osaka Univ. and IMS)*, **Haruo ABE** *(Inst. of Phys. and Chem. Res. and IMS)*, **Yoshifumi TANIMOTO** *(Kanazawa Univ.)*

Recently, we have found magnetic field effects on many chemical reactions as well as on many energy transfer processes. The effects have provided us with new aspects in dynamic behavior of excited species. This new research field can be called "spin chemistry." For some of the effects, however, their mechanisms have not yet been clarified well. Therefore, one of the aims of this joint study is to investigate the mechanisms. Indeed, we have studied the effects on the gas-phase emission of CS_2 and Cs_2 with ns and ps dye lasers. On the other hand, we have made efforts to discover new magnetic field effects. In actuality, we have found the effects on the reactions of excited species (OH, CH, and NO) in flames and on the electron transfer and hydrogen abstraction reactions of chained molecules in solution. We hold a research symposium on this project (January 9th–10th, 1987). This joint study started in April, 1985.

The other members of the program are S. Nagakura (Okazaki National Inst.), H. Sakuragi (Univ. of Tsukuba and IMS), S. Tuchiya (Univ. of Tokyo), K. Mutai (Univ. of Tokyo), Y. Fujimura (Tohoku Univ. and IMS), Y. Hirata (Osaka Univ.), K. Iwai (Nara Women's Univ.), I. Yamazaki (Instrument Center), and R. Nakagaki (Electronic Structure).

Dynamics of Excited Molecules in the Gas Phase Produced by Collisions with Long-lived Excited Rare Gas Atoms

Kozo KUCHITSU *(University of Tokyo)*, **Eizi HIROTA, Kosuke SHOBATAKE, Tamotsu KONDOW** *(University of Tokyo)*, **Kaoru SUZUKI** *(University of Tokyo)*, **Takashi NAGATA** *(University of Tokyo)*, **Hiromichi UEHARA** *(Josai University)*, **and Hiroki NAKAMURA**

This joint program was undertaken in the period between 1985–87 to investigate the following projects:
(a)energy transfer, ionization and reaction processes of simple molecules and molecular clusters in collision with long-lived excited rare gas atoms and slow electrons, and
(b)optically forbidden states of the CN radical produced very efficiently by impact of metastable rare gas atoms.

Studies accomplished in this year are described briefly below:

(1)*Rotational excitation of N_2^+ and CO_2^+ produced by electron impact on N_2 and CO_2*[1,2]

The electron-impact ionization processes,

$$N_2(X^1\Sigma_g^+) + e \rightarrow N_2^+(X^2\Sigma_g^+) + 2e \quad (1)$$
$$CO_2(\tilde{X}^1\Sigma_g^+) + e \rightarrow CO_2^+(\tilde{X}^2\Pi_{3/2g}) + 2e \quad (2)$$

were studied by use of laser-induced fluorescence (LIF) and polarized LIF techniques as a function of electron-impact energy ranging from 25 to 300 eV.

The rotational energy of the nascent production, N_2^+, increased with decreasing electron energy from 2.26 ± 0.16 meV (300K) to 4.24 ± 0.27 meV (25 eV). This behavior is explained in tems of angular momentum transfer through multipole electron-molecule interaction. A slight anisotropic distribution of the rotation vector of $N_2^+(X^2\Sigma_g^+)$ indicates that ejection of a π_u electron is a dominant channel in the ionization process in the energy range of 80–300 eV.

In the case of CO_2, rotational excitation was also found to occur with decreasing electron-impact energy, where the rotational distributions obey Boltzmann behavior.

(2)*Rotational distribution of $NH(A^3\Pi, c^1\Pi)$ produced from NH_3 by impact of metastable helium atoms.*[3]

The dissociative excitation processes,

$$He(2^3S_1) + NH_3 \rightarrow He(1^1S_0) + NH(A^3\Pi/c^1\Pi) + 2H(1s) \quad (3)$$

are found to occur in a helium flowing afterglow by observation of the emission spectra of NH(A-X) and NH(c-a). These NH radicals are rotationally excited, having rotational energies of 0.3–0.5 eV. Their rotational districutions indicate that the rotational excitation of NH is caused by a torque exerted by the separating H atoms.

(3)*Collision of rare gas metastable atoms with cyanogen compounds – formation and spectroscopy of electronically-excited CN radicals*[4-6]

The electronical excited CN radical, CN*, was

produced in a flowing afterglow. Rotational line shifts and intensity anomalies in the CN violet band emission ($B^2\Sigma^+$-$X^2\Sigma^+$) were observed as a function of the ambient pressure of Ar or He in the flow tube. The cross sections, σ, of collisional relaxation in the rotational states of CN($^4\Pi$) and CN($A^2\Pi_i$) were estimated from the pressure dependece of the perturbed line intensities. The ratio of the cross sections for Ar and He was estimated to be σ_{Ar}/σ_{He} = 4.3.

The r-centroid dependences of the relative oscillator strengths of the $A^2\Pi_i$-$X^2\Sigma^+$ and the $B^2\Sigma^+$-$X^2\Sigma^+$ transitions are obtained by the measurements of emission intensities orginating from the same rovibronic level. The results can be explained in terms of the mixing of the $D^2\Pi_i$ state with the $A^2\Pi_i$ state, and the $E^2\Sigma^+$ state with the $B^2\Sigma^+$ state.

On the other hand, the vibrational quantum numbers of the perturbing the $^4\Pi$ state with the $B^2\Sigma^+$ state was determined from the magnitudes of the spin-orbit interaction causing the perturbation at v_B = 14 and 17. It is concluded that the perturbations occur at (v_B, v_π) = (9, 1), (12, 4), (14, 7), (17, 12) and (18, 14).

(4) *Electron attachment to van der Waals clusters*

The studies on the formation of negative ions from a variety of van der Waals clusters in collision with high-Rydberg rare gas atoms and slow electrons were continued. In this year the isotope effects on the electron attachment cross sections fro NH_3/ND_3, CH_3CN/CD_3CN and $(CH_3)_2CO/(CD_3)_2CO$ were investigated. In the cases of NH_3/ND_3 and $(CH_3)_2CO/(CD_3)_2CO$ the cross sections for the deuterated clusters were much smaller than those for the normal clusters, especially when the cluster sizes were small. These isotope effects provide information on the negative ion states of the clusters related to the attachment processes. The dependences of the cross sections on the cluster size can be explained qualitatively by a coupling of the incoming electron and the cluster vibration.

References

1) T. Nagata, A. Nakajima, T. Kondow and K. Kuchitsu, *J. Chem. Phys.* (in press)
2) T. Nagata, A. Nakajima, T. Kondow and K. Kuchitsu, *Chem. Letters* (in press)
3) K. Someda, T. Kondow and K. Kuchitsu, *J. Phys. Chem.* (in press)
4) K. Kanda, M. Thesis, The University of Tokyo (1987).
5) H. Ito, Ph.D. Thesis, The University of Tokyo (1987).
6) H. Ito, Y. Ozaki, K. Suzuki, T. Kondow and K. Kuchitsu, *Chem. Phys. Letters* **139**, 581 (1987).
7) T. Kondow, *J. Phys. Chem.* **91**, 1307 (1987).
8) T. Kondow and K. Kuchitsu, *Mass Spectrosc.* **34**, 339 (1986).

2) Research Symposia

1. Molecular Mechanisms of Oxygen Activation by Metal Complexes
   (January 7th – 9th, 1987)
   Organizer: M. Morishima (Kyoto Univ.)
2. Magnetic Field Effects upon Dynamic Behavior and Chemical Reactions of Excited Molecules
   (January 9th – 10th, 1987)
   Organizer: H. Hayashi (Inst. of Phys. and Chem. Res.)
3. Atom-Molecule Collisions and Chemical Reactions with Nonadiabatic Transitions
   (February 23rd – 25th, 1987)
   Organizer: Y. Kaneko (Tokyo Metropolitan Univ.)
4. Electronic Structure Theories
   (March 9th, 1987)
   Organizer: K. Morokuma (IMS)
5. High-resolution Spectra of Short-lived Molecules
   (March 12th – 14th, 1987)
   Organizer: E. Hirota (IMS)
6. Novel Functional Materials: Organic/Inorganic Intermediates
   (March 19th – 20th, 1987)
   Organizer: H. Inokuchi (IMS)
7. Relaxation Processes of Photoexcited Isolated Molecular Complexes and Clusters
   (March 30th – 31st)
   Organizer: K. Shobatake (IMS)
8. Studies on High-Tc Oxide Superconducters
   (June 4th – 6th, 1987)
   Organizer: F. Takei (Univ. of Tokyo)
9. Molecular Basis of Laser-induced Surface Processes
   (June 26th – 27th, 1987)
   Organizer: H. Masuhara (Kyoto Inst. of Tech.)

3) Cooperative Research

This is one of the most important programs IMS undertakes for conducting its own research of the common interest to both outside and IMS scientists by using the facilities at IMS. During the first half of fiscal

year of 1986 ending on September 30, 74 outside scientists including 6 invited collaborated with IMS scientists; and during the second half of the fiscal year, 80 outside scientists including 4 invited worked in collaboration with IMS scientists, the names and the affiliations of these collaborators are found in the Research Activities.

4) Use of Facility

The number of projects accepted for the Use of Facility Program of the Computer Center during the fiscal year of 1986 amounted to 153 (458 users), and the computer time spent for these projects is 3019 hours (converted to the HITAC M-680 time), and amounts to 53% of the total annual CPU time used.

Fifty four projects (91 users) were accepted for the Use of Facility Program of the Instrument Center during the fiscal year of 1986.

5) UVSOR

Joint studies programs using UVSOR facilities are carried out under one of three categories: 5-a) UVSOR Special Project, 5-b) UVSOR Cooperative Research, and 5-c) Use of UVSOR Facility.

The 8th UVSOR Research Symposium, organized by H. Inokuchi (IMS), was held during December 8th – 9th, 1986.

5-a) UVSOR Special Project

Studies of Negative Ion Formation by Two-Electron Capture of Positive Molecular Ions from Alkali Atoms

Coordinators: **Toshio SUGIURA** *(Univ. of Osaka Prefecture)*
Inosuke KOYANO *(Department of Molecular Assemblies)*

The neutral beam injection into a magnetically-confined fusion reactor is an issue of current concern as a means of auxiliary heating of fusion plasma. One of the most promising techniques for producing the fast ($E \gtrsim 100$ keV) neutral beams required for this purpose is the generation and subsequent neutralization of fast negative ion beams. Basic studies of processes producing negative ions are urgently required for the development of the fast beam sources.

From this point of view, we are conducting the title studies as a special project at the BL3B beam line of the UVSOR facility. One of the main objectives is to investigate the effects of vibrational excitation of the positive molecular ions on the efficiency of this electron capture processes. As a first experiment, we study the H^- formation from H_2^+ by (two-step) two-electron capture from Cs. Vibrationally excited H_2^+ ions are produced by photoionization at the threshold wavelengths for the individual vibrational states and the product H^- ions, obtained by passing them through a Cesium oven, are detected in coincidence with the threshold photoelectrons to select the products coming from a single vibrational state of interest.

Far-infrared Spectroscopy under High Pressure using Synchrotron Radiation

Coordinators: **Takao Nanba** *(Tohoku Univ.)*
Makoto Watanabe *(Research Facilities)*

The transmission measurement system in the far-infrared region under high pressure up to 5 G Pa at low temperature was designed and now under construction at the far-infrared beam line BL6A1 of UVSOR. The experiment at BL6A1 showed that the high brightness of the synchrotron radiation makes possible the spectroscopic study on small specimens even under high pressure using a diamond anvil cell, which has been very difficult by the use of the conventional light source.

Our main subject is the direct observation of the change in the optical phonon spectrum of the single crystal possessing an inversion symmetry after the phase transition induced by high pressure. Such observation has not yet been done because of its Raman inactive character. The measurement will be made in the next fiscal year.

Fluorescence Spectroscopic Studies of Photochemical Reactions Using Synchrotron Radiation as a Light Source

Coordinator: **Kosuke SHOBATAKE** *(Department of Molecular Assemblies)*

This group project is to organize the research efforts aimed at studying the photochemical reactions initiated by irradiation of UV and vacuum uv light using the vapor phase fluorescence apparatus installed on the beam line BL2A at the UVSOR synchrotron radiation facility. The fiscal year of 1986 ending on March 31, 1987 was the last year of this two-year project. For the past year we have succeeded in studying free jet spectroscopy using synchrotron radiation as the light source, which was the main purpose of constructing the fluorescence apparatus. One is now able to carry out direct absorption measurements of free jet molecules and clusters. Brief accounts using the newly introduced technique are made in the Research Activities (IV-N-3~5).

For the past year fluorescence studies of gaseous chemical reactions have been continued. One can now routinely measure absorption, fluorescence excitation, dispersed fluorescence, and time correlated fluorescence decay spectra of gaseous samples in a gas cell in the wavelength region 200–105 nm. Some of the results are presented in the Research Activities IV-N-1~2 of the present issue.

Synchrotron Radiation Photoionization Spectroscopy of Molecules and Molecular Clusters in Supersonic Jets

Coordinator: **Katsumi KIMURA** *(Department of Molecular Assemblies)*

The supersonic molecular beam apparatus constructed on the Beam Line BL2B2 has been further improved during the past one year in several points mainly by H. Shiromaru, in cooperation with several other collaborators who join in this Project. Several kinds of photoionization threshold measurements have been carried out with a quadrupole mass filter. One of the studies in this Project is the determination of the C-H bond dissociation energies of ethylene and acetylene by observation of the threshold energies of H^+ formation by synchrotron radiation, in cooperation with Prof. Y. T. Lee of Berkeley (see IV-K-1). The second subject is the study of water cluster ions by synchrotron radiation: It has been found that various kinds of protonated and unprotonated water cluster ions are produced by photoionization of water-argon and water-CO_2 mixed clusters produced in supersonic jets (see IV-K-2). We have also determined the appearance potentials of small cluster ions from photoionization efficiency curves measured by synchrotron radiation (see IV-K-2).

5-b) UVSOR Cooperative Research

During the first half of fiscal year of 1986, 12 outside scientists including 4 invited collaborated with IMS scientists; and during the second half of the fiscal year, 12 outside scientists including 5 invited worked in collaboration with IMS scientists.

5-c) Use of UVSOR Facility

The number of projects accepted for the Use of UVSOR Facility Program during the fiscal year of 1986 amounted to 59.

FOREIGN SCHOLARS

Visitors from abroad play an important role in research activities and are always welcome at IMS. The following is the list of foreign scientists who visited IMS in the past year (Aug. 1986 – July 1987). The sign *1 indicates an attendant to an Okazaki Conference, *2 an IMS or Japan Society for the Promotion of Science Invited Foreign Scholar, *3 an IMS councillor, *4 an IMS visiting scientist and *5 an IMS adjunct professor or associate professor from abroad.

Prof. J.R. Grover*5	Brookhaven Natl. Lab.	(USA)	Jun. 1986 – Apr. 1987
Prof. S.-O. Oh*2	Kyungpook Natl. Univ.	(Korea)	Jul. – Aug. 1986
Prof. H.-S. Yoo*2	Chungbuk Natl. Univ.	(Korea)	Jul. – Aug. 1986
Prof. D. Kleppner	Massachusetts Inst. of Tech.	(USA)	Aug. 1986
Prof. K. Heinzinger	Max-Planck-Inst. Chem.	(FRG)	Aug. 1986
Prof. R.J. Boyd	Dalhousie Univ.	(Canada)	Aug. 1986
Prof. S.F. Nelsen	Univ. of Wisconsin	(USA)	Aug. 1986
Prof. T.G. Traylor	Univ. of California, San Diego	(USA)	Aug. 1986
Dr. Z. Slanina	Czech. Acad. Sci.	(CSK)	Aug. 1986
Prof. V.S. Letokhov	Inst. Spectroscopy	(USSR)	Aug. 1986
Dr. A. Puretzky	Inst. Spectroscopy	(USSR)	Aug. 1986
Dr. H. Hiraoka	Res. Lab., IBM, San Jose	(USA)	Aug. 1986
Prof. M.S. Jhon	Korea Adv. Inst. Sci. Tech. (KAIST)	(Korea)	Aug. 1986
Dr. T.B. Tang*4	Hong Kong Baptist Coll.	(Hong Kong)	Aug. 1986
Prof. P.V. Schleyer	Univ. Erlangen-Nuernberg	(FRG)	Aug. – Sep. 1986
Dr. M.-W. Ruf	Univ. Kaiserslautern	(FRG)	Aug. – Sep. 1986
Prof. P.N. Skancke*4	Univ. Tromsö	(Norway)	Aug. – Dec. 1986
Prof. E.M. Kosower	Tel-Aviv Univ.	(Israel)	Sep. 1986
Prof. R. Rigler	Karolinska Inst.	(Sweden)	Sep. 1986
Prof. Z.-K. Jiang	Inst. Atom. Mol. Phys., Jilin Univ.	(China)	Sep. 1986
Prof. Z.-W. Wang	Inst. Atom. Mol. Phys., Jilin Univ.	(China)	Sep. 1986
Prof. J.-M. Li*2	Inst. Phys., Beijing, Chinese Acad. Sci.	(China)	Sep. 1986
Dr. P. Froelich	Uppsala Univ.	(Sweden)	Sep. 1986
Dr. J.M. Basset*2	Inst. Rech. Catal., CNRS	(France)	Sep. 1986
Dr. J.P. Gromiec	Inst. Occup. Med., Łódz'	(Poland)	Sep. 1986
Dr. L.A. Gromiec	Technic. Univ. Łódz'	(Poland)	Sep. 1986
Prof. D.J. Klein*1	Texas A and M Univ.	(USA)	Sep. 1986
Prof. A.A. Ovtchinnikov*1	Inst. Chem. Phys., Moscow	(USSR)	Sep. 1986
Prof. W. Weltner Jr.*1	Univ. of Florida	(USA)	Sep. 1986
Prof. T. Oka	Univ. of Chicago	(USA)	Sep. 1986
Prof. G.C. Schatz	Northwestern Univ.	(USA)	Sep. 1986
Prof. K. Müllen	Univ. of Mainz	(FRG)	Sep. 1986
Prof. N.T. Yu	Georgia Inst. of Tech.	(USA)	Sep. 1986
Mr. J. Groot*4	Univ. of York	(UK)	Sep. – Dec. 1986
Prof. R.F. Borkman	Georgia Inst. of Tech.	(USA)	Oct. 1986
Dr. D.K. Evans	AECL Res. Co., Can.	(Canada)	Oct. 1986

Prof. D. Kreysig	Humboldt-Univ. Berlin	(GDR)	Oct. 1986
Prof. A. Bianconi*2	Univ. Roma	(Italy)	Oct. 1986
Prof. R. Sustmann*2	Univ. Essen	(FRG)	Oct. 1986
Prof. A. Rieker	Eberhard-Karls-Univ. Tübingen	(FRG)	Oct. 1986
Prof. M.L. Ginter	Univ. of Maryland	(USA)	Oct. 1986
Dr. R.G. Crystal	Xerox Res. Cent. of Canada	(Canada)	Oct. 1986
Dr. R.H. Marchessault	Xerox Res. Cent. of Canada	(Canada)	Oct. 1986
Prof. W.S. Caughey*2	Colorado State Univ.	(USA)	Oct. 1986
Prof. H. Motz	Oxford Univ.	(UK)	Oct. 1986
Prof. F. Petit	CNRS, ENSC, Lille	(France)	Oct. 1986
Prof. S.R. Leone	Univ. of Colorado	(USA)	Oct. 1986
Dr. K. Kemnitz*4	Columbia Univ.	(FRG)	Oct. – Nov. 1986
Prof. S.M.B. Costa*2	Inst. Super. Tec.	(Portugal)	Oct. 1986 – Feb. 1987
Mrs. P. Wang*2	Inst. Chem., Acad. Sin.	(China)	Oct. 1986 – Sep. 1987
Prof. T. Yan	Inst. High Energy Phys., Acad. Sin.	(China)	Nov. 1986
Dr. C.-Y. Mok*2	Natl. Univ. Singapore	(Singapore)	Nov. 1986
Prof. S. Mu	Yangzhou Teach. Coll	(China)	Nov. 1986
Prof. F. Wang	Changchun Inst. Appl. Chem., Acad. Sin.	(China)	Nov. 1986
Prof. J. Peng	Hunan Univ.	(China)	Nov. 1986
Prof. P. He	Univ. Sci. Tech. China	(China)	Nov. 1986
Prof. T. Liu	Inst. Chem., Acad. Sin.	(China)	Nov. 1986
Dr. S. Zhou	Inst. Chem., Acad. Sin.	(China)	Nov. 1986
Dr. Y. Chang	Inst. Chem., Acad. Sin.	(China)	Nov. 1986
Prof. Z. Liu	Northwest Univ.	(China)	Nov. 1986
Prof. H. Zhang	Shanghai Jiao Tong Univ.	(China)	Nov. 1986
Prof. R. Qian	Inst. Chem., Acad. Sin.	(China)	Nov. 1986
Dr. J. Bei	Inst. Chem., Acad. Sin.	(China)	Nov. 1986
Dr. P. Wu	Inst. Chem., Acad. Sin.	(China)	Nov. 1986
Prof. D. Zhu	Inst. Chem., Acad. Sin.	(China)	Nov. 1986
Dr. M. Qian	Inst. Chem., Acad. Sin.	(China)	Nov. 1986
Dr. M. Guo	Tianjin Inst. Power Sources	(China)	Nov. 1986
Prof. S. Chen	Inst. Chem., Acad. Sin.	(China)	Nov. 1986
Prof. C. Zhao	Northeast Normal Univ.	(China)	Nov. 1986
Prof. X. Sun	Fudan Univ.	(China)	Nov. 1986
Dr. S. Lin	Shanghai Inst. Nucl. Res., Acad. Sin.	(China)	Nov. 1986
Prof. Y. Cao	Inst. Chem., Acad. Sin.	(China)	Nov. 1986, Jul. – Aug. 1987
Dr. S. Li	Inst. Chem., Acad. Sin.	(China)	Nov. 1986
Prof. B. Yan	Inst. Chem., Acad. Sin.	(China)	Nov. 1986
Dr. J.T. Hougen*4	Natl. Bur. of Stand. (NBS)	(USA)	Nov. 1986
Dr. C. Wallace	Natl. Sci. Found. (NSF)	(USA)	Nov. 1986
Prof. D.N. Hendrickson	Univ. of Illinois	(USA)	Nov. 1986
Dr. I. Plazibat*4	Univ. Split	(Yugoslavia)	Nov. 1986 – Sep. 1987
Dr. V.A. Pestunovitch	Irkutsk. Inst. Org. Khim	(USSR)	Dec. 1986
Prof. G.L. Geoffroy	Pennsylvania State Univ.	(USA)	Dec. 1986
Prof. Yu.A. Ustynyug	Lomonosov Moscow State Univ.	(USSR)	Dec. 1986

Prof. M. Stockburger	Max-Planck-Inst. Biophys. Chem.	(FRG)	Dec. 1986
Prof. G.H. Atkinson	Univ. of Arizona	(USA)	Dec. 1986
Prof. H.-S. Yoo*[2]	Chungbuk Natl. Univ.	(Korea)	Dec. 1986 – Feb. 1987
Prof. M. Mizushima	Univ. of Colorado	(USA)	Dec. 1986
Prof. J.T. Groves*[2]	Princeton Univ.	(USA)	Jan. 1987
Prof. P.G. Mezey*[2]	Univ. of Saskatchewan	(Canada)	Jan. – Feb. 1987
Prof. P.-S. Song*[2]	Univ. of Nebraska	(USA)	Jan. – Mar. 1987
Prof. I. Munro*[2]	Daresbury Lab., SERC	(UK)	Jan. – May 1987
Prof. I. Röeggen*[4]	Univ. Tromsö	(Norway)	Jan. – Jun. 1987
Prof. A.L. Verma*[5]	North-Eastern Hill Univ.	(India)	Jan. – Dec. 1987
Dr. B. Dobson	Daresbury Lab., SERC	(UK)	Feb. 1987
Dr. R. Stockbauer*[1]	Natl. Bur. of Stand. (NBS)	(USA)	Feb. 1987
Dr. T.K. Sham*[1]	Brookhaven Natl. Lab.	(USA)	Feb. 1987
Dr. V. Saile*[1]	Hamburg Sychrotronstrahlungs-Lab. HASYLAB, DESY	(FRG)	Feb. 1987
Prof. J. Klein*[1]	Univ. Louis Pasteur	(France)	Feb. 1987
Prof. F.C. Brown*[1]	Univ. of Illiois	(USA)	Feb. 1987
Mr. Y. Wen*[4]	Inst. Chem., Acad. Sin.	(China)	Feb. 1987 – Feb. 1988
Dr. M. Kryszewski	Cent. Mol. Macromol. Stud., Pol. Acad. Sci.	(Poland))	Feb. 1987
Mr. J.J. Wrenn	Massachusetts Inst. of Tech.	(USA)	Feb. 1987
Dr. J. Hautaluoma	Natl. Sci. Found. (NSF)	(USA)	Mar. 1987
Prof. R.S. Becker*[2]	Univ. of Houston	(USA)	Mar. 1987
Dr. U. Bardi	Univ. Firenze	(Italy)	Mar. 1987
Prof. K.E. Gubbins*[2]	Cornell Univ.	(USA)	Mar. 1987
Dr. J. Jackson*[2]	Cornell Univ.	(USA)	Mar. 1987
Mr. W. Chapman*[2]	Cornell Univ.	(USA)	Mar. 1987
Prof. J. Friedrich	Univ. Bayreuth	(FRG)	Mar. 1987
Prof. R.G. Parr*[3]	Univ. of North Carolina	(USA)	Mar. 1987
Dr. B. Brocklehurst	Univ. of Sheffield	(UK)	Mar. 1987
Prof. S.-F. Tan	Natl. Univ. Singapore	(Singapore)	Mar. 1987
Dr. J. Eichler	Hahn-Meitner Inst. Kernforsch.	(FRG)	Mar. – Apr. 1987
Dr. J. Boright	Natl. Sci. Found. (NSF)	(USA)	Apr. 1987
Prof. A. Fontaine*[2]	Univ. Paris-Sud	(France)	Apr. 1987
Prof. R.D. Brown	Monash Univ.	(Australia)	Apr. 1987
Prof. J.C. Polanyi	Univ. of Toronto	(Canada)	Apr. 1987
Dr. G. Black*[5]	SRI Int.	(USA)	Apr. 1987 – May 1988
Mr. A.K. Campen*[4]	Univ. of Southampton	(UK)	Apr. – Oct. 1987
Prof. J.J. Valentini	Univ. of California, Irvine	(USA)	May 1987
Prof. R.F. Curl	Rice Univ.	(USA)	May 1987
Prof. R.D. McKelvey*[2]	Univ. of Wisconsin	(USA)	May – Nov. 1987
Dr. A.J. Dann*[2]	Univ. of Nottingham	(UK)	May 1987 – May 1988
Prof. R.E. Weston	Brookhaven Natl. Lab.	(USA)	Jun. 1987
Dr. K. Kleinermanns	Phys. Chem. Inst., Ruprecht-Karls-Univ.	(FRG)	Jun. 1987
Prof. D. Wertz	North Carolina State Univ.	(USA)	Jun. 1987
Prof. M.K. DeArmond	North Carolina State Univ.	(USA)	Jun. 1987

Prof. F. Wang*[2]	Hefei Natl. Synch. Rad. Lab., Univ. Sci. Tech. China	(China)	Jun. 1987
Dr. D. Jiang	Hefei Natl. Synch. Rad. Lab., Univ. Sci. Tech. China	(China)	Jun. 1987
Prof. G.D. Zhang	Hefei Natl. Synch. Rad. Lab., Univ. Sci, Tech. China	(China)	Jun. 1987
Mr. P.F. Jiang	Hefei Natl. Synch. Rad. Lab., Univ. Sci. Tech. China	(China)	Jun. 1987
Dr. X. Wang	Hefei Natl. Synch. Rad. Lab., Univ. Sci. Tech. China	(China)	Jun. 1987
Dr. J.P. Wang*[4]	Hefei Natl. Synch. Rad. Lab., Univ. Sci. Tech. China	(China)	Jun. 1987
Dr. I. Sasaki	Univ. Paris-Sud	(France)	Jun. 1987
Prof. O.A. Anisimov	Inst. Chem. Kinet. Combust.	(USSR)	Jun. 1987
Dr. S.C. Park*[2]	Kangweon Natl. Univ.	(Korea)	Jun. – Aug. 1987
Mr. X. Xu*[4]	Hefei Natl. Synch. Rad. Lab., Univ. Sci. Tech. China	(China)	Jun. – Aug. 1987
Mr. C.G. Xu*[4]	Hefei Natl. Synch. Rad. Lab., Univ. Sci. Tech. China	(China)	Jun. – Aug. 1987
Mr. D.-K. Jiang*[4]	Hefei Natl. Synch. Rad. Lab., Univ. Sci. Tech. China	(China)	Jun. – Aug. 1987
Prof. P.G. Wolynes*[5]	Univ. of Illinois	(USA)	Jun. 1987 – Jan. 1988
Prof. H. Toftlund*[5]	Univ. Odense	(Denmark)	Jul. 1987 – Mar. 1988
Prof. A.M. Sargeson	Australian Natl. Univ.	(Australia)	Jul. 1987
Prof. D. Xian*[2]	Inst. High Energy Phys., Acad. Sin.	(China)	Jul. 1987
Dr. A.F. Findeis	Natl. Sci. Found. (NSF)	(USA)	Jul. 1987
Prof. J.M. Lee	Chonbuk Natl. Univ.	(Korea)	Jul. – Aug. 1987
Dr. D. Kim*[2]	Korea Stand. Res. Inst.	(Korea)	Jul. – Aug. 1987
Prof. H. Kim*[2]	Seoul Natl. Univ.	(Korea)	Jul. – Sep. 1987

AWARD

Prof. Hirota's Scientific Achievement

Prof. Eizi Hirota received the Award of the Chemical Society of Japan in 1987 for his contribution to "Structural Studies on Short-lived Molecules by High Resolution Spectroscopy".

Since his graduation from the University of Tokyo, Prof. Hirota has been interested in determining precise structure of molecules and has developed theoretical as well as experimental studies. He started his works with electron diffraction and microwave spectroscopy. At the initial stages, he analyzed rotational spectra of molecules in vibrationally excited states and later treated more complicated molecules with rotational isomers and determined the potential barriers for internal rotation. A unique idea was applied to measure microwave spectra of highly symmetric molecules where the molecular symmetry was reduced by isotope substitutions and thus creating dipole moment in the molecules. While working at the Kyushu University in 1970's, he constructed a new spectrometer for the measurement of microwave spectra of short-lived molecules such as free radicals and molecular ions. After he moved to IMS in 1975, he improved the instrumentation which enabled studies on polyatomic radicals such as $CH_3O\cdot$ and $CH_2 = CHO\cdot$. In addition, he constructed many kinds of systems to measure high-resolution infrared spectra of reaction intermediates and developed various novel techniques to get high sensitivity. In particular, he is the first person who applied IR-diode lasers to the high-resolution spectroscopy of short-lived molecules. Through these developments, he has succeeded in the first observation and analysis of a number of important free radicals and molecular ions. Among those works, the first observation of the CH_3 radical and the related extensive studies are the most notable in view of its important role in various chemical processes. These days he is a worldwide leader in this fundamental scientific field. His works have also been greatly contributing to the development of other research fields such as the investigation of interstellar molecules.

LIST OF PUBLICATIONS

N. KOGA and K. MOROKUMA, "Transition State for Carbonyl and Olefin Insertion Reactions", in "Quantum Chemistry: The Challenge of Transition Metals and Coordination Chemistry", A. Veillard Ed., D. Reidel Publishing Co., p.351 (1986).

K. KOGA and K. MOROKUMA, "Mechanism of Carbonyl Insertion Reaction of Pd and Pt Complexes. An ab initio MO Study", *J. Am. Chem. Soc.*, **108**, 6136 (1986).

K. YAMASHITA and K. MOROKUMA, "A Molecular Orbital Study of Protonated N_2O", *Chem. Phys. Lett.*, **131**, 237 (1986).

J. ARAFUNE, N. KOGA, K. MOROKUMA, and T. WATANABE, "Estimate of Molecular Effects on the Neutrino Mass Determination by Triton β Decay", *J. Phys. Soc. Jpn.*, **55**, 3806 (1986).

J. ARAFUNE, N. KOGA, K. MOROKUMA, and T. WATANABE, "Molecular Final-State Interactions in Triton β Decay", *J. Phys. Soc. Jpn.*, **55**, 3813 (1986).

Z. LATAJKA, H. RATAJCZAK, K. MOROKUMA, and W. J. ORVILLE-THOMAS, "Study of Correlation Effects on Stretching Force Constants of the $H_3N\cdots LiF$ Lithium-Bonded and $H_3N\cdots HF$ Hydrogen-Bonded Complexes", *J. Mol. Str.*, **146**, 263 (1986).

K. OHTA and K. MOROKUMA, An Ab Initio MO Study on Electron Transfer in Gas-Phase Hydrated Clusters: $O_2^-(H_2O)_n + O_2 \rightarrow O_2 + O_2^-(H_2O)_n$ (n = 0, 1, and 2), *J. Phys. Chem.*, **91**, 401 (1987).

K. MOROKUMA and H. SUGETA, "Ab Initio Derivative Calculation of Vibrational Circular Dichroism", *Chem. Phys. Lett.*, **134**, 23 (1987).

X. -Y. FU, R. -Z. LIU, and K. MOROKUMA, "An Ab Initio MO Study of the Hydrogen Bond Complex between Cyclopropane and Hydrogen Fluoride", *J. Mol. Sci. (Wuhan, China)* **5**, 21 (1987).

K. YAMANOUCHI, S. KATO, K. MOROKUMA, M. SUGIE, H. TAKEO, C. MATSUMURA, and K. KUCHITSU, "Nuclear Quadrupole Coupling Tensors for Hydrazine, Methylhydrazine, and 1,2-Dimethylhydrazine as Determined by Microwave Spectroscopy and Ab Initio Calculation", *J. Phys. Chem.*, **91**, 828 (1987).

N. KOGA, C. DANIEL, J. HAN, X. Y. FU, and K. MOROKUMA, "Potential Energy Profile of a Full Catalytic Cycle of Olefin Hydrogenation by the Wilkinson Catalyst.", *J. Am. Chem. Soc.*, **109**, 3455 (1987).

K. YAMASHITA, S. YABUSHITA, K. MOROKUMA, and I. KUSUNOKI, "Reply to Comment by Farnell and Ogilvie on "Ab Initio Calculations of Doublet States of NH^+"", *Chem. Phys. Lett.*, **137**, 193 (1987).

S. SAKAI and K. MOROKUMA, "Theoretical Studies on the Acetylene-Vinylidene Rearrangement with a Metal Atom (Li, Be, B, Na, Mg, and Al)", *J. Phys. Chem.*, **91**, 3661 (1987).

S. NAKAMURA, M. TAKAHASHI, R. OKAZAKI, and K. MOROKUMA, "An Ab Initio MO Study of Isomers of HNS_2 and HNO_2", *J. Am. Chem. Soc.*, **109**, 4142 (1987).

P. N. SKANCKE, K. YAMASHITA, and K. MOROKUMA, "A Theoretical Study of Thermal Reactions of Bicyclo[2.1.0]pent-2-ene", *J. Am. Chem. Soc.*, **109**, 4157 (1987).

I. OHMINE, "Energy Dissipation Mechanism of the Optically Excited Molecules in Solvents; A Trajectory Study for a Photoisomerization Process of the π-Conjugated Molecule in Ar and Water", *J. Chem. Phys.*, **85**, 3342 (1986).

H. TANAKA, "Integral Equation and Monte Carlo Study on Hydrophobic Effects: Size Dependence of Apolar Solutes on Solute-Solute Interactions and Structures of Water", *J. Chem. Phys.*, **86**, 1512 (1987).

H. NAKAMURA, A. OHSAKI and M. BAER, "New Implementation to Approximate Quantum Mechanical Treatment of Atom-Diatom Chemical Reactions", *J. Phys. Chem.*, **90**, 6176 (1986).

K. TAKATSUKA and H. NAKAMURA, "Semiclassical Theory in Phase Space for Molecular Processes III. Electronically Nonadiabatic Transitions in Multidimensional Systems", *J. Chem. Phys.*, **85**, 5779 (1986).

M. BAER, H. NAKAMURA and A. OHSAKI, "A Quantum Mechanical Study of Chemical Reaction and Charge Transfer Processes in the $(Ar+H_2)^+$ System", *Chem. Phys. Lett.*, **131**, 468 (1986).

K. NAKASHIMA, H. TAKAGI and H. NAKAMURA, "Dissociative Recombination of H_2^+, HD^+, and D_2^+ by Collisions with Slow Electrons", *J. Chem. Phys.*, **86**, 726 (1987).

M. BAER and H. NAKAMURA, "Quantum Mechanical Studies of Ion-Molecule Reactions: The $He+H_2^+$ and the

$(Ar+H_2)^+$ Systems", *J. Phys. Chem.*, **91** (1987).

K. NASU, "BCS Pairing versus Bipolaron Crystallization in One- and Two- Dimensional Strongly Coupled Electron-Phonon Systems", *Physica,* **143B**, 229 (1986).

K. NASU, "Possibility of Organic Ferromagnet, Polycarbene", *Synthetic Metals,* **19**, 111 (1987).

K. NASU, "Many-Polaron Theory for Superconductivity and CDW in a Strongly Coupled Electron-Phonon System with Quasi Two-Dimensionality, --- An Interpolation between Adiabatic Limit and Inverse-Adiabatic Limit", *Phys. Rev. B.*, **35**, 1748 (1987).

A. MISHIMA and K. NASU, "Effect of Next-Nearest Neighbour Site Transfer Integral and Nearest Neighbour Site Coulomb Interaction on the Quasi-One-Dimensional Organic Ferromagnet, m-Polydiphenylcarbene", *Synthetic Metals,* **19**, 75 (1987).

X. SUN, C. WU, R. FU, S. XIE and K. NASU, "The Vibrational Modes around Soliton in Strong-Coupled One-Dimensional Electron-Lattice Systems", *Phys. Rev.*, **35**, 4102 (1987).

K. OHNO, H. MATSUURA, Y. ENDO, and E. HIROTA, "The Microwave Spectra of Deuterated Silances, Germanes, and Stannanes.", *J. Mol. Spectrosc.*, **118**, 1 (1986).

K. NAKAGAWA, T. KOJIMA, and E. HIROTA, "Diode Laser Spectrum of the ν_8 Band of CH_3SH.", *Bull. Chem. Soc. Jpn.*, **59**, 2935 (1986).

Y. ENDO, S. SAITO, and E. HIROTA, "The Microwave Spectrum of the Thiomethoxy Radical CH_3S.", *J. Chem. Phys.*, **85**, 1770 (1986).

S. SAITO , Y. ENDO, and E. HIROTA, "The Microwave Spectrum of the PF_2 Raidcal in the $\tilde{X}^2B_1$ Ground State.", *J. Chem. Phys.*, **85**, 1778 (1986).

E. HIROTA, "Third-Order Anharmonic Potential Constants and Equilibrium Structures of the Formyl and Hydroperoxyl Radicals.", *J. Mol. Struct.*, **146**, 237 (1986).

Y. ENDO, S. TSUCHIYA, C. YAMADA, E. HIROTA, and S. KODA, "Microwave Kinetic Spectroscopy of Reaction Intermediates: O+Ethylene Reaction at Low Temperature.", *J. Chem. Phys.*, **85**, 4446 (1986).

K. MATSUMURA, K. KAWAGUCHI, E. HIROTA, and T. TANAKA, "Stark Modulation Infrared Diode Laser Spectroscopy of the $\nu_6+\nu_8$ Band of Diacetylene.", *J. Mol. Spectrosc.*, **118**, 530 (1986).

Y. KAWASHIMA, K. KAWAGUCHI, and E. HIROTA, "Detection of HBO by Discharge Modulated Infrared Diode Laser Spectroscopy.", *Chem. Phys. Lett.*, **131**, 205 (1986).

E. HIROTA, "A Simultaneous Determination of Third-Order Vibrational Anharmonicity Constants and Equilibrium Structure--Molecualr Structure of Non-Linear HXY-type Molecules.", *J. Chem. Soc. Jpn. (Nippon Kagaku Kaishi)* (in Japanese), 1438 (1986).

T. SUZUKI and E. HIROTA, "Magnetic Interactions in HCF and HSiF Studied by Sub-Doppler Spectroscopy.", *J. Chem. Phys.*, **85**, 5541 (1986).

T. SUZUKI, S. SAITO, and E. HIROTA, "Hyperfine Coupling Constants of NCO in $\tilde{A}^2\Sigma^+$ by Sub-Doppler Spectroscopy.", *J. Mol. Spectrosc.*, **120**, 414 (1986).

K. KAWAGUCHI and E. HIROTA, "Magnetic Field Modulated Infrared Laser Spectroscopy of the Chloronium ClH_2^+ Ion ν_2 Band.", *J. Chem. Phys.*, **85**, 6910 (1986).

K. KAWASHIMA, Y. ENDO, K. KAWAGUCHI, and E. HIROTA, "Detection and Equilibrium Molecular Structure of a Short-Lived Molecule, HBO, by Microwave Spectroscopy.", *Chem. Phys. Lett.*, **135**, 441 (1987).

C. YAMADA, M. C. CHANG, and E. HIROTA, "Infrared Diode Laser Spectroscopy of the PF Radical.", *J. Chem. Phys.*, **86**, 3804 (1987).

H. KANAMORI and E. HIROTA, "Infrared Laser Kinetic Spectroscopy of a Photofragment CS Generated by Photodissociation of CS_2 at 193 nm: Nascent Vibrational-Rotational-Translational Distribution of CS.", *J. Chem. Phys.*, **86**, 3901 (1987).

Y. ENDO and E. HIROTA, "The Submillimeter-Wave Spectrum of the HCCO Radical.", *J. Chem. Phys.*, **86**, 4319 (1987).

Y. ENDO, H. KANAMORI, and E. HIROTA, "Millimeter- and Submillimeter-Wave Kinetic Spectroscopy of Reaction Intermediates.", *Laser Chem.*, **7**, 61 (1987).

H. SUZUKI, M. OHISHI, N. KAIFU, S. ISHIKAWA, T. KASUGA, S. SAITO, and K. KAWAGUCHI, "Detection of

the Interstellar C_6H radical.", *Publ. Astron. Soc. Japan,* **38**, 911 (1986).

A. MURAKAMI, K. KAWAGUCHI, and S. SAITO, "A Quantum Chemical Calculation of the C_6H radical.", *Publ. Astron. Soc. Japan,* **39**, 189 (1987).

S. SAITO, K. KAWAGUCHI, H. SUZUKI, M. OHISHI, N. KAIFU and S. ISHIKAWA, "Detection of C_6H in the $^2\Pi_{2/1}$ state toward IRC+10216.", *Publ. Astron. Soc. Japan,* **39**, 193 (1987).

S. SAITO, S. YAMAMOTO, and K. KAWAGUCHI, "The Microwave Spectrum of the HBF^+ ion.", *J. Chem. Phys.*, **86**, 2597 (1987).

S. SAITO, K. KAWAGUCHI, S. YAMAMOTO, M. OHISHI, H. SUZUKI, and N. KAIFU, "Laboratory Detection and Astronomical Identification of a New Free Radical, CCS ($^3\Sigma^-$)." *Astroph. J.*, **317**, L 115 (1987).

S. YAMAMOTO, S. SAITO, K. KAWAGUCHI, N. KAIFU, H. SUZUKI, and M. OHISHI, "Laboratory Detection of a New Carbon-Chain Molecule C_3S and its Astronomical Identifications,", *Astroph. J.*, **317**, L 119 (1987)

K. KAWAGUCHI, T. SUZUKI, S. SAITO, and E. HIROTA, "Laser Magnetic Resonance of NH_2 in $\tilde{A}^2A_1$ and Highly Excited Vibrational States of $\tilde{X}^2B_1$.", *J. Opt. Soc. Am.*, **B4**, 1203 (1987).

S. HASHIMOTO, J. TERAOKA, T. INUBUSHI, T. YONETANI, and T. KITAGAWA, "Resonance Raman Study on Cytochrome *c* Peroxidase and Its Intermediate; Presence of the $Fe^{IV}=O$ Bond in Compound ES and Heme-Linked Ionization.", *J. Biol. Chem.*, **261**, 11110 (1986).

T. SUGIHARA and T. KITAGAWA, "Resonance Raman Study of Red-Shifted Retinal Schiff-base.", *Bull. Chem. Soc. Jpn.*, **59**, 2929 (1986).

Y. OZAKI, K. IRIYAMA, H. OGOSHI, T. OCHIAI, and T. KITAGAWA, "Resonance Raman Characterization of Iron-Chlorin Complexes Having Various Spin-, Oxidation- and Ligation-States. I: Comparative Study with Corresponding Iron-Porphyrin Complexes.", *J. Phys. Chem.*, **90**, 6105 (1986).

H. LEE and T. KITAGAWA, "Tautomeric Equilibrium of Salicylidene Schiff Base: UV-Visible Absorption and Raman Spectroscopic Studies.", *Bull. Chem. Soc. Jpn.*, **59**, 2897 (1986).

Y. OZAKI, I. IRIYAMA, H. OGOSHI, T. OCHIAI, and T. KITAGAWA, "Resonance Raman Characterization of Iron-Chlorin Complexes Having Various Spin-, Oxidation-, and Ligation-States. II: Low Frequency Skeletal Vibrations and Fe-Ligand Stretching Modes.", *J. Phys. Chem.*, **90**, 6113 (1986).

H. LEE, M. ABE, R. K. PANDEY, H. -K. LEUNG, K. M. SMITH, and T. KITAGAWA, "Characterization of Low Frequency Resonance Raman Bands of Metallo-protoporphyrin IX: Observation of Isotope Shifts and Normal Coordinate Treatments.", *J. Mol. Struct.*, **146**, 329 (1986).

M. ABE, Y. KYOGOKU, T. KITAGAWA, K. KAWANO, N. OHISHI, A. TAKAI-SUZUKI, and K. YAGI, "Vibrational Analysis of Flavin Derivatives. Part I. Infrared Spectra and Molecular Association of Lumiflavin Derivatives.", *Spectrochim. Acta,* **42A**, 1059 (1986).

N. SHIBAYAMA, H. MORIMOTO, and T. KITAGAWA, "The Properties of Chemically Modified Ni(II)-Fe(II) Hybrid Hemoglobins: Ni(II) Protoporphyrin IX as a Model for a Permanent Deoxy-Heme.", *J. Mol. Biol.*, **192**, 331 (1986).

S. HASHIMOTO, R. NAKAJIMA, I. YAMAZAKI, Y. TATSUNO, and T. KITAGAWA, "Oxygen Exchange Between the Fe(IV)=O Heme and Bulk Water for the A_2 Isozyme of Horseradish Peroxidase.", *FEBS Lett.*, **208**, 305 (1986).

Y. OZAKI, K. IRIYAMA, H. OGOSHI, and T. KITAGAWA, "Ligand-Aided Photoreduction of Iron-porphyrin Complexes Probed by Resonance Raman Spectroscopy.", *J. Am. Chem. Soc.*, **109**, 5000 (1987).

S. MATSUKAWA, K. MAWATARI, Y. YONEYAMA, and T. KITAGAWA, "Functional and Structural Analysis on Abnormal Hemoglobins with Impaired Oxygen Binding Properties.", *J. Protein Chem.*, **6**, 109 (1987).

T. OGURA and T. KITAGAWA, "A Device for Simultaneous Measurements of Transient Raman and Absorption Spectra of Enzymic Reactions: Application to Compound I of Horseradish Peroxidase.", *J. Am. Chem. Soc.*, **109**, 2177 (1987).

K. TOHJI, Y. UDAGAWA, M. HARADA, and A. UENO, "A Development of EXAFS and XANES Measurements in the Laboratory – An Application to Silica Supported Cu-Rh Bimetallic Catalyst.", *J. Chem. Soc. Jpn.*, **1986**, 1553.

Y. HIRASHIMA, H. TSUIKI, A. UENO, K. TOHJI, and Y. UDAGAWA, "EXAFS Study of Binary Oxide-Powder

Composed of TiO_2 and ZrO_2." *J. Catal.*, **102**, 249 (1986).

Z. Z. LIN, T. OKUHARA, M. MISONO, Y. UDAGAWA, and K. TOHJI, "Pronounced Effect of Particle Size on Selectivity Observed for Carbon Monoxide Hydrogenation over Ruthenium-Aluminum Catalyst.", *J. Chem. Soc. Chem. Comm.*, **1986**, 1673.

Y. UDAGAWA, K. TOHJI, Z. Z. LIN, T. OKUHARA, AND M. MISONO, "Catalyst Structure Studied by a Laboratory EXAFS Facilities; Ru/Alumina." *J. de Physique,* **47,** C8-249 (1986).

T. MIZUSHIMA, K. HAYAKAWA, and Y. UDAGAWA, "Stabilization of x-ray Source for EXAFS Measurement (in Japanese)." *Bunko Kenkyu,* **36**, 51 (1986).

Y. SHIMIZUGAWA, C. D. YING, M. OKUNO, H. MORIKAWA, F. MARUMO, Y. UDAGAWA, N. MOCHIDA, and T. SEKIYA, "An EXAFS Study of Local Structure in GeO_2-P_2O_5 Glasses (in Japanese).", *Yogyo Kyokaishi,* **95**, 418 (1987).

K. MOCHIDA, A. FUJII, N. TSUCHIYA, K. TOHJI, and Y. UDAGAWA, "Characterization of Bis(2,4,6-tri-tert-butylphenyl)germanium(II) Using Extended X-ray Absorption Fine Structure.", *Organometallics*, **6**, 610 (1987).

K. TOHJI, D. M. HANSON, and B. X. YANG, "Dispersed Fluorescence of Doubly Charged Molecular Ions Using Synchrotron Excitation.", *J. Chem. Phys.*, **85**, 7492 (1987).

K. KEMNITZ, N. TAMAI, I. YAMAZAKI, N. NAKASHIMA, and K. YOSHIHARA, "Fluorescence Decays and Spectral Properties of Rhodamine B in Submono-, Mono-, and Multilayer Systems", *J. Phys. Chem.*, **90**, 5094 (1986).

H. SHIZUKA, T. OGIWARA, A. NARITA, M. SUMITANI, and K. YOSHIHARA, "NaCl Effect on the Excited-State Proton Dissociation Reaction of Naphthols: Water Structure in the Presence of NaCl", *J. Phys. Chem.*, **90**, 6708 (1986).

M. ITOH, Y. FUJIWARA, M. SUMITANI, and K. YOSHIHARA, "Mechanism of Intramolecular Excited State Proton Transfer and Relaxation Processes in the Ground and Excited states of 3-Hydroxyflavone and the Related Compounds", *J. Phys. Chem.*, **90**, 5672 (1986).

J. N. MOORE, D. PHILLIPS, N. NAKASHIMA, and K. YOSHIHARA, "Photophysics and Photochemistry of Sulphonated Derivatives of 9,10-Anthraquinone: 'Strong' versus 'Weak' Sensitizers", *J. Chem. Soc. Faraday Trans. 2*, **82**, 745 (1986).

K. KEMNITZ, N. NAKASHIMA, and K. YOSHIHARA, "Energy and Electron Transfer of Adsorbed Dyes on Molecular Single Crystals and Other Substrates", in "Ultrafast Phenomena V", Springer Series in Chemical Physics Vol. 46, G. R. Fleming and A. E. Siegman Ed., *Springer Verlag*, p.438 (1986).

N. NAKASHIMA, and K. YOSHIHARA, "Oscillator Strengths of the Ultraviolet Bands of Hot and Relaxed Methallyl, Allyl, and Methyl Radicals", *Laser Chem.*, **7**, 177 (1987).

Y. KAJII, K. OBI, I. TANAKA, N. IKEDA, N. NAKASHIMA, and K. YOSHIHARA, "Deuterium Isotope Effects on Photodecomposition of Alkylbenzenes", *J. Chem. Phys.*, **86**, 6115 (1987).

K. KEMNITZ, N. TAMAI, I. YAMAZAKI, N. NAKASHIMA, and K. YOSHIHARA, "Site-Dependent Fluorescence Lifetimes of Isolated Dye Molecules Adsorbed on Organic Single Crystals and Other Substrates", *J. Phys. Chem.*, **91**, 1423 (1987).

H. SHIZUKA, K. OKAZAKI, H. TANAKA, M. TANAKA, M. ISHIKAWA, M. SUMITANI, and K. YOSHIHARA, "Excited-State Behavior of Phenylethynyldisilanes: An Intramolecular Charge-Transfer Emission", *J. Phys. Chem.*, **91**, 2057 (1987).

H. PETEK and K. YOSHIHARA, "Photochemical Timing. Application to Intramolecular Vibrational Redistribution in *t*-Stilbene", *J. Chem. Phys.*, **87**, 1458 (1987).

M. HIRAMOTO, K. HASHIMOTO, and T. SAKATA, "Electron Transfer and Photoluminescence Dynamics of CdS Particles Deposited on Porous Vycor Glass", *Chem. Phys. Lett.*, **133**, 440 (1987).

K. HASHIMOTO, M. HIRAMOTO, T. SAKATA, H. MURAKI, H. TAKEMURA, and M. FUJIHIRA, "Time-resolved measurements of Luminescence of Ru(II) Complexes Chemically or Physically Immobilized on Semiconductor or Insulator Particles in Various Solvents", *J. Phys. Chem.*, **91**, 6198 (1987).

T. OHNO, S. KATO, S. KAIZAKI, and I. HANAZAKI, "Singlet-Triplet Transitions of Aromatic Compounds Coordinating to a Paramagnetic Chromium(III) Ion", *Inorg. Chem.*, **25**, 3853 (1986).

T. NISHIYA, S. YAMAUCHI, N. HIROTA, M. BABA, and I. HANAZAKI, "Fluorescence Studies of the Intramolecularly Hydrogen-Bonded Molecules o-Hydroxyacetophenone and Salicylamide and Related Molecules", *J. Phys. Chem.*, **90**, 5730 (1986).

H. SAIGUSA, M. ITOH, M. BABA, and I. HANAZAKI, "Intermolecular Dynamics and Exciplex Formation of the 1-cyanonaphthalene/triethylamine van der Waals Complex", *J. Chem. Phys.*, **86**, 2588 (1987).

H. SHINOHARA, K. SATO, Y. ACHIBA, N. NISHI, and K. KIMURA, "The Electronically Excited A States of Ammonia Clusters As Revealed by Two-Phonton Ionization Mass Spectroscopy", *Chem. Phys. Lett.*, **130**, 231 (1986).

T. ICHIMURA, Y. MORI, H. SHINOHARA and N. NISHI, "Photofragment Energy Distributions of p-Dichlorobenzene Molecular Beam Excited by Linearly Polarized Light at 193 nm", *J. Spectrosc. Soc. Japan*, **35**, 299 (1986).

N. NISHI, H. SHINOHARA, K. YAMAMOTO, U. NAGASHIMA and N. WASHIDA, "Fragmentation of Hydrogen-bonded Molecular Clusters on Photoionization", *Faraday Discuss. Chem. Soc.*, **81**, 359 (1986).

M. KAWASAKI, H. SATO, H. SHINOHARA, and N. NISHI, "Photodissociation of Tetramethyltin at 193 nm", *Laser Chem.*, **7**, 109 (1987).

N. NISHI, "Dynamical Study of Surface Photochemistry with an UV Laser: Photodissociation, Photoreaction and Photodesorption of Surface Molecules on Molecular Solids", *Rev. Laser Engineering*, **15**, 878 (1987).

Y. TANIMOTO, M. TAKAYAMA, M. ITOH, R. NAKAGAKI, and S. NAGAKURA, "Magnetic Field Effects on the Photo-induced Electron-transfer Reaction of 1-Acetonaphthone and Diphenylamine in Micellar Solution", *Chem. Phys. Lett.*, **129**, 414 (1986).

R. NAKAGAKI, M. HIRAMATSU, K. MUTAI, Y. TANIMOTO, and S. NAGAKURA, "Photochemistry of Bichromophoric Chain Molecules Containing Electron Donor and Acceptor Moieties. External Magnetic Field Effects upon the Photochemistry of N-[ω-(p-nitrophenoxy)alkyl]anilines", *Chem. Phys. Lett.*, **134**, 171 (1987).

T. IMAMURA, N. TAMAI, Y. FUKUDA, I. YAMAZAKI, S. NAGAKURA, H. ABE, and H. HAYASHI, "External Magnetic Field Effect on the Fluorescence of CS_2 Excited to the V $^1B_2$ State with Nanosecond and Picosecond Dye Lasers", *Chem. Phys. Lett.*, **135**, 208 (1987).

H. SAKURAGI, R. NAKAGAKI, T. OGUCHI, T. ARAI, K. TOKUMARU, and S. NAGAKURA, "Mechanism for Photoisomerization of an Olefin in the Presence of Electron Acceptors as Studied by Magnetic Field Effects", *Chem. Phys. Lett.*, **135**, 325 (1987).

Y. TANIMOTO, N. OKADA, M. ITOH, K. IWAI, K. SUGIOKA, F. TAKEMURA, R. NAKAGAKI, and S. NAGAKURA, "Magnetic Field Effects on the Fluorescence of Intramolecular Electron-Donor-Acceptor Systems", *Chem. Phys. Lett.*, **136**, 42 (1987).

H. KATO, K. YOKOYAMA, M. BABA, N. TAMAI, I. YAMAZAKI, and S. NAGAKURA, "Dynamics of Cs_2 Excited by a Synchronously Pumped Mode-locked Dye Laser, and the Effects of Magnetic Field", *J. Chem. Phys.*, **87**, 1987 (1987).

S. ASADA, K. SEKI, and H. INOKUCHI, "Ultraviolet Photoelectron Spectroscopy of Poly(p-phenylenesulfide)", *Chem. Phys. Lett.*, **130**, 155 (1986).

N. UENO, K. SUGITA, K. SEKI, and H. INOKUCHI, "Low-energy Electron Transmission and Secondary-electron Emission Experiments on Crystalline and Molten Long-chain Alkanes", *Phys. Rev.*, **B34**, 6386 (1986).

K. SEKI, S. ASADA, T. MORI, H. INOKUCHI, I. MURASE, R. ENGELHARDT, and E. -E. KOCH, "UV Photoelectron Spectroscopy of Conducting Polymers and their Model Compounds", *Syn. Metals*, **17**, 629 (1987).

H. INOKUCHI, K. SEKI and N. SATO, "UV Photoelectron Spectroscopy of Organic Molecular Materials", *Physica Scripta*, **T17**, 93 (1987).

K. ISHII, H. NAKAYAMA, P. WU, T. MORI, T. ENOKI, K. IMAEDA, G. SAITO and H. INOKUCHI, "Raman Spectra of the Organic Conductor (TTM-TTF) $I_{2.47}$", *Bull. Chem. Soc. Jpn.*, **60**, 2680 (1987).

H. INOKUCHI, "New Organic Semiconductors; Introduction of Strong Intermolecular Interaction to Molecular Crystals", *Material Sci.*, **8**, 99 (1987).

J. K. JESZKA, K. KIMURA, A. TRACZ, H. INOKUCHI and M. KRYSZEWSKI, "Investigation of CT Complexes in Reticulate Doped Polymers by XPS Spectroscopy", *Material Sci.*, **8**, 103 (1987).

Y. HIGUCHI, N. YASUOKA, M. KAKUDO, Y. KATSUBE, T. YAGI, and H. INOKUCHI, "Single Crystal of Hydrogenase from *Desulfovibrio vulgaris*," Miyazaki F." *J. Biol. Chem.*, **262**, 2823 (1987).

H. INOKUCHI, K. IMAEDA, T. ENOKI, T. MORI, Y. MARUYAMA, G. SAITO, N. OKADA, K. SEKI, Y. HIGUCHI, and N. YASUOKA, High Mobility Organic Semiconductor; Tetrakis (Methyl-telluro)-tetrathiafluvalene (TT_eC_1-TTF), *Nature,* **329**, 39 (1987).

K. SEKI, T. B. TANG, T. MORI, P. J. WU, G. SAITO, K. IMAEDA, Z. R. SHI, T. ENOKI, Y. HIGUCHI, N. YASUOKA, and H. INOKUCHI, "Molecular Fasteners; Extraordinarily Strong Interactions in Tetrakis (alkylthio) tetrathiafluvalenes (TTC_n-TTF_s)", *Studies in Organic Chemistry*, **31**, Physical Organic Chemistry 1986. 575-582

N. SATO, K. SEKI, H. INOKUCHI, and Y. HARADA, "Photoemission from an Amorphous Pentacene Film," *Chem. Phys.*, **109**, 157 (1986).

N. SATO and H. INOKUCHI, "Ionization Potentials of Carbon Tetraiodide and Tetraiodoethylene in the Solid State", *Chem. Phys.*, **113**, 445 (1987).

N. SATO, K. SEKI, and H. INOKUCHI, "Simple Gun for Vapor Deposition of Organic Thin Films", *Rev. Sci. Instrum.*, **58**, 1112 (1987).

N. SATO, H. INOKUCHI, B. M. SCHMID, and N. KARL, "Ultraviolet Photoemission Spectra of Organic Single Crystals," *J. Chem. Phys.*, **83**, 5413 (1985).

N. SATO, H. INOKUCHI, and Edger A. SILINSH, "Reevaluation of Electronic Polarization Energies in Organic Molecular Crystals", *Chem. Phys.*, **115**, 269 (1987).

T. MORI and H. INOKUCHI, "Crystal and Electronic Structures of (BEDT-TTF)$AuCl_2AuCl_4$.", *Chem. Lett.*, **1986**, 2069.

T. MORI and H. INOKUCHI, "Crystal Sturctures of $AuCl_2$ Salts of Bis(ethylenedithio)-tetrathiafulvalene (BEDT-TTF). Existence of Divalent Gold, Au(II).", *Solid State Commun.*, **62**, 525 (1987).

T. MORI and H. INOKUCHI, "Structural and Electrical Properties of $(BEDT\text{-}TTF)_3Cl_2(H_2O)_2$.", *Chem. Lett.*, **1987**, 1657.

R. KATO, H. KOBAYASHI, A. KOBAYASHI, T. MORI, and H. INOKUCHI, "Crystal Structures of $M(DCNQIs)_2$ (DCNQIs = N,N'–dicyanoquinonediimines; M = Li, Na, K, NH_4, Cu, Ag).", *Chem. Lett.*, **1987**, 1579.

A. KOBAYASHI, R. KATO, H. KOBAYASHI, T. MORI, and H. INOKUCHI, "The Organic -Electron Metal System with Interaction Through Mixed-Valence Metal Cation: Electronic and Structural Properties of Radical Salts of Dicyano-Quinodiimine. $(DMeDCNQI)_2Cu$ and $(MeCl\text{-}DCNQI)_2Cu$.", *Solid State Commun.*, **64**, 45 (1987).

T. MORI, F. SAKAI, G. SAITO, and H. INOKUCHI, "Structural and Electrical Properties of $(BEDT\text{-}TTF)_3CuBr_3$.", *Chem. Lett.*, **1987**, 927.

H. KOBAYASHI, R. KATO, A. KOBAYASHI, T. MORI, and H. INOKUCHI, "Thermal Expansion and Stepwise Superconducting Transistion of β-$(BEDT\text{-}TTF)_2$ $(I_3)_{1-x}$ $(AuI_2)_x$.", *Solid State Commun.*, **60**, 473 (1986).

A. KOBAYASHI, R. KATO, H. KOBAYASHI, T. MORI, and H. INOKUCHI, "A New Mechanism of the Structural Phase Transition Accompanied By the Change of the Degree of Charge Transfer in α-$(BPDT\text{-}TTF)[Ni(dmit)_2]_2$.", *Physica*, **143B**, 562 (1986).

T. MORI and H. INOKUCHI, "Crystal Structure of the Mixed-Stacked Salts of Bis(ethylenedithio)tetrathiafulvalene (BEDT-TTF) and Tetracyanoquinodimethane (TCNQ).", *Bull. Chem. Soc. Jpn.*, **60**, 402 (1987).

N. OKADA, G. SAITO, and T. MORI, "Tetratelluradicyclopenta[b,g]naphthalene (TTeDCN).", *Chem. Lett.*, **1986**, 311.

N. OKADA, G. SAITO, and T. MORI, "Tetratelluradicycropenta[b,g]naphthalene (TTeDCN).", *Synth. Metals*, **19**, 589 (1987).

T. MORI, P. WU, K. IMAEDA, T. ENOKI, H. INOKUCHI, and G. SAITO, "Crystal Structures of TTM-TTF Complexes.", *Synth. Metals,* **19**, 545 (1987).

M. KOBAYASHI, T. ENOKI, K. IMAEDA, H. INOKUCHI, and G. SAITO, "Phase Transition of the BEDT-TTF Charge-transfer Complex with ClO_4.", *Physica*, **143B**, 550 (1986).

M. KOBAYASHI, T. ENOKI, K. IMAEDA, H. INOKUCHI, and G. SAITO, "Magnetic Susceptibility of Low-dimensional Organic Conductors with Bis(ethylenedithio)tetrathiafulvalene: $(BEDT\text{-}TTF)_3(ClO_4)_2$ and $(BEDT\text{-}TTF)_2ClO_4(C_2H_3Cl_3)_{0.5}$.", *Phys. Rev.*, **B36**, 1457 (1987).

T. ENOKI, K. IMAEDA, H. INOCKUCHI, and M. SANO, "Novel Electronic Sturcture of the Hydrogen-Potassium Graphite Ternary Intercalation Compounds.", *Phys. Rev.*, **B35**, 9399 (1987).

H. YAMAMOTO, K. SEKI, and H. INOKUCHI, "Ultraviolet Photoelectron Spectroscopy of Solid Iodine.", *J. Chem. Phys.*, **86**, 1775 (1987).

I. KANAZAWA, S. TANIGAWA, R. SUZUKI, Y. MIZUHARA, M. SANO, and H. INOKUCHI, "Two-dimensional Electron Momentum Distribution in Graphite Revealed by Means of Angular Correlation of Positron Anihilation.", *J. Phys. & Chem. Solids*, **48**, 701-705 (1987).

K. IMAEDA, T. ENOKI, G. SAITO, and H. INOKUCHI, "Electronic Properties of 3,3',5,5'-Tetramethylbenzidine Complexes with TCNQ Derivatives.", *Mol. Cryst. Liq. Cryst.*, **141**, 131 (1986).

K. IMAEDA, T. ENOKI, T. MORI, P. WU, M. KOBAYASHI, G. SAITO, and H. INOKUCHI, "Magnetic Property of an Organic Conductor, (TTM-TTF) $(I_3)_{0.823}$.", *Synth. Met.*, **19**, 721 (1987).

K. IMAEDA, T. ENOKI, Z. SHI, P. WU, N. OKADA, H. YAMOCHI, G. SAITO, and H. INOKUCHI, "Electrical Conductivities of Tetrakis(alkylthio)-tetrathiafulvalene (TTC_n-TTF) and Tetrakis(alkyltelluro)-tetrathiafulvalene ($TTeC_n$-TTF).", *Bull. Chem. Soc. Jpn.*, **60**, 3163 (1987).

K. NAKASUJI, H. KUBOTA, T. KOTANI, I. MURATA, G. SAITO, T.ENOKI, K. IMAEDA, H. INOKUCHI, M. HONDA, C. KATAYAMA, and J. TANAKA, "Novel Peri-Condensed Weitz-Type Donors: Synthesis, Physical Properties, and Crystal Structures of 3,10-Dithiaperylene (DTPR), 1,6-Dithiapyrene (DTPY), and Some of Their CT Complexes.", *J. Am. Chem. Soc.*, **108**, 3460 (1986).

Z. HERMAN and I. KOYANO, "Dynamics of Chemical Reactions of Ions from Beam Scattering and State Selected Studies.", *J. Chem. Soc. Faraday Trans.*, **II 83**, 127 (1987).

K. HONMA, K. TANAKA, and I. KOYANO, "State Selected Ion-Molecule Reactions by the TESICO Technique. XIII. Vibrational State Dependence of the Cross Sections in the Reaction $C_2D_2^+(v_2) + H_2$.", *J. Chem. Phys.*, **86**, 688 (1987).

S. NAGAOKA, S. SUZUKI, and I. KOYANO, "Production of Pb^+ Ions Following 5d Core Photoionization of Tetramethyllead as Revealed by a Coincidence Experiment.", *Phys. Rev. Lett.*, **58**, 1524 (1987).

S. SUZUKI and I. KOYANO, "Dynamics of the Reaction $MH^+ + MH \rightarrow MH_2^+ + M$. Separation of Two Microscopic Reaction Mechanisms by TOF Coincidence.", *Radiochimica Acta*, **42**, 123 (1987).

S. SUZUKI and I. KOYANO, "State-Selected Ion/Molecule Reactions by the TESICO Technique. XIV. Separation of Two Microscopic Reaction Mechanisms in the Reaction $CH_3Cl^+ + CH_3Cl \rightarrow CH_4Cl^+ + CH_2Cl$.", *Int. J. Mass Spectrom. Ion Proc.*, **80**, 351 (1987).

I. KOYANO, K. TANAKA, T. KATO, and S. SUZUKI, "State-Selected Charge Transfer and Rearrangement Reactions in Four-Atom Ion-Molecule Systems.", *Faraday Disc. Chem. Soc.*, **84** (1987).

S. NAGAOKA, S. SUZUKI, and I. KOYANO, "Investigation of Fragmentation Processes Following Core Photoionization of Organometallic Molecules in the Vapor Phase.", *Nucl. Instr. Meth.*, (1987) in press.

S. KATSUMATA, K. SATO, Y. ACHIBA, and K. KIMURA, "Excited-State Photoelectron Spectra of the One-Photon Forbidden $C^3\Pi_g$ Rydberg State of Molecular Oxygen", *J. Electron Spectrosc.*, **41**, 325 (1986).

H. SHINOHARA, K. SATO, Y. ACHIBA, N. NISHI, and K. KIMURA, "The Electronically Excited A States of Ammonia Clusters as Revealed by Two-Photon-Ionization Mass Spectroscopy", *Chem. Phys. Letters*, **130**, 231 (1986).

H. SATO, M. KAWASAKI, K. TOYA, K. SATO, and K. KIMURA, "Two-Photon Ionization of trimethylamine. Photoelectron Spectroscopic Evidence for Competition of Ionization and Internal Conversion at the S_2 Excited State", *J. Phys. Chem.*, **91**, 751 (1987).

H. SHIROMARU, Y. ACHIBA, K. KIMURA, and Y.T. Lee, "Determination of the C-H Bond Dissociation Energies of Ethylene and Acetylene by Observation of the Threshold Energies of H^+ Formation by Synchrotron Radiation", *J. Chem. Phys.*, **91**, 17 (1987).

N. HAYASAKA, A. HIRAYA, and K. SHOBATAKE, "Synchrotron Radiation-Assisted Etching of Silicon Surface.",

Jpn. J. Appl. Phys., **26**, L1110 (1987).

K. TABAYASHI and K. SHOBATAKE, "Deuterium Isotope Effect on the Cross Section for the Dissociative Excitation Process. $Ar(^3P_{0,2}) + CH_3CN, CD_3CN \rightarrow Ar + CH_3, CD_3 + CN(B^2\Sigma^+)$", *J. Chem. Phys.*, **87**, 2404 (1987).

K.-H. JUNG, D.K. OH, and K. SHOBATAKE, "Primary Processes in the 121.6 nm Photolysis of Gas Phase Ethyl Bromide.", *J. Photochem.*, **39**, 217 (1987).

I. TOKUE, A. HIRAYA, and K. SHOBATAKE, "Photoexcitation and Photofragment Fluorescence Studies of Methanethiol in Vacuum Ultraviolet", *Chem. Phys.*, **116**, 449 (1987).

S. HIRAYAMA, F. TANAKA, and K. SHOBATAKE, "Excess-Energy-Insensitive Fluorescence Decay of Jet-Cooled 9,10-Dicyanoanthracene", *Chem. Phys. Lett.*, **140**, 447 (1987).

T. NISHII, Y. MARUYAMA, T. INABE, and I. SHIROTANI, "Synthesis and Characterization of Black Phosphorus Intercalation Compounds.", *Synthetic Metals*, **18**, 559 (1987).

H. URAYAMA, G. SAITO, T. INABE, T. MORI, and Y. MARUYAMA, "New Organic Conductors Based on AzaTCNQ.", *Synthetic Metals*, **19**, 469 (1987).

K. OHTA, A. TAKAGI, H. MUROKI, I. YAMAMOTO, K. MATSUZAKI, T. INABE, and Y. MARUYAMA, "Discotic Liquid Crystals of Transition Metal Complexes, 4: Novel Discotic Liquid Crystals Obtained from Substituted Bis(dithiolene)nickel Complexes by a New Method.", *Mol. Cryst. Liq. Cryst.*, **147**, 15 (1987).

M. SATO, M. ONODA, S. SHAMOTO, S. HOSOYA, and Y. MARUYAMA, "Pressure Effect on the Superconducting Transition Temperature of La-Sr-Cu-O System.", *Chem. Lett.*, 1039 (1987).

T. MITSUHASHI, M. GOTO, K. HONDA, Y. MARUYAMA, T. SUGAWARA, T. INABE, and T. WATANABE, "A Twin-TCNQ-type Acceptor: Synthesis of 11,11,12,12,13,13,14,14-Octacyano-1,4:5,8-anthradiquinotetramethane and the Structure of Its (1:1) Tetraethylammonium Salt.", *J. Chem. Soc., Chem. Commun.*, 810, (1987).

R. HORIGUCHI, N. IWASAKI, and Y. MARUYAMA, "Time-Resolved and Temperature-Dependent Fluorescence Spectra of Anthracene and Pyrene in Crystalline and Liquid States.", *J. Phys. Chem.*, **91**, 5135 (1987).

T. INABE, J.G. GAUDIELLO, M.K. MOGUEL, J.W. LYDING, R.L. BURTON, W.J. McCARTHY, C.R. KANNEWURF, and T.J. MARKS, "Cofacial Assembly of Partially Oxidized Metallomacrocycles as an Approach To Controlling Lattice Architecture in Low-Dimensional Molecular "Metals". Probing Band Structure-Counterion Interactions in Conductive $[M(phthalocyaninato)O]_n$ Macromolecules Using Nitrosonium Oxidants.", *J. Am. Chem. Soc.*, **108**, 7595 (1986).

H. HOSHI, M. SAKURAI, Y. INOUE, and R. CHUJO,"Medium Effects on the Molecular Electronic Structure. I. The Formulation of a Theory for the Estimation of a Molecular Electronic Structure Surrounded by an Anisotropic Medium.", *J. Chem. Phys.*, **87**, 1107 (1987).

M. KITAGAWA, H. HOSHI, M. SAKURAI, Y. INOUE, and R. CHUJO, "The large dipole moment of cyclomaltohexaose and its role in determining the guest orientation in inclusion complexes.", *Carbohydr. Res.*, **163**, C1 (1987).

N. HOSHINO, K.A. GOLDSBY, and D.H. BUSCH, "Structure and Dynamic Behavior in Solution of Binuclear Nickel (II) Face-to-Face Complexes with Bis(cyclidene) Ligands.", *Inorg. Chem.*, **25**, 3000 (1986).

H. FUJISHITA, M. SATO, S. SATO and S. HOSHINO, "Charge Density Wave Sate in Mo_8O_{23}", *J. Solid State Chem.*, **66**, 40 (1987).

Y. MATSUDA, M. SATO, M. ONODA, and K. NAKAO, "On the Anomalous Transport Properties of $Li_{0.9}Mo_6O_{17}$", *J. Phys. C.*, **19**, 6039 (1986).

M. ONODA, K. TORIUMI, Y. MATSUDA and M. SATO, "Crystal Structure of Lithium Molybdenum Purple Bronze $Li_{0.9}Mo_6O_{17}$", *J. Solid State Chem.*, **66**, 163 (1987).

H. FUJISHITA, M. SATO, S.M. SHAPIRO and S. HOSHINO, "Inelastic Neutron Scattering Study of the Low Dimensional Conductors $(TaSe_4)_2I$ and Mo_8O_{23}", Proc. 15th Yamada Conf. on Phys. Chem, of Quasi One Dimensional Conductors (1986) Lake Kawaguchi; *Physica*, **143B**, 201 (1986).

Y. MATSUDA, M. ONODA, and M. SATO, "Superconductivity in $Li_{0.9}Mo_6O_{17}$", Proc. 15th Yamada Conf. Phys. Chem. of Quasi One Dimensional Conductors (1986) Lake Kawaguchi; *Physica*, **143B**, 243 (1986).

M. ONODA, H. FUJISHITA, Y. MATSUDA, and M. SATO, "Charge Density Waves in Mo_nO_{3n-1}", Proc. Int. Conf. on Synthetic Metals (1986) Kyoto; *Synth. Metals*, **19**, 947 (1986).

S. SUGAI, S. KURIHARA, and M. SATO, "Lattice Vibrations at the Charge-Density-Wave Phase Transitions in $(TaSe_4)_2I$ and $(NbSe_4)_2I$", Proc 15th Yamada Conf. on Phys. Chem. of Quasi One Dimensional Conductors (1986) Lake Kawaguchi; *Physica*, **143B**, 195 (1986).

C. ESCRIBE-FILIPPINI, J. P. POUGET, B. HENNION, and M. SATO, "Neutron Study of Low Frequency Structural Excitations of $K_{0.3}MoO_3$ in the Peierls Insulating State:, Proc. Int. Conf. on Synthetic Metals (1986) Kyoto; *Synth. Metals*, **19**, 931 (1987).

K. NOMURA, K. KUME, T. SAMBONGI, and M. SATO, "Evidence for Sliding Motion of CDW in $Rb_{0.3}MoO_3$: ^{87}Rb NMR", Proc. 15th Yamada Conf. on Phys. Chem. of Quasi One Dimensional Conductors (1986) Lake Kawaguchi; *Physica*, **143B**, 117 (1986).

H. KUBOTA, M. ONUKI, T.MASUMI, H. ANZAI, and M. SATO, "Dielectric Losses of TTF-TCNQ and $K_{0.3}MoO_3$", Proc. Int. Conf. Synthetic Metals (1986) Kyoto; *Synth. Metals*, **19**, 941 (1987).

M. ONODA, Y. MATSUDA, and M. SATO, "Structure Determination of Low Dimensional Conductor Sodium Purple Bronze $Na_{0.9}MoO_6O_{17}$", *J. Solid State Chem.*, **69**, 67 (1987).

M. SATO, "Structure and the Sliding Motion of CDW's in Blue Bronzes and Other Low Dimensional Conductors (Invited Paper):, Proc. 15th Yamada Conf. on Phys. Chem. of Quasi One Dimensional Conductors (1986) Lake Kawaguchi; *Physica*, **143B**, 90 (1986).

M. SATO, M. ONODA, and Y. MATSUDA, "Structural Transitions in Mo_nO_{3n-1} (n=9 and 10)", *J. Phys. C.*, **20** (1987).

M. SATO, Y. MATSUDA, and H. FUKUYAMA, "Localization and Superconductivity in $Li_{0.9}Mo_6O_{17}$", *J. Phys. C.*, **20**, L137 (1987).

T. EKINO, J. AKIMITSU, Y. MATSUDA, and M. SATO, "Electron Tunneling Study on Superconductivity of $Li_{0.9}Mo_6O_{17}$", *Solid State Commun.*, **63**, 41 (1987).

M. SATO, S. HOSOYA, S. SHAMOTO, M. ONODA, K. IMAEDA, and H. INOKUCHI, "Superconductivity of La-M-Cu-O System (M=Ba, Sr and Ca)", *Solid State Commun.*, **62**, 85 (1987).

S. SHAMOTO, M. ONODA, M. SATO, and S. HOSOYA, "Anisotropy of the Superconducting Critical Magnetic Field H_{c2} of La-M-Cu-O System (M=Sr and Ba)", *Solid State Commun.*, **62**, 479 (1987).

T. EKINO, J. AKIMITSU, M. SATO, and S. HOSOYA, "Electron Tunneling Study of High-T_c Superconductor La-Sr-Cu-O System", *Solid State Commun.*, **62**, 535 (1987).

S. HOSOYA, S. SHAMOTO, M. ONODA, and M. SATO, "High-T_c Superconductivity in New Oxide Systems", *Jpn. J. Appl. Phys.*, **26**, L325 (1987).

S. HOSOYA, S. SHAMOTO, M. ONODA, and M. SATO, "High-T_c Superconductivity in New Oxide Systems II", *Jpn. J. Appl. Phys.*, **26**, L456 (1987).

M. ONODA, S. SHAMOTO, M. SATO, and S. HOSOYA, "Crystal Structures of $(La_{1-x}M_x)_2CuO_{4-\delta}$ (M=Sr and Ba)", *Jpn. J. Appl. Phys.*, **26**, L363 (1987).

S. SHAMOTO, S. HOSOYA, M. ONODA, and M. SATO, "Effect of Vacuum Annealing on the Superconducting Transition Temperature of La-Sr-Cu-O System", *Jpn. J. Appl. Phys.*, **26**, 493 (1987).

T. TAKAHASHI, F. MAEDA, S. HOSOYA, and M. SATO, "Ultraviolet Photoemission Study of High-T_c Superconductor $(La_{1-x}Sr_x)_2CuO_{4-\delta}$", *Jpn. J. Appl. Phys.*, **26**, L349 (1987).

M. ONODA, S. SHAMOTO, M. SATO, and S. HOSOYA, "Crystal Structures of $YBa_2Cu_3O_x$ and $LnBa_2Cu_3O_x$ (Ln=Ho and Dy)", *Jpn. J. Appl. Phys.*, **26**, L876 (1987).

S. SUGAI, M. SATO, and S. HOSOYA, "Raman Study of High T_c Superconductors $(La_{1-x}Sr_x)_2CuO_4$", *Jpn. J. Appl. Phys.*, **26**, L495 (1987).

M. SATO and S. HOSOYA, "Superconductivity of La-M-Cu-O System (M=Ba, Sr and Ca)", Proc. IUPAC CHEMRAWN VI World Conf. on Advanced Materials for Innovations in Energy, Transportation and Communications ID01.

K. FUKUDA, M. SATO, S. SHAMOTO, M. ONODA, and S. HOSOYA, "Magnetic Properties of La_2CuO_4 Single Crystals", *Solid State Commun.*, **63**, 811 (1987).

S. SHAMOTO, M. ONODA, M. SATO, and S. HOSOYA, "Anisotropy of the Superconducting Critical Magnetic Field H_{c2} of La-M-Cu-O System (M=Sr and Ba)", Proc. Int. Conf. Low Temp. Phys.; *Jpn. J. Appl. Phys.*, **26**, S26-3, 1131 (1987).

M. SATO, S. HOSOYA, S. SHAMOTO, and M. ONODA, "High-T_c Superconductivity in La-Ba-Cu-O System (Ln=Lanthanide Atoms)", Proc. Int. Conf. Low Temp. Phys.; *Jpn. J. Appl. Phys.*, **26**, S26-3, 1025 (1987).

M. ONODA, S. SHAMOTO, M. SATO, and S. HOSOYA, "Structural Study of $(La_{1-x}M_x)_2CuO_{4-\delta}$ by X-Ray Four Circle Diffraction", Proc. Int. Conf. Low Temp. Phys.; *Jpn. J. Appl. Phys.*, **26**, S26-3, 1049 (1987).

T. TAKAHASHI, F. MAEDA, T. MIYAHARA, S. HOSOYA, and M. SATO, "Photoelectron Spectroscopy of High-T_c Superconductor $(La_{1-x}Sr_x)_2CuO_{4-\delta}$", Proc. Int. Conf. Low Temp. Phys.; *Jpn. J. Appl. Phys.*, **26**, 1013 (1987).

S. SUGAI, M. SATO, S. HOSOYA, S. UCHIDA, H. TAKAGI, K. KITAZAWA, and S. TANAKA, "Raman and Infrared Studies of Oxide Superconductors $(La_{1-x}M_x)_2CuO_4$", Proc. Int. Conf. Low Temp. Phys.; *Jpn. J. Appl. Phys.*, **26**, S26-3, 1003 (1987).

M. KIMURA, S. MATSUBARA, Y. SAWAKI, and H. IWAMURA, "Electrooxidative Desulfenylation of Michael-Type Thiol Adducts of α,β-Unsaturated Esters, Ketones and Nitriles", *Tetrahedron Lett.*, **27**, 4177 (1986).

K. TAKAGI, K. AOSHIMA, Y. SAWAKI, and H. IWAMURA, "Electron-Relay Chain Reaction of *N*-Methyl-4-β-styrylpyridinium Ion on Colloidal SiO_2", *J. Chem. Soc., Perkin* II, 177 (1986).

Y. SAWAKI, K. ISHIGURO, and H. IWAMURA, "Reactivity of Nitroso Oxides. Oxygen Transfer as an Electrophilic Peroxy Radical", *J. Am. Chem. Soc.*, **109**, 584 (1987).

S. MURATA, T. SUGAWARA, and H. IWAMURA, "Magnetic Interaction of Two Diphenylcarbene Units Linked with an Ethylenic Double Bond", *J. Am. Chem. Soc.*, **109**, 1266 (1987).

K. ISHIGURO, Y. SAWAKI, A. IZUOKA, T. SUGAWARA, and H. IWAMURA, "Electron Spin Resonance Study on the σ- and π-Radical Cations Formed by One-Electron Oxidation of Aryldiazomethanes", *J. Am. Chem. Soc.*, **109**, 2530 (1987).

A. IZUOKA, S. MURATA, T. SUGAWARA, and H. IWAMURA, "Molecular Design and Model Experiments of Ferromagnetic Intermolecular Interaction in the Assembly of High-Spin Organic molecules. Generation and Characterization of the Spin States of Isomeric Bis(phenylmethylenyl)[2.2]paracyclophanes", *J. Am. Chem. Soc.*, **109**, 2631 (1987).

Y. KAWADA, J. ISHIKAWA, H. YAMAZAKI, G. KOGA, S. MURATA, and H. IWAMURA, "Correlation of the Two Torsional Degrees of Freedom about the Bonds From the Bridgehead Carbons to the Sulfur Atom in Bis(9-triptycyl) Sulfide", *Tetrahedron Lett.*, **28**, 445 (1987).

M. IWAMURA, T. ISHIKAWA, Y. KOYAMA, K. SAKUMA, and H. IWAMURA, "1-Pyrenylmethyl Esters. Photolabile Protecting Groups for Carboxylic Acids", *Tetrahedron Lett.*, **28**, 679 (1987).

H. TUKADA, K. MUTAI, and H. IWAMURA, "(3-Nitrenophenyl)methylene: a Ground State Quintet Molecule Having Both Carbenic and Nitrenic Atoms", *J. Chem. Soc., Chem. Commun.*, 1159 (1987).

E.C. LIM, R.J. LOCKE, B.T. LIM, T. FUJIOKA, and H. IWAMURA, "Conformation and Electronic Relaxation of Molecular Triplet Excimers; Triplet Excimers of Naphthalene and Related Molecules", *J. Phys. Chem.*, **91**, 1298 (1987).

M. KIMURA, K. KOIE, S. MATSUBARA, Y. SAWAKI, and H. IWAMURA, "A Novel Electrooxidative Methoxylation of Cyanomethyl Sulphides", *J. Chem. Soc., Chem. Commun.*, 122 (1987).

M. IWAMURA, K. TOKUDA, N. KOGA, and H. IWAMURA, "Photoreactivity of 1-Pyrenylmethyl Esters. Dependence on the Structure of the Carboxylic Acid Moieties and the Nature of the Excited States", *Chemistry Lett.*, 1729 (1987).

K. ISHIGURO, Y. SAWAKI, and H. IWAMURA, "Diazomethane Radical Cations as Dipolarophiles in the Dimeric Olefin Formation from Diazo-compounds", *Chemistry Lett.*, 1853 (1987).

K. ISOBE, S. TERO-KUBOTA, H. TANAKA, Y. NAKAMURA S. OKEYA, and K. SAITO, "Synthesis and Photochemical Behavior of μ-*p*-Xylene-α,α′-diyldimolybdenum (II).", *J. Organometal, Chem.*, **329**, C21 (1987).

M. TANAKA, I. TSUJIKAWA, K. TORIUMI, and T. ITO, "The Structure of the Linear Chain Tetraammine-

platinum(II)diiodotetraammineplatinum(IV) Hydrogensulfate Dihydrate, $[Pt(NH_3)_4][PtI_2(NH_3)_4](HSO_4)_4 \cdot 2H_2O$", *Acta Cryst.*, **C42**, 1105 (1986).

K. TORIUMI, M. YAMASHITA, H. ITO, and T. ITO, "Structure of One-Dimensional Pd^{II}-Pd^{IV} Mixed-Valence Complexes, $[Pd^{II}L][Pd^{IV}Cl_2L]Y_4$ (Y=ClO_4 and PF_6), and Their Parent Pd^{II} and Pd^{IV} Complexes, $[Pd^{II}L](ClO_4)_2$ and $[Pd^{IV}Cl_2L](NO_3)_2 \cdot HNO_3 \cdot H_2O$, with 1,4,8,11-Tetraazacyclotetradecane(L)", *Acta Cryst.*, **C42**, 963 (1986).

K. TORIUMI, M. YAMASHITA and I. MURASE, "Crystal Structures of Bromo-Bridged One-Dimensional Mixed-Metal Compounds, $[Ni^{II}(en)_2][Pt^{IV}Br_2(en)_2](ClO_4)_4$ and $[Pd^{II}(en)_2][Pt^{IV}Br_2(en)_2](ClO_4)_4$", *Chem. Lett.*, 1753, (1986).

Y. MAEDA, H. OSHIO, Y. TAKASHIMA, M. MIKURIYA, and M. HIDAKA, "Crystal Structure, Mössbauer Spectra, and Magnetic Properties of $[Fe(acpa)_2]PF_6$ and Crystallographic Changes in Fast Electronic Relaxation between S=1/2 and S=5/2", *Inorg. Chem.*, **25**, 2958 (1986).

H. OSHIO, K. KITAZAKI, J. MISHIRO, N. KATO, Y. MAEDA, Y. TAKASHIMA, "New Spin-crossover Iron(III) Complexes with Large Hysterisis Effects and Time Dependence of their Magnetism", *J. Chem. Soc. Dalton Trans.*, 1341 (1987).

H. OSHIO, S. TERO-KUBOTA, and T. ITO, "Photochemical Behavior of Aluminum-Ethyl Complex with Tetraaza Macrocyclic Ligand, $Al(C_{22}H_{22}N_4)(C_2H_5)$", *Bull. Chem. Soc. Jpn.*, **60**, 3047 (1987).

M. MIKURIYA, S. KIDA, and I. MURASE, "Crystal and Molecular Structure of a Thiolate-bridged Binuclear Nickel(II) Complex, $[Ni_2\{SCH(CH_2CH_2NH_2)_2\}_2]Br_2$", *Bull. Chem. Soc. Jpn.*, **60**, 1180 (1986).

M. MIKURIYA, S. KIDA, and I. MURASE, "Crystal and Molecular structure of a Novel Mixed-spin Binuclear Nickel(II) Complex with N,N′,N″,N″-Tetrakis(2-aminoethyl)-1,4,8,11-tetraazacyclotetradecane", *J. Chem. Soc., Dalton Trans.*, 1261 (1987).

M. MIKURIYA, S. KIDA, and I. MURASE, "Preparation and Crystal Structures of Binuclear Copper(II) Complexes of N,N′,N″,N″-Tetrakis(2-aminoethyl)-1,4,8,11-tetraazacyclotetradecane Containing Azide, Cyanide, or Thiocyanate Ion", *Bull. Chem. Soc. Jpn.*, **60**, 1355 (1987).

M. MIKURIYA, S. KIDA, and I. MURASE, "Crystal and Molecular Structure of $[Cu_2(taec)X](ClO_4)_3 H_2O$(taec=N,N′,N″,N″-Tetrakis(2-aminoethyl)-1,4,8,11-tetraazacyclotetradecane; X=I, F, NO_2, and CH_3COO; n=0,1, or 2). Effect of Incorporation of an Anion X on the Structure of the Complex Cation", *Bull. Chem. Soc. Jpn.*, **60**, 1681 (1987).

M. NAKAMURA, H. OKAWA, T. ITO, M. KATO, and S. KIDA, "Proton NMR Spectroscopic Investigation on Stereoselectivity in Cobalt(III) Complexes of Various 3-Substituted 1-Phenyl-1,3-propanediones", *Bull. Chem. Soc. Jpn.*, **60**, 539 (1987).

M. SUZUKI, S. MURATA, A. UEHARA, and S. KIDA, "Synthesis and Characterization of a Dinuclear Manganese(II, III) Mixed Valence Complex with the Dinucleating Ligand, L-py", *Chem. Lett.*, 281, (1987).

S. ISHIGURO and H. OHTAKI, "Thermodynamic and Structural Studies on Metal Complexes in Various Solvents", *Coord. Chem. Section B*, **15**, 237 (1987).

S. ISHIGURO, B.G. JELIAZKOVA, and H. OHTAKI, "A Calorimetric Study of *N,N*-Dimethylformamide Complexes of Copper(II) in Acetonitrile", *J. Solution Chem.*, **16**, 1 (1987).

S. ISHIGURO, K. OZUTSUMI, and H. OHTAKI, "Calorimetric and Spectrophotometric Studies of Chloro Complexes of Nickel(II) and Zinc(II) Ions in *N,N*-Dimethylformamide", *Bull. Chem. Soc. Jpn.*, **60**, 531 (1987).

S. ISHIGURO, K. OZUTSUMI, L. NAGY, and H. OHTAKI, "Calorimetric and Spectrophotometric Studies of Bromo Complexes of Copper(II) in *N,N*-Dimethylformamide", *Bull. Chem. Soc. Jpn.*, **60**, 1691 (1987).

S. ISHIGURO, L. NAGY, and H. OHTAKI, "Calorimetric and Spectrophotometric Studies of Ternary Copper(II) Complexes with Bromide Ions and 2,2′-Bipyridil in *N,N*-Dimethylformamide", *Bull. Chem. Soc. Jpn.*, **60**, 2053 (1987).

S. ISHIGURO, L. NAGY, and H. OHTAKI, "A Calorimetric Study of Ternary Zinc(II) Complexes with Chloride Ions and 2,2′-Bipyridil in *N,N*-Dimethylformamide", *Bull. Chem. Soc. Jpn.*, **60**, 2865 (1987).

B.-T. WANG, Y. SASAKI, K. OKAZAKI, K. KANESATO, and K. SAITO, "Kinetics of Ligand Substitution and Oxidation Reactions of the (2-Phosphonomethyl)9mino diacetato aquaoxovandium(IV) Ion.", *Inorg. Chem.*, **25**, 3745 (1986).

A. NAGASAWA, H. KIDO, T.M. HATTORI, and K. SAITO, "Ligand Isotopic Exchange Kinetics of Tris(acetylacetonato)aluminium(III) in Acetylacetone under Atomospheric and Elevated Pressures.", *Inorg. Chem.*, **25**, 4330 (1986).

K. SAITO, A. NAKAMURA, H. TAKEI, and B.-T. BATEER, "Heterogeneous Olefin hydrogenation Catalysis of Metal Cluster Compounds consisting of Rhodium-Boron Cluster Anion and Rare Earth Cations.", *J. Catal*, **106**, 292 (1987).

Y. SASAKI, K. ENDO, A NAGASAWA, and K. SAITO, "Reinvestigation of the Pressure Effect upon an Outer-Sphere Electron-Transfer Reactions between Aquapentamminecobalt(III) and Hexacycnoferrate(II) in Aqueous Solution", *Inorg. Chem.*, **25**, 4845 (1986).

M. EBIHARA, Y. SASAKI, S. TERO-KUBOTA, and K. SAITO, "A Kinetic Study of Pressure Effect upon an Outer-Sphere Electron Transfer Reaction Invoving Free Radicals.", *Bull. Chem. Soc. Jpn.*, **60**, 391 (1987).

Y. SASAKI, T. NINOMIYA, A. NAGASAWA, K. ENDO, and K. SAITO, "Large Positive Activation Volumn for the Intramolecular Electron-Transfer Reaction from Iron(II) to Cobalt(III) in (μ-Pyrazine-N,N')-(pentamminecobalt(III))pentacyanoiron(II) in Aqueous Solution.", *Inorg. Chem.*, **26**, 2164 (1987).

H. KATO, Y. YAMAGUCHI, M. YAMADA, S. FUNAHASHI, Y. NAKAGAWA, and H. TAKEI, "Neutron scattering study of magnetic excitations in oblique easy-axis antiferromagnet $FeTiO_3$.", *J. Phys. C.*, **19**, 6993 (1986).

Y. TODATE, Y. ISHIKAWA, K. TAJIMA, S. TOMOYOSHI, and H. TAKEI, "Spin dynamics in a quasi-two dimentional antiferromagnet $MnTiO_3$", *J. Phys. Soc. Japan*, **55**, 4464 (1986).

H. TAKEYA, H. TAKEI, Y. KOIKE, T. FUKASE, T. SHISHIDO, N. TOYOTA, and Y. SYONO, "Shock-loading effects on superconducting and ferromagnetic transitions of $ErRh_4B_4$", *Jpn. J. Appl. Phys.*, **25**, 1954 (1986).

T. SHISHIDO, N. TOYOTA, and H. TAKEI, "Growth and superconductivity of Nb_5Sn_2Ga crystals", *Jpn. J. Appl. Phys.*, **25**, 1600 (1986).

H. TAKEI, N. KOBAYASHI, H. YAMAUCHI, T. SHISHIDO, and T. FUKASE, "Magnetic and superconducting properties of the cubic perovskite YRh_3B", *J. Less-Common Metals*, **125**, 233 (1986).

A. ITO, H. ARUGA, E. TORIKAI, M. KIKUCHI, Y. SYONO, and H. TAKEI, "Time-dependent phenomena in a short-range ising spin-glass, $Fe_{0.5}Mn_{0.5}TiO_3$", *Phys. Rev. Letters*, **57**, 483 (1986).

J.M. NEWSAM, Y. ENDOH, Y. ISHIKAWA, and H. TAKEI, "Powder neutron diffraction studies of the mixed ilmenite system $Fe_{0.6}Co_{0.4}TiO_3$", *J. Phys. C.*, **19**, 1273 (1986).

E. TORIKAI, A. ITO, Y. TAKEDA, K. NAGAMINE, K. NISHIYAMA, Y. SYONO, and H. TAKEI, "Spin dynamics in mixed antiferromagnet with competing anisotropies $Fe_{0.6}Co_{0.4}TiO_3$ probed by positive muons", *Solid State Commun.*, **58**, 839 (1986).

H. TAKEI, S. HOSOYA, S. TSUNEKAWA, M. KIKUCHI, and T. KOBAYASHI, "Oxidation of copper chevrel compound $Cu_xMo_6S_8(x\sim2)$", *Mat. Res. Bull.*, **21**, 713 (1986).

Y. KOIKE, T. FUKASE, N. KOBAYASHI, S. HOSOYA, and H. TAKEI, "Quenched superconductivity by rapid cooling down to low temperatures below Tc_2 in single-crystal $HoMo_6S_8$", *Solid State Commun.*, **60**, 771 (1986).

T. SHISHIDO and H. TAKEI, "Crystal growth of CsCl-type $Rh_{50}Al_{50-x}Cu_x$ from copper solution", *J. Less-Common Metals*, **119**, 75 (1986).

Y. YAMAGUCHI, H. KATO, H. TAKEI, A.I. GOLDMAN, and G. SHIRANE, "Re-examination of the magnetic structure of $FeTiO_3$", *Solid State Commun.*, **59**, 865 (1986).

S. TSUNEKAWA, K. IMAEDA, and H. TAKEI, "Nonstoichiometry and superconductivity in $La_xMo_6S_y$", *Mat. Res. Bull.*, **22**, 585 (1987).

H. TAKEI, "Ternary superconductors of sulfides and borides", *SERAMIKKUSU*, **22**, 568 (1987), in Japanese.

N. MOMOZAWA, M. MITA, and H. TAKEI, "Single crystal growth of $(Ba_{1-x}Sr_x)_2Zn_2Fe_{12}O_{22}$ from high temperature solution", *J. Crystal Growth*, **83**, 403 (1987).

Y. NAKAZAWA, M. ISHIKAWA, T. TAKABATAKE, H. TAKEYA, T. SHIBUYA, K. TERAKURA, and H. TAKEI, "Characterization of the high T_c superconductor $(Ba_{0.7}Y_{0.3})CuO_{3-x}$", *Jpn. J. Appl. Phys.*, **26**, L682 (1987).

Y. IYE, T. TAMEGAI, H. TAKEYA, and H. TAKEI, "The Anisotropic upper critical field of single crystal

$YBa_2Cu_3O_x$", *Jpn. J. Appl. Phys.*, **26**, L1057 (1987).

T. SAITO, H. MANABE, T. YAMAGATA, and H. IMOTO, "First Synthesis of Octahedral Tungsten Cluster Chloro Complexes with Trialkylphosphines and Their Conversion to η^1-Ethyl Derivatives.", *Inorg. Chem.*, **26**, 1362 (1987).

S. TERO-KUBOTA, H. OSHIO, T. ITO, V.L. GOEDKEN, and J. HIGUCHI, "Time-Resolved and Conventional ESR Studies of the Excited Triplet States of Dibenzotetraazamacrocyclic Complexes of Al(III) and Ge(IV)", *Chem. Phys. Lett.*, **131**, 430 (1986).

M. ISHII, S. FUNAHASHI, and M. TANAKA, "Variable Pressure and Temperature Nuclear Magnetic Resonance Study of Solvent Exchange on Manganese(II) Ion in *N,N*-Dimethylformamide. Influence of Solvent Molecular Size on Solvent Exchange Mechanism.", *Chem. Lett.*, **871** (1987).

S. FUNAHASHI, N. UCHIYAMA, M. ISHII, and M. TANAKA, "Kinetics of Imidazole Addition to the Axial Site of the Iron(II) Complex of 2,3,9,10-Tetraphenyl-1,4,8,11-tetraaza-1,3,8,10-cyclotetradecatetraene in Dimethyl Sulfoxide. Evidence for a Dissociative-Interchange Mechanism.", *Inorg. Chim. Acta*, **128**, 169 (1987).

H. KASHIWAGI, F. HIROTA, U. NAGASHIMA, and T. TAKADA, "Ab Initio MO Calculations on the Chlorophyll-Water System and Estimation of the Structure of the Special Pair.", *Int. J. Quant. Chem.*, **30**, 311 (1986).

K. OHNO, K. MOROKUMA, F. HIROTA, H. HOSOYA, S. IWATA, Y. OSAMURA, H. KASHIWAGI, S. YAMAMOTO, K. KITAURA, N. KOSUGI, H. NAKATSUJI, S. OBARA, K. TANAKA, M. TOGASHI, and S. YAMABE, "Quantum Chemistry Literature Data Base–Bibliography of Ab Initio Calculations for 1985", *J. Mole, Struct.*, (Theochem), **135**, 1 (1986).

A. CHAIKEN, G. ROTH, T. ENOKI, N.C. YEH, M.S. DRESSELHAUS, and P. TEDROW, "Superconducting Properties of Ternary Graphite Intercalation Compounds", *Mat. Res. Soc. Symp. Proc.*, **56**, 461 (1986).

N.C. YEH, T. ENOKI, L. SALAMANCA-RIBA, and G. DRESSELHAUS, "Structural and Electronic Properties of Potassium Hydrogen Intercalated Graphite", *Mat. Res. Soc. Symp. Proc.*, **56**, 467 (1986).

T. ENOKI, K. IMAEDA, H. INOKUCHI, and M. SANO, "Novel Electronic Structure of the Hydrogen-Potassium-Graphite Ternaray Intercalation Compounds", *Phys. Rev.*, **B35**, 9399 (1987).

M. TANAKA, A. KAWAMOTO, J. TANAKA, M. SANO, T. ENOKI, and H. INOKUCHI, "Electronic Structure of (BEDT-TTF)$CuCl_2$ Complex", *Bull. Chem. Soc. Jpn.*, **60**, 2531 (1987).

I. YAMAZAKI, N. TAMAI, and T. YAMAZAKI, "Picosecond Fluorescence Spectroscopy on Molecular Association in Langmuir-Blodgett Films", *Ultrafast Phenomena V*, eds. by G.R. Fleming and A.E. Siegman, Springer Ser. Chem. Phys. Vol. **46** (Springer, Berlin, Heidelberg 1986) pp.444-446.

I. YAMAZAKI, N. TAMAI, and T. YAMAZAKI, "Picosecond Fluorescence Spectroscopy on Excimer Formation and Excitation Energy Transfer of Pyrene in Langmuir-Blodgett Monolayer Films", *J. Phys. Chem.*, **91**, 3572 (1987).

I. YAMAZAKI, F.M. WINNIK, M.A. WINNIK, and S. TAZUKE, "Excimer Formation in Pyrene-Labelled Hydroxypropylcelluose in Water: Picosecond Fluorescence Studies", *J. Phys. Chem.*, **91**, 4213 (1987).

N. TAMAI, T. YAMAZAKI, I. YAMAZAKI, and N. MATAGA, "Fractal Behaviors in Two-Dimensional Excitation Energy Transfer on Vesicle Surfaces", *Ultrafast Phenomena V*, eds. by G.R. Fleming and A.E. Siegman, Springer Ser. Chem. Phys. Vol. **46** (Springer, Berlin, Heidelberg 1986) pp.449-453.

T. TAMAI, T. YAMAZAKI, and I. YAMAZAKI, "Two-Dimensional Excitation Energy Transfer Between Chromophoric Carbazole and Anthracene in Langmuir-Blodgett Monolayer Films", *J. Phys. Chem.*, **91**, 841-845 (1987).

N. TAMAI, T. YAMAZAKI, I. YAMAZAKI, A. MIZUMA and N. MATAGA, "Excitation Energy Transfer Between Dye Molecules Adsorbed on Vesicle Surface", *J. Phys. Chem.*, **91**, 3503-3508 (1987).

A. MATSUI, K. MIZUNO, N. TAMAI, and I. YAMAZAKI, "Transient Free-Exciton Luminescence and Exciton-Lattice Interaction in Pyrene Crystals", *Chem. Phys.*, **113**, 111-117 (1987).

A. ITAYA, A. KURAHASHI, H. MASUHARA, N. TAMAI, and I. YAMAZAKI, "Dynamic Fluorescence Microprobe Method Utilizing Total Internal Reflection Phenomenon", *Chem. Letters*, **1979** (1987).

Y. TANIGUCHI, M. MITSUYA, N. TAMAI, I. YAMAZAKI, and H. MASUHARA, "Fluorescence Spectra of

Vacuum-Deposited Films of ω-(1-Pyrenyl)alkanoic Acids", *Chem. Phys. Lett.*, **130**, 516-520 (1986).

M. MIMURO, N. TAMAI, T. YAMAZAKI, and I. YAMAZAKI, "Excitation Energy Transfer in Spinach Chloroplasts: Analysis by the Time-Resolved Fluorescence Spectrum at −196°C in Picosecond Time Range", *FEBS Letters*, **213**, 119-122 (1987).

M. MIMURO, I. YAMAZAKI, N. TAMAI, T. YAMAZAKI, and Y. FUJITA, "Analysis of Pigment System I Chl a Fluorescence at Room Temperature by the Steady State and the Time-Resolved Spectrum in Picosecond Time Range", *Progress in Photosynthesis Research*, Vol. **1**, ed. by J. Biggins, (Martinus Nijhoff, Dordrecht, 1987), pp. 91-94.

K. KIMURA and S. BANDOW, "Paramagnetic Enhancement in the Magnetic Susceptibility of Ultrafine Magnesium Particles", *Phys. Rev. Lett.*, **58**, 1359 (1987).

S. BANDOW, K. KIMURA, K. KON-NO, and A. KITAHARA, "Magnetic Properties of Magnetite Ultrafine Particles Prepared by W/O Microemulsion Method", *Jap. J. Appl. Phys.*, **26**, 713 (1987).

K. KIMURA "Metal Colloids Produced by Means of Gas Evaporation Technique. IV. Size Distribution of Small Mg and In Particles", *Bull. Chem. Soc. Jpn.*, **60**, 3093 (1987).

J.K. JESZKA, K. KIMURA, A. TRACZ, H. INOKUCHI, and M. KRYSZEWSKI, "Investigations of CT Complexes in Reticulate Doped Polymers by XPS Spectroscopy", *Material Sci.*, **VIII. No.1-2**, 103 (1987).

H. TAKAYA, T. OHTA, N. SAYO, H. KUMOBAYASHI, S. AKUTAGAWA, S. INOUE, I. KASAHARA, and R. NOYORI, "Enantioselective Hydrogenation of Allylic and Homoallylic Alcohols.", *J. Am. Chem. Soc.*, **109**, 1596 (1987).

K. MASHIMA, K. JYODOI, A. OHYOSHI, and H. TAKAYA, "Reaction of $(\eta^5\text{-}C_5H_5)_2$ $\overline{TiOC[=Re(CO)_4Re(CO)_5]CH_2CH_2}$ with *tert*-Butylisocyanide: Molecular Structure of a New Zwitterionic Complex Involving η^2-Imidoyltitanium and Acyldirhenium Carbonyl Moieties.", *Organometallics*, **6**, 885 (1987).

T. OHTA, H. TAKAYA, M. KITAMURA, K. NAGAI, and R. NOYORI, "Asymmetric Hydrogenation of Unsaturated Carboxylic Acids Catalyzed by BINAP–Ruthenium(II) Complexes.", *J. Org. Chem.*, **52**, 3174 (1987).

R. NOYORI, T. OHKUMA, M. KITAMURA, H. TAKAYA, N. SAYO, H. KUMOBAYASHI, and S. AKUTAGAWA, "Asymmetric Hydrogenation of β-Keto Carboxylic Esters." *J. Am. Chem. Soc.*, **109**, 5856 (1987).

M. KITAMURA, K. MANABE, R. NOYORI, and H. TAKAYA, "Kinetic Resolution of 4-Hydroxy-2-cyclopentenone by Rhodium-catalyzed Asymmetric Isomerization." *Tetrahedron Lett.*, **28**, 4719 (1987).

M. KITAMURA, Yi HSIAO, R. NOROYI, and H. TAKAYA, "General Asymmetric Synthesis of Benzomorphans and Morphinans via Enantioselective Hydrogenation." *Tetrahedron Lett.*, **28**, 4829 (1987).

T. MITANI, Y. KANEKO, S. TANUMA, Y. TOKURA, T. KODA, and G. SAITO,"Electric Conductivity and Phase Diagram of a Mixed-stack Charge-transfer Crystal: Tetrathiafulvalene-p-chloranil.", *Phys. Rev.*, **B35**, 427 (1987).

T. MITANI, Y. TOKURA, K. TAKAOKA, T. KODA, and G. SAITO, "Phase Transition of the Mixed-stack Charge-transfer TTF-p-chloranil Single Crystals.", *Synth. Metals*, **19**, 515 (1987).

Y. WADA, T. MITANI, M. YAMASHITA, and T. KODA, "Charge Transfer Excitons in Halogen-bridged Mixed Valence Complexes", *Synth. Metals*, **19**, 907 (1987).

Y. TOKURA, H. OKAMOTO, T. KODA, T. MITANI, and G. SAITO, "Domain Wall Dynamics in Mixed-stack Charge-transfer Crystal", *Physica*, **143b**, 527 (1986).

Y. KANEKO, S. TANUMA, Y. TOKURA, T. KODA, T. MITANI, and G. SAITO, "Optical Reflectivity Spectra of the Mixed-stack Organic Charge-transfer Crystal Tetrathiafulvalene-p-chloranil under Hydrostatic Pressure", *Phys. Rev.*, **B35**, 8024 (1987).

Y. TAKAGI and K. YOSHIHARA, "XV International Quantum Electronics Conference", *Technical digest*, **MBB3**, p.4 (1987).

T. NANBA, Y. URASHIMA, M. IKEZAWA, M. WATANABE, E. NAKAMURA, K. FUKUI, and H. INOKUCHI, "Far-Infrared Spectroscopy by Synchrotron Radiation at the UVSOR Facility", *J. Infrared & Millimeter Waves*, **7**, 1769 (1986).

T. MURATA, T. MATSUKAWA, M. MORI, M. OBASHI, S. NAOÉ, H. TERAUCHI, Y. NISHIHATA, O.

MATSUDO, and J. YAMAZAKI, "A Double Crystal Monochromator for Soft X-Ray Beam Line of UVSOR", *J. Phys. (France)*, **47**, *Suppl.*, **C8**, 135 (1986).

K. NAKAMURA, Y. SASAKI, M. WATANABE, and M. FUJITA, "Polarized Reflection Spectra of Orthorhombic Indium Bromide in 2-30 eV Region", *Physica Scripta*, **35**, 557 (1987).

T. KASUGA, "Ion-Clearing System of UVSOR Storage Ring", *Jpn. J. Appl. Phys.*, **25**, 1711 (1986).

T. KATAYAMA, A. NODA, N. TOKUDA, H. YONEHARA, and M. YOSHIZAWA, "Helical Type Kicker for Stochastic Momentum Cooling", *Jpn. J. Appl. Phys.*, **25**, 1919 (1986).

Review Articles and Textbooks

K. NASU, "Dynamics of Free Exciton Self-Localization", *Optical Properties of Solids, and Electron-Lattice Interaction* ed. by K. NASU, Special Volume of Solid State Physics (April 1987, Tokyo, AGNE GIJUTSU CENTER, in Japanese) p.75.

K. NASU, "Contemporary Problems in the Theory for Tunneling", *Physics and Application of Tunneling Phenomena* ed. by Y. Takeuchi Collected papers in the 23-th Symposium (1987, March 12-13, Institute for Electric-Communication, Tohoku Univ. Sendai, Japan. in Japanese), p.78.

E. HIROTA and S. SAITO, "Spectroscopy and Structures of Free Radicals and Molecular Ions.", *Revs. Chem. Interm.*, **7**, 353 (1987).

E. HIROTA, "Structures of Molecular Ions.", *Chemistry* (in Japanese), **42**, 568 (1987).

T. KITAGAWA and T. OGURA, "Resonance Raman Study on Catalytic Intermediates of Cytochrome *c* Oxidase.", in "*Time-Resolved Vibrational Spectroscopy*" G.H. Atkinson, Ed. Gordon and Breach Science Publishers, pp. 83-100.

T. KITAGAWA and Y. OZAKI, "Infrared and Raman Spectra of Metalloporphyrins", *Structure and Bonding*, **64**, pp.71- (1987).

T. KITAGAWA, "Resonance Raman Spectra of Reaction Intermediates of Heme Enzymes.", in "*Advances in Spectroscopy*" R.J.H. Clark and R.E. Hester, Eds. Wiley & Sons, Vol. **13**, pp.443-481 (1986).

T. KITAGAWA, "Application of Resonance Raman Spectroscopy to Biological Science", *Physics* (in Japanese), **66**, 724-730 (1986).

T. KITAGAWA, "Infrared and Raman Study on Hemoglobin Cooperativity" in *Tanpakushitsu, Kakusan, Koso* (in Japanese), **32**, 584-593 (1987).

S. HASHIMOTO and T. KITAGAWA, "Resonance Raman Study on the Structure in the Heme Vicinity of Peroxidases" in "*Nippon Kagaku Zasshi*" in Japanese, pp.1613-1622 (1986).

K. KAMOGAWA and T. KITAGAWA, "Application of Raman Difference Spectroscopy to Solution Chemistry" in *Bunko Kenkyu*" "in Japanese" **36**, 3-19 (1987).

T. KITAGAWA and T. OGURA, "Application of Raman Spectroscopy to Biological Science" in "*Bunko Kenkyu*" "in Japanese" **36**, 147-162 (1987).

N. KAKUTA, "Behaviours of the Hydrogen on Metal Surfaces (Roles of Surface Hydrogen over CO Hydrogenation Catalysts).", *Hyomen*, **24**, 607 (1986).

N. NAKASHIMA, and K. YOSHIHARA, "Hot Molecule Mechanism in Photochemistries of Benzene, Alkylbenzenes, and Olefins", in "*Physical Organic Chemistry 1986*", M. Kobayashi Ed., Elsevier, (1986).

K. YOSHIHARA, "Flash Photolysis and Spectroscopy by Prof. G. Porter", in "*Classic Papers in Chemistry*", Ser. II, Vol. 4, K. Tokumaru, Ed., Japan Science Societies Press, Tokyo, pp.225-244 (1986).

T. SAKATA, "Molecular Processes on Electrode Surfaces", *Kagaku to Kogyo* (in Japanese), **39**, 827 (1986).

T. SAKATA, "Photocatalyst", *The Energy Conservation* (in Japanese), **39**, 48 (1987).

T. SAKATA, "Photoexcitation of Semiconductor and the Basis of Photocatalysis---Photoinduced Electron Transfer at Semiconductor Interface", *Nippon Syashin Gakkaishi* (in Japanese), **50**, 207 (1987).

T. SAKATA, "Light and Molecules---Absorption, Emission and Spectra",*Kagaku to Kyoiku* (in Japanese), **35**, 393 (1987).

N. NISHI, "Cluster Beam Chemistry", *Kagaku to Kogyo* (in Japanese), **40**, 270 (1987).

I. KOYANO and K. SHOBATAKE, "Synchrotron Radiation Spectroscopy. VI. Gas-Phase Studies of Processes of Chemical Interest.", *Bunko Kenkyu* (in Japanese), **35**, 493 (1986).

I. KOYANO, "Photoionization.", in "Molecular Science Series" 11 (in Japanese), I. Tanaka ed., Kyoritsu Publ. Co. Ltd., pp.285-342 (1987).

H. INOKUCHI, K. SHOBATAKE, and M. WATANABE, "UVSOR and Its Application to Molecular Science.", *Kasokuki Kagaku* (in Japanese), **1**, 15 (1986).

K. SHOBATAKE, "1986 Nobel Prize Winners in Chemistry----- Understanding of Chemical Reactions at Microscopic Levels.", *Chemistry* (in Japanese), **42**, 9 (1987).

K. SHOBATAKE, "1986 Novel Prize Winners in Chemistry. Chemical Reaction Dynamics--- Visualizing How Chemical Reactions Proceed---.", *Chemistry Today* (in Japanese), **1987**, 12 (1987).

K. KIMURA, "Molecular Dynamic Photoelectron Spectroscopy using Resonant Multiphoton Ionization for Photophysics and Photochemistry", *Internat. Rev. Phys. Chem.*, **6**, 195 (1987).

Y. ACHIBA, K. SATO, and K. KIMURA, "Dynamical Aspects of Molecular Clusters Studied by Multiphoton Ionization Technique", in "*Microclusters*", ed. by S. Sugano, Y. Nishina and S. Ohnishi, Springer-Verlag, Berlin, p.115 (1987).

M. SATO, "Superconductivity and Charge Density Waves in Transition Metal Oxides and Bronzes", *Nippon Kessho Gakkai-shi*, **29**, 190 (1987).

K. ISHIGURO, Y. SAWAKI, A. IZUOKA, T. SUGAWARA, and H. IWAMURA, "Studies on Cation Radical Species Generated by One-Electron Oxidation of Diazomethanes", in "*Studies in Organic Chemistry. Physical Organic Chemistry 1986*", M. Kobayashi, Ed., Elsevier, Amsterdam, Vol. 31, p.67, 1987.

T. SUGAWARA, S. MURATA, and H. IWAMURA, "Detection and Characterization of 2-(9-Fluorenyl)phenylnitrene as an Intermediate in the Photorearrangement of 1-Azatriptycene", in "*Studies in Organic Chemistry. Physical Organic Chemistry 1986*", M. Kobayashi, Ed., Elservier, Amsterdam, Vol. 31, p.99, 1987.

H. IWAMURA and A. IZUOKA, "High-Spin Organic Molecules and Molecular Assemblies. Approaches to Organic Ferromagnets", *Nippon Kagaku Kaishi* (in Japanese), 595 (1987).

H. IWAMURA, "Strongly Magnetic Organic Materials", *Kagaku to Kogyo* (in Japanese), **40**, 585 (1987).

K. SAITO and K. KASHIWABARA, "Preparation, Circular Dichroism and Substitution Reactions of Platinum(II) Complexes with Asymmetric Olefin Ligands.", *J. Organom. Chem.*, **330**, 291 (1987).

H. KASHIWAGI, "Calculations of Molecular Science and Features of Supercomputer System at the Institute for Molecular Science.", *Computer Center News of Hokkaido University*, Vol. 19, No. 4, pp.3 (1987).

H. KASHIWAGI, "Computational Chemistry for Heme and Electrons.", *Protein, Nucleic Acid and Enzyme*, 1987-5, Vol. 32, No. 6, pp.711 (1987).

I. YAMAZAKI, "Picosecond Time-Resolved Fluorescence Spectroscopy and Its Application to Surface Molecular Dynamics" *Zairyo Gijutsu* (in Japanese), **5**, 200-208 (1987).

I. YAMAZAKI, "Photosynthesis Primary Processes Studied with Picosecond Time-Correlated Photon-Counting Method" *The Review of Laser Engineering* (in Japanese), **15**, 595-605 (1987).

I. YAMAZAKI, "Photosynthetic Light-Harvesting Antenna System and Its Artificial Analogue of Langmuir-Blodgett Multilayers" *Radiation Chemistry* (in Japanese), No. **44**, 200-202 (1987).

K. KIMURA, "Preparation of Metal Small Particles and thier Magnetic Properties", *Zairyo Gijutsu* (in Japanese), **5**, 350 (1987).

G. SAITO and T. MITANI, "The Neutral-to-Ionic Phase Transition and Soliton Formation in the Charge Transfer Complex", *KAGAKU* (in Japanese), **42**, 136 (1987).

T. NANBA, M. IKEZAWA, M. WATANABE and H. INOKUCHI, "Far Infrared Solid State Spectroscopy by the Use of Synchrotron Radiation", *Kotai Butsuri* (in Japanese), **22**, 93 (1987).

T. KASUGA and M. WATANABE, "Overview of the UVSOR Facility", *BNL Report*, **BNL 51959**, pp.83-93 (1986).

Institute for Molecular Science, Myodaiji, Okazaki 444, Japan